WILDFIRE IMPACTS ON SOIL CARBON POOLS AND MICROBIAL COMMUNITIES IN MIXED-CONIFER FORESTS OF CALIFORNIA

By

Jaron Adkins

A DISSERTATION

Submitted to
Michigan State University
in partial fulfillment of the requirements
for the degree of

Crop and Soil Sciences − Doctor of Philosophy
Ecology, Evolutionary Biology, and Behavior − Dual Major

2021

ABSTRACT

WILDFIRE IMPACTS ON SOIL CARBON POOLS AND MICROBIAL COMMUNITIES IN MIXED-CONIFER FORESTS OF CALIFORNIA

By

Jaron Adkins

Forest ecosystems are important reservoirs for long term carbon (C) storage. Forests of the western United States account for 20-40% of total U.S. carbon C sequestration, and nearly half of the total C in these forests is stored in soil. However, many forests in the western U.S are experiencing wildfire conditions that diverge from historical fire regimes. Prior to Euro-American settlement, California's mixed-conifer forests typically experienced frequent surface fires of low to moderate burn severity, but, due to the combined effects of altered forest structure and climate change, now experience fires that are larger and more severe than historical conditions. Fires have numerous direct and indirect effects on the soil biological, chemical, and physical characteristics that influence the soil C cycle. Understanding how altered soil characteristics influence the cycling and persistence of soil C, and how they vary with severity, is important for managing forests for C storage and for predicting fire-climate feedbacks. My dissertation work incorporates observational and manipulative experiments to understand the direct and indirect effects of burn severity on soil C cycling and microbial communities over the short to intermediate term, with a particular focus on the distribution of soil C between active and slow cycling pools.

Soil C can be conceptualized as discrete pools of variable persistence in soil. The active C pool is quickly decomposed, contributing to the return of CO_2 to the atmosphere, whereas the non-active C pool is more stable and contributes to long term C storage. I leveraged a burn

severity gradient resulting from a wildfire in a California mixed-conifer forest to determine the structure and kinetics of these C pools at an intermediate time point in post-fire recovery (i.e. three years). I found that the size of the non-active C pool was smaller in burned areas than unburned areas, and the kinetic rate of the non-active C pool was negatively related to burn severity. I also characterized the soil microbial communities across this severity gradient and identified the environmental characteristics responsible for differences. I found that fungal-to-bacterial ratio and oligotroph-to-copiotroph bacteria ratio decreased with burn severity, and these effects were driven by differences in live and dead tree basal area, soil nutrients, and pH. Leveraging another burn severity gradient, I then determined whether differences in microbial communities and soil C pools were related one-year post-fire in a mixed-conifer forest. I again found lower non-active C pool kinetic rates, and higher abundances of copiotrophic bacteria in burned compared to unburned areas. Differences in soil C pool kinetics were related to tree basal area, soil nutrients, and bacterial communities.

I determined the short-term impacts of fire on soil C pools and cycling using lab experiments in which I manipulated soil heating intensity and pyrogenic organic matter (PyOM) additions. I found that high intensity soil heating can decrease microbial biomass C (MBC) accumulation, whereas PyOM had minimal effects on MBC in the short-term. Finally, I found that the size of the active C pool increased with soil heating intensity, while the kinetic rate of the non-active C pool decreased; PyOM primarily increased the size of the non-active C pool. Taken as a whole, my research suggests that fire induces short-term soil C losses by increasing the size of the active C pool, but, over the intermediate-term, residual soil C is more persistent. Fire severity is predicted to increase globally throughout the 21st century, and my research contributes to understanding how forest C storage will be affected by disrupted wildfire regimes.

This dissertation is dedicated to Hayden, who taught me the meaning of resilience
And to Shane, whose example and support gave me the courage to take this journey.

ACKNOWLEDGMENTS

I would like to thank my committee members for their support throughout my studies. Thank you to my dissertation advisor, Dr. Jessica Miesel, for giving me the opportunity to pursue my research interests, helping me do my best work, and treating me with compassion when I needed it. Thank you to Dr. Kathryn Docherty for your patient training and positive responses to all my attempts. Thank you to Dr. Phillip Robertson for reminding me to focus on the big picture and providing encouragement. Thank you to Dr. Lisa Tiemann for always being willing to give help, feedback, and advice.

This work would not have been possible without financial support from Michigan State University, the Department of Plant, Soil and Microbial Sciences, the Department of Forestry, and the National Science Foundation Graduate Research Fellowship Program. I would like to thank the staff of the USDA Forest Service at the Plumas National Forest and the Lassen National Forest for their logistical support. I thank the staff of the Duke University Research Forest for providing access to their properties and facilitating sample collection.

I would like to thank all the staff and faculty in the Department of Plant, Soil, and Microbial Sciences and the Department of Forestry who formally or informally supported me during my time at Michigan State University. Finally, I would like to extend my most appreciative thanks to all my lab colleagues and fellow graduate students with whom I have been fortunate to share this journey.

TABLE OF CONTENTS

LIST OF TABLES

LIST OF FIGURES

KEY TO ABBREVIATIONS

AIC	Aikake Information Criterion
ANOVA	Analysis of Variance
C	Carbon
C_a	Active Carbon Pool
C_r	Resistant Carbon Pool
C_s	Slow Carbon Pool; Non-Active Carbon Pool
Csoc	Total Soil Organic C
CO_2	Carbon Dioxide
CUE	Carbon Use Efficiency
DBH	Diameter at Breast Height
DME	Dry Mass Equivalent
dNBR	Differenced Normalized Burn Ratio
EOC	Extractable Organic Carbon
FAME	Fatty Acid Methyl Ester
F:B	Fungal-to-Bacterial Ratio
GLM	Generalized Linear Model
IAR	Inhibitor Additivity Ratio
k_a	Kinetic Rate of Active Carbon Pool
k_r	Kinetic Rate of Resistant Carbon Pool
k_s	Kinetic Rate of Slow Carbon Pool; Kinetic Rate of Non-Active Carbon Pool

KCl	Potassium Chloride
MAT	Mean Annual Temperature
MBC	Microbial Biomass Carbon
MRT	Mean Residence Time
N	Nitrogen
NH_4	Ammonium
NO_3	Nitrate
O:C	Oligotroph-to-Copiotroph Ratio
OTU	Operational Taxonomic Unit
P	Phosphorus
PcOA	Principal Coordinates Analysis
PERMANOVA	Permutational Analysis of Variance
PLFA	Phospholipid Fatty Acid
PLSR	Partial Least Squares Regression
POM	Particulate Organic Matter
PyC	Pyrogenic Carbon
PyOM	Pyrogenic Organic Matter
RdNBR	Relative Differenced Normalized Burn Ratio
RMSE	Root Mean Square Error
SBS	Soil Burn Severity
SEM	Structural Equation Model
SOM	Soil Organic Matter
TIN	Total Inorganic Nitrogen

WFPS	Water Filled Pore Space
WHC	Water Holding Capacity

CHAPTER 1:

SOIL CARBON POOLS AND FLUXES VARY ACROSS A BURN SEVERITY GRADIENT THREE YEARS AFTER WILDFIRE[1]

1.1 ABSTRACT

Carbon (C) storage in soils contributes to the strength and stability of total ecosystem C sinks, but both aboveground and belowground C is vulnerable to loss during fire. The distribution of soil C and nitrogen (N) among various defined pools – e.g., active, slow and resistant C, and ammonium and nitrate as forms of inorganic N – determines the C storage capacity of forests and the nutrient availability for plant communities recovering from wildfires. Projections of increased wildfire severity due to a warming climate and frequent droughts raise concerns about parallel increases in fire's impacts on the sizes and mineralization kinetics of soil C and N pools, with potentially long-lasting effects on the strength of the forest C sink and on the ability of forests to recover from disturbance. Therefore, I sought to determine how the sizes and mineralization rates of soil C and N pools vary across a gradient of fire severity three years after the Chips Fire burned 30,500 ha of Sierra Nevada mixed-conifer forest. I measured total C and N in forest floor and mineral soil (0-5 cm), the pool sizes and mean residence times of the active, slow, and resistant C in mineral soil, and the pool sizes and mineralization rates of inorganic N in mineral soil. Forest floor total C was lower in areas that experienced high severity fire than in unburned reference areas, an effect likely attributable to greater combustion of forest floor material in high severity areas. Mineral soil C content did not vary with fire severity. Over

[1] *Originally published as:* Adkins J., Sanderman J., Miesel J.R., 2019. Soil carbon pools and fluxes vary across a fire severity gradient three years after a wildfire burned Sierra Nevada mixed-conifer forest. Geoderma 333, 10-22.

a 300-day lab incubation, mineral soil CO_2-C efflux rates were consistently lower in soils from areas that experienced high severity fire relative to unburned reference areas and were associated with longer mean residence times of the slow C pool. Forest floor N content was lower in high severity areas than unburned areas, whereas mineral soil total N did not vary with vary with fire severity. Mineral soil ammonium and total inorganic N concentrations increased significantly with fire severity in field-fresh soils, but this trend was no longer apparent after a 300-day lab incubation, indicating that site-specific factors control N availability among fire severity levels. My results indicate that future increases in wildfire severity in mixed-conifer forest may alter the strength of the forest C sink by impacting the amount C stored in forest floor, the stability of mineral soil C, and the availability of N to recovering plant communities.

1.2 INTRODUCTION

Changes to the size and persistence of soil carbon (C) pools in temperate forests have the potential to influence atmospheric CO_2 concentrations (Trumbore 2000; Lutzow et al. 2006) because of the major role these ecosystems play in global C dynamics. For example, temperate forests accounted for ~30% of the global forest C sink from 1990-2007 (Pan et al. 2011), and store 48% of ecosystem C in their soils (Pan et al. 2011). The majority of soil C is stored as soil organic matter (SOM), a continuum of materials that remains in soil for days to centuries, depending on the physiochemical properties of the SOM and the surrounding matrix, and the physical accessibility of the organic compounds to decomposers (Schmidt et al. 2011). The SOM continuum is often modelled as three distinct C pools with variable turnover times: an active C pool (C_a) with a mean residence time (MRT) of days to months, a slow pool (C_s) with a MRT of years to decades, and a resistant pool (C_r), potentially stable for centuries (Trumbore 1997; Paul et al. 2006). The turnover rates and distribution of C among these three C pools are sensitive to

changes in environmental conditions and disturbance regimes (Trumbore 1997; Jackson et al. 2017) and influence the strength of the ecosystem C sink (Luo and Weng 2011).

Wildfires are one of the most common forest disturbances in the conterminous United States, burning more than 17,000 km^2 y^{-1} and causing 13.40 Tg C y^{-1} of direct C emissions during 1990-2012 (Chen et al. 2017). In addition to causing combustion emissions, high-severity wildfires can transform forest stands from C sinks to C sources when C losses via decomposition exceed photosynthetic C gains during post-fire forest recovery (Kashian et al. 2006). When climate and fire regimes are stable, wildfire emissions are balanced by the C uptake of vegetative regrowth during ecosystem recovery, ecosystems transition from C sources back to C sinks, and the net ecosystem C flux is zero (Bowman et al. 2009; Loehman et al. 2014). However, altered disturbance regimes disrupt this equilibrium by affecting the magnitude of C losses and temporal patterns of ecosystem recovery (Luo and Weng 2011). Fire regimes have shifted in ecosystems worldwide: for example, the global average area burned increased by more than 20% in the second half of the 20th century compared to the first half (Flannigan et al. 2013). In western United States forests (west of 102º W longitude), wildfire frequency increased four-fold, total area burned increased six-fold, and the length of the fire season increased by 78 days during 1987-2003 compared to 1970-1986 (Westerling et al. 2006). In the Sierra Nevada mountain range, the proportion of burned area that experienced high severity fires nearly doubled between 1984 and 2006 (Miller et al. 2009b).

Wildfire severity is a measure of the magnitude of effects of wildfire on ecosystem biomass (Keeley 2009), and is correlated with C stock losses from aboveground vegetation and dead wood in mixed-conifer (Campbell et al. 2007; Meigs et al. 2009) and ponderosa pine (*Pinus ponderosa*) forests (Meigs et al. 2009). The increasing occurrence of high burn severity in an

ecosystem that historically experienced frequent fires of primarily low to moderate severity has the potential to alter forest composition and successional pathways and destabilize forest C stocks, particularly when coupled with the warming temperatures and increased drought frequency expected in climate projections (Earles et al. 2014; Liang et al. 2017b). Landsat-derived spectral data available since 1982 have greatly expanded the scale and ease with which burned areas can be mapped (García and Caselles 1991). The increasing availability of fire severity data has expanded both interest in and ability to assess the impacts of fire on aboveground components of the ecosystem, whereas the ability to determine effects on belowground C stocks remains challenging because Landsat imagery is more sensitive to changes in vegetation than soil (Miller and Thode 2007; Miller et al. 2009a). The storage of C in pools with long residence times increases the strength and stability of the total ecosystem C sink (Luo and Weng 2011). Thus, the size, structure, and turnover times of soil C pools have potential to influence the transition of forests from C sources to C sinks during recovery from wildfire and may either moderate or exacerbate the response to shifting patterns of fire severity.

Meta-analyses have indicated that wildfires in general decrease soil C stocks in the forest floor layer (Nave et al. 2011), but the response of mineral soil C varies with climatic zones, forest type, soil depth, fire type (i.e., wildfire vs. prescribed fire), and time since fire (Johnson and Curtis 2001; Nave et al. 2011; Wang et al. 2012). Wildfire-induced changes in soil N stocks generally mirror those of soil C stocks in temperate regions, in which forest floor N stocks generally decrease (Nave et al. 2011; Wang et al. 2012), whereas the effects on mineral soil N vary with soil depth and fire type (Wan et al. 2001; Nave et al. 2011). None of the meta-analyses to date have directly assessed the impacts of fire severity or fire intensity (i.e., energy flux resulting from a fire) on soil C and N, a shortcoming acknowledged by several researchers (Nave

et al. 2011; Wang et al. 2012). However, studies that separate the effects of prescribed fires and wildfires on soil C and N have found that wildfires cause greater losses to forest floor C and N stocks and mineral soil C concentrations than prescribed fires (Nave et al. 2011; Wang et al. 2012). Because prescribed fires are often of lower intensity and result in lower severity relative to wildfires, the differences in impacts between prescribed fires and wildfires reported to date suggest that soil C and N storage may also differ across contrasting levels of fire severity (Alcañiz et al. 2018).

Because of the large proportion of C stored in soil, the size and turnover times of the C_a, C_s, and C_r pools determines the strength and stability of the ecosystem C sink in recovering forests (Luo and Weng 2011). Fernández et al. (1999) used a two-pool model to assess the impacts of wildfire on labile and recalcitrant soil C pools and their associated kinetics in *P. sylvestris* and *P. pinaster* forests in northwest Spain and found that wildfire increased the size and mineralization rate of the labile C pool in soils to 5 cm depth, an effect that persisted for several months, but was no longer apparent after one year. Two years after the wildfire, the labile C pools in burned soils and their mineralization rates were lower than or equal to those in unburned soils; meanwhile, the mineralization rate of the recalcitrant C pool in burned soils was consistently lower than that of unburned soils over the two year study (Fernández et al. 1999). The study sites Fernández et al. (1999) used experienced only high intensity fires, and the effects of fire severity level were not considered. To my knowledge, the relationship between wildfire severity and the C_a, C_s, and C_r pools and their associated kinetics has yet to be assessed: this information is important for understanding long term effects of wildfire on forest C storage (Birdsey et al., 2006). For example, lower mineralization rates and larger sizes of the C_r and C_s

pools may partially offset total ecosystem C losses by increasing the overall MRT, and thus the sink strength, of forest C (Luo and Weng 2011).

Fire directly influences the soil C pool structure through the formation of pyrogenic carbon (i.e., carbon associated with char; PyC), which is generated via the thermal decomposition of biomass and encompasses a spectrum of materials from slightly charred plant matter to highly condensed soot and micrographine sheets (Bird et al. 2015). PyC was initially viewed solely as a resistant C pool, but emerging evidence shows that PyC consists of an active, slow, and resistant pool (Kuzyakov et al. 2014). The relative sizes of these PyC pools depends on combustion temperature (Bird et al. 2015) and source material (Hatton et al., 2016, Michelotti and Miesel 2015), and the amount of PyC generated during fires has been shown to increase with fire severity (Miesel et al. 2015; Maestrini et al. 2017) and fire intensity (Czimczik et al. 2003; Sawyer et al. 2018). Pyrogenic C contributes directly to soil total C pools, but also influences soil C pools indirectly via impacts on mineralization kinetics of native soil C. For example, PyC induces short-term positive and long-term negative priming effects (Maestrini et al. 2015), and soil C mineralization rates decrease with increasing PyC concentrations (Michelotti and Miesel 2015). Thus, severity-based differences in PyC accumulation may have downstream impacts on C flux rates from the soil to the atmosphere.

Low soil inorganic N content often limits plant productivity in coniferous forests (Vitousek and Howarth 1991), whereas enhancing N availability can increase soil C stocks by increasing soil C inputs (Nave et al. 2009) and decreasing C loss via respiration (Janssens et al. 2010). Therefore, the sizes of inorganic N pools in post-fire soils are likely to affect the recovery of aboveground (Grogan et al. 2000) and belowground C stocks. Increases in soil ammonium (NH_4^+) and nitrate (NO_3^-) concentrations are typical after wildfires, across a variety of ecosystem

types (Wan et al. 2001). Maximum increases in soil NH_4^+ and NO_3^- concentrations are approximately tenfold greater than pre-fire conditions, generally returning to pre-fire levels after one year for NH_4^+, and within five years for NO_3^- (Wan et al. 2001). Studies ranging from two days to 26 months after fires have variously attributed the N pulse to pyrolysis of forest floor material (Covington and Sackett 1992), ash deposition (Christensen 1973), decreased uptake by vegetation due to plant mortality (Ficken and Wright 2017), and decreased uptake by microbes (Koyama et al. 2012).

Fire also impacts N cycling in soil, over short- and longer time periods after fire. For example, a meta-analysis of N mineralization response to fires showed that fires stimulate a short term (< 3 months) increase in N mineralization, but decrease N mineralization rates over the long term (at least 3 years), a decrease that is greater for prescribed fires than wildfires (Wang et al. 2012). In addition to the direct effects of increased N availability on N mineralization rates, changes to N mineralization may result from changes to soil moisture and temperature that in turn influence microbial activity (Turner et al. 2007), or from increases in PyC concentrations (Michelotti and Miesel 2015). Together, results from these studies suggest that fire severity level may have an important influence on N mineralization rates in a recovering forest.

Direct assessments of soil C and N pools and dynamics after wildfires are needed to improve estimates of the amount and stability of C stored in forest ecosystems (Birdsey et al. 2006). Meta-analyses separating the effects of wildfire and prescribed fire on soil C and N content, as well as research on the influence of fire severity on soil PyC suggest that the distribution of soil C and N among different pools may be influenced by severity (Nave et al. 2011; Wang et al. 2012; Miesel et al. 2015; Maestrini et al. 2017). However, specific estimates of the sizes and turnover rates of the C_a, C_s, and C_r pools are lacking. Therefore, I conducted a

field study to investigate patterns in soil C and N across a fire severity gradient three years after wildfire. My specific objectives were to quantify: 1) total C and N content in forest floor and mineral soil, 2) the sizes of the char pool in forest floor and the PyC pool in mineral soil, 3) the sizes and MRTs of mineral soil C_a, C_s, and C_r pools, 4) the sizes and mineralization rates of inorganic N pools in mineral soil, and 5) the influence of mineral soil PyC on C and N mineralization rates, across contrasting fire severity levels, including unburned reference areas.

1.3 MATERIALS AND METHODS

1.3.1 Site description

I investigated the area affected by the Chips Fire (Lat: 40.095 Long: -121.199; Fig.1.1), which was ignited by lightning on July 28, 2012 and burned 30,500 ha of the Plumas and Lassen National Forests prior to containment on August 31, 2012 by United States Forest Service wildland firefighting crews. Fire severity estimates based on the Relative Differenced Normalized Burn Ratio (RdNBR), which is calculated from Landsat imagery (Eidenshink et al. 2007), indicate that approximately 6,300 ha burned at high severity, 9,600 ha at moderate severity, and 12,500 ha at low severity (MTBS 2017). RdNBR based severity estimates are sensitive to changes to soil color and moisture, but primarily detect changes to vegetation chlorophyll and water content and is therefore considered an aboveground severity metric (Miller and Thode 2007; Safford et al. 2008; Miller et al. 2009a). RdNBR values are calibrated to the amount of basal area mortality, resulting in a three-level severity classification where < 25% basal area mortality is classified as low severity, 25-75% basal area mortality is classified as moderate severity, and >75% mortality is classified as high severity (Miller et al. 2009a). The forest type of my study area is classified as California mixed-conifer (Ruefenacht et al. 2008), consisting of *P. ponderosa, P. lambertiana, P. jeffreyi, Abies concolor, Pseudotsuga menziesii,*

Calocedrus decurrens, and *Quercus kelloggii*. *Ceanothus* spp. and *Arctostaphylos* spp. shrub species are also common.

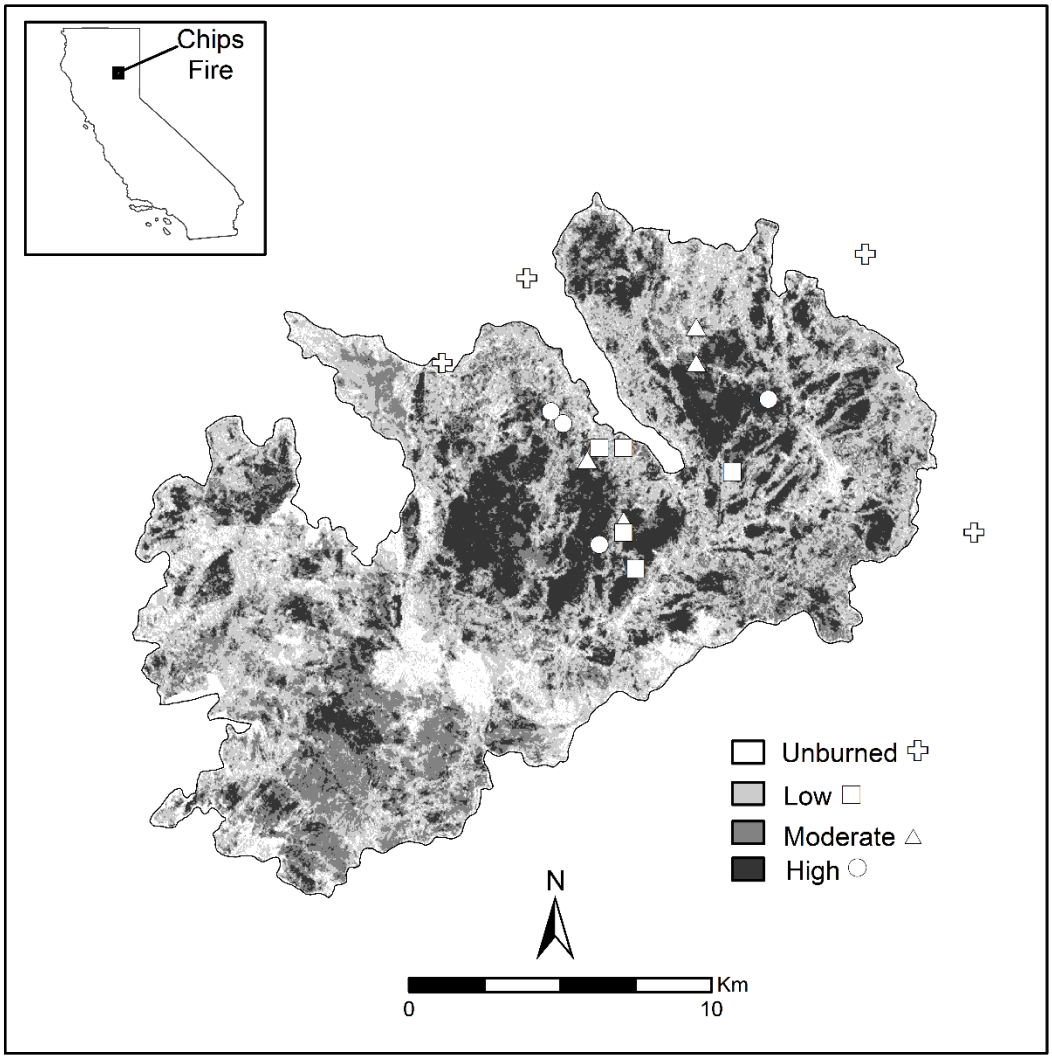

Figure 1.1 Locations of field plots at different fire severity levels in the Chips Fire. The Chips Fire burned mixed-conifer forest in the Plumas and Lassen National Forests, California, USA in 2012. The border denotes the fire perimeter, the color gradient indicates different severity levels, and the symbols indicate the location of field plots. Unburned plots were sited outside of the fire perimeter in mixed-conifer stands of similar composition.

Prior to Euro-American settlement in the mid-19th century, the mean fire return interval of the region's mixed-conifer forests ranged from 11 to 34 years (Mallek et al. 2013), and less than 10% of annual burned area experienced high severity fires (Mallek et al. 2013; Miller and

Safford 2017). However, a policy of fire suppression has been in place in the United States since the early 20th century (Dombeck et al. 2004), leading to greater tree and fuel density in mixed-conifer forests, and the percentage of burned area that experienced high severity fire increased to 25% by 1984-2009 (Mallek et al. 2013). At the Plumas National Forest Supervisor's Office in Quincy, CA, the 30 year mean annual precipitation is 1080 mm, more than 75% of which occurs in winter and spring, and mean annual temperature is 10.6º C (NCEI-NOAA 2017).

My field plots were established in 2014 as part of a broader forest inventory performed by the USDA Forest Service. Between July 6, 2015 and July 28, 2015 (i.e., three years post-fire), I sampled 17 plots (4 unburned, 5 low severity, 4 moderate severity, 4 high severity) for forest floor and mineral soil (Fig 1.2). I selected plots that had relatively similar topographic characteristics across severity levels. Selected plots had an elevation range of 1217-1641 m, slopes < 50%, and a variety of slope aspects (Table 1.1). Plots were established 100-1000 m from roads and trails in areas without post-fire salvage logging to minimize the influence of direct human activity on my research plots. Unburned reference plots were located within 2000 m of the fire perimeter in mixed-conifer stands of similar composition. The average distance between any two plots was 6.4 km, with a minimum distance of 400 m. A portion of the forest burned by the Chips Fire had been burned previously by the Storrie Fire in 2000 and was excluded from this study. Most of the area burned by the Chips Fire had not burned in the last century. My field sites comprised two soil series: Skalan, a loamy-skeletal, isotic, mesic Vitrandic Haploxeralf, and Kinkel, a loamy-skeletal, mixed, superactive, mesic Ultic Palexeralf. These acidic soils are gravelly loams that form from metamorphic parent material and are free of calcium and carbonates. Typical pedons consist of 2.5-5 cm thick O horizons, 7.5-17.5 cm thick A horizons, and Bt horizons to bedrock (Soil Survey Staff).

Table 1.1 Topographic characteristics of research plots for each wildfire severity level. Aspect count shows number of plots per aspect category.

Severity	Elevation (m)	Slope (%)	Aspect (count)			
			N	E	S	W
Unburned	1359-1593	22-29	0	2	1	1
Low	1217-1399	12-36	1	0	1	3
Moderate	1466-1591	18-43	0	1	2	1
High	1451-1641	31-49	0	4	0	0

Figure 1.2 Photographs depicting aboveground (a-d) and soil surface (e-h) characteristics of unburned mixed-conifer forest stands, and stands that had experienced low, moderate, and high severity fire, respectively, three years previously. The high severity stand in image d had accumulated patchy leaf litter, whereas the high severity stand in image h exhibited bare mineral soil. Image h illustrates the high gravel content of the soils.

1.3.2 Field methods

At each plot, I sampled forest floor and mineral soil 17 m from the plot center at azimuths of 0º, 120º, and 240º, for a total of 51 forest floor samples and 51 mineral soil samples. The forest floor includes the plant litter and duff layers, and is equivalent to the combined Oi, Oe, and Oa horizons in the USDA Soil Taxonomy classification system (Perry et al. 2008). I collected all forest floor material from within a 15 cm radius circular sampling frame and then collected mineral soil to 5 cm depth using a stainless-steel scoop. I collected one additional volumetric

mineral soil sample from each plot to estimate bulk density by collecting mineral soil to 5 cm using a 10 cm diameter sampling cylinder. Samples were shipped within one week to the laboratory for processing. Forest floor samples were air-dried, and mineral soils were stored and shipped on ice and then refrigerated (4 ºC) until processing.

1.3.3 Lab methods

Soil processing and C and N analysis

Small amounts of gravel were present in the lower duff layer in the forest floor samples, likely due to mixing with the mineral soil surface over time as the forest floor layer developed after past fires, as a result of annual freeze/thaw cycles, erosion from wind and spring snowmelt, or bioturbation (Fig. 1.2h). I removed any gravel present in the forest floor by hand to the maximum extent possible, and then processed each sample at 22,000 RPM for 60 second cycles in a Waring commercial lab blender (Conair Inc., Stamford, CT, USA) until all the material passed a 2 mm mesh screen. A blender was used rather than a plant mill to avoid damaging mill blades with any residual mineral material present in the forest floor samples that was impossible to remove by hand. I then pulverized a subsample of the blended forest floor in a SPEX 8000D Mixer/Mill (SPEX Sample Prep LLC, Metuchen, NJ, USA) for further analysis. I oven-dried the pulverized forest floor material at 60º C and subsampled for determination of total C, total N, and char content. I sieved the field-moist mineral soil samples (2 mm mesh screen), and subsampled to determine total C, total N, PyC, C_r, inorganic N (NH_4^+ and NO_3^-), and to establish the laboratory incubation to determine C_a, C_s, and soil CO_2 efflux. The subsamples for mineral soil total C, total N, and PyC analysis were oven dried at 105º C to completely remove moisture and pulverized as described above. Subsamples for C_r analysis were oven dried at 60º C. I

measured total C and N in forest floor and mineral soil samples using a Costech dry combustion elemental analyzer (Costech Analytical Technologies Inc., Valencia, CA, USA).

Determination of forest floor char

Throughout this article, I use the term "char" to refer to pyrogenic (charred) material in the forest floor, for which associated C was not determined, whereas I use "PyC" to denote C associated with pyrogenic material in the mineral soil, determined through chemical oxidation. Char concentrations in forest floor samples were predicted from a Fourier transform infrared spectroscopy-based chemometric model developed from a series of laboratory-based standards. Mid-infrared spectra were acquired on dried and finely ground samples on a Bruker Vertex 70 (Bruker Optics, Billerica, MA USA) equipped with a Si-based wide-range beam-splitter and detector with cesium iodide windows. Samples were run neat (i.e., undiluted) using a Pike Autodiff diffuse reflectance accessory (Pike Technologies, Madison, WI). I acquired spectra from 6000-180 cm^{-1} at a 4 cm^{-1} resolution. For each set of samples, a background spectrum was obtained (average of 60 scans) and this was subtracted from the sample reflectance spectra (also an average of 60 scans). A previously validated, partial least squares regression (PLSR) model developed using The Unscrambler X software (CAMO Inc.) was used to predict char concentration. This model was developed using known mixtures of pine needle litter and char produced from pine needles or pine wood at temperatures of 300 and 550° C, so that char concentrations varied from 0 to 100% in 5% increments (J. Miesel, personal communication). A two-factor PLSR model successfully captured this variance in char with 20-fold cross-validation indicating an R^2 of 0.97 with a root mean square error (RMSE) of 5.0%. Two sub-samples from separate low severity plots and one sub-sample from a high severity plot were poorly represented

(i.e., fell outside of 2 s.d.) by the calibration model as determined by Mahalanobis and inlier distance metrics. These three samples were excluded from further analysis.

Determination of mineral soil PyC

I measured mineral soil PyC concentrations using a weak nitric acid digestion technique (Kurth et al. 2006). I digested 0.5 g mineral soil in 10 mL 1 M nitric acid + 20 mL 30% hydrogen peroxide at 100º C in a block digester (SEAL Analytical Inc., United Kingdom). The soil C present after digestion is considered PyC and was measured by elemental analysis as described above.

Determination of mineral soil C pools and CO_2-C efflux

I incubated soils to determine potential soil CO_2-C efflux rates and the size and kinetics of the C_a and C_s pools. I weighed 30 g subsamples of fresh (field-moist), sieved mineral soil into 120 mL specimen cups and adjusted soil moisture to 40% water filled pore space (WFPS). The cups were placed in 1 L glass jars, 5 mL DI water was added to the bottom of each jar to maintain humidity, and the soils were incubated in the dark for 300 days at ambient temperature (22º C). Soil moisture change was determined bi-weekly via change in microcosm mass and was readjusted to 40% WFPS. I measured CO_2 evolution on days 10, 14, 28, 42, 58, and 90 and every 30 days thereafter until day 300. This incubation length is similar to the length recommended by Robertson et al. (1999) for determining mineral soil C pool sizes. At each measurement event, I flushed the air in jars to ambient CO_2 concentrations, then tightly sealed them for 24-48 hours before sampling a 1 mL gas aliquot through septa fitted to the jar lids. I measured CO_2 concentration of the aliquot using a LI-COR LI-820 CO_2 gas analyzer (LI-COR Inc., Lincoln, NE, USA), which was continuously flushed with CO_2-free air. I determined CO_2 concentrations via comparison to a calibration curve constructed using standards of known CO_2 concentration. I

calculated CO_2-C efflux rates as the increase in CO_2-C concentrations in the jars during the time they were sealed. I standardized CO_2-C efflux rates to the total amount of soil C present in each microcosm.

Determination of resistant mineral soil C

I estimated mineral soil C_r concentrations as non-hydrolysable C using a modified version of the acid digestion method described by Paul et al. (1997). Briefly, I slaked 5 g oven-dried soil in 20 mL DI water with eight 4 mm glass beads overnight to disrupt soil aggregates. Undecomposed plant material is resistant to hydrolysis and can bias estimates of C_r (Paul et al. 1997), so I passed the soil solution through a 53 µm sieve to remove plant residues. Thereafter, 0.5 g of the sieved soil was refluxed with 10 mL 6 M hydrochloric acid at 116º C for 2 hours in a Mars 6 microwave digester (CEM Corporation, Matthew, NC, USA). The C present after digestion is considered C_r and was measured by elemental analysis as described above.

Determination of mineral soil inorganic N pools and mineralization rates

I extracted fresh mineral soils for NH_4^+-N and NO_3^--N by shaking 10 g field-moist soils in 50 mL 2 M potassium chloride (KCl) on a shaker table for 1 hour. I then separated the extract from the soil via filtration with Whatman grade 5 (2.5 µm) filter paper (GE Healthcare UK Limited, Little Chalfont, Buckinghamshire, UK). I determined the extract NH_4^+-N concentration spectrophotometrically by reacting the extracts with ammonia salicylate and ammonia cyanurate in a 96-well plate (Sinsabaugh et al. 2000), after which I measured absorbance at 595 nm (BioTek Elx800, BioTek Instruments Inc., Winuski, VT, USA). I determined the concentration of NO_3^--N in the extracts spectrophotometrically by reacting the extracts with vanadium (III), sulfanilamide, and N-(1-naphthyl)-ethylenediamine dihydrochloride in a 96-well plate, after which I measured absorbance at 540 nm (Doane and Horwáth 2003). I converted absorbance

values to concentrations via comparison to standard curves produced using $(NH_4)_2SO_4$ and KNO_3 reference solutions. I calculated total inorganic nitrogen (TIN) as the sum of NH_4^+-N and NO_3^--N. I repeated this procedure after the 300-day lab incubation, and calculated net ammonification, net nitrification, and net N mineralization over the course of the incubation.

1.3.4 Statistical analysis

I used linear mixed models to assess the responses of soil C and N pools to fire severity. All models included fire severity, elevation, slope, and aspect as explanatory variables. I conservatively assumed the azimuth subsamples within each plot were non-independent by including a plot-identifier as a random effect. Models assessing inorganic N concentrations included total N as an additional covariate. Models assessing instantaneous CO_2-C efflux rates during the lab incubation included fixed effects of incubation day, severity, day by severity interactions, and a random day effect. Models assessing cumulative CO_2-C efflux during the lab incubation included a fixed effect of log incubation day, day by severity interactions, and a random day effect. Models assessing the influence of PyC on mineral soil CO_2-C efflux and N transformations included fire severity as a random effect rather than as a fixed effect. For all models, the statistical significance of each explanatory variable was assessed using Type 3 Sums of Squares, and variables that were non-significant at $\alpha = 0.05$ were sequentially removed from models until all remaining explanatory variables were significant or no variables remained. If severity was not significant at $\alpha = 0.05$, but exhibited *p*-values ≤ 0.10, I pooled low, moderate, and high severity treatments into a single burned treatment to determine whether fire had a significant effect on the response variable even if differences in severity did not. For each model, I tested my assumption of non-independence among subplots by comparing Aikake Information Criterion (AIC) values and residual standard errors between models that did or did not include

plot-identifier random effects (Pinheiro and Bates 2000). If the model without the random effect had both a lower AIC value ($\Delta AIC \geq 2$) and improved residual standard errors, I considered subplots independent. When assumptions of normality were not met for a model, I box-cox transformed the response variable using the car package (Fox and Weisberg 2011) in the statistical programming software R (R Core Team 2019) to select an appropriate value for λ. If the 95% confidence interval for λ included 0, the response variable was log transformed. Linear mixed-models were performed in R using the nlme package (Pinheiro et al. 2019). When Type 3 Sums of Squares indicated that fire severity or aspect were significant model parameters, I performed means separations tests using Tukey's adjustment for multiple comparisons using the lsmeans package (Lenth 2016).

I used non-linear regression to fit a three-pool constrained model to CO_2 evolution data resulting from the lab incubation according to the method of Paul et al. (2001) to determine the size and kinetics of mineral soil C_a and C_s pools. Briefly, CO_2 evolution was fit to the following first-order kinetics model:

$$dC/dt = C_a \times k_a e^{(-ka \times day)} + C_s \times k_s e^{(-ks \times day)} + C_r \times k_r^{(-kr \times day)} \quad \text{(eq 1.1)}$$

where C_a is the size of the active C pool, and k_a is its mineralization rate coefficient, C_s is the slow C pool and k_s is its mineralization rate coefficient, and C_r is the size of the resistant C pool and k_r is its mineralization rate coefficient. In this model, C_a, k_a, and k_s are determined via non-linear regression, the C_r pool is determined by acid hydrolysis prior to model fitting, and k_r is based on an assumed MRT of 1000 years. C_s is constrained to be ($C_{soc} - C_r - C_a$), where C_{soc} is total soil organic C content. Mineralization rate constants are also presented as MRT (1/k) for ease of interpretation and are scaled to field values using a Q_{10} value of 2.0 and a MAT of 10.6° C. The respiration rates for soils from one of the unburned plots did not decrease over the 300-

day incubation and were not fit to the model nor included in any subsequent statistical analyses. Non-linear regression was performed with SAS software using PROC NLIN (SAS software, version 9.3, SAS Institute Inc., Cary, NC, USA). Bonferroni adjusted comparisons of resulting parameters (e.g. C_a, k_a) among severity levels were performed using PROC GLIMMIX in SAS.

1.4 RESULTS

1.4.1 Total carbon and nitrogen content

I found significant differences among fire severity levels in forest floor total C content ($p = 0.014$). High severity areas had 82% less forest floor mass and 71% lower forest floor total C content than unburned areas (Table 1.2, Fig. 1.3a). Aspect was the only significant predictor of forest floor C concentrations: plots located on eastern aspects had a mean forest floor C concentration of 47.3% compared to a grand mean of 43.0% for all plots (Table 1.3). Forest floor N contents were 85% smaller in high severity areas than in unburned areas ($p = 0.014$; Fig. 1.3b), whereas there were no differences in forest floor N concentrations. Forest floor C:N ratios varied with fire severity ($p = 0.003$): high severity areas had higher C:N ratios than unburned and moderate severity areas (Table 1.2).

For mineral soil samples, there were no differences in total C or N content (Fig. 1.3), total C or total N concentrations, or C:N ratios among severity levels (Table 1.2). Mineral soil C content increased with elevation at a rate of 0.12 ± 0.05 g C m^{-2} per 100 m increase in elevation on the log response scale ($p = 0.038$; Table 1.3), and mineral soil N content increased with elevation at a rate of 0.11 ± 0.03 g N m^{-2} per 100 m increase in elevation on the log response scale ($p = 0.003$).

Table 1.2 Forest floor mass, carbon concentrations, nitrogen concentrations, C:N ratios, char mass fraction, and total char mass; and mineral soil (0-5 cm) carbon concentrations, nitrogen concentrations, C:N ratios, pyrogenic carbon mass fraction, and total pyrogenic carbon mass among fire severity levels. Values are means ± SE. Lowercase letters within rows indicate significant differences among fire severity levels at $\alpha = 0.05$.

	Unburned (N = 4)	Low (N = 5)	Moderate (N = 4)	High (N = 4)
Forest Floor				
Mass (kg m^{-2})	4.57 ± 1.46 a	1.63 ± 0.33 ab	1.71 ± 0.58 ab	0.80 ± 0.41 b
C Concentration (%)	42.39 ± 1.28 a	39.98 ± 2.25 a	41.71 ± 3.87 a	48.85 ± 1.40 a
N Concentration (%)	0.80 ± 0.09 a	0.73 ± 0.03 a	0.86 ± 0.08 a	0.63 ± 0.07 a
C:N	60.77 ± 4.88 b	64.27 ± 1.54 ab	54.70 ± 5.50 b	90.52 ± 8.52 a
Char Mass Fraction (mg g^{-1})	180.72 ± 26.64 ab	294.44 ± 53.15 a	273.13 ± 75.42 a	160.75 ± 6.56 b
Total Char Mass (g m^{-2})	739.51 ± 246.82 a	580.24 ± 200.91 a	621.02 ± 356.27 a	120.55 ± 63.42 a
Mineral Soil (0-5 cm)				
C Concentration (%)	4.98 ± 0.48 a	4.69 ± 0.22 a	5.02 ± 0.29 a	6.33 ± 0.46 a
N Concentration (%)	0.20 ± 0.02 a	0.20 ± 0.12 a	0.20 ± 0.03 a	0.26 ± 0.02 a
C:N	28.92 ± 4.00 a	27.73 ± 2.10 a	28.45 ± 1.62 a	28.63 ± 1.53 a
PyC Mass Fraction (mg g^{-1})	10.56 ± 1.88 a	8.42 ± 2.56 a	10.50 ± 2.04 a	11.70 ± 2.68 a
Total PyC Mass (g m^{-2})	310.79 ± 56.54 a	201.83 ± 45.44 a	358.83 ± 80.15 a	299.23 ± 57.8 a

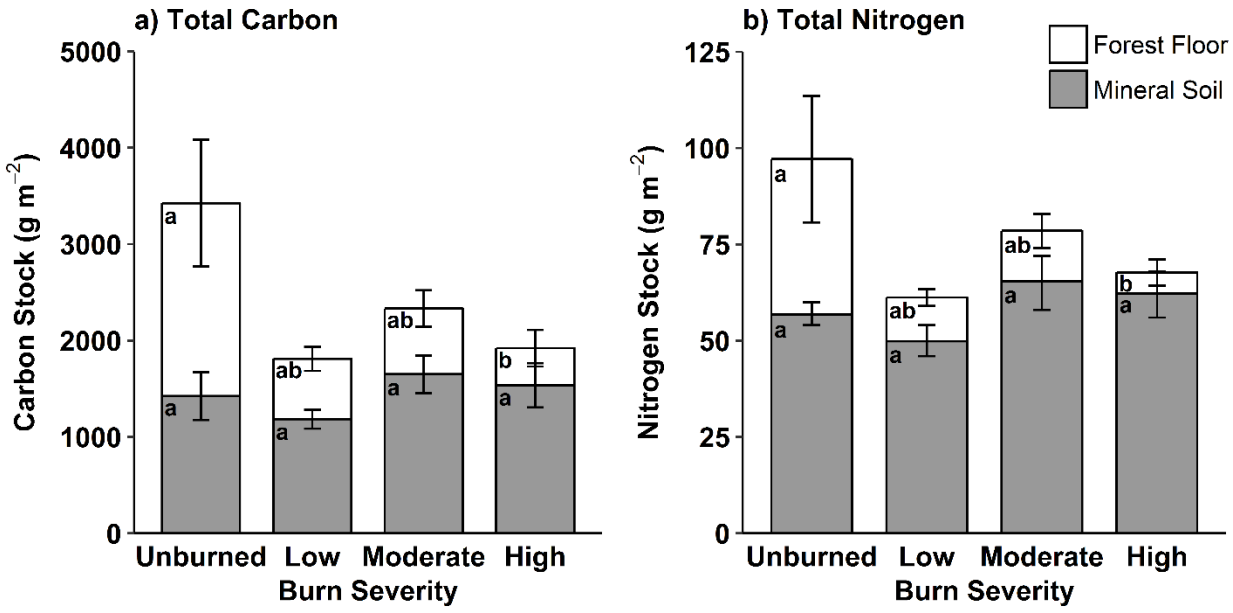

Figure 1.3 Mean (± SE) carbon (a) and nitrogen (b) stocks in forest floor and 0-5 cm mineral soil for each severity level three years after the 2012 Chips wildfire burned mixed-conifer forest in northern California. Stocks are presented as mass per unit area. Lowercase letters indicate significant differences among fire severity levels at $\alpha = 0.05$.

1.4.2 Carbon and nitrogen pools

Pyrogenic carbon in forest floor and mineral soil

Low and moderate severity areas had higher mass fraction of char in the forest floor than high severity areas ($p = 0.008$; Table 1.2), but there were no differences in total content of forest floor char among severity levels (Table 1.2). Forest floor char mass fraction decreased by 5.1 ± 2.2 mg g^{-1} for every percent increase in slope ($p = 0.038$; Table 1.3). There were no differences in mineral soil PyC mass fraction or total PyC content among severity levels (Table 1.2), but there was a significant effect of aspect on PyC mass fraction ($p = 0.005$; Table 1.3). Eastern aspects had higher PyC mass fractions (1.19 ± 0.15 mg g^{-1}) than western aspects (0.64 ± 0.09 mg g^{-1}). Mineral soil total PyC content increased with elevation at a rate of 0.16 ± 0.08 g m^{-2} per 100 m increase in elevation on the log response scale.

Table 1.3 Model parameters for models for which a topographic explanatory variable was statistically significant. Prior to log transformation, elevation parameter estimates are change in response variable ± SE per 100 m increase in elevation. Aspect parameter estimates are untransformed means. Lowercase letters for aspect parameter estimates represent significant differences at $\alpha = 0.05$.

	Parameter	Estimate	*F*	*p*
Forest Floor				
C Concentration (%)	Aspect: North	42.80 ± 4.64 ab	-	-
	Aspect: East	47.26 ± 0.99 a	-	-
	Aspect: South	41.08 ± 2.12 ab	-	-
	Aspect: West	38.74 ± 1.80 b	-	-
Char Mass Fraction (mg g^{-1})	Severity	See main text		
	Slope (%)	-5.12 ± 2.20	5.43	0.038
Mineral Soil (0-5 cm)				
Total C Content (g m^{-2})*	Intercept	6.92 ± 0.13	2833.23	< 0.001
	Elevation (100 m)	0.12 ± 0.05	5.30	0.038
Total N Content (g m^{-2})*	Intercept	3.77 ± 0.08	2347.67	< 0.001
	Elevation (100 m)	0.11 ± 0.03	12.87	0.003
PyC Mass Fraction (mg g^{-1})†	Aspect: North	0.71 ± 0.15 ab	-	-
	Aspect: East	1.19 ± 0.23 a	-	-
	Aspect: South	1.26 ± 0.32 ab	-	-
	Aspect: West	0.64 ± 0.09 b	-	-
Total PyC Content (g m^{-2})*	Intercept	5.09 ± 0.19	3693.09	< 0.001
	Elevation (100 m)	0.16 ± 0.08	4.40	0.042
NO_3^- Concentration (µg g^{-1})	Intercept	-1.10 ± 0.77	2.04	0.162
	Elevation (100 m)	0.87 ± 0.30	8.50	0.011

*Response log transformed; parameter estimates on log scale
†Response box-cox transformed; parameter estimates on original scale

Mineral soil C pools and CO_2-C efflux

Non-linear regression indicated that there were differences in the sizes and kinetics of soil C pools among fire severity levels (Fig. 1.4a; Table 1.4). High severity areas had significantly larger C_a pools than low and moderate severity areas when estimated on a soil mass fraction basis (Table 1.4), and when estimated as a proportion of C_{soc}, C_a pools were smaller in burned areas than unburned areas (Table 1.4). My statistical models indicated that the size of the C_s pools varied with severity when estimated on a soil mass fraction basis ($p = 0.011$), but mean comparisons indicated that differences between severity levels were not significant, despite high severity areas exhibiting C_s pools that were 64% larger than those in unburned areas ($p = 0.078$;

Table 1.4). There were no differences in C_r pools among severity levels. The mineralization rate coefficient (k_a) associated with the C_a pool did not vary significantly with severity, but high severity areas had the smallest k_s (corresponding to a longer MRT_s), and low severity areas had a smaller k_s than unburned areas (Table 1.4).

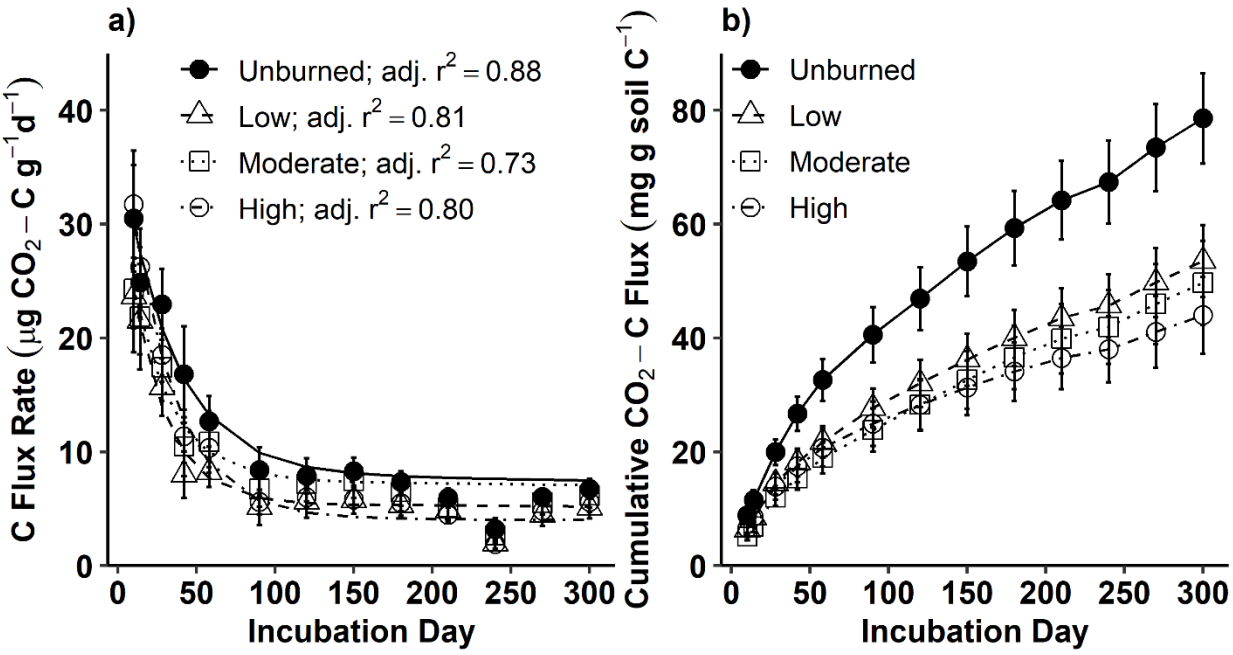

Figure 1.4 Mean (± SE) CO_2-C efflux rate (points) over a 300-day laboratory incubation of mineral soils (0-5 cm) fit with 3-pool carbon models (lines) using non-linear regression (a) and mean (± SE) cumulative CO_2-C efflux over the incubation period(b). Soils were collected from contrasting levels of fire severity three years after the Chips wildfire, which burned California mixed-conifer forest in 2012. CO_2-C efflux rateis presented as carbon respired per unit dry soil mass per day, and cumulative CO_2-C efflux is carbon respired per unit soil carbon.

Table 1.4 Size of active (C_a), slow (C_s), and resistant (C_r) soil carbon pools, their sizes proportional to total soil organic carbon (C_a:C_{soc}, C_s:C_{soc}, C_r:C_{soc}), and corresponding decomposition rate constants (k_x) and mean residence times (MRT_x; $1/k_x$) for 0-5 cm mineral soil for each wildfire severity. C_a, C_s, and C_r are expressed on a dry soil mass basis, k_a and MRT_a are expressed as days, and k_s, k_r, MRT_s are expressed as years. C_a, k_a, and k_s were determined via non-linear regression of CO_2 evolution data from a 300 day lab incubation, C_r was determined via acid hydrolysis, and C_s is assumed to be the difference between total soil organic carbon and C_a + C_r. Lab-based values of MRT were scaled to field conditions using a Q_{10} correction of 2.0. Values are means ± SE. Lowercase letters within rows represent significant differences among severity levels at $\alpha = 0.05$.

	Unburned (N = 3)	Low (N = 5)	Moderate (N = 4)	High (N = 4)
C_a (g kg^{-1})	0.99 ± 0.15 ab	0.67 ± 0.08 b	0.64 ± 0.08 b	1.08 ± 0.11 a
C_s (g kg^{-1})	28.89 ± 3.49 b*	35.81 ± 5.22 ab	36.40 ± 6.18 ab	46.96 ± 5.14 a*
C_r (g kg^{-1})	10.79 ± 0.68 a	11.59 ± 1.23 a	15.05 ± 1.65 a	15.30 ± 1.21 a
C_a:C_{soc} (%)	2.68 ± 0.33 a	1.58 ± 0.16 b	1.39 ± 0.25 b	1.68 ± 0.19 b
C_s:C_{soc} (%)	69.90 ± 2.01 a	73.91 ± 0.97 a	68.95 ± 1.83 a	73.80 ± 1.52 a
C_r:C_{soc} (%)	27.42 ± 1.98 a	24.51 ± 0.90 a	29.66 ± 1.80 a	24.52 ± 1.50 a
k_a (d^{-1})	0.030 ± 0.006 a	0.044 ± 0.009 a	0.040 ± 0.010 a	0.035 ± 0.005 a
k_s (y^{-1})	0.102 ± 0.011 a	0.055 ± 0.006 b	0.074 ± 0.007 ab	0.031 ± 0.005 c
k_r(y^{-1})	0.0025[a]	0.0025[a]	0.0025[a]	0.0025[a]
Lab MRT				
MRT_a (d)	33.40 ± 6.90 a	22.81 ± 4.56 a	24.94 ± 6.18 a	28.43 ± 4.16 a
MRT_s (y)	9.82 ± 1.06 c	18.26 ± 1.95 b	13.43 ± 1.25 bc	31.86 ± 5.19 a
Field MRT				
MRT_a (d)	84.55 ± 17.46 a	57.73 ± 11.54 a	63.15 ± 15.65 a	71.96 ± 10.54 a
MRT_s (y)	24.86 ± 2.67 c	46.24 ± 4.93 b	34.00 ± 3.17 bc	80.65 ± 13.13 a

[a]Based on an assumed MRT of 1000 years and constrained in non-linear regression model.
*p = 0.071

I fit a non-linear regression to all the plots within each severity level, obtaining a single estimate for each C pool and associated kinetics at each severity level (Fig. 1.4a, Table 1.4). I were thus unable to estimate the influence of topographic variables on these parameters, except for the C_r pool, which was measured separately using acid hydrolysis. However, I calculated instantaneous CO_2-C efflux rates (Fig. 1.4a) and cumulative CO_2-C efflux (Fig. 1.4b) over the duration of the incubation and determined the influence of severity and topography on these parameters. For instantaneous efflux rates, there were significant effects of incubation day (p < 0.001), severity (p < 0.001), severity by day interaction (p = 0.001), and hillslope (p = 0.004). For cumulative CO_2-C flux, there were significant effects of incubation day (p < 0.001), severity (p = 0.032), severity by day interaction (p < 0.001), and aspect (p = 0.008). The significant

severity by day interaction indicates the need to examine severity-based differences on each measurement day. When analyzing CO_2-C efflux over time, analyses based on instantaneous efflux rates are more statistically valid than those based on cumulative C flux (Hess and Schmidt 1995), so I limit my reporting of differences in cumulative C flux to those present only on the final incubation day (i.e., day 300), in contrast to a more detailed reporting of differences in instantaneous CO_2-C efflux rates (Table 1.5).

Table 1.5 Table of *F* and *p*-values for determining statistically significant differences in instantaneous CO_2-C efflux rates during a lab incubation of mineral soils (0-5 cm) collected three years after the 2012 Chips Fire in Sierra Nevada mixed-conifer forest.

			Severity			
Incubation day	*F*	*p*	Unburned (N = 3)	Low (N = 5)	Moderate (N = 4)	High (N = 4)
10	2.07	0.118	--	--	--	--
14	1.18	0.328	--	--	--	--
28	7.22	<0.001	a	b	b	b
42	4.26	0.010	a	b	b	b
58	2.27	0.095	--	--	--	--
90	2.68	0.060	--	--	--	--
120	3.62	0.021	a	ab	ab	b
150	5.64	0.003	a	b	b	b
180	4.53	0.008	a	b	ab	b
210	3.18	0.034	a	ab	ab	b
240	2.83	0.050	a	ab	ab	b
270	3.86	0.016	a*	ab	b*	b
300	4.22	0.011	a*	ab	b*	b

* $p < 0.10$.

On incubation days 28, 42, and 150, soils from unburned areas exhibited higher CO_2-C efflux rates than burned soils from all severity levels (Table 1.5, Fig. 1.4a). Carbon efflux rates for unburned soils were significantly greater than low and high severity soils on day 180 and were greater than soils from high severity areas on day 120, and from day 210 until the end of the incubation. At the conclusion of the incubation, cumulative CO_2-C efflux for unburned soils was significantly greater than for soils from low and moderate severity areas (Fig. 1.4b). Despite exhibiting the lowest overall mean cumulative CO_2 –C efflux, soils from high severity areas were not significantly different from any other areas.

Mineral soil inorganic N pools

There were significant differences among severity levels in mineral soil TIN and NH_4^+-N concentrations in fresh, pre-incubated (i.e., incubation day 0) mineral soils (p = 0.003 and p = 0.009, respectively; Fig. 1.5). There was a general trend of greater TIN and NH_4^+-N concentrations at higher severity, although there were no differences between low severity areas and unburned or moderate severity areas, and high and moderate severity soils were not significantly different from one another (Fig. 1.5a and 1.5c). Mineral soil total N concentration was a significant covariate explaining TIN; TIN increased by 4.3 ± 1.8 μg g^{-1} for every percent increase in total N concentration (p = 0.020). There were no significant differences in NO_3^--N concentrations among severity levels for day 0 soils (Fig. 1.5c), but NO_3^--N concentrations increased with elevation at a rate of 0.87 μg g^{-1} 100 m^{-1}. After the 300-day lab incubation, there were no longer differences in NH_4^+-N, NO_3^--N, or TIN concentrations (Fig. 1.5b and 1.5c). There were no differences in net ammonification, net nitrification, or net N mineralization rates among severity levels over the course of the incubation (Fig. 1.6).

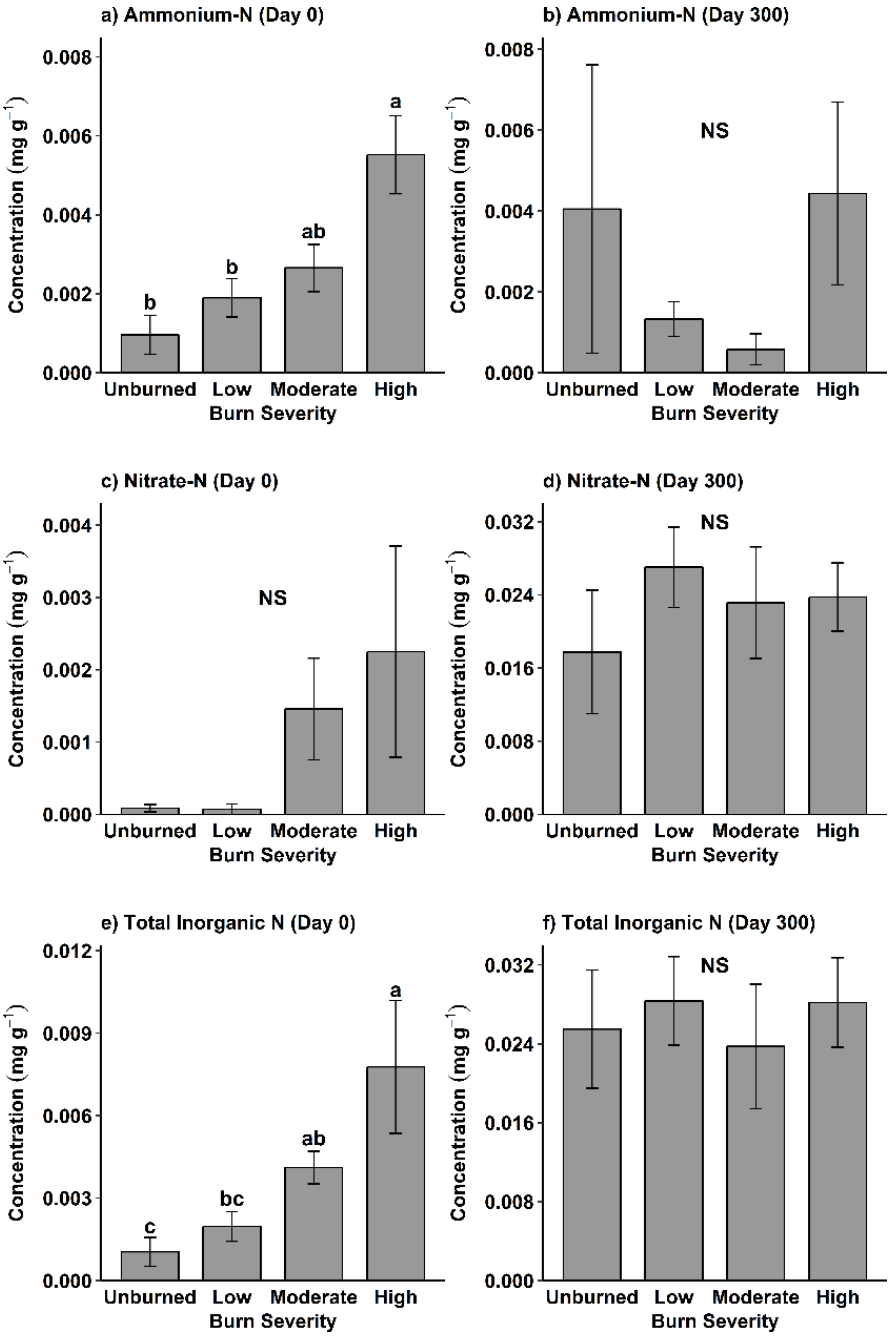

Figure 1.5 Concentration of ammonium nitrogen (a), nitrate nitrogen (c), and total inorganic nitrogen (e) in fresh mineral soils (0-5 cm), and concentration of ammonium nitrogen (b), nitrate nitrogen (d), and total inorganic nitrogen (f) after a 300 day lab incubation. Soils were collected from contrasting levels of fire severity three years after the Chips wildfire, which burned northern California mixed-conifer forest in 2012. Means (± SE) for each severity level are displayed. Concentrations are presented on a dry soil mass basis. Lowercase letters indicate significant differences among severity levels at $\alpha = 0.05$. NS indicates there were no significant differences among severity levels.

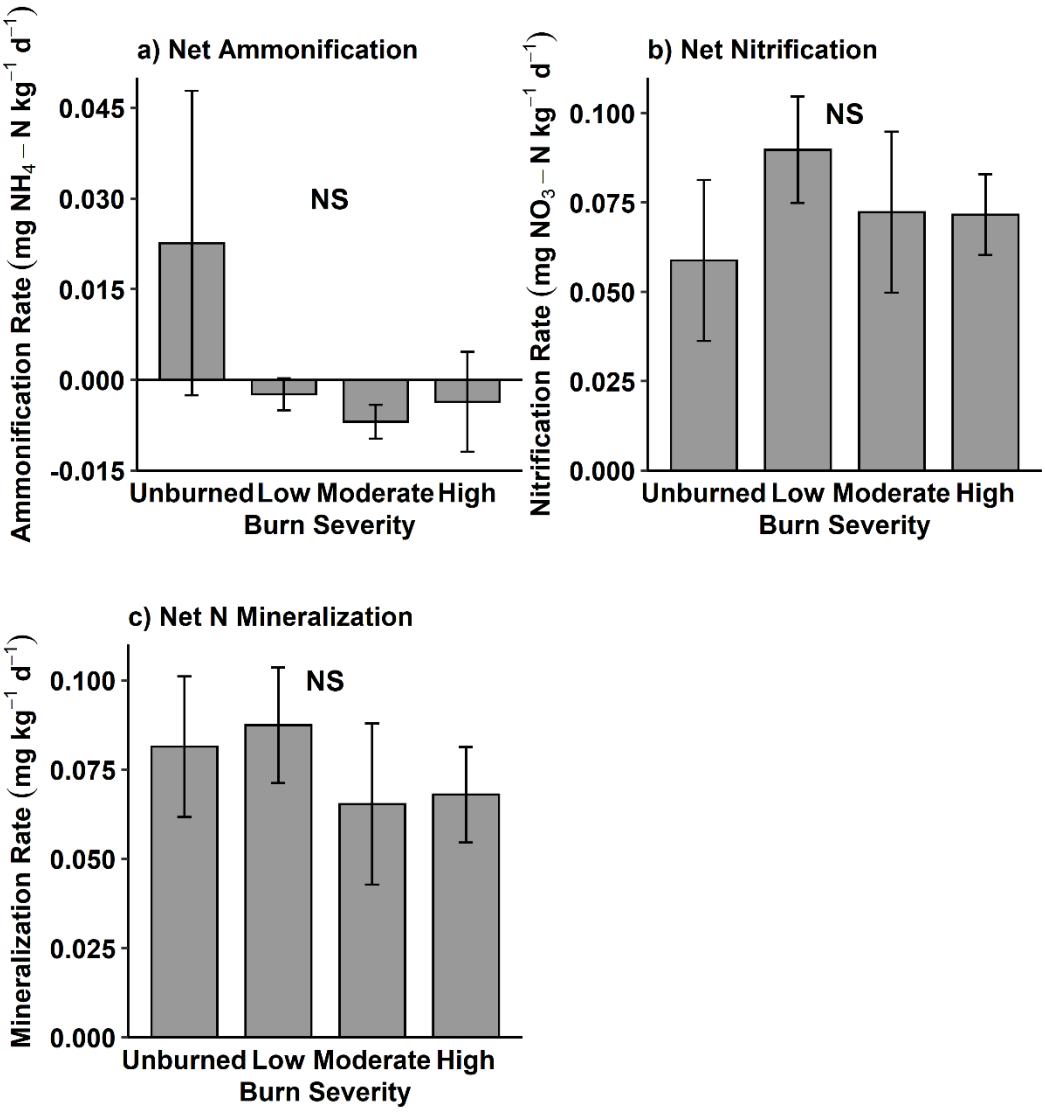

Figure 1.6 Mean (± SE) net ammonification (a), net nitrification (b), and net nitrogen mineralization (c) for mineral soil (0-5 cm) for each severity level over the course of a 300 day lab incubation. Soil were collected three years after the 2012 Chips wildfire burned mixed-conifer forest in northern California mixed-conifer forest. NS indicates there were no significant differences among severity levels.

1.4.3 Influence of pyrogenic carbon on mineral soil carbon and nitrogen pools and fluxes

There was a significant positive correlation between PyC mass fraction and C_r mass fraction ($p < 0.001$, Pearson's $r = 0.64$). The PyC pool was 58% of the size of the C_r pools on average. There was no relationship between either PyC mass fraction or total PyC mass and

inorganic N concentrations, C efflux, net ammonification, net nitrification, or net N mineralization rates over the course of the lab incubation (data not shown).

1.5 DISCUSSION

1.5.1 Soil carbon and nitrogen content

The smaller forest floor total C and N contents in high severity areas can be attributed to differences in forest floor mass, because C and N concentrations did not significantly vary among severity levels. The loss of forest floor may have long-term impacts on soil C and N cycling because the litter layer is a source of C and N inputs to mineral soil (Heckman et al. 2013), and less forest floor insulation may result in higher temperatures and lower moisture content in mineral soils (Kasischke and Johnstone 2005), thereby influencing soil microbial activity. Higher soil temperatures will have a tendency to increase microbial activity, whereas moisture limitation will decrease microbial activity (Chapin et al. 2011). This may result in bursts of microbial activity following precipitation events that are more intense but shorter in duration in areas that experienced high severity fire compared to lower severity and unburned areas. California's mixed-conifer forests may be especially sensitive to the effects of temperature and moisture, because they are seasonally dry and prone to frequent drought. Changes to soil temperature and moisture may affect the amount of C retained in microbial biomass versus lost to respiration (i.e., carbon use efficiency). Carbon use efficiency declines with increasing temperature due to greater respiratory costs and heat stress (Manzoni et al. 2012) and declines with increasing soil moisture variability due to physiological and osmotic stress (Tiemann and Billings 2011). Loss of the litter layer may also alter the soil microbial community structure. Forest litter is preferentially colonized by fungi (Chapin et al. 2011), and loss of the litter layer

may shift the microbial community towards bacterial dominance, thereby altering decomposition pathways.

1.5.2 Pyrogenic carbon pools

The lower char mass fraction in high severity areas compared to low and moderate severity areas may have resulted from greater forest floor combustion efficiency, or from increased inputs of killed but uncharred biomass in the years following the fire. Despite the lower char mass fraction in high severity areas, there were no differences in total forest floor char content. This is likely due to decreased forest floor mass in high severity areas offsetting the greater char mass fraction. I did not directly measure PyC concentration of forest floor char, but C concentrations are generally greater for charred material than for uncharred biomass (Czimczik et al. 2002; Maestrini and Miesel 2017). The magnitude of C enrichment in char depends on source material and pyrolysis temperature; for example, C concentrations range from approximately 60% for charred pine needles pyrolyzed at 300º C to more than 90% for charred pine wood pyrolyzed at 550º C (Maestrini and Miesel 2017). The digestion-resistant C fraction (i.e. PyC) ranges from approximately 10% for pine needles charred at 300º C to approximately 90% for pine wood charred at 550º C. Using these values as constraints, this would translate to forest floor char-C contents ranging from 73 to 109 g char-C m^{-2} (12 to 109 g PyC m^{-2}) for high severity areas and contents ranging from 444 to 666 g char-C m^{-2} (44 to 599 g PyC m^{-2}) for the unburned areas. The greater mass fraction of char in forest floor from low and moderate severity areas may eventually lead to changes in C pool structure and dynamics as the char becomes incorporated into the mineral soil. An experiment in a beech-dominated temperate forest indicated that the MRT of charred biomass in soil is one to two orders of magnitude longer than unburnt biomass; the same experiment indicated that PyC can promote the formation of SOM-

stabilizing aggregates (Singh et al. 2014). Furthermore, a meta-analysis by Maestrini et al., (2015) indicated that upon incorporation into mineral soil, PyC induces a positive priming effect to the native soil C over short time periods (20-200 days), but results in an overall negative priming effect over the long term (> 200 days). Longer MRTs, promotion of aggregate formation, and a negative priming effect should all serve to increase the size and MRTs of the C_s and C_r pools as charred biomass becomes incorporated into the mineral soil.

1.5.3 Mineral soil carbon pools and CO_2-C efflux

Wildfires release stored C immediately through combustion, but can also cause delayed C losses as fire-killed plant biomass decomposes, thereby transforming forests from C sinks to C sources until losses are offset by C accumulation during forest regeneration (Kashian et al. 2006). Using a Differenced Normalized Burn Ratio (dNBR) severity classification, Meigs et al., (2009) determined that the amount of time required for forest stands to transition from C source to sink is shorter for stands that experienced low or moderate severity fire than high severity fire, where net primary production is lower due to greater plant mortality. The structure and dynamics of mineral soil C pools govern the amount of C lost via respiration versus the amount retained in the mineral soil (Post and Kwon 2000; Six and Jastrow 2002). Soil C pools thus determine the magnitude of overall C losses following wildfires and the time required to transition forests back to C sinks. The low soil CO_2-C efflux rates I observed in soils from high severity areas indicate that these stands are experiencing similar C losses to low and moderate severity stands, three years after fire. I also found that the MRT for the C_s pool increased following wildfire, a trend that was most pronounced among high severity areas, suggesting that soil C stability is greater in soils from high severity areas than other burned and unburned areas. The C_s pool accounts for more than 70% of soil C in high severity areas, indicating that CO_2-C efflux is likely to remain

low in these soils until more labile C is incorporated into the C_s pool. The greater C stability and corresponding lower CO_2-C efflux in high severity soils suggests that the strength of the C source is not enhanced by soil respiration in these stands, and supports Meigs et al., (2009) finding that the sink-source relationship in recovering forests is driven by plant production rather than soil respiration. There was no relationship between PyC and CO_2-C efflux, but the absence of differences in mineral soil PyC pools among burned and unburned areas suggests that PyC had not been incorporated into the mineral soil three years after the wildfire. Previous research in sites impacted by the Chips fire has indicated that high severity areas contain a greater proportion of PyC in aboveground C pools than low-to-moderate severity areas (Maestrini et al. 2017), but lateral transport of PyC due to erosion may exceed the rates of vertical mixing following wildfires in the region (Abney et al. 2017), perhaps accounting for the lack of differences in soil PyC pools among severity levels.

Of the three C pools addressed in this study, C_a is most accessible for microbial processing (Bremer et al. 1994; Six and Jastrow 2002), and thus strongly influences soil biological activity and site fertility (Mandal et al. 2008). The C_a pool is sensitive to environmental change and is an early indicator of the impact of changing environmental conditions on soil C dynamics (Bremer et al. 1994). Large C_a pools are indicative of labile (i.e., easily decomposable) C inputs from plant residues and root exudates (Paul et al. 1999; Collins et al. 2000; Hoosbeek et al. 2006). According to the severity classification system I used, high severity wildfire results in 75-100% basal area mortality (Miller et al. 2009a), yet I found that high severity areas had proportionally similarly sized C_a pools compared to soils from low and moderate severity areas, and larger C_a pools than low and moderate severity areas when estimated on a soil mass fraction basis. The larger C_a pools in high severity areas relative to low

and moderate areas could result from greater incorporation of root necromass into mineral soils in these areas. Tree root survival is low following high severity fire in mixed-conifer forests (Meigs et al. 2009), stimulating root decomposition (Campbell et al. 2016), and perhaps providing a sustained source of belowground C_a inputs. Root decomposition could also account for the tendency for C_s pool size to increase with severity and for the longer MRT_s in the burned plots. Root-derived C has been shown to account for a greater proportion of soil C and have longer MRT values than C derived from aboveground biomass (Rasse et al. 2005). In fact, my field-scaled MRT_s values are similar to the estimated MRT for *Pseuodotsuga menziesii* coarse root necromass of approximately 50 years (Janisch et al. 2005).

Another possible explanation for the larger C_a pools in high severity plots is the potential for fast-growing, early successional plant species to incorporate labile C and N into the soil, a possibility that is supported by the greater TIN and NH_4^+-N concentrations in the high severity plots. Nitrogen-fixing shrubs are often early colonizers following wildfires in mixed-conifer forests (Conard et al. 1985), and high severity patches create canopy openings that favor shrub establishment (Meigs et al. 2009; Knapp et al. 2012; Collins and Roller 2013). In fact, I observed a greater proportion of *Ceanothus cordulatus*, an early successional N-fixing shrub, in high severity areas than other areas (personal observation; Knapp et al. 2012).

My results are novel because they are the first to describe the structure and dynamics of mineral soil C pools—properties that determine the status of soils as C sources or sinks—among contrasting levels of fire severity. Fernández et al. (1999) described two mineral soil C pools following wildfire in Galician pine forest, but they did not account for fire severity nor differentiate between the slow and resistant C pools. Nevertheless, my finding of greater MRT for the C_s pool agrees with the observation of Fernández et al. (1999) of decreased mineralization

rates in a recalcitrant C pool. My findings of a larger C_a pool in high severity areas than in low and moderate severity areas three years after wildfire contrasts with Fernández et al. (1999) finding decreases in the size of the labile C pool during a two-year post-fire monitoring period. I also found no differences in the MRT of the C_a pool among severity levels, whereas Fernández et al. (1999) found decreases in the mineralization of the labile C pool that persisted for at least two years. These contrasting results highlight the need for additional studies assessing the mineralization kinetics and distribution of soil C among different pools following wildifres across contrasting ecoystem types and on short and long timescales.

1.5.4 Inorganic nitrogen pools

Fires have been known to create a pulse of inorganic N to the soil (DeBano et al. 1979), because NH_4^+ is a product of forest floor pyrolysis (Covington and Sackett 1992). However, the resulting spike in NH_4^+-N generally dissipates after about a year as NH_4^+ is transformed to NO_3^- (Wan et al. 2001). My observations of a persistent six-fold increase in both NH_4^+-N and TIN in high severity soils relative to unburned soils three years after fire suggests either that high severity fires directly induce a more persistent increase in NH_4^+-N than low and moderate severity fires, or that indirect, post-fire effects drive soil inorganic N pools. For example, elevated TIN could have resulted from increased N inputs from colonization by N-fixing plants (e.g., from the *C. cordulatus* plants I observed; Oakley et al. 2003), decreased N uptake by plants due to greater plant mortality in areas of higher severity (Grogan et al. 2000; Ficken and Wright 2017), continuous root decomposition, or differences in the activity rates of soil microbial communities (Smithwick et al. 2005). If the loss of forest floor resulted in drier soils in high severity areas, the elevated NH_4^+-N could also be the result of decreased nitrification rates (Turner et al. 2007). A sustained increase in TIN may support forest regeneration after severe

wildfires because N is a limiting nutrient in coniferous forests (Vitousek and Howarth 1991). Furthermore, fertilization experiments suggest that increased TIN may strengthen the soil C sink by increasing SOM formation (Bradford et al. 2008) and by decreasing soil C respiration, effects postulated to result from microbial groups switching energy sources from N-containing recalcitrant C sources to N-poor but more labile C substrates that can be metabolized more efficiently (Janssens et al. 2010). However, elevated TIN may also have undesirable effects on the ecosystem if lower N-uptake by plants in high severity areas leads to increased leaching of NO_3^- from soil, resulting in contamination of streams and groundwater (Vitousek et al. 1979). After my 300-day lab incubation, there were no longer any differences in NH_4^+-N or TIN concentrations, nor were there differences in ammonification, nitrification, or N mineralization rates, suggesting that site characteristics are the dominant drivers of differences in inorganic N pools. However, my lab incubation did not include living plant biomass, therefore I could not account for the effects of plant N uptake on soil N mineralization, or competition between plants and microbes for inorganic N. Because I measured initial and day 300 inorganic N concentrations, my calculations of net mineralization that occurred represent a relatively coarse time scale, and therefore did not capture any patterns of short term mineralization that may have differed among severity levels

1.6 CONCLUSIONS

My study found that wildfire severity influences soil C and N pool structure and dynamics. I found that less soil C is stored in areas of high fire severity, but that C may be more stable as evidenced by longer MRT_s. The large C_a pools and TIN concentrations indicate soils in high severity areas maintain the nutrient cycling processes necessary to support forest regeneration, and low CO_2-C efflux rates and long MRT of the C_s pool indicate future soil C

losses will be low. This suggests that the recovery of forest C will likely be constrained by vegetation regeneration rather than soil C cycling processes. If fires in mixed-conifer forests continue to occur with increasingly high-severity effects, these forests may not completely reaccumulate C stored in aboveground and belowground pools. Further research is needed to determine whether greater soil sink strength in high severity areas will offset lower aboveground production under future severity scenarios. Determining the mechanisms responsible for greater soil C stability in high severity areas (e.g. PyC inputs, shrub colonization, root decomposition, etc.) will aid in managing forests for C sequestration. Whether high severity fire consistently leads to larger and/or more persistent increases in TIN than low and moderate severity fire and the role of TIN in driving forest recovery also warrants further investigation.

REFERENCES

REFERENCES

Abney RB, Sanderman J, Johnson D, et al (2017) Post-wildfire erosion in mountainous terrain leads to rapid and major redistribution of soil organic carbon. Front Earth Sci 5:1–16. doi: 10.3389/feart.2017.00099

Alcañiz M, Outeiro L, Francos M, Úbeda X (2018) Effects of prescribed fires on soil properties: A review. Sci Total Environ 613–614:944–957. doi: 10.1016/j.scitotenv.2017.09.144

Bird MI, Wynn JG, Saiz G, et al (2015) The pyrogenic carbon cycle. Annu Rev Earth Planet Sci 43:273–298. doi: 10.1146/annurev-earth-060614-105038

Birdsey R, Pregitzer K, Lucier A (2006) Forest carbon management in the United States. J Environ Qual 35:1461. doi: 10.2134/jeq2005.0162

Bowman DMJS, Balch JK, Artaxo P, et al (2009) Fire in the earth system. Science 324:481–484. doi: 10.1126/science.1163886

Bradford MA, Fierer N, Reynolds JF (2008) Soil carbon stocks in experimental mesocosms are dependent on the rate of labile carbon, nitrogen and phosphorus inputs to soils. Funct Ecol 22:964–974. doi: 10.1111/j.1365-2435.2008.01404.x

Bremer E, Janzen HH, Johnston AM (1994) Sensitivity of total, light fraction and mineralizable organic matter to management practices in a Lethbridge soil. Can J Soil Sci 74:131–138. doi: 10.4141/cjss94-020

Campbell J, Donato D, Azuma D, Law B (2007) Pyrogenic carbon emission from a large wildfire in Oregon, United States. J Geophys Res Biogeosciences. doi: 10.1029/2007JG000451

Campbell JL, Fontaine JB, Donato DC (2016) Carbon emissions from decomposition of fire-killed trees following a large wildfire in Oregon, United States. J Geophys Res Biogeosciences 121:718–730. doi: 10.1002/2015JG003165

Chapin FS, Matson PA, Vitousek PM (2011) Principles of Terrestrial Ecosystem Ecology. Springer New York, New York, NY

Chen G, Hayes DJ, David McGuire A (2017) Contributions of wildland fire to terrestrial ecosystem carbon dynamics in North America from 1990 to 2012. Global Biogeochem Cycles 31:878–900. doi: 10.1002/2016GB005548

Christensen NL (1973) Fire and the nitrogen cycle in california chaparral. Science 181:66–68. doi: 10.1126/science.181.4094.66

Collins BM, Roller GB (2013) Early forest dynamics in stand-replacing fire patches in the northern Sierra Nevada, California, USA. Landsc Ecol 28:1801–1813. doi: 10.1007/s10980-013-9923-8

Collins HP, Elliott ET, Paustian K, et al (2000) Soil carbon pools and fluxes in long-term Corn Belt agroecosystems. Soil Biol Biochem 32:157–168. doi: 10.1016/S0038-0717(99)00136-4

Conard SG, Jaramillo AE, Cromack K, Rose S (1985) The role of the genus *Ceanothus* in western forest ecosystems. Portland, OR

Covington W, Sackett S (1992) Soil mineral nitrogen changes following prescribed burning in ponderosa pine. For Ecol Manage 54:175–191. doi: 10.1016/0378-1127(92)90011-W

Czimczik CI, Preston CM, Schmidt MWI, et al (2002) Effects of charring on mass, organic carbon, and stable carbon isotope composition of wood. Org Geochem 33:1207–1223. doi: 10.1016/S0146-6380(02)00137-7

Czimczik CI, Preston CM, Schmidt MWI, Schulze E-D (2003) How surface fire in Siberian scots pine forests affects soil organic carbon in the forest floor: Stocks, molecular structure, and conversion to black carbon (charcoal). Global Biogeochem Cycles. doi: 10.1029/2002GB001956

DeBano LF, Eberlein GE, Dunn PH (1979) Effects of burning on chaparral soils: I. soil nitrogen. Soil Sci Soc Am J 43:504–509. doi: 10.2136/sssaj1979.03615995004300030015x

Doane TA, Horwáth WR (2003) Spectrophotometric determination of nitrate with a single reagent. Anal Lett 36:2713–2722. doi: 10.1081/AL-120024647

Dombeck MP, Williams JE, Wood CA (2004) Wildfire policy and public lands: Integrating scientific understanding with social concerns across landscapes. Conserv Biol 18:883–889. doi: 10.1111/j.1523-1739.2004.00491.x

Earles JM, North MP, Hurteau MD (2014) Wildfire and drought dynamics destabilize carbon stores of fire-suppressed forests. Ecol Appl 24:732–740. doi: 10.1890/13-1860.1

Eidenshink JC, Schwind B, Brewer K, et al (2007) A project for monitoring trends in burn severity. Fire Ecol 3:3–21.

Fernández I, Cabaneiro A, Carballas T (1999) Carbon mineralization dynamics in soils after wildfires in two Galician forests. Soil Biol Biochem 31:1853–1865. doi: 10.1016/S0038-

0717(99)00116-9

Ficken CD, Wright JP (2017) Contributions of microbial activity and ash deposition to post-fire nitrogen availability in a pine savanna. Biogeosciences 14:241–255. doi: 10.5194/bg-14-241-2017

Flannigan MD, Cantin AS, de Groot WJ, et al (2013) Global wildland fire season severity in the 21st century. For Ecol Manage 294:54–61. doi: 10.1016/j.foreco.2012.10.022

Fox J, Weisberg S (2011) An R companion to applied regression., 2nd edn. Sage, Thousand Oaks, CA

García MJL, Caselles V (1991) Mapping burns and natural reforestation using thematic mapper data. Geocarto Int 6:31–37. doi: 10.1080/10106049109354290

Grogan P, Burns TD, Chapin III FS (2000) Fire effects on ecosystem nitrogen cycling in a Californian bishop pine forest. Oecologia 122:537–544. doi: 10.1007/s004420050977

Hatton PJ, Chatterjee S, Filley TR, et al (2016) Tree taxa and pyrolysis temperature interact to control the efficacy of pyrogenic organic matter formation. Biogeochemistry 130:103–116. doi: 10.1007/s10533-016-0245-1

Heckman K, Campbell J, Powers H, et al (2013) The influence of fire on the radiocarbon signature and character of soil organic matter in the Siskiyou National Forest, Oregon, USA. Fire Ecol 9:40–56. doi: 10.4996/fireecology.0902040

Hess TF, Schmidt SK (1995) Improved procedure for obtaining statistically valid parameter estimates from soil respiration data. Soil Biol Biochem 27:1–7. doi: 10.1016/0038-0717(94)00166-X

Hoosbeek MR, Li Y, Scarascia-Mugnozza GE (2006) Free atmospheric CO_2 enrichment (FACE) increased labile and total carbon in the mineral soil of a short rotation Poplar plantation. Plant Soil 281:247–254. doi: 10.1007/s11104-005-4293-x

Jackson RB, Lajtha K, Crow SE, et al (2017) The ecology of soil carbon: Pools, Vulnerabilities, and biotic and abiotic controls. Annu Rev Ecol Evol Syst 48:annurev-ecolsys-112414-054234. doi: 10.1146/annurev-ecolsys-112414-054234

Janisch JE, Harmon ME, Chen H, et al (2005) Decomposition of coarse woody debris originating by clearcutting of an old-growth conifer forest. Ecoscience 12:151–160.

Janssens IA, Dieleman W, Luyssaert S, et al (2010) Reduction of forest soil respiration in response to nitrogen deposition. Nat Geosci 3:315–322. doi: 10.1038/ngeo844

Johnson DW, Curtis PS (2001) Effects of forest management on soil C and N storage: Meta analysis. For Ecol Manage 140:227–238. doi: 10.1016/S0378-1127(00)00282-6

Kashian DM, Romme WH, Tinker DB, et al (2006) Carbon storage on landscapes with stand-replacing fires. Bioscience 56:598–606. doi: 10.1641/0006-3568(2006)56[598:CSOLWS]2.0.CO;2

Kasischke ES, Johnstone JF (2005) Variation in postfire organic layer thickness in a black spruce forest complex in interior Alaska and its effects on soil temperature and moisture. Can J For Res 35:2164–2177. doi: 10.1139/x05-159

Keeley JE (2009) Fire intensity, fire severity and burn severity: A brief review and suggested usage. Int J Wildl Fire 18:116–126. doi: 10.1071/WF07049

Knapp EE, Phillip Weatherspoon C, Skinner CN (2012) Shrub seed banks in mixed conifer forests of northern California and the role of fire in regulating abundance. Fire Ecol 8:32–48. doi: 10.4996/fireecology.0801032

Koyama A, Stephan K, Kavanagh KL (2012) Fire effects on gross inorganic N transformation in riparian soils in coniferous forests of central Idaho, USA: Wildfires v. prescribed fires. Int J Wildl Fire 21:69–78.

Kurth VJ, MacKenzie MD, DeLuca TH (2006) Estimating charcoal content in forest mineral soils. Geoderma 137:135–139. doi: 10.1016/j.geoderma.2006.08.003

Kuzyakov Y, Bogomolova I, Glaser B (2014) Biochar stability in soil: Decomposition during eight years and transformation as assessed by compound-specific ^{14}C analysis. Soil Biol Biochem 70:229–236. doi: 10.1016/j.soilbio.2013.12.021

Lenth R V. (2016) Least-squares means: The R package lsmeans. J Stat Softw 69:1–33. doi: 10.18637/jss.v069.i01

Liang S, Hurteau MD, Westerling AL (2017) Response of Sierra Nevada forests to projected climate–wildfire interactions. Glob Chang Biol 23:2016–2030. doi: 10.1111/gcb.13544

Loehman RA, Reinhardt E, Riley KL (2014) Wildland fire emissions, carbon, and climate: Seeing the forest and the trees – A cross-scale assessment of wildfire and carbon dynamics in fire-prone, forested ecosystems. For Ecol Manage 317:9–19. doi: 10.1016/j.foreco.2013.04.014

Luo Y, Weng E (2011) Dynamic disequilibrium of the terrestrial carbon cycle under global change. Trends Ecol Evol 26:96–104. doi: 10.1016/j.tree.2010.11.003

Lutzow M v., Kogel-Knabner I, Ekschmitt K, et al (2006) Stabilization of organic matter in temperate soils: mechanisms and their relevance under different soil conditions - a review. Eur J Soil Sci 57:426–445. doi: 10.1111/j.1365-2389.2006.00809.x

Maestrini B, Alvey EC, Hurteau MD, et al (2017) Fire severity alters the distribution of pyrogenic carbon stocks across ecosystem pools in a Californian mixed-conifer forest. J Geophys Res Biogeosciences 122:2338–2355. doi: 10.1002/2017JG003832

Maestrini B, Miesel JR (2017) Modification of the weak nitric acid digestion method for the quantification of black carbon in organic matrices. Org Geochem 103:136–139. doi: 10.1016/j.orggeochem.2016.10.010

Maestrini B, Nannipieri P, Abiven S (2015) A meta-analysis on pyrogenic organic matter induced priming effect. GCB Bioenergy 7:577–590. doi: 10.1111/gcbb.12194

Mallek CM, Safford H, Viers J, Miller JD (2013) Modern departures in fire severity and area vary by forest type, Sierra Nevada and southern Cascades, California, USA. Ecosphere 4:1–28. doi: 10.1890/ES13-00217

Mandal B, Majumder B, Adhya TK, et al (2008) Potential of double-cropped rice ecology to conserve organic carbon under subtropical climate. Glob Chang Biol 14:2139–2151. doi: 10.1111/j.1365-2486.2008.01627.x

Manzoni S, Taylor P, Richter A, et al (2012) Environmental and stoichiometric controls on microbial carbon-use efficiency in soils. New Phytol 196:79–91. doi: 10.1111/j.1469-8137.2012.04225.x

Meigs GW, Donato DC, Campbell JL, et al (2009) Forest fire impacts on carbon uptake, storage, and emission: The role of burn severity in the eastern Cascades, Oregon. Ecosystems 12:1246–1267. doi: 10.1007/s10021-009-9285-x

Michelotti L, Miesel J (2015) Source Material and Concentration of Wildfire-Produced Pyrogenic Carbon Influence Post-Fire Soil Nutrient Dynamics. Forests 6:1325–1342. doi: 10.3390/f6041325

Miesel JR, Hockaday WC, Kolka RK, Townsend PA (2015) Soil organic matter composition and quality across fire severity gradients in coniferous and deciduous forests of the southern boreal region. J Geophys Res Biogeosciences 120:1124–1141. doi: 10.1002/2015JG002959

Miller JD, Knapp EE, Key CH, et al (2009a) Calibration and validation of the relative differenced Normalized Burn Ratio (RdNBR) to three measures of fire severity in the Sierra Nevada and Klamath Mountains, California, USA. Remote Sens Environ 113:645–656. doi: 10.1016/j.rse.2008.11.009

Miller JD, Safford HD (2017) Corroborating evidence of a pre-Euro-American low- to moderate-severity fire regime in yellow pine–mixed conifer forests of the Sierra Nevada, California, USA. Fire Ecol 13:58–90. doi: 10.4996/fireecology.1301058

Miller JD, Safford HD, Crimmins M, Thode AE (2009b) Quantitative evidence for increasing forest fire severity in the Sierra Nevada and southern Cascade Mountains, California and Nevada, USA. Ecosystems 12:16–32. doi: 10.1007/s10021-008-9201-9

Miller JD, Thode AE (2007) Quantifying burn severity in a heterogeneous landscape with a relative version of the delta Normalized Burn Ratio (dNBR). Remote Sens Environ 109:66–80. doi: 10.1016/j.rse.2006.12.006

MTBS (2017) Monitoring trends in burn severity. https://www.mtbs.gov.

Nave LE, Vance ED, Swanston CW, Curtis PS (2009) Impacts of elevated N inputs on north temperate forest soil C storage, C/N, and net N-mineralization. Geoderma 153:231–240. doi: 10.1016/j.geoderma.2009.08.012

Nave LE, Vance ED, Swanston CW, Curtis PS (2011) Fire effects on temperate forest soil C and N storage. Ecol Appl 21:1189–1201.

NCEI-NOAA (2017) National centers for environmental information. https://www.ncei.noaa.gov.

Oakley BB, North MP, Franklin JF (2003) The effects of fire on soil nitrogen associated with patches of the actinorhizal shrub *Ceanothus cordulatus*. Plant Soil 254:35–46. doi: 10.1023/A:1024994914639

Pan Y, Birdsey RA, Fang J, et al (2011) A large and persistent carbon sink in the world's forests. Science 333:988–993. doi: 10.1126/science.1201609

Paul EA, Follett RF, Leavitt SW, et al (1997) Radiocarbon dating for determination of soil organic matter pool sizes and dynamics. Soil Sci Soc Am J 61:1058–1067. doi: 10.2136/sssaj1997.03615995006100040011x

Paul EA, Harris D, Collins HP, et al (1999) Evolution of CO2 and soil carbon dynamics in biologically managed, row-crop agroecosystems. Appl Soil Ecol 11:53–65. doi: 10.1016/S0929-1393(98)00130-9

Paul EA, Morris SJ, Conant RT, Plante AF (2006) Does the acid hydrolysis-incubation method measure meaningful soil organic carbon pools? Soil Sci Soc Am J 70:1023–1035. doi: 10.2136/sssaj2005.0103

Perry DA, Oren R, Hart SC (2008) Forest Ecosystems. Johns Hopkins University Press, Baltimore

Pinheiro J, Bates D, Debroy S, Sarkar D (2019) nlme: Linear and nonlinear mixed effects models.

Pinheiro JC, Bates DM (2000) Mixed-effects models in S and S-Plus. Springer-Verlag, New York

Post WM, Kwon KC (2000) Soil carbon sequestration and land-use change: Processes and potential. Glob Chang Biol 6:317–327. doi: 10.1046/j.1365-2486.2000.00308.x

R Core Team (2019) R: A language and environment for statistical computing.

Rasse DP, Rumpel C, Dignac MF (2005) Is soil carbon mostly root carbon? Mechanisms for a specific stabilisation. Plant Soil 269:341–356. doi: 10.1007/s11104-004-0907-y

Robertson GP, Wedin D, Groffman PM, et al (1999) Soil carbon and nitrogen availability. In: Robertson GP, Coleman DC, Bledsoe CS, Sollins P (eds) Standard soil methods for long-term ecological research. Oxford University Press, New York, pp 258–271

Ruefenacht B, Finco MV, Nelson MD, et al (2008) Conterminous U.S. and Alaska Forest Type Mapping Using Forest Inventory and Analysis Data. Photogramm Eng Remote Sens 74:1379–1388. doi: 10.14358/PERS.74.11.1379

Safford HD, Miller JD, Schmidt D, et al (2008) BAER soil burn severity maps do not measure fire effects to vegetation: A comment on Odion and Hanson (2006). Ecosystems 11:1–11. doi: 10.1007/s10021-007-9094-z

Sawyer R, Bradstock R, Bedward M, Morrison RJ (2018) Fire intensity drives post-fire temporal pattern of soil carbon accumulation in Australian fire-prone forests. Sci Total Environ 610–611:1113–1124. doi: 10.1016/j.scitotenv.2017.08.165

Schmidt MWI, Torn MS, Abiven S, et al (2011) Persistence of soil organic matter as an ecosystem property. Nature 478:49–56. doi: 10.1038/nature10386

Singh N, Abiven S, Maestrini B, et al (2014) Transformation and stabilization of pyrogenic organic matter in a temperate forest field experiment. Glob Chang Biol 20:1629–1642. doi: 10.1111/gcb.12459

Sinsabaugh RL, Reynolds H, Long TM (2000) Rapid assay for amidohydrolase (urease) activity in environmental samples. Soil Biol Biochem 32:2095–2097. doi: 10.1016/S0038-0717(00)00102-4

Six J, Jastrow JD (2002) Organic matter turnover. Encycl Soil Sci 936–942. doi: 10.1081/E-ESS-120001812

Smithwick EAH, Turner MG, Mack MC, Chapin FS (2005) Postfire soil N cycling in northern conifer rorests affected by severe, stand-replacing wildfires. Ecosystems 8:163–181. doi: 10.1007/s10021-004-0097-8

Soil Survey Staff Official soil series descriptions. In: Nat. Resour. Conserv. Serv. United States Dep. Agric. www.nrcs.usda.gov.

Tiemann LK, Billings SA (2011) Changes in variability of soil moisture alter microbial community C and N resource use. Soil Biol Biochem 43:1837–1847. doi: 10.1016/j.soilbio.2011.04.020

Trumbore S (2000) Age of soil organic matter and soil respiration: radiocarbon constraints of belowground C dynamics. Ecol Appl 10:399–411.

Trumbore SE (1997) Potential responses of soil organic carbon to global environmental change. Proc Natl Acad Sci 94:8284–8291. doi: 10.1073/pnas.94.16.8284

Turner MG, Smithwick EA, Metzger KL, et al (2007) Inorganic nitrogen availability after severe stand-replacing fire in the Greater Yellowstone ecosystem. Proc Natl Acad Sci U S A 104:4782–4789. doi: 10.1073/pnas.0700180104

Vitousek PM, Gosz JR, Grier CC, et al (1979) Nitrate losses from disturbed ecosystems. Science 204:469–474.

Vitousek PM, Howarth RW (1991) Nitrogen limitation on land and in the sea : How can it occur? Biogeochemistry 13:87–115.

Wan S, Hui D, Luo Y (2001) Fire effects on nitrogen pools and dynamics in terrestrial ecosystems: A meta-analysis. Ecol Appl 11:1349–1365.

Wang Q, Zhong M, Wang S (2012) A meta-analysis on the response of microbial biomass, dissolved organic matter, respiration, and N mineralization in mineral soil to fire in forest ecosystems. For Ecol Manage 271:91–97. doi: 10.1016/j.foreco.2012.02.006

Westerling AL, Hidalgo HG, Cayan DR, Swetnam TW (2006) Warming and earlier spring increase western U.S. forest wildfire activity. Science 313:940–943. doi: 10.1126/science.112883

CHAPTER 2:

HOW DO SOIL MICROBIAL COMMUNITIES RESPOND TO FIRE IN THE INTERMEDIATE TERM? INVESTIGATING DIRECT AND INDIRECT EFFECTS[2]

2.1 ABSTRACT

Fires transform soil microbial communities directly via heat-induced mortality and indirectly by altering plant and soil characteristics. Emerging evidence suggests the magnitude of changes to some plant and soil properties increases with burn severity, but the persistence of changes varies among plant and soil characteristics, ranging from months to years post-fire. Thus, which environmental attributes shape microbial communities at intermediate time points during ecosystem recovery, and how these characteristics vary with severity, remains poorly understood. I identified the network of properties that influence microbial communities three years after fire, along a burn severity gradient in Sierra Nevada mixed-conifer forest. I used phospholipid fatty acid (PLFA) analysis and bacterial 16S-rDNA amplicon sequencing to characterize the microbial community in mineral soil. Using structural equation modelling, I applied a systems approach to identifying the interconnected relationships among severity, vegetation, soil, and microbial communities. Dead tree basal area, soil pH, and extractable phosphorus increased with severity, whereas live tree basal area, forest floor mass, and the proportion of the ≥53 µm soil fraction decreased. Forest floor loss was associated with decreased soil moisture across the severity gradient, decreased live tree basal area was associated with

[2] *Originally published as:* Adkins J., Docherty K., Gutknecht J., Miesel J.R., 2020. How do soil microbial communities respond to fire in the intermediate term? Investigating direct and indirect effects associated with fire occurrence burn severity. Science of The Total Environment 745, 140957.

.

increased shrub coverage, and increased dead tree basal area was associated with increases in total and inorganic soil nitrogen. Soil fungal abundance decreased across the severity gradient, despite a slightly positive response of fungi to lower soil moisture in high severity areas. Bacterial phylogenetic diversity was negatively related to severity and was driven by differences in nutrients and soil texture. The abundance of *Bacteroidetes* increased and the abundance of *Acidobacteria* decreased across the severity gradient due to differences in soil pH. Overall, I found that the effects of burn severity on vegetation and soil physicochemical characteristics interact to shape microbial communities at an intermediate time point in ecosystem recovery.

2.2 INTRODUCTION

Wildfire activity has increased globally over the past several decades (Flannigan et al. 2013). In the western United States, wildfire frequency increased four-fold and total burned area increased six-fold during 1987-2003 compared to 1970-1986 (Westerling et al. 2006); from 1984-2011, total wildfire area in the region increased by >350 km^2 y^{-1}, and the number of wildfires > 405 ha increased by seven fires per year (Dennison et al. 2014). Burn severity, which is a measure of the magnitude of fire's impact to aboveground and belowground organic matter (Keeley 2009), has also increased. In the mixed-conifer forests of California's Sierra Nevada mountain range, the proportion of high severity fire has more than quadrupled compared to pre-settlement (Miller and Safford 2017), including approximately doubling between 1984-2006 (Miller et al. 2009b). Fire disturbances can influence ecosystem functions for months to years by impacting plant and microbial communities (Treseder et al. 2004; Holden et al. 2016; Pérez-Valera et al. 2019). Soil microbial community structure may affect the resilience of the community to future disturbances (Jansson and Hofmockel 2020), and has been linked to key soil ecosystem processes, including CO_2 flux (Bier et al. 2015). Responses of microbial

communities to fire may thus affect ecosystem stability and govern the transition of an ecosystem from a C source to a C sink during forest recovery (Balser et al. 2006), but the timescale over which these impacts persist remains poorly characterized.

Knowledge of the plant and soil characteristics that shape microbial communities at intermediate time points during post-fire recovery is currently limited (Dove et al. 2020; McLauchlan et al. 2020). Most existing publications describing impacts of fire on microbial communities focus on changes that occur within one year (e.g. Weber et al., 2014; Whitman et al., 2019; Xiang et al., 2014) or several decades (e.g. Cutler et al., 2017; LeDuc et al., 2013; Treseder et al., 2004) post-fire, and boreal forests are currently over-represented (Xiang et al. 2014a; Holden et al. 2016; Whitman et al. 2019) relative to other ecosystem types. Furthermore, despite decades-long calls for studies assessing the role of burn severity in shaping microbial communities (Hart et al. 2005; Pressler et al. 2018), relatively few publications have accounted for severity (but see Holden et al., 2016; Sáenz de Miera et al., 2020; Weber et al., 2014; Whitman et al., 2019; Xiang et al., 2014). Therefore, it is relatively unknown how forecasted increases in fire activity will influence the environmental drivers and characteristics of microbial communities at intermediate time points during post-fire recovery. This is a critical knowledge gap, as the response of microbial communities to changing fire regimes may either exacerbate or modulate the magnitude of fire feedbacks to climate change. For example, fire can cause decreases in fungal biomass and increases in copiotrophic bacteria, which may lead to increases in post-fire soil C efflux because bacterial biomass has faster turnover times compared to fungal biomass (Rousk and Bååth 2011), and copiotrophic bacteria are associated with faster decomposition rates compared to oligotrophic taxa (Orwin et al. 2018).

Immediate, direct effects of fire on soil microbial communities are driven by soil heating, which alters community structure via differential survival of heat-sensitive versus heat-resistant microbes. For example, lower fungal biomass is frequently observed in recently burned ecosystems relative to unburned controls (Dooley and Treseder 2012; Pressler et al. 2018), as fungi may be more sensitive to soil heating than bacteria (Neary and DeBano 2005). Relatedly, the spore-forming ability of the bacterial phyla *Firmicutes* and *Actinobacteria* may convey heat resistance and explain the increase in their dominance in the immediate aftermath of fires (Prendergast-Miller et al. 2017; Whitman et al. 2019). Fire also appears to favor microorganisms that exhibit a copiotrophic growth strategy. Predicted 16S-rRNA gene copy number, a trait associated with rapid growth rates, increases in response to fire in environments ranging from Mediterranean shrubland (Pérez-Valera et al. 2019) to Canadian boreal forests (Whitman et al. 2019). As post-fire ecosystem succession progresses, the direct impacts of fire on microbes may become less important as environmental characteristics become dominant drivers of microbial communities (Hart et al. 2005; Ferrenberg et al. 2013). Fires may influence microbial communities over intermediate (i.e. 1-10 years) and long timescales (>10 years) by changing the soil environment (i.e. soil pH, nutrient status, organic matter pools, texture, moisture, and temperature) (Certini 2005; Hart et al. 2005; Neary and DeBano 2005). Fire induced losses to plant biomass can indirectly influence the soil environment and microbial community by leading to less soil nutrient and water uptake by plants, fewer litter inputs, and decreased influence of plant canopy on soil temperature (Hart et al. 2005; Neary et al. 2005; Ficken and Wright 2017).

The persistence of fire-induced changes varies for different plant and soil properties and can range from months or years (e.g. pH, nutrient status; Certini, 2005; Wan et al., 2001) to decades (e.g. plant canopy coverage, soil organic matter pools; Fornwalt et al., 2018; Neary et

al., 2005). The magnitude of these changes likely depends on burn severity, but only a few studies have investigated the links between severity and soil properties or how plant communities modulate these changes. Studies that have directly assessed relationships between burn severity and soil properties in mixed-conifer forests have found that severity affects the magnitude of change to pH (Weber et al. 2014), total inorganic nitrogen (TIN) concentrations, forest floor (i.e. organic horizon) mass (Adkins et al. 2019b), forest floor pyrogenic C (i.e. charcoal associated C; PyC) concentrations (Maestrini et al. 2017), and soil texture (Ulery and Graham 1993). Differential impacts of burn severity on soil properties may lead to differences in microbial communities across severity gradients. For example, soil pH affects microbial diversity and community structure (Lauber et al. 2009; Rousk et al. 2010; Docherty et al. 2015), loss of forest floor may decrease habitat availability for fungi (Joergensen and Wichern 2008; Baldrian et al. 2012), and increases in PyC may favor lignolytic microbes adapted to decomposing aromatic substrates (Czimczik and Masiello 2007).

The direct and indirect effects of fire on soils represent a system level change to the microbial environment. A systems approach to assessing changes in microbial communities will improve understanding of the linkages between fire and microbial communities by disentangling the interconnected effects of fire on soil and vegetation. Previous research on the impacts of fire on soil microbial communities has tended to focus solely on soil characteristics, and researchers have called for studies that consider vegetation, soil, and microbes as an interacting network (Pressler et al. 2018). Here, I examined the impacts of burn severity on soil microbial community structure via plant and soil properties three years after a wildfire burned California mixed-conifer forest in the Sierra Nevada mountain range. I took a systems approach to understanding the impacts of burn severity by utilizing structural equation models (SEM) that accounted for

impacts of severity, plant coverage, and soil properties on microbial communities. My overarching hypothesis is that soil microbial community structure varies with burn severity, and that such differences can be explained by severity-associated differences in mineral soil nutrient concentrations, soil moisture content, and soil texture. I also hypothesized that plant coverage would influence microbial communities only indirectly via impacts on soil nutrients. Lastly, I hypothesized that accounting for burn severity instead of fire occurrence only would better explain changes to the microbial community by accounting for more of the variability in plant and soil characteristics in the post-fire environment. I used two methodological approaches which examine different characteristics of soil microbial communities. I used phospholipid fatty acid (PLFA) analysis to quantify total microbial biomass and the abundance of ecologically distinct guilds of microbes, including general fungi, Gram-positive bacteria, and Gram-negative bacteria. I used 16S-rDNA amplicon sequencing to examine bacterial communities at a finer resolution, characterizing the abundance of bacteria at the phylum level, bacterial phylogenetic diversity, and the ratio of oligotrophic-to-copiotrophic (O:C) bacterial taxa.

2.3 METHODS

2.3.1 Site description and field methods

My study was conducted in mixed-conifer forest (Ruefenacht et al. 2008) in the northern Sierra Nevada mountain range, California, USA (Plumas and Lassen National Forests; Fig. S2.1). The forest is dominated by *Pinus ponderosa* Lawson & C. Lawson, *P. lambertiana* Douglas, *P. jeffreyi* Balf., *Abies concolor* (Gord. & Glend.) Lindl. ex Hildebr., *Pseudotsuga menziessi* (Mirb.) Franco, and *Calocedrus decurrens* (Torr.) Florin, with lesser cover by *Quercus kelloggi* Newberry. Soils in my plots were from the Skalan soils series, a loamy-skeletal, isotic, mesic Vitrandic Haploxerlaf, and the Kinkel series, a loamy-skeletal, mixed, superactive, mesic

Ultic Palexeralf. During the period from approximately 1500-1850 C.E., the mean fire rotation in the region was 23 years for dry mixed-conifer forests and 31 years for moist mixed-conifer forests of the Sierra Nevada and Cascade mountain ranges in California; between 6-8% of burned forest experienced high severity fires on average (Mallek et al. 2013). The proportion of high severity fires in mixed-conifer forests increased to 25-30% for the period from 1984-2009 (Mallek et al. 2013). The 30 year mean annual precipitation is 1080 mm and mean annual temperature is 10.6 ºC (determined at the nearest weather station, Quincy, CA). My study focuses on the Chips Fire (Lat: 40.095 Long: -121.199), which was ignited by lightning and burned approximately 32,000 ha between July 28 to August 31, 2012.

Extended differenced Normalized Burn Ratios (dNBR) fire severity estimates, determined via Landsat TM imagery at a 30 m resolution, are collected in the growing season after fire occurrence, and are sensitive to post- versus pre-fire changes in vegetation and soil exposure (Parsons et al. 2010). The dNBR metric is correlated with absolute change in biomass and thus the magnitude of soil heating (i.e. more biomass burned equals greater heat flux) (Safford et al. 2008). dNBR therefore represent a combination of effects to both vegetation and soil, so I refer to dNBR as "total burn severity" throughout this paper. dNBR values (including unburned pixels) are continuous, but can be thresholded into severity categories: approximately 20% of the area affected by the Chips Fire was classified as high severity, 30% as moderate severity, 38% as low severity, and 12% as unburned (MTBS 2017). Immediately after wildfires, the USDA Burned Area Emergency response team often assesses soil burn severity (SBS). During the SBS mapping process, dNBR maps are modified based on field assessment of soil conditions, including loss to soil litter and duff layers, ash color and depth, soil structure, soil water repellency, and damage to fine roots (Parsons et al. 2010).

The USDA Forest Service established permanent plots and evaluated forest composition and structure across categories of total burn severity in summer 2014 (Alvey 2016; Maestrini et al. 2017). I randomly selected 17 of these plots (4 unburned, 6 low SBS, 5 moderate SBS, and 2 high SBS; dNBR range 1-1004) for soil and tree basal area sampling in summer 2015 (i.e. three years post-fire; Fig. S2.1). Plot level shrub coverage estimates were provided by USDA Forest Service staff based on measurements performed in 2014 (i.e. two years post-fire) within a 16 m sampling radius following a standard protocol for the Common Stand Exam (USDA 2015). Although it is possible that small changes in shrub cover may have changed between 2014 and 2015, shrub data from 2014 were the only data available as they were not assessed at the plot level during my soil sampling. Because the shrub species present at this site are perennial species, I assumed that shrub cover in 2014 represented cover in 2015. Plot characteristics and sampling methods have been described in detail previously (Maestrini et al. 2017; Adkins et al. 2019b). Briefly, plot elevation ranged from 1217-1641 m asl and were located on a variety of aspects with slopes < 50%. At each plot, I measured tree diameters at breast height (DBH) for all live and dead stems >10 cm DBH within an 11.3 m sampling radius, and I used these values to calculate live and dead tree basal areas at the plot level. I collected forest floor and mineral soil at azimuths of 0º, 120º, and 240º at 17 m from the plot center, resulting in a total of 51 forest floor samples and 51 mineral soil samples. The forest floor comprises the plant litter and duff layers, and is equivalent to the combined Oi, Oe, and Oa horizons in the USDA Soil classification system (Perry et al. 2008). At each sampling azimuth, I measured forest floor depth, collected all forest floor material from within a 15 cm diameter circular sampling frame, and collected mineral soil to 5 cm using a stainless-steel scoop. I stored mineral soils on ice for 2-7 days after collection and shipped them to the lab on ice. Subsamples for PLFA and DNA

analysis were stored at -80 ºC, and the remainder of the soils were refrigerated at 4 ºC until processing.

2.3.2 Laboratory methods

Soil processing and chemical analyses

Detailed methods for bulk sample processing and chemical analysis have been described previously (Adkins et al. 2019b). Briefly, I determined total forest floor dry mass, and pulverized forest floor subsamples by sequentially processing in a Waring commercial lab blender (Conair Inc., Stamford Ct, USA) and a ball mill (SPEX Sample Prep LLC, Metuchen, NJ, USA). I oven-dried the pulverized forest floor at 60 ˚C and determined C and N concentrations via elemental analysis (Costech Analytical Technologies Inc., Valencia, CA, USA). I sieved field-moist mineral soils (2 mm) and subsampled for determination of total C, N, PyC, ammonium (NH_4), nitrate (NO_3), extractable phosphorus (P), pH, proportion of sand + particulate organic matter (sand+POM), soil moisture, PLFA, and 16S-rDNA analysis. For C, N and PyC analysis, I oven-dried subsamples at 105 ˚C (C and N) or 60 ˚C (PyC) and pulverized in a ball mill prior to analysis. I used field-moist subsamples for NH_4, NO_3, and extractable P analysis, and air-dried subsamples for pH determination. I oven-dried subsamples at 60 ˚C for determination of sand+POM proportion. I determined soil moisture gravimetrically as the mass difference between subsamples oven-dried at 105 ˚C and field-moist samples. I determined PyC concentrations using weak nitric acid digestion (Kurth et al. 2006; Maestrini et al. 2017). I measured NH_4 and NO_3 concentrations spectrophotometrically following extraction with 2 M KCl (Sinsabaugh et al. 2000; Doane and Horwáth 2003). I measured P concentration after extraction with 0.5 M $NaHCO_3$ (Olsen et al. 1954). I determined pH using a 1:2 (w:v) soil slurry (Oakton pH 700, Oakton Instruments, Vernon Hills, IL, USA). I quantified sand+POM as the

mass proportion of dispersed soil that did not pass through a 53 μm sieve during wet sieving (Cambardella and Elliott 1993).

PLFA analysis

I performed PLFA analysis using a modified version of the Bligh and Dyer method (Bligh and Dyer 1959; Schmidt et al. 2015). I freeze-dried 6 g mineral soil subsamples and extracted fatty acids three times using a 0.9:1:2 mixture of 0.15 M citrate buffer:chloroform:methanol. I separated the phases using a 0.9:1 ratio of citrate buffer:chloroform to isolate lipids in the chloroform phase. I separated lipid classes via silica acid chromatography, followed by methylation of phospholipids through alkaline methanolysis.

I analyzed the isolated FAMEs on a Gas Chromatograph System (Agilent 7890, Agilent Technologies Inc., Santa Clara, CA, USA). I converted peak areas to nmol lipid g soil^{-1} using internal standards. I used the sum of all lipids with less than 19 carbons as an index for microbial biomass. I used specific lipids as biomarkers to distinguish microbial groups within the community. I considered the sum of 18:1 ω9c and 18:2 ω6,9c lipids as general fungal indicators, the sum of monounsaturated (excluding 16:1 ω5c) and cyclopropyl lipids as Gram-negative bacterial indicators, and the sum of all iso- and anteiso-branched lipids as Gram-positive bacterial indicators. I considered the sum of 14:0, 15:0, 16:0, and 18:0 lipids as non-specific bacterial indicators. I used the ratio of mean abundances of fungal biomarkers to bacterial biomarkers (excluding 16:1 ω5c) as an index for fungal:bacterial lipid ratio (F:B). Two soil subsamples (one from a high severity plot and one from an unburned plot) were lost during PLFA processing and were excluded from further analysis.

DNA extraction and sequence analysis

I extracted DNA from 0.25 g of fresh soil using a DNA isolation kit (MoBIO PowerSoil, MoBIO laboratories, Carlsbad, CA), according to the manufacturer's instructions. I used Illumina-MiSeq to amplify the V4 region of the 16S-rRNA gene using 515f/806r universal primers (Caporaso et al. 2010). DNA sequences were processed using the QIIME (v 1.9) bioinformatics pipeline (Caporaso et al. 2010). I merged forward and reverse sequence reads using the pandaseq (v 2.6) algorithm (Masella et al. 2012), and I removed chimeric sequences *de novo* using the USEARCH (v 6.1) algorithm (Edgar 2010). I clustered sequences into operational taxonomic units (OTUs) using a 97% similarity threshold via comparison to the SILVA SSURef database (v 128) (Quast et al. 2013). I removed contaminant OTUs using the *filter_otus_from_otu_table.py* command, and I removed OTUs associated with Archaea, mitochondria, and chloroplasts using the *filter_taxa_from_otu_table.py* command. I calculated OTU relative abundance at the phylum level using the *summarize_taxa.py* command. I determined Faith's phylogenetic diversity for each sample by passing the *PD_whole_tree* option to the *alpha_diversity.py* command (Faith 1992). I calculated O:C as the ratio of the sum of relative abundances of all taxa classified within the phyla *Acidobacteria* and *Verrucomicrobia* to the sum of the relative abundances of all taxa classified within *Actinobacteria*, β-*proteobacteria*, *Firmicutes,* and *Bacteroidetes* (Fierer et al. 2007; Fierer et al. 2012a; Ramirez et al. 2012). After sequence processing, there were 19,527-45,893 sequences per sample (mean=30,570; SD=4827). I did not rarefy my samples because rarefying reduces statistical power and is not useful when library size varies by less than ten-fold (McMurdie and Holmes 2014; Weiss et al. 2017). Raw sequence data are accessible from the NCBI Sequence Read Archive (SRA) under project ID PRJNA632607, accession numbers SAMN14195883-5931.

2.3.3 Statistical methods

Univariate relationships between fire, soil, vegetation, and microbial characteristics

I assessed univariate relationships using maximum-likelihood linear mixed models constructed in the nlme package (v 3.1.140) (Pinheiro et al. 2019) in the R statistical computing environment (v 3.6.1) (R Core Team 2019). My linear models included a plot-identifier as a random effect, and either fire occurrence, total burn severity, or SBS as the explanatory variable; I treated fire occurrence and SBS as categorical variables and total burn severity as a continuous variable. The four unburned plots were included in my severity models. I examined residual distributions to assess the assumption of normality and determined that lipid-derived absolute abundance and microbial biomass values should be log-transformed. I determined whether fire occurrence, total burn severity, or SBS best explained each response by comparing Akaike Information Criterion (AIC) values among the models. For models assessing the response of vegetation, I compared only fire occurrence and total burn severity models. I performed differential expression analysis and assessed the $\log_2$-fold change in individual bacterial OTUs in response to fire occurrence using the edgeR package (v 3.28.1) (Robinson et al. 2010). I aggregated OTUs within bacterial families and calculated mean $\log_2$-fold change to identify families that exhibited different abundances in burned and unburned areas.

Multivariate relationships between fire, soil, vegetation, and microbial communities

I assessed the relationships between fire occurrence, burn severity, and lipid-based and 16S-based communities by performing permutational analysis of variance (PERMANOVA) analysis on Bray-Curtis dissimilatory matrices. Dissimilatory matrices were based on the relative abundances (%) of lipids and bacterial phyla, and PERMANOVAs were performed using the *adonis2* function within the vegan package (v 2.5.6) (Oksanen et al. 2019). I assessed

relationships of fire occurrence and severity, vegetation, soil characteristics, and whole microbial communities using PCoA analysis within the vegan package. I calculated the correlations of variables with the resulting principle coordinates using the *envfit* function in vegan.

System scale relationships between fire, soil, vegetation, and microbial communities using structural equation modelling

I constructed SEMs using the piecewiseSEM package (v 2.1.0) (Lefcheck 2016) and the nlme package (Pinheiro et al. 2019). Piecewise SEM is a multivariate statistical technique that incorporates multiple explanatory and response variables into a single causal network, represented as a set of regression equations (Lefcheck 2016). SEMs quantify path coefficients for direct and indirect drivers of an explanatory variable on a response variable, which can be combined into a single compound coefficient to assess the overall effect (Grace 2006). I used SEMs to determine direct and indirect drivers of the absolute abundance (nmol lipid g^{-1} soil) of lipid-derived microbial guilds and the absolute abundance (count of sequences within phyla) of the four most abundant bacterial phyla determined using 16S-rDNA analysis. I recognize that there are potential issues with the use of absolute rather than relative abundance of 16S-rDNA due to differences in sample sequence depth and rRNA gene copy number among phyla. However, due the similarity in library sizes among my samples, using absolute versus relative abundance is unlikely to affect my results. Moreover, the use of proportional abundance for analyzing microbiome data has been found to increase false positive rates and spurious correlations (Friedman and Alm 2012; McMurdie and Holmes 2014).

I also constructed SEMs for microbial biomass, F:B, bacterial phylogenetic diversity, and O:C. I constructed an initial SEM metamodel composed of multivariate linear mixed models with vegetation and soil characteristics as response variables. The component linear mixed

models assessing the response of vegetation included total burn severity as the explanatory variable, and the mixed model assessing shrub cover also initially included live and dead tree basal area as explanatory variables. Component mixed models assessing soil characteristics included total burn severity and the three plot-level vegetation characteristics as explanatory variables. The model assessing mineral soil moisture also included the overlaying forest floor mass as an explanatory variable. After initial fit, the SEM metamodel was modified by sequentially removing explanatory variables that exhibited p-values ≥ 0.15. The resulting SEM metamodel was then used as a starting model to construct SEMs describing drivers of individual microbial community characteristics.

All initially fit SEMs included a direct link between the microbial characteristic of interest and total burn severity, and direct links from each soil and vegetation variable to the microbial characteristic. SEMs describing lipid-derived microbial groups also included a direct link to microbial biomass, and SEMs describing 16S-derived microbial groups included a direct link to F:B. All SEM paths were initially fit using linear mixed models that included a plot identifier as a random effect. I evaluated the assumption of conditional independence between explanatory variables in my SEMs by examining the significance of correlation coefficients provided in the output of the *psem* function in the piecewiseSEM package. If the correlation between explanatory variables was highly significant (i.e. $p \leq 0.005$) I specified correlated errors between those variables in my SEMs. I then sequentially removed the least significant path from the SEM until all paths exhibited p-values ≤ 0.15. I assessed the goodness of fit for each SEM using Fisher's C-value. A non-significant Fisher's C-value ($p>0.05$) indicates that the modeled relationships are supported by the data (Lefcheck 2016). I then fitted an alternate version of the SEM in which fire occurrence was substituted for total burn severity, and the relative support for

these models was compared using the full-model AIC (Shipley and Douma 2020). I considered an SEM including severity versus fire occurrence to have more support if the full-model ΔAIC between the models was ≥ 2. Path coefficients in all SEMs are presented on the standardized scale implemented in the piecewiseSEM package, which standardizes coefficients by multiplying the raw coefficient by the ratio of the standard deviation of the explanatory variable to the standard deviation of the response variable. I considered path coefficients statistically significant at α=0.05.

2.4 RESULTS

2.4.1 Relationships between vegetation and soil characteristics and fire occurrence and severity

Univariate analyses

Live and dead tree basal area and shrub coverage were significantly related to fire occurrence and total burn severity (Fig. 2.1). AIC values indicated that total burn severity had more support than fire occurrence for explaining dead tree basal area, which increased with total burn severity (Fig 2.1b). AIC values did not indicate a preference for total burn severity versus fire occurrence for explaining live tree basal area or shrub coverage. Live tree basal area was ~3.7 times lower in burned areas compared to unburned areas (Fig. 2.1c), and shrub coverage was ~3.9 times higher in burned areas compared to unburned areas (Fig. 2.1e).

AIC values indicated that fire occurrence had more explanatory power than total burn severity for differences in forest floor mass. Forest floor mass was ~3.5 times lower in burned areas compared to unburned areas (Fig. 2.2a). Total burn severity was supported over fire occurrence for explaining differences in mineral soil sand+POM proportion, pH, total C, total N, TIN, and extractable P (Figs. 2.2 and 2.3). Sand+POM was negatively associated with total burn

severity (Fig. 2.2d), and pH was positively associated with total burn severity (Fig. 2.2f). Total soil N, TIN, and extractable P all increased with total burn severity (Figs. 2.3d, 2.3f, and 2.3h). For all univariate models (including for microbial groups), AIC values indicated that SBS only had more explanatory power than both fire occurrence and total burn severity for TIN concentrations (Fig. S2.2), so I do not discuss SBS extensively in the remainder of this paper (but see supplemental figures).

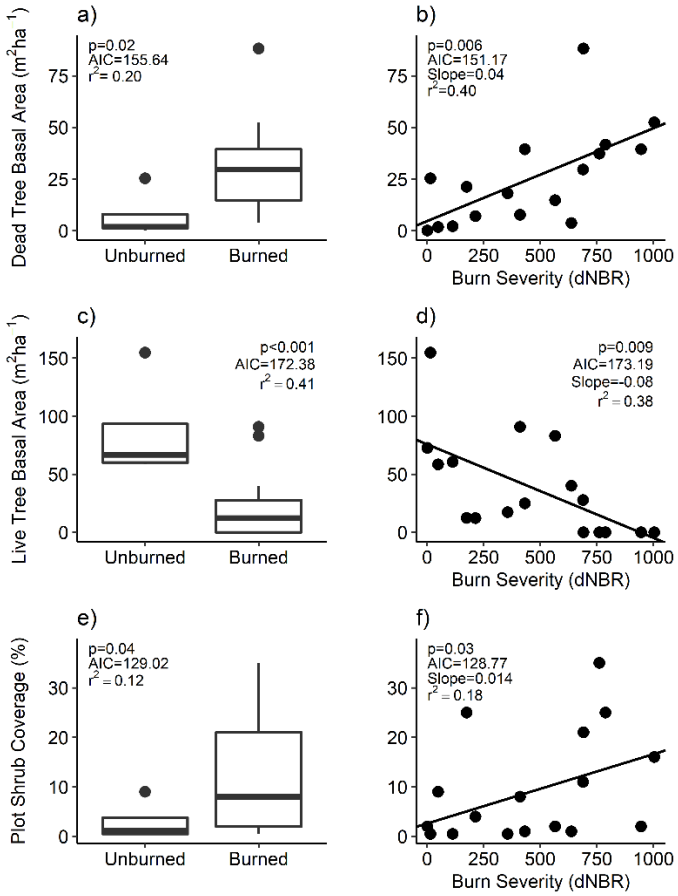

Figure 2.1 Relationship of fire occurrence (column 1) and dNBR (column 2) to live tree basal area, dead tree basal area, and shrub coverage in 17 plots within the Chips Fire perimeter.

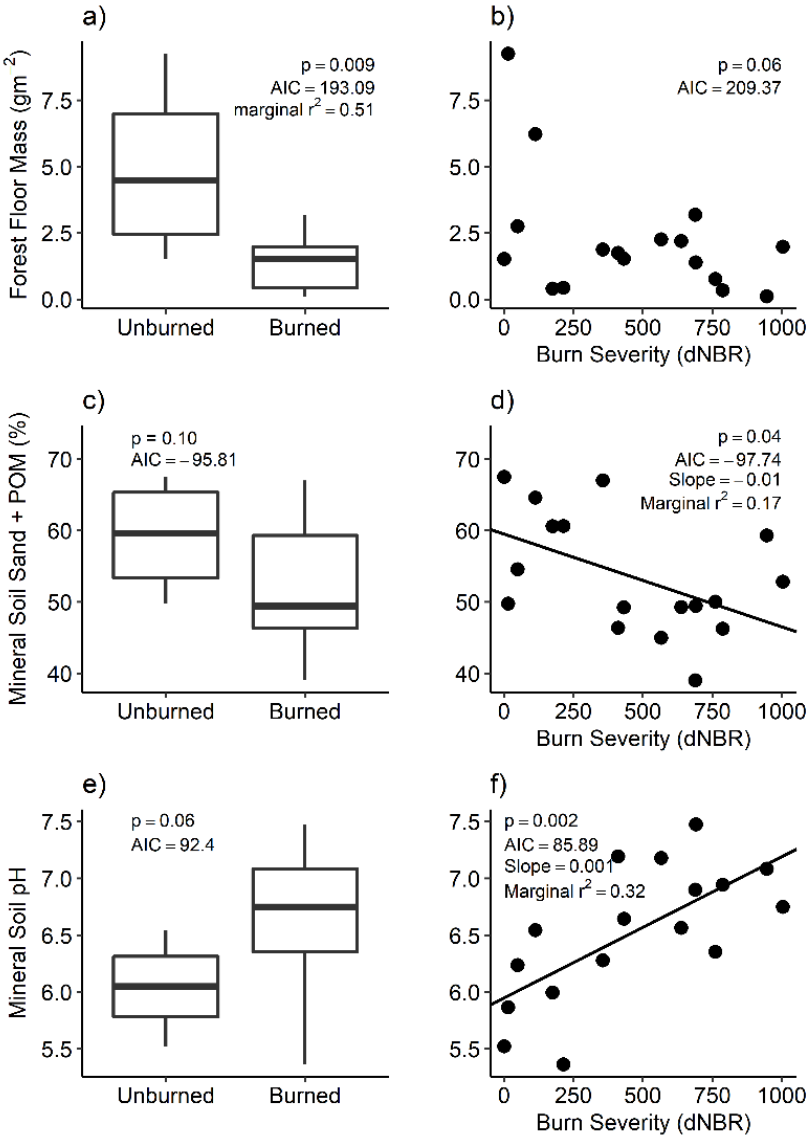

Figure 2.2 Relationship of fire occurrence (column 1), soil burn severity (column 2), and total burn severity (column 3) to forest floor mass, mineral soil sand+POM (5 cm) and mineral soil pH. Marginal r^2 values are provided for soil properties that linear mixed models indicated were significantly affected by the explanatory variable of interest at α=0.05. Capital letters in soil burn severity figures denote Tukey-adjusted significant differences among severity levels. Slope values are provided in total burn severity figures for properties that were significantly affected at α=0.05.

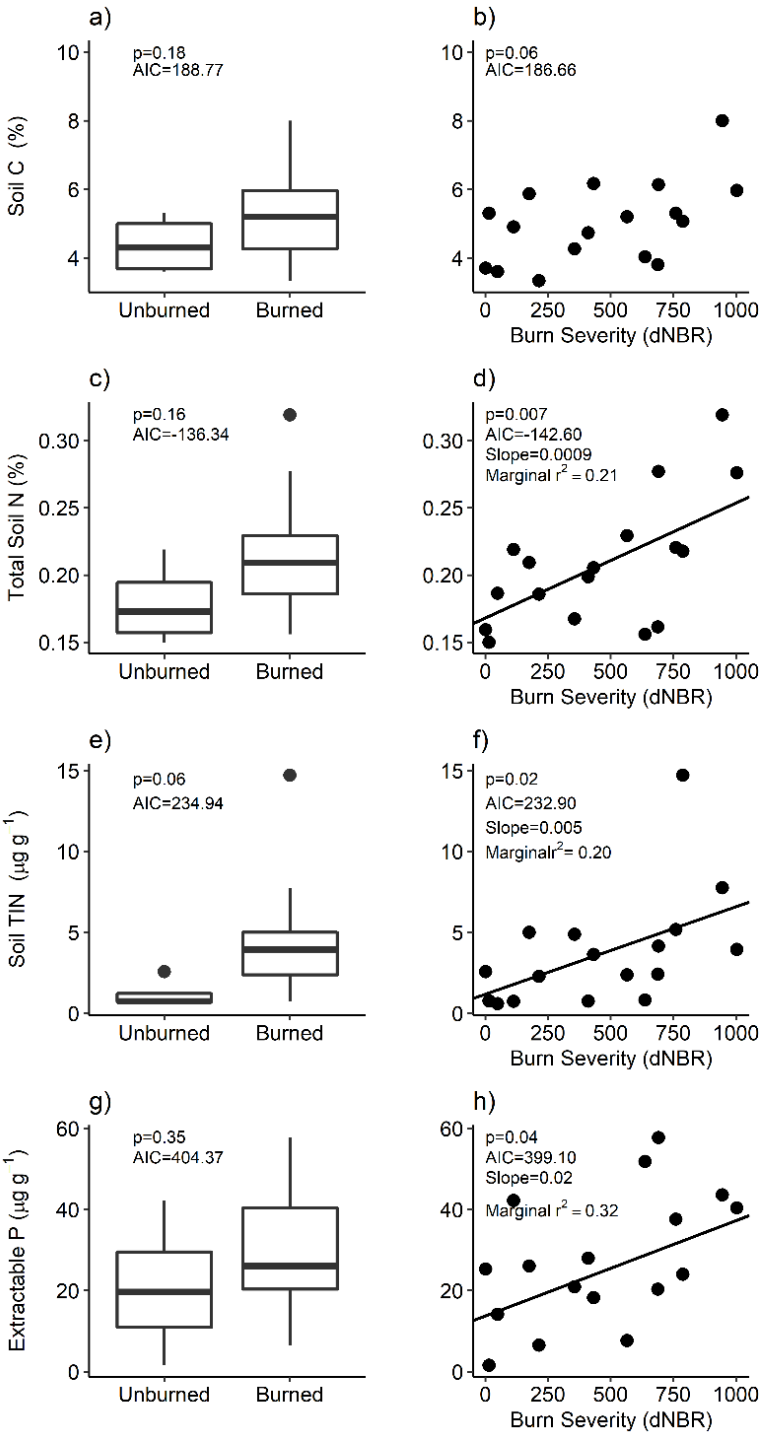

Figure 2.3 Relationship of fire occurrence (column 1), soil burn severity (column 2), and total burn severity (column 3) to soil properties for mineral soils collected to 5 cm depth. Marginal r^2 values are provided for soil properties that linear mixed models indicated were significantly affected by the explanatory variable of interest at α=0.05. Capital letters in soil burn severity figures denote Tukey-adjusted significant differences among severity levels. Slope

values are provided in total burn severity figures for properties that were significantly affected at α=0.05.

SEM analyses

My SEM metamodel revealed direct and indirect drivers of severity on soil characteristics (Fig. 2.4), some of which were not captured by univariate analyses. Similar to my univariate analyses, SEM revealed direct relationships between total burn severity and live tree basal area, dead tree basal area, extractable P, and pH. Additionally, I found a direct, negative link between total burn severity and sand+POM that was tempered by a negative relationship between live tree basal area and sand+POM, leading to a compound path coefficient between total burn severity and sand+POM of -0.40. For other characteristics, the relationship with severity was entirely indirect. Total burn severity affected forest floor mass indirectly via a negative association with live tree basal area (compound coefficient=-0.42). Forest floor mass was positively associated with soil moisture, leading to an indirect negative relationship between moisture and total burn severity (compound coefficient=-0.20). The positive relationship between total burn severity and shrub coverage was driven by the negative relationship between live tree basal area and shrub coverage (compound coefficient=0.31). The positive relationship between total burn severity and total N was driven by a positive relationship with dead tree basal area (compound coefficient=0.30). The positive relationship between total burn severity and TIN was driven by total N and a negative relationship between TIN and live tree basal area (compound path coefficient=0.31).

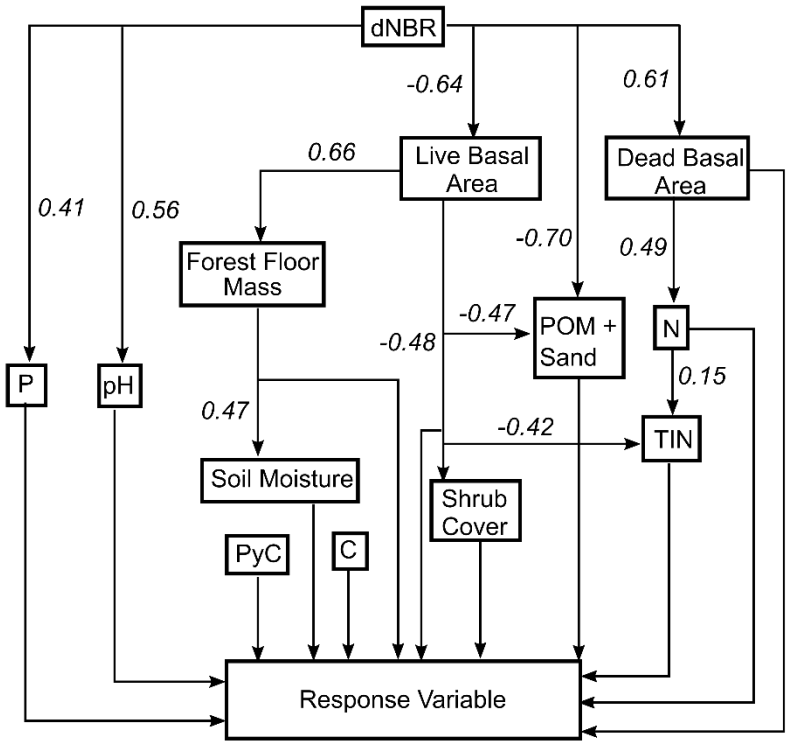

Figure 2.4 General model depicting initially fitted structural equation model of direct and indirect links between fire severity metrics and PLFA-based microbial group absolute abundance and 16S-based bacteria phylum absolute abundance. Microbial biomass was also included as an explanatory variable of PLFA-based microbial group abundance, and fungal-to-bacterial ratio (F:B) was included as an explanatory variable for 16S-based models. Paths were fit using linear mixed models with a random plot effect. Standardized coefficients are displayed for links between total burn severity (dNBR) and endogenous variables. Forest floor mass was negatively related to soil burn severity; soil burn severity is a categorical variable, so a coefficient is not displayed. Abbreviations: N= nitrogen concentration, PyC = pyrogenic carbon concentration, C = carbon concentration, TIN = total inorganic nitrogen concentration, P = phosphorus concentration, POM + Sand = proportion of particulate organic matter plus sand soil fraction

2.4.2 Relationships between soil microbial communities and fire occurrence and severity

Microbial abundance based on lipid indicators

Fire affected lipid communities primarily by impacting fungal lipids. PERMANOVAs of a Bray-Curtis dissimilatory matrix indicated that lipid communities were significantly related to fire occurrence (r^2=0.11; p=0.002) and total burn severity (r^2=0.14; p=0.001). Based on AIC,

total burn severity best explained the relative abundance of general fungal lipids and F:B. Fire occurrence had more explanatory power for the relative abundance of Gram-negative bacteria; neither fire occurrence nor total burn severity had more power for explaining the relative abundance of total bacterial lipids, Gram-positive lipids, or total microbial biomass. Despite differences in AIC values, based on univariate analyses, the only lipid group significantly related to fire occurrence or burn severity was the relative abundance of general fungal lipids, which exhibited a negative relationship with total burn severity (Fig. 2.5a; slope=-0.008; marginal r^2=0.17; p=0.038).

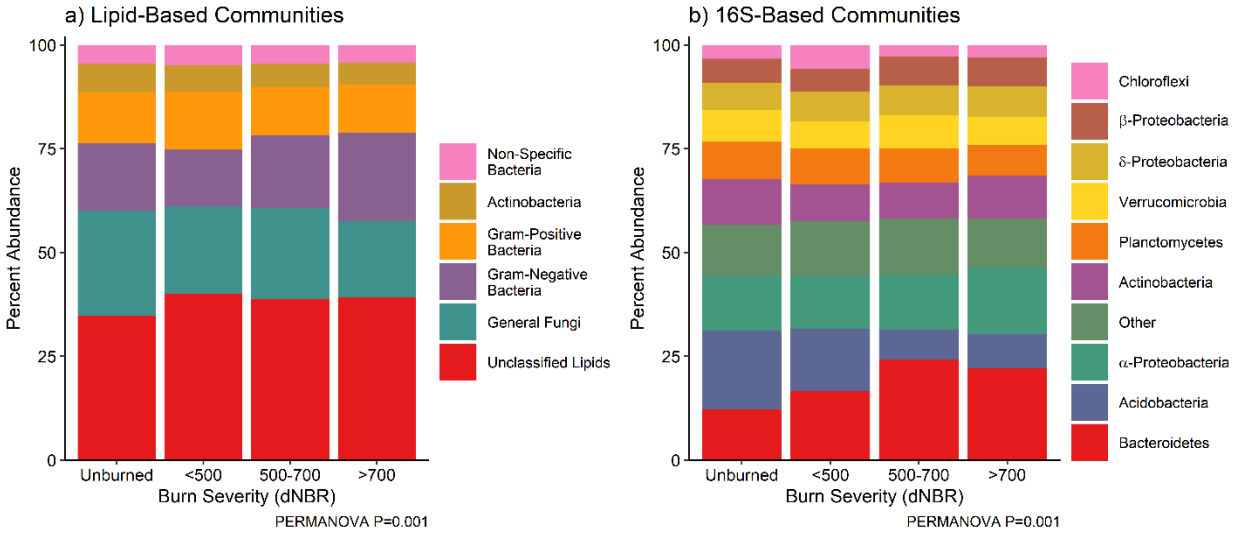

Figure 2.5 Relative abundance of microbial groups based on PLFA analysis (a and b) and the nine most abundant bacterial phyla (c and d) across a gradient of soil burn severity and total burn severity in mineral soils (0-5 cm). Total burn severity is grouped by approximate dNBR quartiles in my data.

Bacterial composition and diversity based on 16S-rDNA analysis

Fire occurrence and burn severity had numerous effects bacterial communities, analyzed with 16S-rDNA methods. Each soil sample harbored bacterial sequences representing 3,959.49 ± 153.69 bacterial OTUs. PERMANOVAs of bacterial communities indicated that they were significantly related to fire occurrence (r^2=0.12; p=0.002) and total burn severity (r^2=0.24;

p=0.001). AIC values indicated that neither fire occurrence nor total burn severity better explained Faith's phylogenetic diversity, which was negatively related to fire occurrence (Fig. 2.6c). Total burn severity best explained differences in O:C ratio, which was negatively related to burn severity (Fig. 2.6f).

Among all soil samples, the most abundant bacterial groups were *Bacteroidetes* (18.65 ± 1.35%), α-*Proteobacteria* (13.89 ± 0.56%), *Acidobacteria* (12.50 ± 1.44%), and *Actinobacteria* (9.65 ± 0.40%) (Fig. 2.5b). Based on AIC values, total burn severity better explained differences in *Bacteroidetes* and *Acidobacteria* relative abundance, whereas fire occurrence best explained α-*Proteobacteria* and *Actinobacteria* relative abundance. *Bacteroidetes* relative abundance increased with total burn severity (slope=0.012; marginal r^2=0.42; $p < 0.001$). The mean log_2-fold change in abundance of *Bacteroidetes* OTUs in response to fire was 0.58 ± 0.06 (Fig S2.4). The five most abundant families in *Bacteroidetes* (*Chitinophagaceae*, *Cytophagaceae*, *Sphingobacteriaceae*, *Flavobacteriaceae*, and unclassified *env.OPS 17)* all exhibited significantly positive log_2-fold change in abundance in response to fire occurrence.

α-*Proteobacteria* relative abundance was not significantly related to fire occurrence at the class level (p=0.48). The mean log_2-fold change in abundance of α-*Proteobacteria* OTUs in response to fire was 0.20 ± 0.05 (Fig. S2.5). *Acidobacteria* relative abundance was negatively related to burn severity (Fig. 2.5b; slope=-0.015; marginal r^2=0.49; $p<0.001$); the mean log_2-fold change in abundance of *Acidobacteria* OTUs in response to fire was -0.59 ± 0.05 (Fig. S2.6). All four identified families within *Acidobacteria* exhibited negative log_2-fold response to fire occurrence. *Actinobacteria* relative abundance decreased from 11.06 ± 0.40% in unburned areas to 9.22 ± 0.45% in burned areas (marginal r^2=0.08; p=0.007); the mean log_2-fold change in abundance of *Actinobacteria* OTUs in response to fire was 0.03 ± 0.05 (Fig. S2.7). At the family

level, OTUs within some families (e.g., *Frankiaceae* and *Mycobacteriaceae*) exhibited negative log_2-fold response to fire occurrence, while *Micrococcaceae* exhibited a positive response.

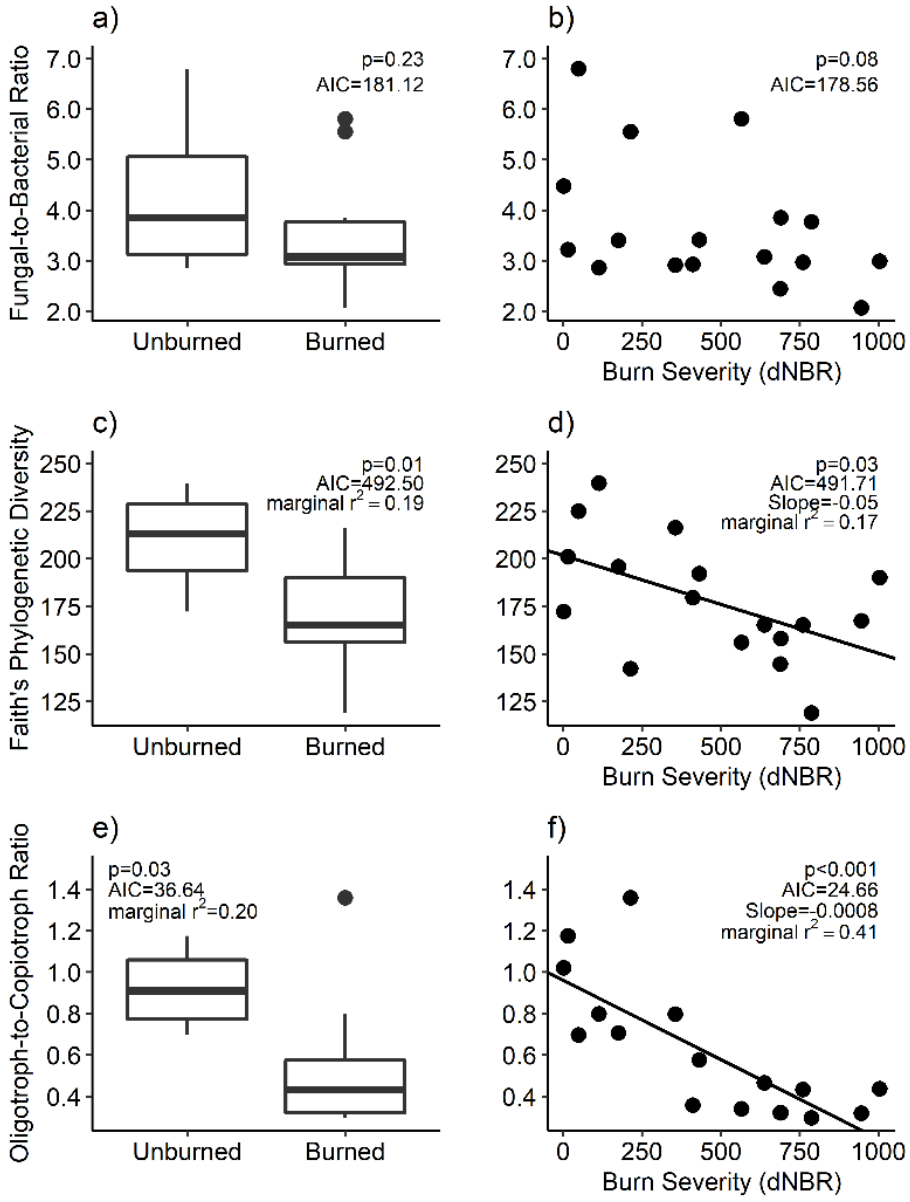

Figure 2.6 Relationship of microbial community characteristics including lipid-based fungal-to-bacterial ratio,16S-based Faith's phylogenetic diversity, and 16S-based oligotrophic:copiotrophic bacterial taxa ratio, with fire occurrence (column 1), soil burn severity (column 2), and total burn severity (column 3) in mineral soils (0-5 cm). Marginal r^2 values are provided for microbial community characteristics that linear mixed models indicated were significantly affected by the explanatory variable of interest at α=0.05. Capital letters in soil burn severity figures denote Tukey-adjusted significant differences among severity levels. Slope

values are provided in total burn severity figures for characteristics that were significantly affected at α=0.05.

2.4.3 Direct and indirect soil and vegetation drivers of soil microbial community characteristics

Principle coordinates analysis

For lipid communities, the first and second PCoA axes explained 33.59% and 22.06% of community variation, respectively (Fig. 2.7a). In addition to fire occurrence (r^2=0.14; p=0.001) and total burn severity (r^2=0.47, p=0.001), four environmental variables were significantly correlated with the PCoA ordination: dead tree basal area (r^2=0.22; p=0.009), pH (r^2=0.48; p=0.001), sand+POM (r^2=0.28; p=0.003), and extractable P (r^2=0.19; p=0.011).

For 16S-rDNA-based soil microbial communities, the first and second PCoA axes explained 48.87% and 11.13% of community variation, respectively (Fig. 2.7b). In addition to fire occurrence (r^2=0.15; p=0.004) and total burn severity (r^2=0.47; p=0.001), eight environmental variables were significantly correlated with the PCoA ordination: dead tree basal area (r^2=0.19; p=0.005), shrub coverage (r^2=0.15; p=0.033), pH (r^2=0.60; p=0.001), soil moisture (r^2=0.25; p=0.001), sand+POM (r^2=0.25; p=0.002), TIN (r^2=0.16; p=0.031), extractable P (r^2=0.16; p=0.024), and forest floor mass (r^2=0.15; p = 0.033).

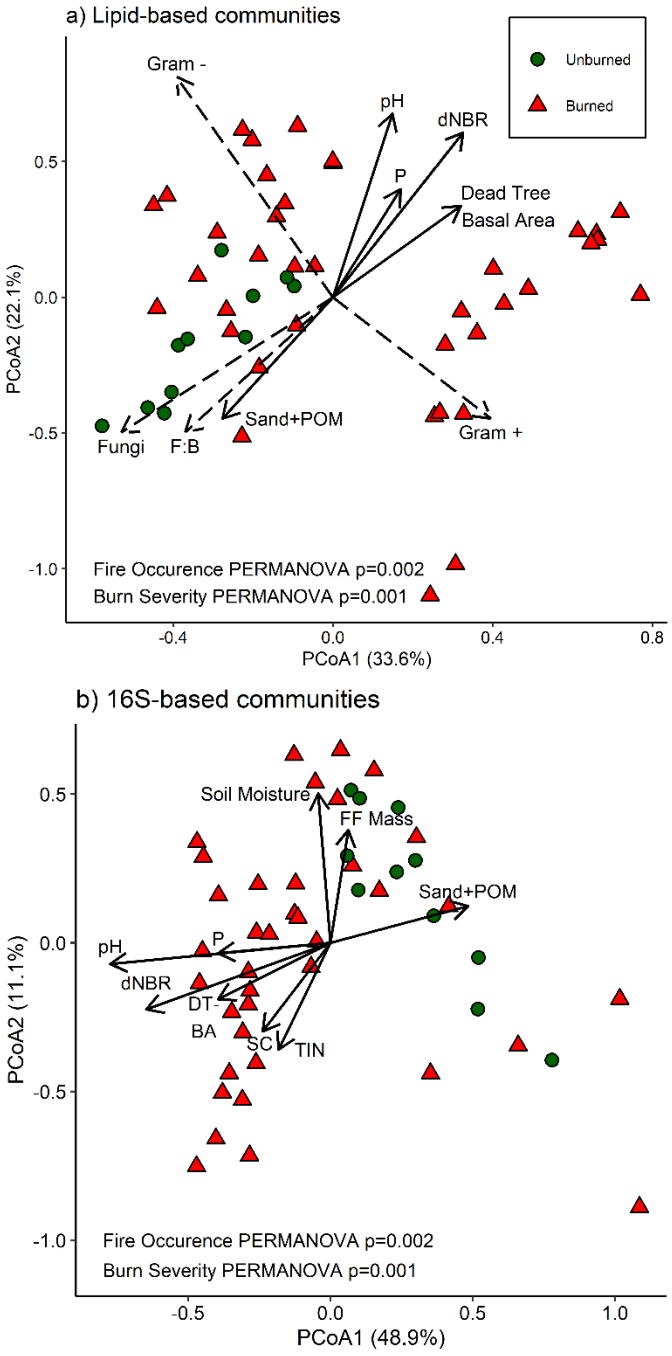

Figure 2.7 Principle coordinates analysis (PCoA) plots of lipid-based communities (a) and 16S-rDNA based bacterial communities at the phylum level (b) in mineral soils (0-5 cm). Vectors represent variables that are significantly correlated with one of the PCoA axes, and vector lengths are scaled based on r^2 values. Solid vectors represent environmental or edaphic variables, and dashed vectors in a) represent microbial groups based on lipid groupings. Abbreviations: F:B = fungi-to-bacteria ratio, FF Mass = forest floor mass, P = extractable phosphorus concentration, TIN = total inorganic nitrogen concentration, DT-BA = dead tree basal area, SC = shrub coverage

SEM analysis

SEM models revealed relationships between severity and microbial communities that were not captured by univariate analysis, and full-model AIC values indicated that SEMs including total burn severity had more explanatory power than fire-occurrence models for every microbial characteristic measured (Table 2.1). Microbial biomass was positively related to live tree basal area, shrub coverage, sand+POM, and total N, resulting in a negative relationship with total burn severity that was not captured by univariate analysis. Absolute fungal abundance was directly, negatively related to total burn severity. Additionally, fungal abundance responded negatively to soil moisture, leading to an indirect, positive relationship between total burn severity and fungal abundance. There was also an indirect negative relationship between fungal abundance and burn severity via the relationship of total burn severity with total microbial biomass. My SEMs also revealed relationships between severity and F:B, total bacterial, Gram-negative, and Gram-positive bacterial abundances that were not captured by univariate analyses. F:B was directly, negatively influenced by total burn severity, and indirectly influenced via soil moisture and total N. Total bacterial lipid abundance was negatively influenced by total burn severity via the total microbial biomass path. Gram-negative bacteria had a direct positive link to total burn severity, but relationships with live tree basal area, P, and microbial biomass resulted in an overall negative relationship between severity and Gram-negative bacteria. Gram-positive bacteria was indirectly linked to total burn severity via relationships with live tree basal area, soil moisture, TIN, pH, and microbial biomass, leading to a negative relationship with severity.

SEMs revealed that total burn severity affected the absolute abundances of *Bacteroidetes* and *Acidobacteria* directly and indirectly via pH mediated impacts. There was an indirect, positive relationship between total burn severity and *Bacteroidetes* via the positive response of

Bacteroidetes to pH, and an indirect, negative relationship between total burn severity and *Acidobacteria* due to the negative response of *Acidobacteria* to pH. The abundance of $\alpha-$*Proteobacteria* was indirectly related to severity via the influence of pH, live tree basal area, and TIN. *Actinobacteria* absolute abundance was associated with dead tree basal area and sand+POM, effects that offset one another and resulted in an essentially neutral relationship between severity and *Actinobacteria*. There was an indirect, negative relationship between total burn severity and bacterial phylogenetic diversity via associated decreases in sand+POM and increases in TIN and P. Total burn severity negatively influenced O:C via a direct, negative link and an indirect, negative link via pH; these negative links were tempered by an indirect, positive link via shrub coverage.

Table 2.1. Structural equation models describing drivers of soil microbial communities three years after fire in mixed-conifer forest. Standardized coefficients are presented for paths that were significant at $\alpha=0.05$, but non-significant paths were retained in the final model at $p \leq 0.15$. The compound coefficient between total burn severity (dNBR) and the microbial characteristic of interest represents the combined direct and indirect effects of severity. Abundance of microbial groups determined via PLFA are presented on the log scale, and abundance of microbial groups determined via 16S-rDNA are sequence counts. Full-model AIC values are presented for the final models that included severity and for models in which fire occurrence (burned versus unburned) was substituted for severity. Abbreviations: C = total carbon, DBA = dead tree basal area, F:B = fungal-to-bacterial ratio, FFM = forest floor mass, LBA = live tree basal area, MB = microbial biomass, N = total nitrogen concentration, O:C = oligotroph-to-copiotroph ratio, P = extractable phosphorus, PyC = pyrogenic carbon SC = shrub coverage, , SM = soil moisture, SP = sand+POM, TIN = total inorganic nitrogen

Response Variable	Structural Equation Model	dNBR Compound Coefficient	Model Fisher's C (p-value)	Full-Model AIC
Microbial Biomass	Biomass=0.57LBA + 0.42N + 0.49SC + 0.31SP LBA=-0.64dNBR N=0.49DBA SC=-0.48LBA SP=-0.70dNBR – 0.47LBA DBA=0.61dNBR	-0.22	30.54 (0.062)	Severity: 216.13 Fire Occurrence: 224.53
General Fungi	Abundance =– 0.14dNBR + 0.93MB − 0.11SM MB=0.57LBA + 0.42N + 0.49SC + 0.31SP SM=0.47FFM LBA=−0.64dNBR N=0.49DBA SC=−0.48LBA SP=−0.70dNBR – 0.47LBA FFM=0.66LBA DBA=0.61dNBR	-0.32	70.16 (0.41)	Severity: 216.18 Fire Occurrence: 230.41

Table 2.1 (cont'd)

Gram Positive Bacteria	Abundance=–0.10LBA + 1.02MB − 0.08pH + 0.05SM − 0.08TIN LBA=−0.64dNBR MB=0.57LBA + 0.42N + 0.49SC + 0.31SP pH=0.56dNBR SM=0.47FFM TIN=−0.30LBA + 0.24N N=0.49DBA SC=−0.48LBA SP=-0.70dNBR – 0.47LBA FFM=0.66LBA DBA=0.61dNBR	-0.24	78.76 (0.75)	Severity: 119.18 Fire Occurrence: 134.09
Gram Negative Bacteria	Abundance=0.11dNBR+ 0.16LBA + 0.95MB + 0.08P LBA=−0.64dNBR MB=0.57LBA + 0.42N + 0.49SC + 0.31SP P=0.41dNBR N=0.49DBA SC=−0.48LBA SP=–0.70dNBR – 0.47LBA DBA=0.61dNBR	-0.17	54.11 (0.32)	Severity: 193.52 Fire Occurrence: 213.36
Total Bacteria	Abundance = 1.00MB MB=0.57LBA + 0.42N + 0.49SC + 0.31SP LBA=−0.64dNBR N=0.49DBA SC=−0.48LBA SP=-0.70dNBR – 0.47LBA DBA=0.61dNBR	-0.22	64.88 (0.20)	Severity: 157.97 Fire Occurrence: 169.5
Fungal−to−Bacterial Ratio	F:B=−0.51dNBR+ 0.33N − 0.40SM N=0.49DBA SM=0.66FFM DBA=0.61dNBR FFM=0.66LBA LBA=−0.64dNBR	-0.33	66.66 (0.52)	Severity: 420.23 Fire Occurrence: 454.55

Table 2.1 (cont'd)

Bacteroidetes	Abundance=0.29dNBR + 0.48pH pH=0.56dNBR	0.56	0.00 (1.00)	Severity: 761.37 Fire Occurrence: 768.15
α−Proteobacteria	Abundance=0.42LBA + 0.39pH − 0.38PyC + 0.49TIN LBA=−0.64dNBR pH=0.56dNBR TIN=−0.30LBA + 0.24N N=0.49DBA DBA=0.61dNBR	0.10	44.27 (0.38)	Severity: 797.49 Fire Occurrence: 812.71
Acidobacteria	Abundance=−0.47dNBR − 0.44pH − 0.18PyC + 0.21SP pH=0.56dNBR SP=–0.70dNBR – 0.47LBA LBA=−0.64dNBR	-0.80	19.81 (0.34)	Severity: 782.2 Fire Occurrence: 804.83
Actinobacteria	Abundance=0.39DBA + 0.54SP DBA=0.61dNBR SP=−0.70dNBR− 0.47LBA LBA=−0.64dNBR	0.02	3.78 (0.71)	Severity: 829.24 Fire Occurrence: 837.64
Bacterial Phylogenetic Diversity	BPD=0.34C − 0.43P + 0.36SP – 0.43TIN P=0.41dNBR SP=−0.70dNBR − 0.47LBA TIN=−0.30LBA + 0.24N LBA=−0.64dNBR N=0.49DBA DBA=0.61dNBR	-0.45	86.23 (0.59)	Severity: 837.10 Fire Occurrence: 853.86
Oligotroph−to−Copiotroph Ratio	O:C=−0.36dNBR − 0.66pH − 0.24SC pH=0.56dNBR SC=−0.48LBA LBA=−0.64dNBR	-0.80	35.47 (0.49)	Severity: 18.49 Fire Occurrence: 37.02

2.5 DISCUSSION

2.5.1 A systems approach revealed direct and indirect drivers of severity on plant, soil, and microbial characteristics

My results demonstrate that burn severity influences microbial communities at the ecosystem scale via simultaneous and interacting effects on plant and soil characteristics. I found evidence to support my overarching hypothesis that severity shapes microbial communities primarily via soil properties, both through direct linkages and indirectly by altering vegetation characteristics. My PCoA analyses identified severity, and vegetation and soil properties related to severity, as drivers of microbial community structure. My results agree with a previous study that found that bacterial communities were related to soil NH_4, pH, and moisture one year after a wildfire in boreal forest in China, but that study did not find that microbial community structure differed between the two burn severity categories they considered (Xiang et al. 2014a). The absence of a relationship with severity in Xiang's et al. (2014) study could suggest that one year after fire, fire occurrence alone is sufficient for explaining differences in microbial communities. Severity may become more important later through the trajectory of forest recovery if impacts of severity on plant communities become more dominant drivers of soil properties (e.g. by three years post-fire as in my study) (Hart et al. 2005). This illustrates the importance of taking an ecosystem recovery approach by simultaneously assessing plant and soil effects on microbial communities.

By leveraging a systems approach to assessing impacts of burn severity on microbial communities, after enough time for differentiation of stands recovering to different burn severities, I disentangled direct versus indirect drivers of soil microbial communities. I found some support for my hypothesis that vegetation characteristics functioned as indirect, rather than

direct, drivers of soil microbial communities via an influence on soil properties, however there were several instances where vegetation properties were directly linked to microbial groups (Table 2.1). Direct links between vegetation and microbial groups could be caused by differences in the amount or type of litter inputs to soil, mutualistic relationships with mycorrhizae and rhizospheric bacteria, or losses in canopy shading affecting soil temperature (Hart et al. 2005).

I found support for my hypothesis that accounting for burn severity instead of fire occurrence only would better explain changes to the microbial community. Full-model AICs indicated that SEMs that included severity had more explanatory power than fire occurrence in every instance, despite univariate model AICs indicating that fire occurrence was more supported for explaining differences in some microbial groups. This may be because severity-based linear models capture more of the variability of the responses of soil and vegetation characteristics to fire and tend to exhibit lower AIC values than fire-occurrence linear models (for example, see Figs 2.1- 2.3).

2.5.2 Burn severity has direct and indirect effects on fungal abundance

My systems approach provided evidence that the direct negative impacts of fire on fungal abundance persist three years post-fire and that these impacts are modulated by indirect effects of burn severity on soil moisture via live tree basal area and forest floor mass. The direct negative link between total burn severity and absolute fungal abundance could be due to soil heating causing increased fungal mortality (Neary and DeBano 2005) or slower fungal recovery compared to bacteria (D'Ascoli et al. 2005; Mabuhay et al. 2006). The greater tolerance of bacteria compared to fungi for high soil pH has been invoked to explain decreases in fungal abundance in recently burned ecosystems (Dooley and Treseder 2012), but I did not observe

relationships between pH and fungal abundance. Instead, I found that soil moisture and total N were the only edaphic characteristics directly related to fungal abundance.

The negative relationship between soil moisture and fungi may result in stronger decreases in fungal abundance in high severity areas during the wetter winter and spring months compared to the drier summer and fall. This is because fire-induced changes to forest structure can affect soil moisture in two different ways that may vary in importance seasonally. Decreased plant biomass can reduce soil water uptake and evapotranspiration, thereby increasing soil moisture (Neary and DeBano 2005). Conversely, decreases in canopy and forest floor cover can increase soil exposure to solar radiation, increasing evaporation (Holden et al. 2015). More than 75% of the annual precipitation in my study area occurs during the winter and spring (NCEI-NOAA 2017); thus, in the spring months when snowmelt and precipitation is abundant, decreased plant evapotranspiration may lead to greater soil moisture in high severity stands compared to lower severity stands, whereas in the summer and fall months when precipitation is limited, increased evaporation may lead to lower soil moisture. As a result, fungal abundance may be even lower in high severity areas during the wet months than the dry months when I collected my samples. Changes in soil fungal abundance could impact the soil C cycle by altering the types of C substrates utilized and because fungal biomass has slower turnover than bacterial biomass (Rousk and Bååth 2011). Therefore, decreases in fungal abundance may increase the post-fire CO_2 efflux, acting as a positive feedback between fire and climate change.

2.5.3 Burn severity impacts on bacterial communities are driven by nutrients, pH, and soil texture

Bacterial phylogenetic diversity was lower in burned areas than unburned areas, but the impacts of severity on diversity only became clear when accounting for soil nutrients and

texture. This provides context to a meta-analysis by Pressler et al. (2018), which found no significant effects of fire on bacterial diversity, although individual studies have found negative relationships between fire and bacterial diversity (Pérez-Valera et al. 2017; Sáenz de Miera et al. 2020). The apparent lack of response of bacterial diversity to fire in many studies may be due to those studies not accounting for indirect effects of fire on diversity via soil nutrients. Fire-induced increases in extractable soil P and TIN are ephemeral, often dissipating within two years (Wan et al. 2001; Certini 2005). Therefore, decreases in bacterial diversity in response to fire may be short-lived and difficult to detect, especially following low-severity fires where the nutrient spike is smaller or dissipates earlier (Adkins et al. 2019b). Links between microbial communities and soil nutrients may result in seasonally dynamic community characteristics. Increased liberation of P and TIN from plant litter during periods of greater decomposition (e.g. in warm, wet spring months; Dove et al., 2020) could lead to apparently lower phylogenetic diversity compared to periods when low decomposition limits nutrient availability. Decreases in bacterial biodiversity may affect soil C and nutrient cycles by decreasing functional diversity and redundancy (Wagg et al. 2019). For example, a meta-analysis of studies that manipulated soil microbial diversity indicated that soil respiration rates increase with diversity; however, the diversity levels in manipulative experiments may not match the high biodiversity present in natural ecosystems, and thus may overestimate the impacts on the C cycle (de Graaff et al. 2015). In contrast to the effects of post-fire decreases in fungal abundance, decreases in microbial diversity may down-regulate the post-fire CO_2 efflux.

Soil pH was a primary correlate of changes in abundance of the two most abundant bacterial phyla in my study (i.e. *Bacteroidetes, Acidobacteria*). The relationship to pH may explain the commonly observed increases of *Bacteroidetes* abundance (Weber et al. 2014; Xiang

et al. 2014a; Pérez-Valera et al. 2019) and decreases of *Acidobacteria* abundance (Weber et al. 2014; Rodríguez et al. 2018; Whitman et al. 2019) in response to fire, because increased soil pH is a typical response to fire (Certini 2005). *Bacteroidetes* and *Acidobacteria* phyla are among the most dominant bacterial phyla in biomes across the globe (Janssen 2006; Fierer et al. 2012b; Docherty et al. 2015), and due to the different growth strategies of these phyla (Fierer et al. 2007; Ho et al. 2017), their relative abundances likely play an important role in soil C cycling (e. g. Fierer et al., 2007). The changes in *Bacteroidetes* and *Acidobacteria* abundance drove the decrease in O:C I observed across the severity gradient. This is a contrast to suggestions by other authors that copiotrophic taxa should give way to oligotrophic taxa as soon as 16 weeks after wildfire (Ferrenberg et al. 2013). However, rather than the pH driven changes I observed, the shift to oligotrophic taxa in other burned systems may be due to losses in soil organic matter (Ferrenberg et al. 2013). Nutrient availability was not a primary driver of O:C as others have found (Fierer et al. 2007; Fierer et al. 2012a; Ramirez et al. 2012), which may reflect increased competition by plants for soil nutrients in burned ecosystems. Indeed, I found that TIN was negatively related to live tree basal area.

Although bacterial taxa are often classified as oligotrophic or copiotrophic at the phylum level, lower taxonomic rankings (e.g. family and genera) can exhibit variable growth strategies (Ho et al. 2017), and divergent responses to fire (Whitman et al. 2019). For example, although I found that the average $\log_2$-fold change of *Bacteroidetes* OTUs in burned versus unburned areas was positive, OTUs within the most abundant *Bacteroidetes* families exhibited both positive and negative responses to fire occurrence. *Chitinophagaceae, Cytophagaceae*, *Sphingobacteriaceae,* and *Flavobacteriaceae* OTUs exhibited higher abundance in burned areas, agreeing with research that has identified OTUs from these families as positive fire responders within one year

post-fire in a boreal forest in Canada (Whitman et al. 2019) and ponderosa pine and mixed-conifer forests in New Mexico (Weber et al. 2014). The response of groups within the *Acidobacteria* phylum have varied among studies. I and others found that *Acidobacteria* OTUs from *Blastocatellaceae* (subgroup 4) and *Solibacteraceae* (subgroup 3) displayed lower abundance in burned areas (Whitman et al. 2019), but subgroup 4 genera have also been associated with burned soils (Weber et al. 2014). Likewise, my finding that *Acidobacteriaceae* (subgroup 1) OTUs displayed lower abundance in burned areas supports previous observations (Weber et al. 2014), but others have identified a positive response of OTUs from this family (Whitman et al. 2019). Although I found *Actinobacteria* phylum abundance was lower in burned areas, OTUs from my study's most abundant *Actinobacteria* family, *Micrococcaceae,* exhibited greater abundance in burned areas, as others have found (Weber et al. 2014; Sáenz de Miera et al. 2020). *Mycobacteriaceae* OTUs exhibited lower abundance in burned areas, in contrast to a study that found that *Mycobacteria* were dominant in both burned and unburned soils in a pine-oak forest in New Jersey, USA (Mikita-Barbato et al. 2015). Some *Mycobacteria* are effective degraders of aromatic compounds (Bastiaens et al. 2000), and thus might exhibit higher abundance when fire increases soil PyC. However, *Mycobacteria* abundance is also higher at low pH (Norby et al. 2007), so fire-driven increases in pH may limit this response.

2.6 CONCLUSIONS

I found that that burn severity affects the magnitude of persistent effects on the soil microbial community by influencing vegetation and soil characteristics in mixed-conifer forest. I also found that remotely sensed severity estimates (dNBR) mostly outperformed field-validated soil burn severity estimates for explaining changes in soil properties, for soil samples at an intermediate (three years) time point after fire. This is an important finding that has potential to

expand research capabilities at intermediate post-fire time points because dNBR can be easily calculated in areas where Landsat imagery is available. I linked changes to microbial communities to environmental properties that correlate with severity and are slow to recover from fire (e.g. forest floor mass, live tree basal area). This suggests that changes to microbial communities may persist for years after fire, which may lead to broad-scale effects on ecosystem functions, especially if forecasted increases in fire activity result in greater extent of high severity burns. My systems approach to addressing the influence of fire on microbial communities demonstrates the importance of considering the interconnectedness of environmental characteristics for understanding drivers of microbial community recovery from fire, and I recommend that researchers apply this approach to future studies. The systems approach could also be extended to investigate how plant, soil, and microbial characteristics interact to influence ecosystem functions over multiple timescales. For example, previous research has demonstrated that fire alters soil C flux rates for years to decades (Adkins et al. 2019b; Dove et al. 2020). The fire-induced changes to microbial communities I observed—particularly the decreased fungal abundance and O:C—could have long-term impacts on the soil C cycle across the severity gradient by replacing slow C cycling microbial groups with fast C cycling groups. A systems approach could elucidate whether changes in C flux are driven by microbial community changes or whether other environmental characteristics are dominant drivers.

APPENDIX

SUPPLEMENTAL FIGURES

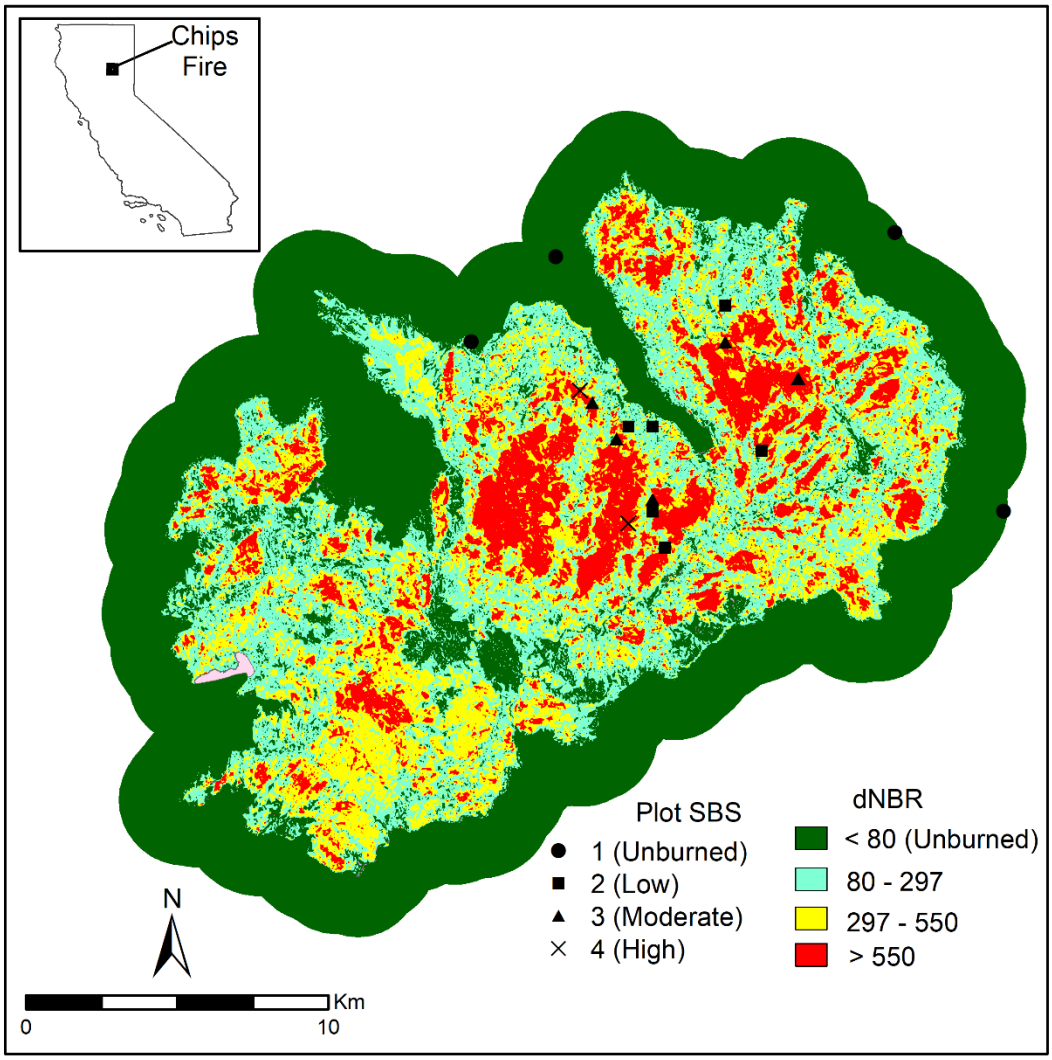

Figure S2.1 Locations of field plots within a burn severity matrix resulting from the Chips Fire. dNBR values are grouped into unburned, low, moderate, and high severity thresholds identified by the Monitoring Trends in Burn Severity team.

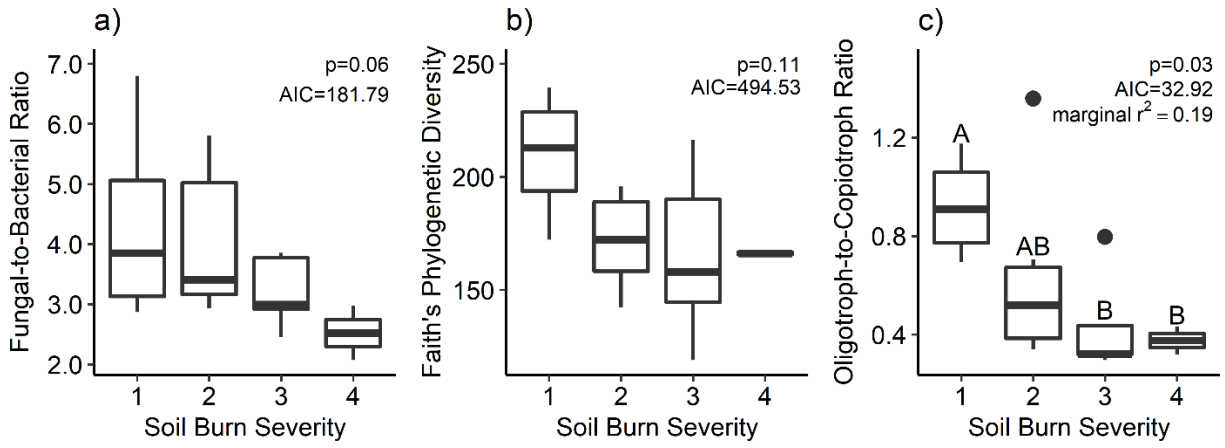

Figure S2.3 Relationship of lipid-based fungal-to-bacterial ratio, 16S-based Faith's phylogenetic diversity, and 16S-based oligotrophic:copiotrophic bacterial taxa ratio with soil burn severity in mineral soils (0-5 cm). Soil burn severity values of 1 are unburned plots, 2 are low SBS, 3 are moderate SBS, and 4 are high SBS. Marginal r^2 values are provided for microbial community characteristics that linear mixed models indicated were significantly affected by soil burn severity α=0.05. Capital letters in figures denote Tukey-adjusted significant differences among soil burn severity levels.

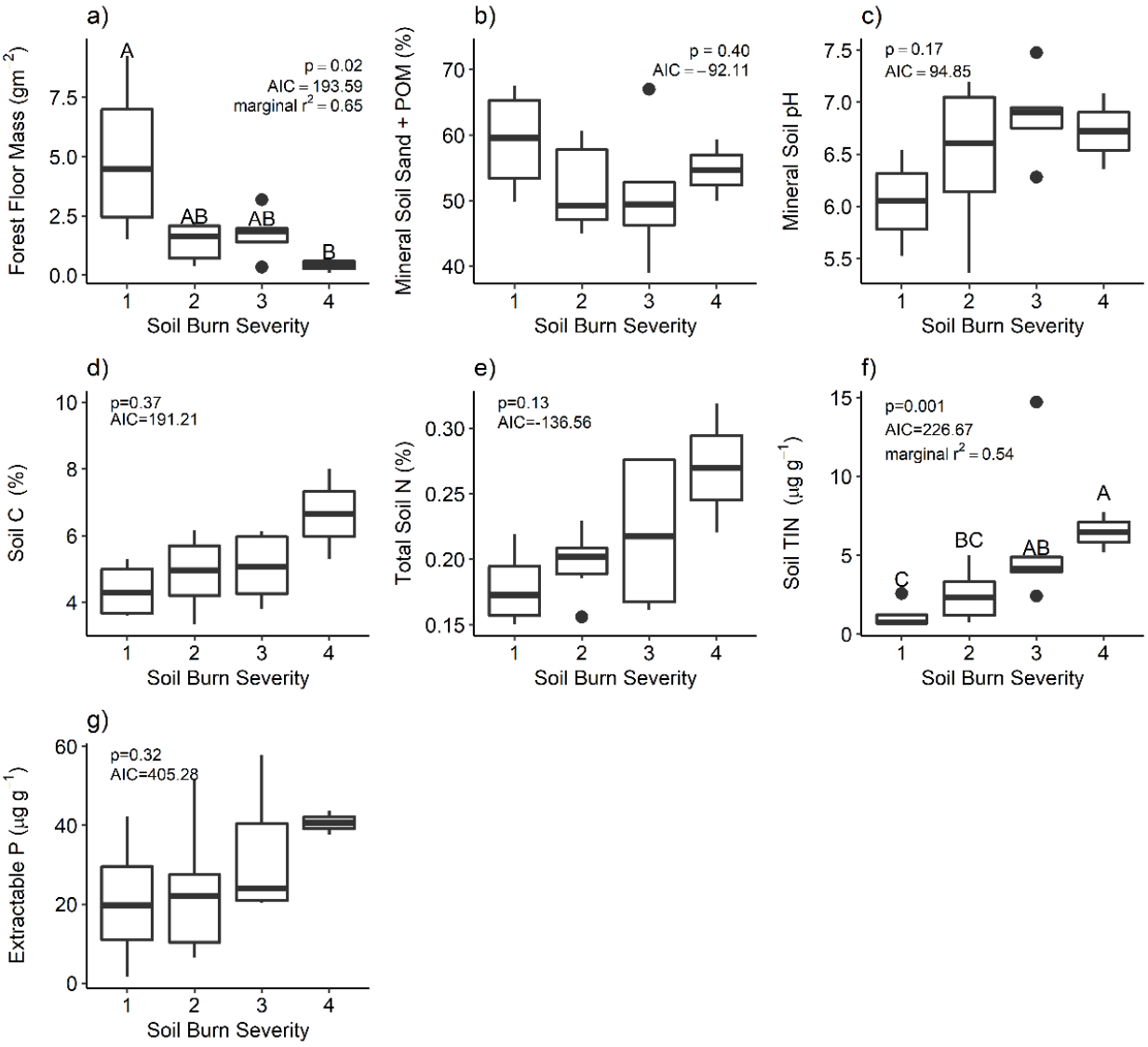

Figure S2.2 Relationship of soil burn severity with soil properties. Soil burn severity values of 1 are unburned plots, 2 are low SBS, 3 are moderate SBS, and 4 are high SBS. Marginal r^2 values are provided for soil properties that linear mixed models indicated were significantly affected by the soil burn severity at α=0.05. Capital letters denote Tukey-adjusted significant differences among soil burn severity levels.

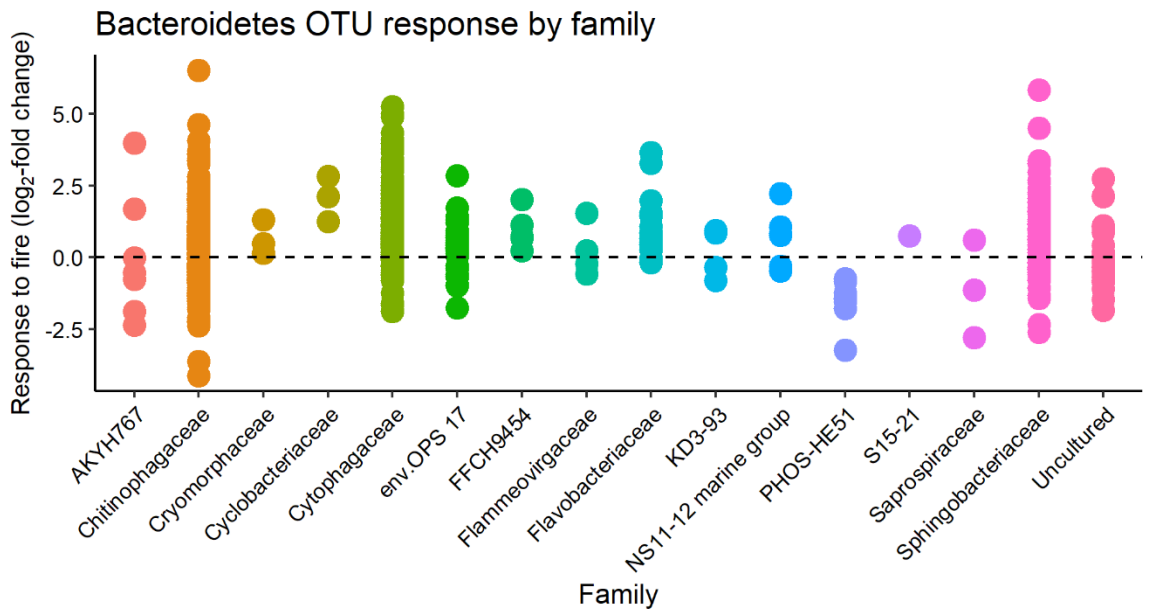

Figure S2.3 Log2-fold response to fire for OTUs grouped by family within *Bacteroidetes* for mineral soils collected to 5 cm three years after the Chips Fire burned mixed-conifer forest in the Sierra Nevada Mountain Range, California, USA in 2012.

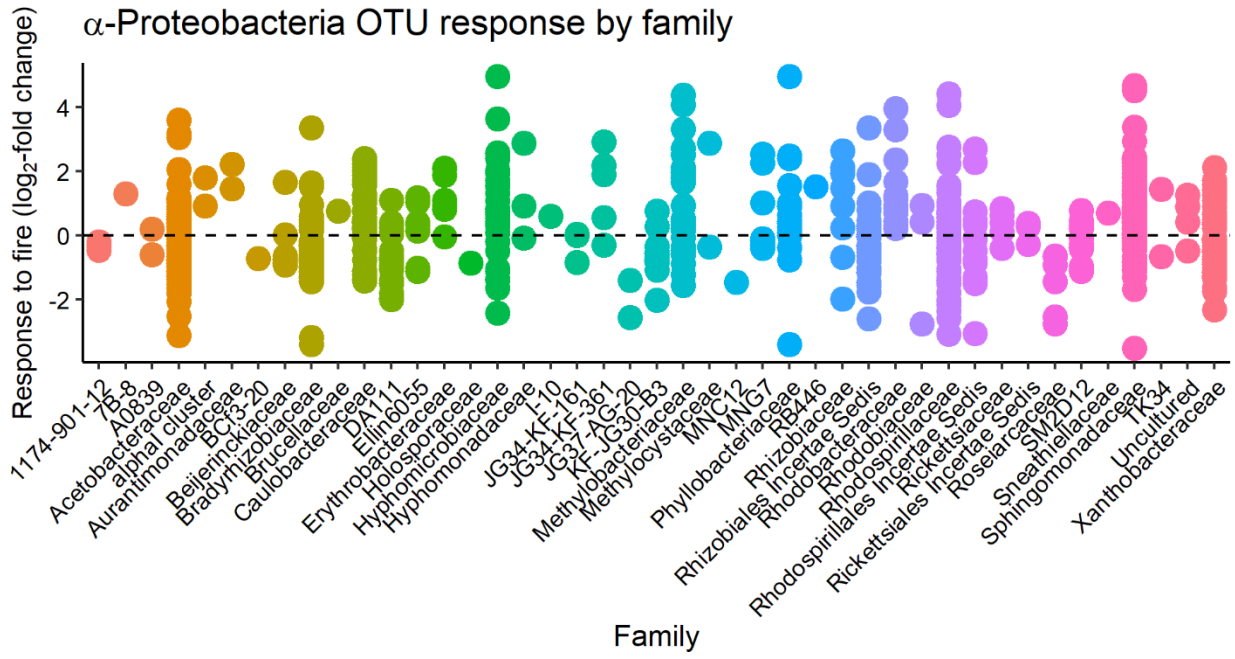

Figure S2.4 Log2-fold response to fire for OTUs grouped by family within *α-Proteobacteria* for mineral soils collected to 5 cm.

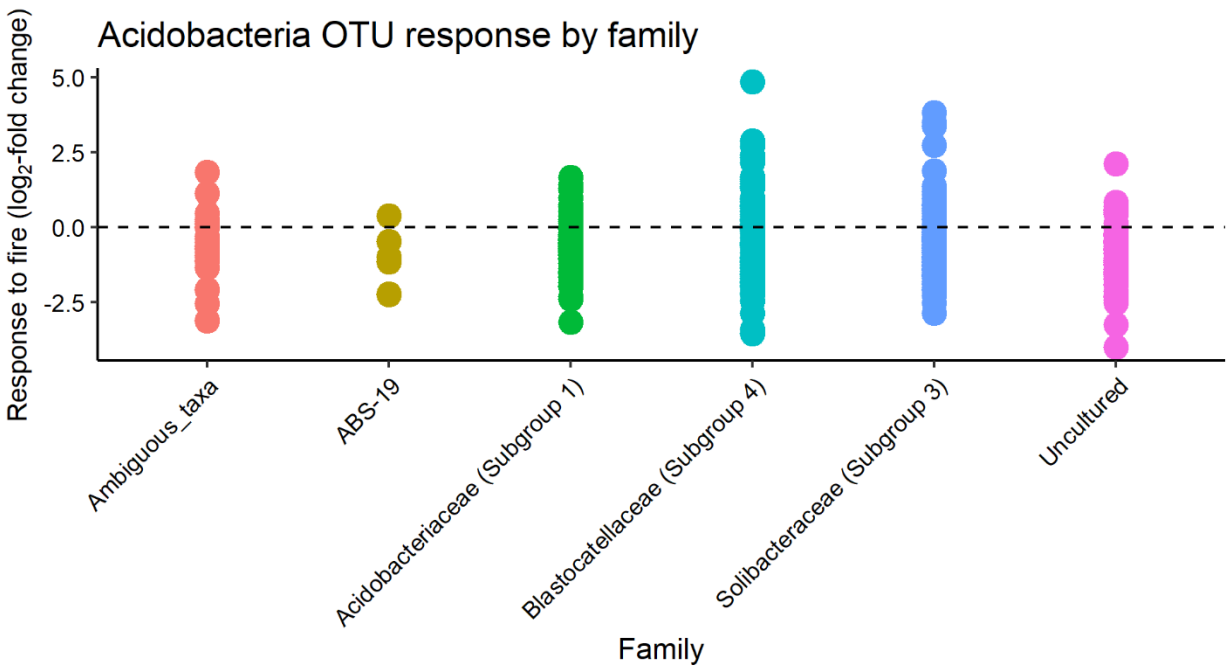

Figure S2.5 Log$_2$-fold response to fire for OTUs grouped by family within *Acidobacteria* for mineral soils collected to 5 cm.

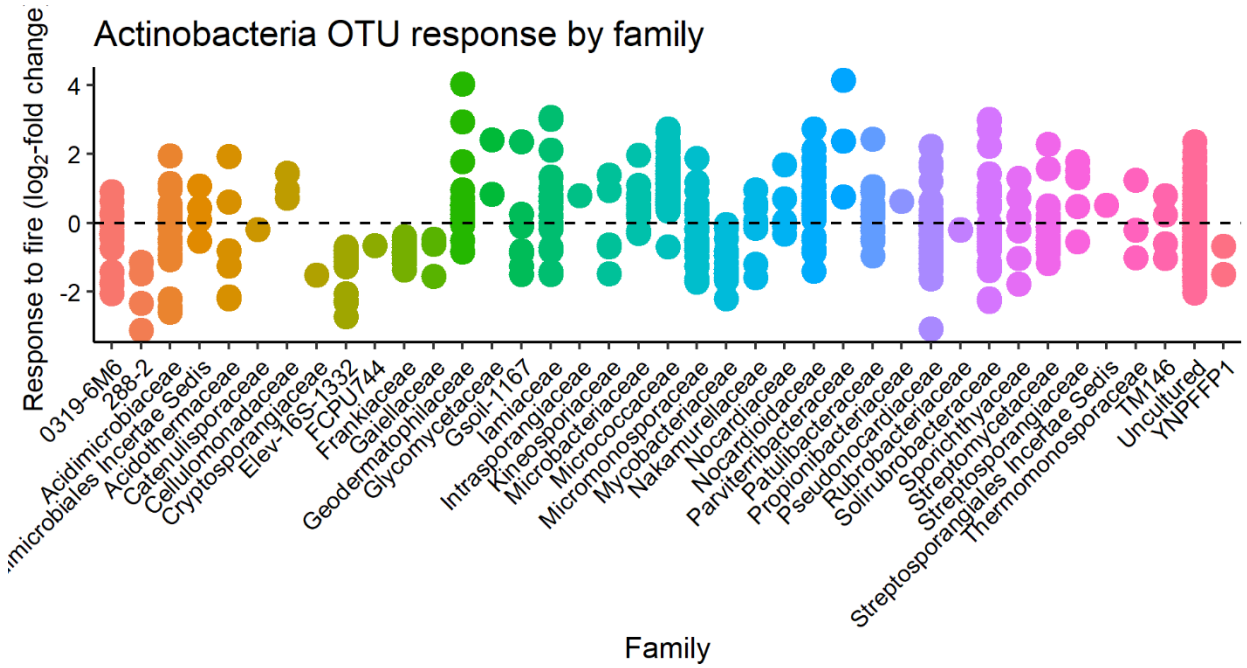

Figure S2.6 Log$_2$-fold response to fire for OTUs grouped by family within *Actinobacteria* for mineral soils collected to 5 cm.

REFERENCES

REFERENCES

Adkins J, Sanderman J, Miesel J (2019) Soil carbon pools and fluxes vary across a burn severity gradient three years after wildfire in Sierra Nevada mixed-conifer forest. Geoderma 333:10–22. doi: 10.1016/j.geoderma.2018.07.009

Alvey EC (2016) Early seral mixed-conifer forest structure and composition following a wildfire reburn in the Sierra Nevada. Humboldt State University

Baldrian P, Kolaiřík M, Štursová M, et al (2012) Active and total microbial communities in forest soil are largely different and highly stratified during decomposition. ISME J 6:248–258. doi: 10.1038/ismej.2011.95

Balser TC, McMahon KD, Bart D, et al (2006) Bridging the gap between micro - and macro-scale perspectives on the role of microbial communities in global change ecology. Plant Soil 289:59–70. doi: 10.1007/s11104-006-9104-5

Bastiaens L, Springael D, Wattiau P, et al (2000) Isolation of Adherent Polycyclic Aromatic Hydrocarbon (PAH) - Degrading Bacteria Using PAH-Sorbing Carriers. 66:1834–1843.

Bier RL, Bernhardt ES, Boot CM, et al (2015) Linking microbial community structure and microbial processes: An empirical and conceptual overview. FEMS Microbiol Ecol 91:1–11. doi: 10.1093/femsec/fiv113

Bligh EG, Dyer WJ (1959) A rapid method of total lipid extraction and purification. Can J Biochem Physiol 37:911–917.

Cambardella CA, Elliott ET (1993) Methods for physical separation and characterization of soil organic matter fractions. Geoderma 56:449–457. doi: 10.1016/0016-7061(93)90126-6

Caporaso JG, Kuczynski J, Stombaugh J, et al (2010) QIIME allows analysis of high- throughput community sequencing data Intensity normalization improves color calling in SOLiD sequencing. Nat Publ Gr 7:335–336. doi: 10.1038/nmeth0510-335

Certini G (2005) Effects of fire on properties of forest soils: a review. Oecologia 143:1–10. doi: 10.1007/s00442-004-1788-8

Cutler NA, Arróniz-Crespo M, Street LE, et al (2017) Long-Term Recovery of Microbial Communities in the Boreal Bryosphere Following Fire Disturbance. Microb Ecol 73:75–90. doi: 10.1007/s00248-016-0832-7

Czimczik CI, Masiello C a. (2007) Controls on black carbon storage in soils. Global Biogeochem Cycles 21:1–8. doi: 10.1029/2006GB002798

D'Ascoli R, Rutigliano FA, De Pascale RA, et al (2005) Functional diversity of the microbial community in Mediterranean maquis soils as affected by fires. Int J Wildl Fire 14:355. doi: 10.1071/WF05032

de Graaff M-A, Adkins J, Kardol P, Throop HL (2015) A meta-analysis of soil biodiversity impacts on the carbon cycle. 1:257–271. doi: 10.5194/soil-1-257-2015

Dennison PE, Brewer SC, Arnold JD, Moritz MA (2014) Large wildfire trends in the western United States, 1984-2011. Geophys Res Lett 41:2928–2933. doi: 10.1002/2014GL059576

Doane TA, Horwáth WR (2003) Spectrophotometric determination of nitrate with a single reagent. Anal Lett 36:2713–2722. doi: 10.1081/AL-120024647

Docherty KM, Borton HM, Espinosa N, et al (2015) Key edaphic properties largely explain temporal and geographic variation in soil microbial communities across four biomes. PLoS One 10:1–23. doi: 10.1371/journal.pone.0135352

Dooley SR, Treseder KK (2012) The effect of fire on microbial biomass: A meta-analysis of field studies. Biogeochemistry 109:49–61. doi: 10.1007/s10533-011-9633-8

Dove NC, Safford HD, Bohlman GN, et al (2020) High-severity wildfire leads to multi-decadal impacts on soil biogeochemistry in mixed-conifer forests. Ecol Appl 0:1–18. doi: 10.1002/eap.2072

Edgar RC (2010) Search and clustering orders of magnitude faster than BLAST. Bioinformatics 26:2460–2461. doi: 10.1093/bioinformatics/btq461

Faith DP (1992) Conservation evaluation and phylogentic diversity. Biol Conserv 61:1–10. doi: 10.1890/0012-9658(2006)87[1465:ATTFHF]2.0.CO;2

Ferrenberg S, O'neill SP, Knelman JE, et al (2013) Changes in assembly processes in soil bacterial communities following a wildfire disturbance. ISME J 7:1102–1111. doi: 10.1038/ismej.2013.11

Ficken CD, Wright JP (2017) Contributions of microbial activity and ash deposition to post-fire nitrogen availability in a pine savanna. Biogeosciences 14:241–255. doi: 10.5194/bg-14-241-2017

Fierer N, Bradford MA, Jackson RB (2007) Toward an ecological classification of soil bacteria. Ecology 88:1354–1364. doi: 10.1890/05-1839

Fierer N, Lauber CL, Ramirez KS, et al (2012a) Comparative metagenomic, phylogenetic and physiological analyses of soil microbial communities across nitrogen gradients. ISME J 6:1007–1017. doi: 10.1038/ismej.2011.159

Fierer N, Leff JW, Adams BJ, et al (2012b) Cross-biome metagenomic analyses of soil microbial communities and their functional attributes. Proc Natl Acad Sci 109:21390–21395. doi: 10.1073/pnas.1215210110

Flannigan MD, Cantin AS, de Groot WJ, et al (2013) Global wildland fire season severity in the 21st century. For Ecol Manage 294:54–61. doi: 10.1016/j.foreco.2012.10.022

Fornwalt PJ, Stevens-Rumann CS, Collins BJ (2018) Overstory structure and surface cover dynamics in the decade following the hayman fire, Colorado. Forests 9:1–17. doi: 10.3390/f9030152

Friedman J, Alm EJ (2012) Inferring Correlation Networks from Genomic Survey Data. PLoS Comput Biol 8:1–11. doi: 10.1371/journal.pcbi.1002687

Grace JB (2006) Structural Equation Modeling and Natural Systems. Cambridge Univ Press, West Nyack, GB

Hart SC, DeLuca TH, Newman GS, et al (2005) Post-fire vegetative dynamics as drivers of microbial community structure and function in forest soils. For Ecol Manage 220:166–184. doi: 10.1016/j.foreco.2005.08.012

Ho A, Di Lonardo DP, Bodelier PLE (2017) Revisiting life strategy concepts in environmental microbial ecology. FEMS Microbiol Ecol 93:1–14. doi: 10.1093/femsec/fix006

Holden SR, Berhe AA, Treseder KK (2015) Decreases in soil moisture and organic matter quality suppress microbial decomposition following a boreal forest fire. Soil Biol Biochem 87:1–9. doi: 10.1016/j.soilbio.2015.04.005

Holden SR, Rogers BM, Treseder KK, Randerson JT (2016) Fire severity influences the response of soil microbes to a boreal forest fire. Environ Res Lett 11:035004. doi: 10.1088/1748-9326/11/3/035004

Janssen PH (2006) Identifying the dominant soil bacterial taxa in libraries of 16S rRNA and 16S rRNA Genes. Appl Environ Microbiol 72:1719–1728. doi: 10.1128/AEM.72.3.1719-1728.2006

Jansson JK, Hofmockel KS (2020) Soil microbiomes and climate change. Nat Rev Microbiol 18:35–46. doi: 10.1038/s41579-019-0265-7

Joergensen RG, Wichern F (2008) Quantitative assessment of the fungal contribution to microbial tissue in soil. Soil Biol Biochem 40:2977–2991. doi: 10.1016/j.soilbio.2008.08.017

Keeley JE (2009) Fire intensity, fire severity and burn severity: A brief review and suggested usage. Int J Wildl Fire 18:116–126. doi: 10.1071/WF07049

Kurth VJ, MacKenzie MD, DeLuca TH (2006) Estimating charcoal content in forest mineral soils. Geoderma 137:135–139. doi: 10.1016/j.geoderma.2006.08.003

Lauber CL, Hamady M, Knight R, Fierer N (2009) Pyrosequencing-based assessment of soil pH as a predictor of soil bacterial community structure at the continental scale. Appl Environ Microbiol 75:5111–5120. doi: 10.1128/AEM.00335-09

LeDuc SD, Lilleskov EA, Horton TR, Rothstein DE (2013) Ectomycorrhizal fungal succession coincides with shifts in organic nitrogen availability and canopy closure in post-wildfire jack pine forests. Oecologia 172:257–269. doi: 10.1007/s00442-012-2471-0

Lefcheck JS (2016) piecewiseSEM: Piecewise structural equation modelling in r for ecology, evolution, and systematics. Methods Ecol Evol 7:573–579. doi: 10.1111/2041-210X.12512

Mabuhay JA, Nakagoshi N, Isagi Y (2006) Soil microbial biomass, abundance, and diversity in a Japanese red pine forest: First year after fire. J For Res 11:165–173. doi: 10.1007/s10310-005-0201-8

Maestrini B, Alvey EC, Hurteau MD, et al (2017) Fire severity alters the distribution of pyrogenic carbon stocks across ecosystem pools in a Californian mixed-conifer forest. J Geophys Res Biogeosciences 122:2338–2355. doi: 10.1002/2017JG003832

Mallek CM, Safford H, Viers J, Miller JD (2013) Modern departures in fire severity and area vary by forest type, Sierra Nevada and southern Cascades, California, USA. Ecosphere 4:1–28. doi: 10.1890/ES13-00217

Masella AP, Bartram AK, Truszkowski JM, et al (2012) PANDAseq: paired-end assembler for illumina sequences. BMC Bioinformatics 13:31. doi: 10.1186/1471-2105-13-31

McLauchlan KK, Higuera PE, Miesel J, et al (2020) Fire as a fundamental ecological process: research advances and frontiers. J Ecol 1365-2745.13403. doi: 10.1111/1365-2745.13403

McMurdie PJ, Holmes S (2014) Waste Not, Want Not: Why Rarefying Microbiome Data Is Inadmissible. PLoS Comput Biol. doi: 10.1371/journal.pcbi.1003531

Mikita-Barbato RA, Kelly JJ, Tate RL (2015) Wildfire effects on the properties and microbial

community structure of organic horizon soils in the New Jersey Pinelands. Soil Biol Biochem 86:67–76. doi: 10.1016/j.soilbio.2015.03.021

Miller JD, Safford HD (2017) Corroborating evidence of a pre-Euro-American low- to moderate-severity fire regime in yellow pine–mixed conifer forests of the Sierra Nevada, California, USA. Fire Ecol 13:58–90. doi: 10.4996/fireecology.1301058

Miller JD, Safford HD, Crimmins M, Thode AE (2009) Quantitative evidence for increasing forest fire severity in the Sierra Nevada and southern Cascade Mountains, California and Nevada, USA. Ecosystems 12:16–32. doi: 10.1007/s10021-008-9201-9

MTBS (2017) Monitoring trends in burn severity. https://www.mtbs.gov.

NCEI-NOAA (2017) National centers for environmental information. https://www.ncei.noaa.gov.

Neary D., DeBano L. (2005) Wildland fire in ecosystems effects of fire on soil and water.

Neary DG., Ryan KC., DeBano LF (eds) (2005) Wildland Fire in Ecosystems: effects of fire on soil and water. U.S. Dept. of Agriculture, Forest Service, Rocky Mountain Research Station, Ogden, UT

Norby B, Fosgate GT, Manning EJB, et al (2007) Environmental mycobacteria in soil and water on beef ranches : Association between presence of cultivable mycobacteria and soil and water physicochemical characteristics §. 124:153–159. doi: 10.1016/j.vetmic.2007.04.015

Oksanen J, Blanchet FG, Friendly M, et al (2019) vegan: Community Ecology Package.

Olsen SR, Cole CV, Watanable FS, Dean LA (1954) Estimation of available phosphorus in soils by extraction with sodium bicarbonate.

Orwin KH, Dickie IA, Holdaway R, Wood JR (2018) A comparison of the ability of PLFA and 16S rRNA gene metabarcoding to resolve soil community change and predict ecosystem functions. Soil Biol Biochem 117:27–35. doi: 10.1016/j.soilbio.2017.10.036

Parsons A, Robichaud PR, Lewis S a, et al (2010) Field guide for mapping post-fire soil burn severity. Gen. Tech. Rep. RMRS-GTR-243

Pérez-Valera E, Goberna M, Faust K, et al (2017) Fire modifies the phylogenetic structure of soil bacterial co-occurrence networks. Environ Microbiol 19:317–327. doi: 10.1111/1462-2920.13609

Pérez-Valera E, Goberna M, Verdú M (2019) Fire modulates ecosystem functioning through the

phylogenetic structure of soil bacterial communities. Soil Biol Biochem 129:80–89. doi: 10.1016/j.soilbio.2018.11.007

Perry DA, Oren R, Hart SC (2008) Forest Ecosystems. Johns Hopkins University Press, Baltimore

Pinheiro J, Bates D, Debroy S, Sarkar D (2019) nlme: Linear and nonlinear mixed effects models.

Prendergast-Miller MT, de Menezes AB, Macdonald LM, et al (2017) Wildfire impact: Natural experiment reveals differential short-term changes in soil microbial communities. Soil Biol Biochem 109:1–13. doi: 10.1016/j.soilbio.2017.01.027

Pressler Y, Moore JC, Cotrufo MF (2018) Belowground community responses to fire: meta-analysis reveals contrasting responses of soil microorganisms and mesofauna. Oikos 1–19. doi: 10.1111/oik.05738

Quast C, Pruesse E, Yilmaz P, et al (2013) The SILVA ribosomal RNA gene database project: Improved data processing and web-based tools. Nucleic Acids Res 41:590–596. doi: 10.1093/nar/gks1219

R Core Team (2019) R: A language and environment for statistical computing.

Ramirez KS, Craine JM, Fierer N (2012) Consistent effects of nitrogen amendments on soil microbial communities and processes across biomes. Glob Chang Biol 18:1918–1927. doi: 10.1111/j.1365-2486.2012.02639.x

Robinson MD, McCarthy DJ, Smyth GK (2010) edgeR: a Bioconductor package for differential expression analysis of digital gene expression data. Bioinformatics 26:139–140.

Rodríguez J, González-Pérez JA, Turmero A, et al (2018) Physico-chemical and microbial perturbations of Andalusian pine forest soils following a wildfire. Sci Total Environ 634:650–660. doi: 10.1016/j.scitotenv.2018.04.028

Rousk J, Bååth E (2011) Growth of saprotrophic fungi and bacteria in soil. FEMS Microbiol Ecol 78:17–30. doi: 10.1111/j.1574-6941.2011.01106.x

Rousk J, Bååth E, Brookes PC, et al (2010) Soil bacterial and fungal communities across a pH gradient in an arable soil. ISME J 4:1340–1351. doi: 10.1038/ismej.2010.58

Ruefenacht B, Finco MV, Nelson MD, et al (2008) Conterminous U.S. and Alaska Forest Type Mapping Using Forest Inventory and Analysis Data. Photogramm Eng Remote Sens 74:1379–1388. doi: 10.14358/PERS.74.11.1379

Sáenz de Miera LE, Pinto R, Gutierrez-Gonzalez JJ, et al (2020) Wildfire effects on diversity and composition in soil bacterial communities. Sci Total Environ. doi: 10.1016/j.scitotenv.2020.138636

Safford HD, Miller JD, Schmidt D, et al (2008) BAER soil burn severity maps do not measure fire effects to vegetation: A comment on Odion and Hanson (2006). Ecosystems 11:1–11. doi: 10.1007/s10021-007-9094-z

Schmidt J, Schulz E, Michalzik B, et al (2015) Carbon input and crop-related changes in microbial biomarker levels strongly affect the turnover and composition of soil organic carbon. Soil Biol Biochem 85:39–50. doi: 10.1016/j.soilbio.2015.02.024

Shipley B, Douma JC (2020) Generalized AIC and chi-squared statistics for path models consistent with directed acyclic graphs. Ecology 101:e02960. doi: 10.1002/ecy.2960

Sinsabaugh RL, Reynolds H, Long TM (2000) Rapid assay for amidohydrolase (urease) activity in environmental samples. Soil Biol Biochem 32:2095–2097. doi: 10.1016/S0038-0717(00)00102-4

Treseder KK, Mack MC, Cross A (2004) Relationships among fires, fungi, and soil dynamics in Alaskan boreal forests. Ecol Appl 14:1826–1838.

Ulery AL, Graham RC (1993) Forest Fire Effects on Soil Color and Texture. Soil Sci Soc Am J 57:135–140. doi: 10.2136/sssaj1993.03615995005700010026x

USDA (2015) FSVEG Common Stand Exam User Guide. USDA Forest Service, Washington, DC

Wagg C, Schlaeppi K, Banerjee S, et al (2019) Fungal-bacterial diversity and microbiome complexity predict ecosystem functioning. Nat Commun 10:1–10. doi: 10.1038/s41467-019-12798-y

Wan S, Hui D, Luo Y (2001) Fire effects on nitrogen pools and dynamics in terrestrial ecosystems: A meta-analysis. Ecol Appl 11:1349–1365.

Weber CF, Lockhart JS, Charaska E, et al (2014) Bacterial composition of soils in ponderosa pine and mixed conifer forests exposed to different wildfire burn severity. Soil Biol Biochem 69:242–250. doi: 10.1016/j.soilbio.2013.11.010

Weiss S, Xu ZZ, Peddada S, et al (2017) Normalization and microbial differential abundance strategies depend upon data characteristics. Microbiome 5:1–18. doi: 10.1186/s40168-017-0237-y

Westerling AL, Hidalgo HG, Cayan DR, Swetnam TW (2006) Warming and earlier spring increase western U.S. forest wildfire activity. Science 313:940–943. doi: 10.1126/science.1128834

Whitman T, Whitman E, Woolet J, et al (2019) Soil bacterial and fungal response to wildfires in the Canadian boreal forest across a burn severity gradient. Soil Biol Biochem 138:107571. doi: 10.1016/j.soilbio.2019.107571

Xiang X, Shi Y, Yang J, et al (2014) Rapid recovery of soil bacterial communities after wildfire in a Chinese boreal forest. Sci Rep 4:1–8. doi: 10.1038/srep03829

CHAPTER 3:

DETERMINING LINKS BETWEEN BACTERIAL LIFE-STRATEGIES AND SOIL CARBON POOLS ONE-YEAR POST-FIRE

3.1 ABSTRACT

Wildfire and burn severity influence soil microbial community structure during post-fire recovery. If post-fire differences in microbial communities affect the dynamics of soil carbon (C) pools, these altered microbial communities could govern the transition of forests from C sources to C sinks during post-fire recovery. For example, fire may change the abundance of copiotrophic and oligotrophic bacterial taxa, which have the potential to influence the kinetic rates of soil C pools due to differences in C-acquisition strategies and nutrient requirements. I assessed differences in soil bacterial community structure and soil C pool kinetics one year after a wildfire in a mixed-conifer forest in northern California, USA. I determined whether differences in bacterial communities and C pool kinetics were related to copiotrophic versus oligotrophic life history strategies. Specifically, I assessed how bacterial taxa were related to the availability of inorganic nitrogen, phosphorus, and the active C pool. I further assessed whether bacterial taxa that have traditionally been classified as oligotrophs or copiotrophs were correlated with C pool kinetic rates. I found that bacteria classified as copiotrophs at the phylum level exhibited greater abundance in burned areas compared to unburned areas, whereas oligotrophic phyla exhibited lower abundance in burned versus unburned areas. I found that soil C persistence increased with burn severity, as evidenced by decreases in the kinetic rate of the non-active C pool. The kinetic rate of the non-active C pool was positively related to *Elusimicrobia* abundance, a suspected oligotrophic phylum. At the phylum level, copiotrophs were positively correlated with nutrient availability and the active C pool, but genera within the same phylum exhibited both positive and negative relationships with nutrient and labile C availability

(assessed as active C pool size). Overall, my results suggest that bacterial life-strategies are related to soil C pool kinetics, but phylum-level life-strategy classifications do not capture the breadth of bacterial metabolic diversity. Phylum-level classifications may therefore be ineffective at predicting how changes in bacterial communities influence ecosystem functions.

3.2 INTRODUCTION

Wildfire frequency and severity have increased in the forests of the western United states over the past several decades (Westerling 2006; Dennison et al. 2014), a trend that is predicted to continue (Flannigan et al. 2009). Increased burn severity influences soil carbon (C) cycling for years to decades post-fire by altering soil C pool structure, efflux rates, and decomposition (Holden et al. 2016; Adkins et al. 2019b; Dove et al. 2020). Understanding drivers of post-fire soil C flux is important because the balance between soil C efflux and photosynthetic C gains governs the transition of ecosystems from C sources to C sinks during ecosystem recovery (Kashian et al. 2006). Because soil microbes drive the soil C cycle, it is important to understand how microbial communities are affected by wildfire.

Linking microbial community composition to ecosystem function is an important research direction in microbial ecology (Prosser and Martiny 2020), but is challenging for broad scale ecosystem functions, because such functions are the integrative results of reactions performed by a wide swath of microbial groups (Treseder et al. 2012; Fierer 2017). Additionally, broad scale functions are dependent on other biotic and abiotic mechanisms (Schmidt et al. 2011). In the case of soil C flux, it has been posited that microbial access to substrates, rather than microbial community structure, dictates flux rate and magnitude (Schmidt et al. 2011; Schimel and Schaeffer 2012). However, emerging evidence suggests that microbial structure influences the soil C cycle. A meta-analysis of studies that manipulated microbial diversity

indicated that C respiration was positively related to bacterial diversity (de Graaff et al. 2015). Microbial diversity and community complexity have been shown to influence decomposition and ecosystem multifunctionality in an experimental grassland (Wagg et al. 2019) and C use efficiency in an experimental forest (Domeignoz-Horta et al. 2020).

The amount of C respired versus retained in soils is dependent on the structure and stability of soil C pools (Trumbore 2000; Kuzyakov 2011; Torn et al. 2013). Soil C can be conceptualized as distinct C pools with variable turnover times: an active C pool (C_a) with a mean residence time of days to months and a non-active pool (C_s) with a mean residence time of years to decades (Paul et al. 2006). The sizes of the active and non-active C pools and their associated kinetic rates (k_a and k_s, respectively) can be quantified by measuring soil C respiration over long-term lab incubations (Collins et al. 2000; Kuzyakov 2011). In this approach, C pools are a function of biological processes rather than intrinsic chemical characteristics (see Schmidt et al., 2011). Microbial activity therefore reflects soil C pool kinetics, but whether differences in microbial community structure influence the respective cycling rates of the two C pools is unknown.

Disturbance-induced changes to microbial communities could alter ecosystem processes if the microbial community is not resistant or resilient to disturbance or not functionally redundant with the pre-disturbance community (Allison and Martiny 2008; Treseder et al. 2012). In the case of fires, microbial community composition in forest soil is often not resistant or resilient over the short- to intermediate-term, as they exhibit decreases in diversity and changes in community composition that persist from months to years post-fire (Weber et al. 2014; Rodríguez et al. 2017; Rodríguez et al. 2018; Whitman et al. 2019; Sáenz de Miera et al. 2020; Adkins et al. 2020). Altered microbial community composition may not lead to changes in soil

function if sufficient functional redundancy exists between pre-fire and post-fire soils. However, post-fire soil microbial communities appear to be functionally distinct, becoming predominated by more copiotrophic bacterial taxa compared to oligotrophic taxa, an effect that increases with burn severity (Ferrenberg et al. 2013; Adkins et al. 2020). Furthermore, due to changes to soil pH and differential heat tolerance, bacteria are more predominant than fungi in post-fire soils for a decade or more post-fire (Dooley and Treseder 2012; Pressler et al. 2018), so bacterial communities may play a particularly important role in ecosystem processes in recovering forests over the short- to intermediate-term.

The classification of bacterial taxa as copiotrophic or oligotrophic represents a trait-based framework for describing bacterial community structure (Fierer 2017), and these taxa may differ in their effects on the soil C cycle. Copiotrophs consume labile C, have high nutrient requirements, and exhibit high growth rates. In contrast, oligotrophs exhibit slow growth rates, but have high substrate affinity and may outcompete copiotrophs when nutrient content and/or organic matter quality is low (Fierer et al. 2007; Ramirez et al. 2012). These ecological strategies are reflected at the gene level: metagenomic and metabolic approaches have revealed that soils abundant in copiotrophs harbor more genes associated with carbohydrate utilization and protein degradation, and fewer genes and enzymes associated with recalcitrant C degradation, organic N decomposition, and P scavenging (Fierer et al. 2012a; Ramirez et al. 2012; Hartman et al. 2017). The combined influences of oligotroph vs. copiotroph abundance, nutrient content, and organic matter quality may thus alter soil C pool kinetics. For example, if two soils have equally large stocks of labile C (i.e. easily decomposable C), but differ in their abundance of copiotrophic taxa (for example due to differences in soil nutrient contents), the soil with greater copiotroph abundance might exhibit larger k_a values due the capacity of copiotrophs for rapid growth. In

contrast, soils with large stocks of recalcitrant C (e.g. lignin, pyrogenic C) might exhibit larger k_s values when oligotroph abundance is high due to their higher substrate affinity and their greater ability to mine nutrients.

Consistent patterns have emerged in post-fire differences in phylum-level bacterial community composition among many ecosystem types, and these differences are often reflected by divergent responses of oligotrophic and copiotrophic taxa to fire and burn severity. The copiotrophic phyla *Bacteroidetes*, *Actinobacteria*, and *Firmicutes* tend to exhibit higher abundance post-fire, whereas the oligotrophic phylum *Acidobacteria* exhibits lower abundance (Weber et al. 2014; Xiang et al. 2014b; Pérez-Valera et al. 2019; Whitman et al. 2019). Changes in bacterial phyla abundance are likely due to a combination of direct and indirect effects of fire on soils. For example, spore-forming, heat resistant taxa such as *Actinobacteria* and *Firmicutes* are more likely to survive soil heating events (Prendergast-Miller et al. 2017). These and other copiotrophic phyla (e.g. *Bacteroidetes*, *Proteobacteria*) may also positively respond to the fire-induced increases in total inorganic nitrogen (TIN), active C pools, and dissolved organic C (Fernández et al. 1997; Wan et al. 2001; Wang et al. 2012). Changes to both microbial communities and nutrient availability have been demonstrated to scale with burn severity in mixed-conifer forests (Adkins et al. 2019b; Adkins et al. 2020); thus, C-cycling processes that are driven by microbial community structure likely vary with burn severity. Consistent responses to fire among certain bacterial genera have also emerged. The genera *Masillia,* a potential aromatic-C degrader, *Arthrobacter,* a fast-growing and stress-tolerant taxa, and *Flavisolibacter* have frequently been found to increase in abundance following fires (Weber et al. 2014; Pérez-Valera et al. 2017; Rodríguez et al. 2017; Whitman et al. 2019; Sáenz de Miera et al. 2020). Although a few studies have accounted for the role of burn severity in shaping

microbial communities (Weber et al. 2014; Whitman et al. 2019; Sáenz de Miera et al. 2020), most have not, and identifying the influence of severity on post-fire microbial communities has been identified as a key information need in fire ecology research (Hart et al. 2005; Pressler et al. 2018).

The numerous interacting direct and indirect effects of fire and burn severity on soil and bacterial properties highlights the importance of employing a systems approach to understanding disturbance effects on the soil C cycle. Understanding the relationships between soil characteristics and the C cycle will improve predictions of the impacts of changing fire regimes on the C sink strength of forests, and understanding the influence of bacterial communities on soil functions is necessary for improving ecosystem models (Schimel and Schaeffer 2012; Treseder et al. 2012; Graham et al. 2016). Additionally, the variability in soil biological, physical, and chemical properties across burn severity gradients make fire-prone forests valuable ecological systems for testing trait-based frameworks of bacterial communities (see Fierer, 2017b). Here, my overarching objectives are to 1) determine how C pool structure and kinetics are related to soil properties and bacterial communities one-year post fire, and 2) how the oligotroph-copiotroph framework can explain post-fire differences in soil bacterial communities. In service of these objectives, I addressed four hypotheses. I hypothesized that 1) changes in C pool structure in kinetics across a burn severity gradient can be explained by accounting for soil properties; 2) bacterial OTUs that have previously been identified as positive fire responders will be positively correlated with burn severity; 3) bacterial taxa that are more abundant in burned areas will primarily be copiotrophs and therefore positively related to nutrient availability and C_a size; and 4) copiotrophic taxa abundance will be positively associated with k_a, whereas oligotrophic taxa abundance will be positively associated with k_s.

3.3 MATERIALS AND METHODS

3.3.1 Site description

My study was conducted in mixed-conifer forest in the Klamath National Forest, located in northern California, USA. The forest type is a California mixed-conifer forest (Ruefenacht et al. 2008), which consists of *Pinus ponderosa* Lawson & C. Lawson, *P. lambertiana* Douglas, *P. jeffreyi* Balf., *Abies concolor* (Gord. & Glend.) Lindl. ex Hildebr., *Pseudotsuga menziessi* (Mirb.) Franco, *Calocedrus decurrens* (Torr.) Florin, *Arbutus menziesii* Pursh. and *Quercus kelloggi* Newberry. Soils of my study area belong to the Skalan series and its associates (Soil Survey Staff 2015); Skalan is a loamy-skeletal, isotic, mesic Vitrandic Haploxeralf that forms in weathered gneiss residuum and is slightly acidic (Soil Survey Staff 2018). The mean annual precipitation is 1290 mm and mean annual temperature is 9.0 °C (NCEI-NOAA 2017). My study focuses on areas affected by the Beaver Fire (Lat: 41.88993, Long: -122.87056; Fig. S3.1), a wildfire that burned ~13,000 ha between July 30, 2014 to August 31, 2014. Burn severity estimates based on the Differenced Normalized Burn Ratio (dNBR) indicate that the Beaver Fire resulted in ~4800 ha of burned area classified as high severity, ~4600 ha classified as moderate severity, ~3700 ha classified as low severity, and ~750 ha within the fire perimeter was unburned (MTBS 2017). dNBR severity estimates are based on Landsat reflectance images collected in the growing seasons immediately before and after fire occurrence, and reflect post- versus pre-fire changes in vegetation and soil exposure (Parsons et al. 2010), resulting in continuous dNBR values assigned to both burned and unburned plots. dNBR values for unburned plots are typically < 100, whereas the upper limit for burned plots can exceed 1000.

3.3.2 Field methods

Between August 3, 2015 and August 10, 2015 (i.e. one-year post-fire), I sampled 10 plots (4 unburned, 6 burned; dNBR 0-863). At each plot, I determined live and dead tree basal area and sampled for forest floor and mineral soil. I measured tree diameters at breast height (DBH) for all live and dead trees >10 cm DBH within an 11.3 m sampling radius, and I used these values to calculate live and dead tree basal area at the plot level. I sampled forest floor and mineral soil 15 m from the plot center at azimuths of 0º, 90º, 180 º and 270º, for a total of 40 forest floor and 40 mineral soil samples collected. The forest floor includes the plant litter and duff layers, and is equivalent to the combined Oi, Oe, and Oa horizons in the USDA Soil Taxonomy classification system (Perry et al. 2008). I collected all forest floor material from within a 15 cm radius circular sampling frame. I inserted a 5 cm radius metal cylinder into the mineral soil to 5 cm and collected mineral soil using a stainless-steel scoop. I collected one additional volumetric mineral soil sample from the center of each plot to estimate bulk density using the same sampling method. Forest floor samples were stored at ambient temperature for ~14 days prior to being transported to the lab. Mineral soil samples were stored under refrigeration for 2-7 days and shipped to the lab on ice. Upon arrival at the lab, the forest floor samples were air-dried, and mineral soils were sieved (2 mm) and sub-sampled for DNA analysis. Sub-samples for DNA analysis were stored at -80 ºC, and the remainder of the mineral soils were refrigerated at ~4º C until analyses.

3.3.3 Lab methods

Soil processing and chemical analyses

I processed the forest floor in a blender to pass a 2 mm mesh screen and then pulverized a subsample of the blended material in a ball mill (SPEX Sample Prep LLC, Metuchen, NJ, USA).

I oven-dried the pulverized forest floor material at 65º C and prior to determination of total C and N. I used the sieved mineral soil for determination of total C, N, pyrogenic-C (PyC), NO_3-N, NH_4-N, extractable P, and pH. I oven-dried the mineral soil sample to be used for C and N analysis at 105º C and then pulverized the subsamples as described above. I analyzed one forest floor sample and one mineral soil sample from each subplot for total C and N concentrations on a dry combustion elemental analyzer (Costech Analytical Technologies Inc., Valencia, CA, USA), using atropine as the quantification standard. I quantified mineral soil PyC concentrations by digesting 0.5 g mineral soil from each subplot in 10 mL 1.0 M HNO_3 + 20 mL 30% H_2O_2 at 100˚ C for 16 hours (Kurth et al. 2006) and analyzing post-digested soils for residual C and N.

I extracted a 10 g sample of fresh mineral soil from each subplot for NH_4^+-N and NO_3^--N in 50 mL 2.0 M KCl for 1 hour. I filtered the resulting soil extracts through 2.5 µm pore-size filter paper (GE Healthcare UK Limited, Little Chalfont, Buckinghamshire, UK). I determined the extract NH_4^+ concentrations spectrophotometrically by reacting with ammonia salicylate and ammonia cyanurate (Sinsabaugh et al. 2000), and measuring absorbance at 595 nm (BioTek Elx800, BioTek Instruments Inc., Winuski, VT, USA). I determined the concentrations of NO_3^- in the extracts spectrophotometrically by reacting the extracts with vanadium (III) chloride, sulfanilamide, and N-(1-naphthyl)-ethylenediamine dihydrochloride and measuring absorbance at 540 nm (Doane and Horwáth 2003). I extracted 2.5 g subsamples of fresh mineral soils for phosphorus (P) in 40 mL 0.5 M $NaHCO_3$ and determined P concentration using the Olsen method (Olsen et al. 1954). I measured mineral soil pH of a 1:2 (w:v) soil slurry with a benchtop pH meter (Oakton pH 700, Oakton Instruments, Vernon Hills, IL, USA).

Determination of carbon pool structure and kinetics

I incubated soils to determine the size and kinetic rates of the C_a and C_s pools and potential soil C flux rates. I adjusted a 30 g sample of fresh mineral soil from each subplot to 40% water filled pore space (WFPS) in 120 mL specimen cups. The specimen cups were placed in 1 L glass jars, and the soils were incubated in the dark for 300 days at ambient temperature (~23 ºC) with biweekly adjustments of soil moisture to 40% WFPS. I measured CO_2 evolution on days 10, 14, 28, 42, 58, 90, and every 30 days thereafter until day 300. Prior to each measurement event, I flushed the jars to ambient CO_2 concentrations, then tightly sealed the jars for 24-48 hours before sampling a 1 mL gas aliquot through septa fitted to the jar lids. I measured CO_2 concentration of the aliquot using an infrared gas analyzer (LI-COR Inc., Lincoln, NE, USA), and calculated CO_2-C efflux as the difference in CO_2-C concentrations between the soil containing jars and blank jars that contained only a specimen cup and DI water.

DNA extraction and bioinformatic analysis

DNA was extracted from 0.25 g of soil using the MoBIO PowerSoil DNA isolation kit (MoBIO laboratories, Carlsbad, CA), according to the manufacturer's instructions. Illumina-MiSeq was used to amplify the V4 region of the 16S-rRNA gene using 515f/806r universal primers (Caporaso et al. 2010) at the Michigan State University Genomics Core. I processed DNA sequences using the QIIME2 bioinformatics pipeline (Bolyen et al. 2019). I denoised, merged forward and reverse reads, and removed chimeras using the q2-DADA2 plugin (Callahan et al. 2016). I inferred phylogenetic trees by applying MAFFT multiple sequence alignment (Katoh and Standley 2013) and FastTree 2 (Price et al. 2010) using the q2-phylogeny plugin. With the q2-diversity plugin, I used the phylogenetic tree to calculate OTU richness, Faith's phylogenetic diversity (Faith 1992), Shannon's diversity, Pileou's evenness, and a weighted

UniFrac distance matrix (Lozupone and Knight 2005). I used the q2-feature-classifier plugin (Bokulich et al. 2018) with the classify_sklearn action (Pedregosa et al. 2011) to classify taxonomic composition of my samples employing a Naïve Bayes classifier trained on the SILVA SSURef database version 132 using a 99% similarity threshold (Quast et al. 2013). I filtered OTUs associated with Archaea, Eukaryotes, mitochondria, and chloroplasts. I calculated oligotroph-to-copiotroph ratio at the phylum level as the ratio of the sum of relative abundances of all taxa classified within the phyla *Acidobacteria* and *Verrucomicrobia* to the sum of the relative abundances of all taxa classified within the phyla *Actinobacteria*, *Firmicutes*, and *Bacteroidetes* (Fierer et al. 2007; Fierer et al. 2012a; Ramirez et al. 2012).

I predicted metagenomic functional potential of soil bacterial communities using the PICRUST2 (Phylogenetic Investigation of Communities by Reconstruction of Unobserved States) software (Douglas et al. 2019). PICRUST2 uses HMMER software (hmmer.org) to perform multiple sequence alignment via hidden Markov models, places reads in a reference tree using EPA-ng (Barbera et al. 2018), and outputs a tree file with Gappa (Czech et al. 2020). PICRUST2 then performs hidden-state prediction of gene families (Louca and Doebeli 2017), and uses MinPath (Ye and Doak 2009) to infer the relative abundance of MetaCyc metabolic pathways (Caspi et al. 2018). MetaCyc is a metabolic pathway database in which pathways are hierarchically grouped according to metabolic function. I focused my analysis on degradation pathway groups related to C cycling, including carbohydrate degradation, alcohol degradation, amine degradation, amino acid degradation, aromatic compound degradation, carboxylate degradation, fatty acid and lipid degradation, nucleoside and nucleotide degradation, and secondary metabolite degradation pathways.

3.3.4 Statistical analysis

Fire and severity effects on soil properties and tree basal area

I performed all statistical analysis in the R statistical computing environment (R Core Team 2019). I used linear mixed models (R Package: *nlme*; Pinheiro et al., 2016) to determine the impacts of wildfire occurrence and burn severity (dNBR) on live and dead tree basal area, total C and N, C:N ratio, PyC, NH_4^+-N, NO_3^--N, TIN, extractable P, pH, gravimetric soil moisture, and forest floor mass. To account for legacy effects of soil properties related to topography, all models initially included elevation, slope, and aspect as covariates. Topographic variables that were not significant at $\alpha < 0.05$ were sequentially removed from the models. All models included plot-identifier as a random effect, and the NH_4^+-N, NO_3^--N, and TIN models included total N as a covariate. I determined that inorganic N variables did not meet assumptions of normality, so I normalized these variables using Box-Cox transformations (Box and Cox 1964). I determined whether wildfire occurrence or dNBR was a better predictor of differences by fitting separate models that included either fire occurrence (burned or unburned) or burn severity as an explanatory variable and comparing model AIC values. I selected fire occurrence or severity as the better predictor if the model containing that variable was ≥ 2.0 AIC points lower than the alternative model.

Fire and severity effects on soil C pools and fluxes

I assessed the impacts of fire and severity on soil C flux rates and cumulative soil C flux over my soil incubation using the following fixed effects portion of linear mixed models:

$$\text{C Flux (cumulative or rate)} = \beta_o + \beta_1 \times \text{Incubation Day} + \beta_2 \times \ln(\text{Incubation Day}) + \beta_3 \times \text{Fire Variable} + \beta_4 \times \ln(\text{Incubation Day}) \times \text{Fire Variable} \quad (1)$$

where β_i represents the model-fitted intercept or slope coefficient and fire variable is either fire occurrence or burn severity. Each model also initially included all topographic variables and a plot-identifier random effect. Non-significant topographic variables were sequentially removed, and selection of fire occurrence or severity as a more suitable predictor was performed using AIC values as described above.

I assessed the size and mineralization rates of the C_a and C_s pools using non-linear mixed models. I assessed the sizes of the C_a and C_s pools and their mineralization rate constants using the following fixed effects portion a two-compartment first-order kinetics model (Kuzyakov 2011):

$$^{Rate}CO_2 = C_a \times k_a e^{(-ka \times day)} + C_s \times k_s e^{(-ks \times day)} \quad \text{(eq. 2)}$$

where $^{Rate}CO_2$ is the soil CO_2 efflux rate at each measurement event, C_a is the size of the active C pool, k_a is its mineralization coefficient, C_s is the size of the non-active C pool and k_s is its mineralization rate coefficient. In this model, C_s is constrained to be $C_{SOC} - C_a$, where C_{SOC} is total soil organic C content. I did not include a passive pool in this model because research shows that methods of isolating passive C pools do not result in biologically meaningful estimates (Greenfield et al. 2013).

I determined whether fire occurrence or severity affected soil C pools by first fitting a global non-linear model that included all 40 incubation replicates. I performed model selection procedures for random effects in non-linear models as described by Pinhero and Bates (2000), which resulted in the inclusion of a plot identifier as a random effect associated with C_a and k_s, and no random effect associated with k_a. I assessed how wildfire impacted the size or kinetic rates of the C_a and C_s pools by adding fire occurrence or severity as a covariate to the non-linear models. Selection of fire occurrence or severity as a more suitable predictor variable was

performed using AIC values as previously described. In addition to the global model, I fit separate non-linear models for each incubation replicate to obtain independent estimates of C_a, k_a, and k_s for use in elastic net regularization analysis and structural equation modelling (described below). Five incubation replicates (two replicates from separate unburned plots, and one each from plots with dNBR values of 108, 350, and 478) did not converge during non-linear regression due to consistently high respiration rates throughout the incubation and were excluded from further analysis. After exclusion, each of the ten plots still had C pool parameter estimates from at least three subplots.

Fire and severity effects on soil bacterial communities and imputed metagenomes

I assessed the impacts of wildfire and burn severity on Faith's phylogenetic diversity, OTU richness, Shannon's diversity, Pielou's evenness, O:C, and the relative abundance of the ten most abundant bacterial phyla using linear mixed models and AIC model-selection as described above. The ten most abundant bacterial phyla represented all phyla that exhibited >0.5% relative abundance and 94.1% of the total abundance. I used multivariate statistical approaches (R Package: *vegan*; Oksanen et al., 2017) to determine the impacts of fire occurrence, burn severity, and soil properties on bacterial community structure. Using a weighted UniFrac distance matrix of the bacterial community, I employed principle coordinates analysis (PCoA), and full and partial Mantel tests to determine the relationships between plant and soil characteristics and bacterial communities. Additionally, I performed PCoA and Mantel tests on a Bray-Curtis distance matrix of imputed MetaCyc metabolic pathways, hierarchically grouped into common C-degradation pathways.

I identified positive and negative fire responsive bacterial OTUs using species indicator analysis with fire occurrence as the explanatory variable, relative abundance of OTUs as

response variables, and point biserial correlation as the output statistic (R Package: *indicspecies*; De Caceres and Legendre, 2009). I assessed which positive fire-responder OTUs were also positively related to severity by performing linear mixed-model analysis on the relative abundance of each fire-responsive OTU with dNBR as the explanatory variable and unburned plots excluded from the analysis.

Links between ecosystem characteristics and soil carbon pools

I determined properties linked to the size and kinetic rates of soil C pools using structural equation modeling. I constructed an initial SEM meta-model composed of linear mixed models that included live tree basal area, dead tree basal area, forest floor mass, total C, PyC, total N, TIN, extractable P, pH, and soil moisture as response variables (R Package: *piecewiseSEM*; Lefcheck, 2016). All component linear mixed models initially included explanatory variables of severity and any topographic variable (i.e. elevation, slope, aspect) that my previous analyses (see above) indicated was significantly related to the response variable of interest. All edaphic response variables initially also included live and dead tree basal area as explanatory variables. The TIN linear model also included total N as an explanatory variable, and the soil moisture model included overlying forest floor mass as an explanatory variable. All linear-mixed models included a plot-identifier as a random effect. I used severity instead of fire occurrence in my SEMs, because AIC values indicated that severity had more explanatory power for more soil variables (Table 3.1), and previous research indicates that severity-based SEMs outperform fire occurrence SEMs (Adkins et al. 2020). The initial SEM model was modified by sequentially removing paths that exhibited p-values > 0.05, resulting in an SEM meta-model upon which all further models were based.

I assessed relationships of soil properties, live and dead tree basal area, and topography with C pools using separate SEMs for each C pool parameter (i.e. C_a, k_a, k_s). Each SEM included C_a, k_a, or k_s as the response variable, and the initial explanatory variables included all soil and topography variables, and live and dead tree basal area. Variables that were not significant at α=0.05 were sequentially removed from the model. I did not construct SEMs for C_s because this pool dominated the total C stock so SEMs would likely identify factors impacting total C stock size rather than C_s pool size. My SEMs satisfy the recommendations of 5 observations per variable (Grace et al. 2015), and local-estimation approaches to SEM like those used here have smaller sample size requirements since there only need to be enough degrees of freedom to fit any component model (Shipley et al. 2001).

Relationships between bacteria, C pools, and soil nutrients

I used correlation analyses and elastic net regularization to assess relationships between $\log_2$ bacterial abundance at the levels of phylum and genus with C pools, soil TIN and P, and pH, soil variables that are commonly associated with bacterial copiotrophic versus oligotrophic life-strategies. I considered C_a pools size an indicator of labile C availability. I performed univariate correlations between all bacterial phyla and the selected soil variables. At the genus level, I performed correlations within phyla that my linear mixed-models indicated were related to burn severity and that previous research indicates exhibit either copiotrophic or oligotrophic life strategy (i.e. *Acidobacteria*, *Actinobacteria*, *Bacteroidetes*, *Proteobacteria*, and *Verrucomicrobia*). All correlations were performed using Spearman's rank correlation to account for non-normality of bacterial abundance data and I considered correlations significant at α=0.05.

I also performed elastic net regularization (R Package: *glmnet*; Friedman et al., 2010) to identify bacteria phyla and metabolic pathways that are predictive of C pool parameters. Elastic

net regularization selects the best set of predictors (i.e. phyla or metabolic pathways) for a given response by using LASSO and ridge regression, but does not assign significance values to selected predictors; elastic net regularization is frequently used with sparse datasets when the number of potential predictors is larger than the number of observations, as is often the case for genomic data (Friedman et al. 2010; Wagg et al. 2019).

3.4 RESULTS

3.4.1 Relationships between fire, tree basal area, and soil properties

Linear mixed models

My AIC-based model selection indicated that fire occurrence had more explanatory power for models assessing total soil C, NH_4^+-N and TIN, whereas severity had more explanatory power for dead tree basal area, forest floor mass, total N, pH, and soil moisture (Table 3.1). Neither explanatory variable had more power for live tree basal area, C:N, NO_3^--N, and extractable P.

Concentrations of NH_4^+-N, NO_3^--N, and TIN were higher in burned stands than unburned stands (Table 3.1). Additionally, total N was a significant covariate for NH_4^+-N, NO_3^--N, and TIN, all of which were all positively related to total N ($p<0.001$, $p=0.041$, and $p<0.001$, respectively). Univariate relationships between total N and NH_4^+-N, NO_3^--N, and TIN were not significant indicating total N was not the primary driver of changes to inorganic N. Dead tree basal area increased with both severity ($p=0.005$) and elevation ($p=0.017$). Live tree basal area was not related to severity and increased with elevation ($p=0.034$). Forest floor mass was negatively associated with severity ($p=0.002$) and positively related to elevation ($p=0.001$). Mineral soil gravimetric moisture was negatively related to severity ($p=0.004$), and positively related to elevation ($p<0.001$). Soil pH increased in association with severity ($p=0.007$). Mineral

soil total C and N, C:N, PyC, and extractable P were not significantly affected by fire occurrence or burn severity. Total N was positively related to elevation (p=0.012) and C:N was negatively related to elevation (p=0.045). Hillslope and aspect were not related to any of the considered properties.

Table 3.1 Relationship of fire occurrence and burn severity (dNBR) to soil properties as determined via linear mixed models. Linear mixed models also included elevation, hillslope, and aspect as topographic covariates. Relationships between soil properties and topographic variables are described in the main text. Lowercase letters represent differences in soil properties between unburned and burned forest stands at α=0.05. dNBR coefficient is the model-determined slope parameter and represents change in soil property per unit increase in dNBR. Bold text indicates that ΔAIC was ≥ 2 between models that included burn status *versus* dNBR, indicating that one of these variables should be preferred for predicting change in the relevant soil property.

	Unburned mean ± SE (n=4)	Burned mean ± SE (n=6)	dNBR coefficient	Fire occurrence model AIC	dNBR model AIC
Live Tree Basal Area (m^2 ha^{-1})	77.7 ± 26.5 a	33.3 ± 11.6 a	-0.046	100.19	98.79
Dead Tree Basal Area (m^2 ha^{-1})	5.4 ± 5.4 b	21.6 ± 5.6 a	0.044*	78.60	**76.07**
Forest floor Mass (kg $m^{-2)}$)	2.60 ± 0.48 a	0.95 ± 0.39 b	-0.0026*	485.46	**463.69**
Total C (g kg^{-1})	66.2 ± 13.3 a	68.8 ± 10.3 a	0.0043	**206.30**	208.35
Total N (g kg^{-1})	2.7 ± 0.5 a	2.8 ± 0.8 a	-0.0011	-61.16	**-64.56**
C:N	34.0 ± 11.5 a	37.9 ± 8.0 a	0.023	356.07	357.73
PyC Proportion (% Total C)	14.3 ± 3.3 a	12.8 ± 2.0 a	-0.000065	-94.95	-96.16
NH_4^+-N (µg g^{-1})$^{\Psi}$	1.28 ± 0.52 a	11.9 ± 4.6 b	0.0016*	**45.06**	49.90
NO_3^--N (µg g^{-1}) $^{\Psi}$	0.29 ± 0.29 a	5.21 ± 3.18 b	0.00057*	16.28	15.97
TIN (µg g^{-1}) $^{\Psi}$	1.57 ± 0.75 a	17.1 ± 7.7 b	0.0019*	**61.20**	65.88
Extractable P (µg g^{-1})	35.0 ± 4.2 a	45.0 ± 4.6 a	0.0084	334.54	336.47
pH	6.14 ± 0.05 a	6.54 ± 0.11 b	0.00090*	64.11	**58.43**
Soil Moisture (g kg^{-1})	88.9 ± 16.0 a	56.6 ± 20.7 a	-0.0041*	216.60	**208.42**
Bulk Density (kg m^{-3})	1.17 ± 0.19 a	1.26 ± 0.16 a	-0.000045	13.05	13.18

$^{\Psi}$ Response variables for inorganic N models were box-cox transformed prior to statistical analysis and slope value is on box-cox scale. Unburned/burned means are on original scale. Inorganic N models included total N concentration as a covariate.

***** Coefficient significantly different from zero at α = 0.05.

Structural equation models

My SEM meta-model revealed relationships between severity and soil properties that were not captured by my linear mixed-models (Fig 3.1). Soil moisture was directly, negatively linked to severity (p=0.03), indirectly, negatively linked via forest floor mass (p=0.001), and indirectly, positively linked via dead tree basal area (p=0.047), leading to a standardized

compound path coefficient of -0.52 between severity and soil moisture (marginal r^2=0.63). Although my univariate analysis did not reveal a relationship between severity and total N (section 2.1.1), my SEM indicated that N was negatively linked to severity, a relationship that was partially offset by a positive relationship between N and dead tree basal area, leading to compound path coefficient of -0.40 between N and severity (marginal r^2=0.69). After accounting for dead tree basal area, elevation was no longer a significant predictor of total N.

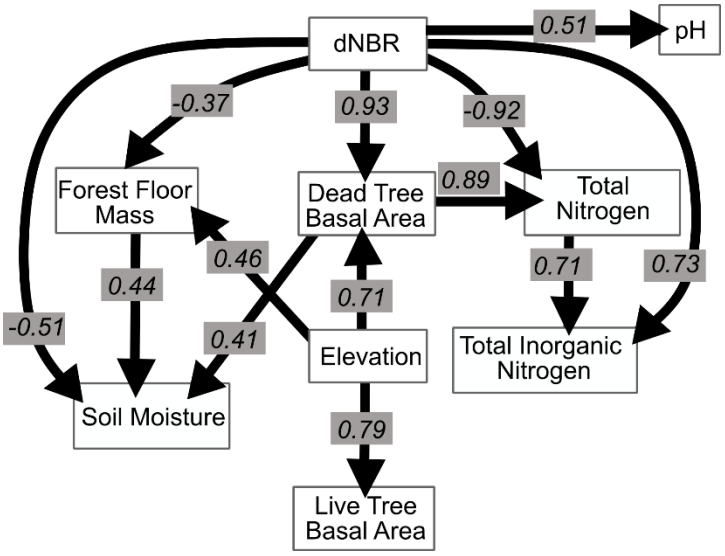

Figure 3.1 Causal diagram depicting structural equation model of direct and indirect links between burn severity, topography, live and dead tree basal area, and soil properties. Paths were fit using linear mixed models with a random plot effect. Standardized coefficients are displayed for all links. All retained paths exhibited p-values ≤ 0.05.

3.4.2 Relationship of wildfire and burn severity to soil C pools and fluxes

AIC-based comparisons of mixed-models assessing soil CO_2 efflux rate over my 300-day incubation did not suggest a preference for fire occurrence versus severity-based models (Fig. 3.2). However, AIC values indicated fire occurrence had more explanatory power when assessing the same data as cumulative CO_2-C flux (Fig S3.2). There was a negative main effect of fire occurrence on flux rate (p=0.01) and a positive interaction effect of fire occurrence ×

ln(day) (p=0.007) (Fig. 3.8). Together, these effects indicate that initial flux rates were lower in burned soils, and, over the course of the incubation, flux rates decreased more slowly in burned soils compared to unburned soils. Flux rates were positively related to elevation, but, when the data was assessed as cumulative CO_2-C flux, elevation was not a significant predictor.

AIC-based model selection of my global non-linear mixed models quantifying soil C pool structure and kinetics indicated that a fire occurrence model had more explanatory power than a severity model (ΔAIC=3.08). k_s decreased from 0.00017 in unburned soils to 0.000070 in burned soils (p=0.002). This is equivalent to C_s MRT increasing from 16.1 years to 39.2 years. The sizes of the C_a and C_s pools and k_a were not significantly different between burned and unburned soils. Modeled C_a was 1220 ± 210 mg kg soil^{-1} (2.08 ± 0.37% of total C), and k_a was 0.028 ± 0.002 (MRT=35.7 days).

The SEMs indicated that C_a was directly positively related to severity, but the relationship was offset by dead tree basal area, forest floor mass, and total N such that there was only a minimal change in C_a with severity (Table 3.2). SEMs indicated that k_a was indirectly linked to severity via a relationship with pH. SEMs indicated that k_s was indirectly linked to severity via the path between dead tree basal area and total N. k_s was directly positively related to live tree basal area and PyC.

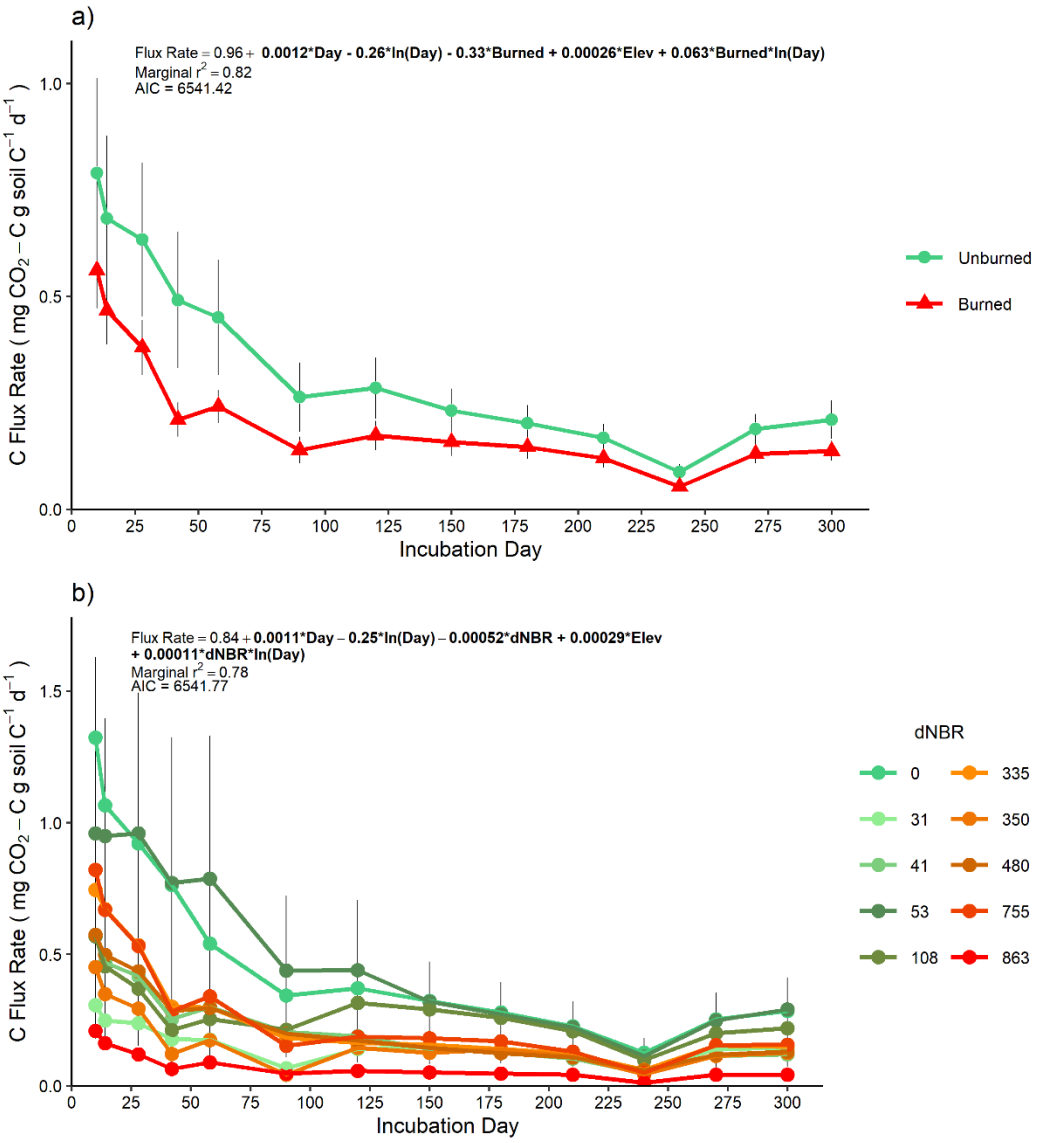

Figure 3.2 Mean (± SE) CO_2-C efflux rate (points) over a 300-day laboratory incubation of mineral soils (0-5 cm) grouped by fire-occurrence (a) and severity (b). Colored lines represent change in CO_2-C efflux rates between sampling days and vertical bars represent standard errors. In panel a, SE is based on n=4 unburned plots and n=6 burned plots. In panel b, SE is based on n=3 or 4 subplots per plot.

Table 3.2 Structural equation models explaining direct and indirect links to C-pool parameters. Path coefficients were standardized and only coefficients exhibiting p-values ≤ 0.05 were retained in the models. Abbreviations: DBA=dead tree basal area; FFM= forest floor mass; LBA=live tree basal area; N=total nitrogen; PyC=pyrogenic carbon

Response Variable	Structural Equation Model	dNBR Compound Coefficient	Fisher's C (p-value)
C_a	C_a=**1.68dNBR − 1.45DBA** + **0.63FFM + 0.70N +0.85ELEV** (m. r^2=0.54) FFM=−**0.37dNBR** + **0.46ELEV** (m. r^2=0.84) N=−**0.92dNBR** + **0.89DBA** (m. r^2=0.69) DBA=**0.93dNBR + 0.79ELEV** (m. r^2=0.72)	0.03	6.29 (0.39)
k_a	k_a=**0.51pH** (m. r^2=0.24) pH=**0.51dNBR** (m. r^2=0.35)	0.26	1.64 (0.44)
k_s	k_s=**0.26LBA + 0.40N + 0.56PyC** (m. r^2=0.63) LBA=**0.79ELEV** (m. r^2=0.62) N=−**0.92dNBR** + **0.89DBA** (m. r^2=0.69) DBA=**0.93dNBR + 0.79ELEV** (m. r^2=0.72)	-0.04	25.30 (0.12)

3.4.3 Relationships between wildfire, burn severity, bacterial communities, and imputed metabolic pathways

Bacterial diversity

Fire occurrence and severity negatively impacted Faith's phylogenetic diversity, with AIC values indicating no preference for fire occurrence or severity-based models (Figs. 3.3a and 3.3b). AIC-based model selection indicated that the severity model better explained OTU richness, which was negatively correlated with severity (Figs. 3.3c and 3.3d). Shannon's diversity and Pielou's evenness were not associated with either fire occurrence or severity (data not shown). Fire occurrence had more explanatory power for changes in phyla-level oligotroph-to-copiotroph ratios, which decreased from 1.08 in unburned soils to 0.48 in burned soils (Figs 3.3e and 3.3f).

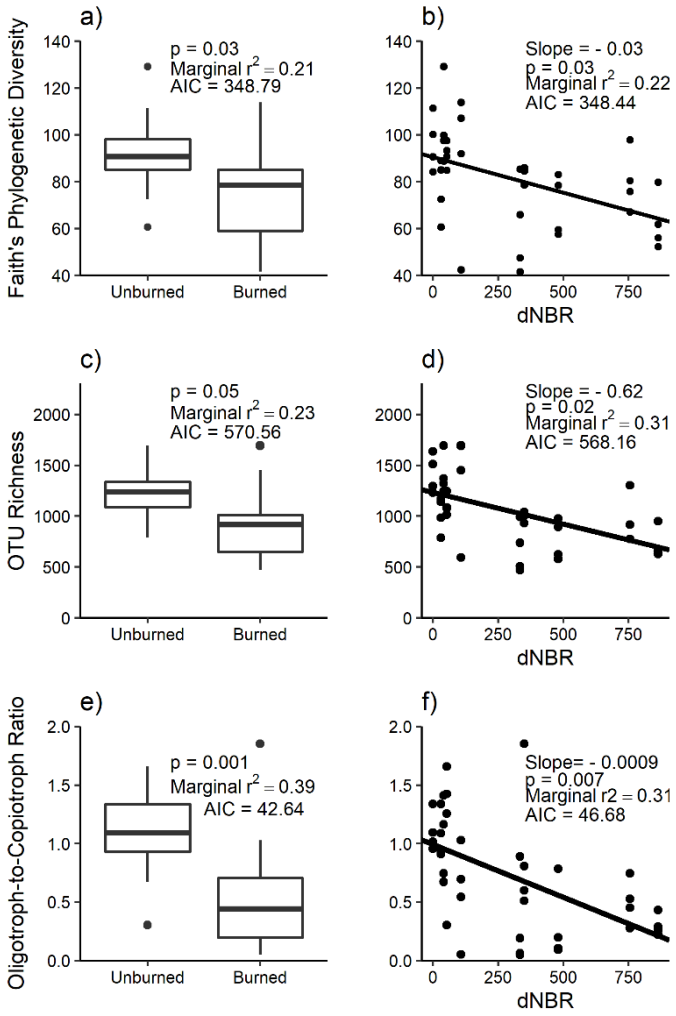

Figure 3.3 Relationship between fire occurrence and severity for selected microbial community characteristics, including Faith's phylogenetic diversity (a and b), OTU richness (c and d), and oligotrophic-to-copiotrophic taxa ratio (e and f).

Bacterial community structure

I performed PCoA on a weighted UniFrac distance matrix and found that the first axis explained 54.9% of variation, and the second axis explained an additional 8.7% (Fig. 3.4). Fire occurrence (r^2=0.24, p<0.001) and severity (r^2=0.57, p<0.001) were both significantly correlated with the PCoA ordination. Several soil properties were also significantly correlated with the ordination, including NH_4-N concentration (p=0.002), TIN concentration (p=0.008), P concentration (p=0.009), pH (p<0.001), soil moisture (p=0.010), and forest floor mass (p=0.003).

Mantel tests between the weighted UniFrac matrix and a Bray-Curtis matrix of soil properties indicated the two matrices were significantly related (Mantel statistic r=0.246, p=0.008).

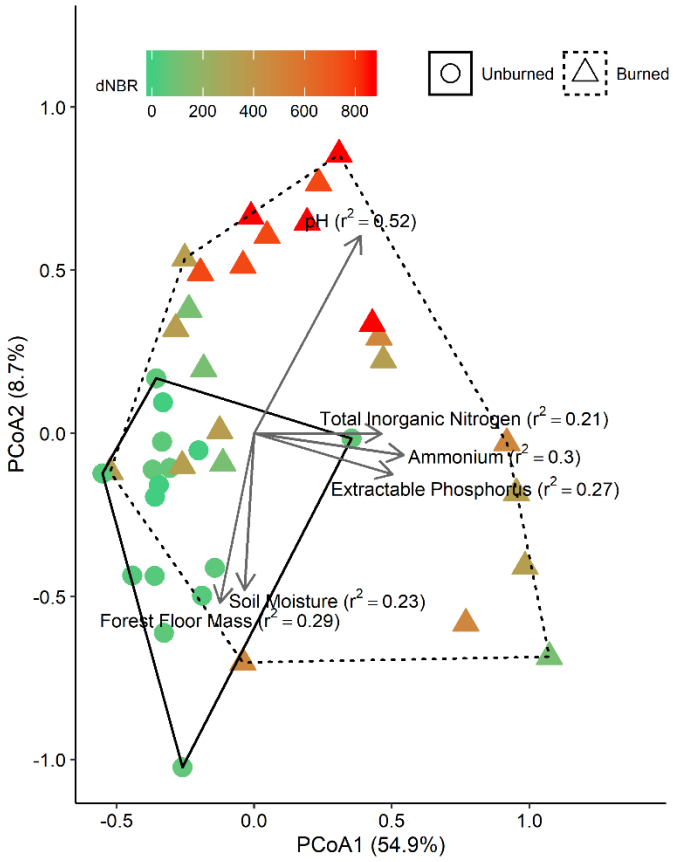

Figure 3.4 Principle coordinates analysis (PCoA) plots based on a weighted UniFrac distance matrix of bacterial communities in mineral soils (0-5 cm). Each point represents the bacterial community from a single subplot. Vectors represent variables that are significantly correlated with one of the PCoA axes, and vector lengths are scaled based on r^2 values. Solid and dashed hulls depict the ordination space that encompasses all burned and unburned samples, respectively.

I assessed the relationship between wildfire occurrence and severity and the relative abundances of the ten most abundant bacterial groups using univariate linear mixed models. AIC values indicated that the fire occurrence models had more explanatory power for assessing differences in *Bacteroidetes, Acidobacteria, Verrucomicrobia,* and *Planctomycetes* relative abundance. The relative abundances of *Bacteroidetes, Actinobacteria, and Firmicutes* were

higher in burned areas than unburned areas (Fig. 3.5). The relative abundances of *Acidobacteria, Verrucomicrobia,* and *Planctomycetes* relative abundance were lower in burned areas than unburned areas. There was no significant effect of fire occurrence or burn severity on α-*Proteobacteria, γ-Proteobacteria, δ-proteobacteria* or *Gemmatimonadetes* relative abundance.

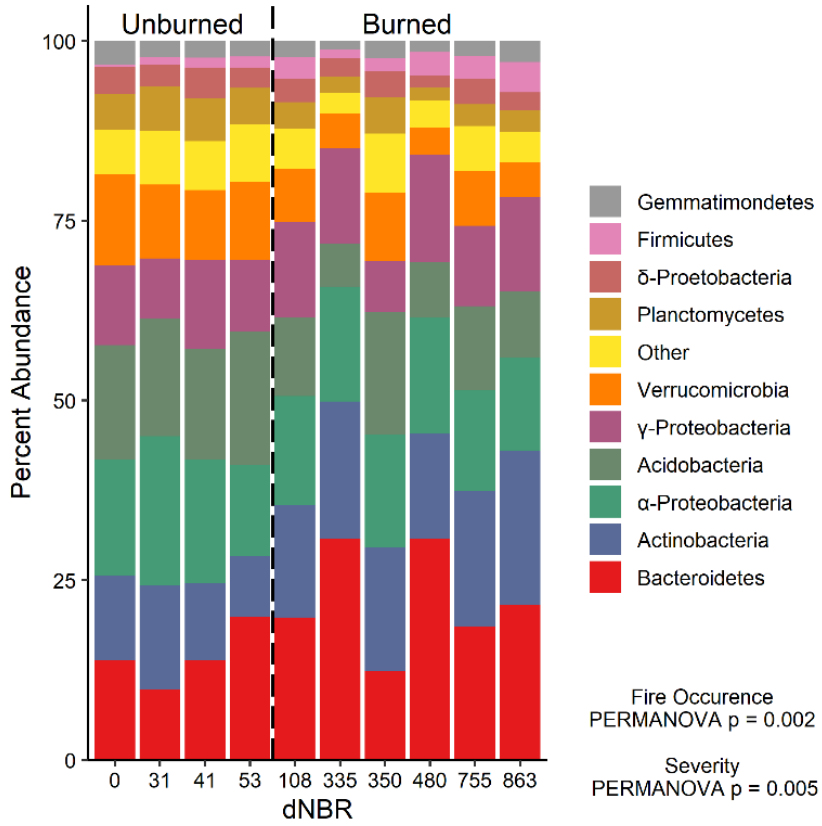

Figure 3.5 Relative abundance of the ten most abundant bacterial phyla across a gradient of burn severity in mineral soils (0-5 cm). The ten most abundant phyla accounted for ~94% of the total bacterial community. Abundances at each dNBR level are the means of four subplots.

Bacterial OTUs

Indicator species analysis identified 53 OTUs as indicators of burned soils (i.e. positive fire responders) and 74 OTUs as indicators of unburned soils (i.e. negative fire responders) (data not shown). The positive fire responders most commonly belonged to the *Actinobacteria* and *Bacteroidetes* phyla, as well as to the *α-proteobacteria* class, which respectively accounted for 28.6%, 23.2%, and 26.8% of the positive responder OTUs. The seven OTUs that exhibited the

strongest positive response to fire (point biserial correlation >0.60) came from the genera *Massilia* (*γ-proteobacteria*), *Roseomonas* (*α-proteobacteria*), *Segetibacter* (*Bacteroidetes*; 2 OTUs), *Blastoccus* (*Actinobacteria*), unclassified *Micrococcaceae* genus (*Actinobacteria*), and unclassified *Burkholderiaceae* genus (*γ-proteobacteria*). The negative fire responders most frequently belonged to the *Planctomycetes* phylum, which accounted for 14.7% of these responders, and to the *α-proteobacteria* and *γ-proteobacteria* classes, which accounted for 18.7% and 17.3%, respectively. The five OTUs that exhibited the strongest negative response came from the genera *Cytophaga* (*Bacteroidetes*), IS-44 (*γ-proteobacteria*), *Mycobacterium* (*Actinobacteria*), uncultured *Elsteraceae* genus (*α-proteobacteria*), and uncultured *Gemmataceae* genus (*Planctomycetes*).

I identified 15 OTUs as positively associated with severity based on linear mixed models (Fig. 3.6). Of the 15 OTUs, six were from the *Bacteroidetes* phylum, two were from *Actinobacteria*, and one was from *Verrucomicrobia*. Four severity responders were from the *α-proteobacteria* class, one was from the *γ-proteobacteria* class, and one was from the *δ-proteobacteria* class. The abundances of all of the severity-associated OTUs were positively correlated with either TIN or P (data not shown).

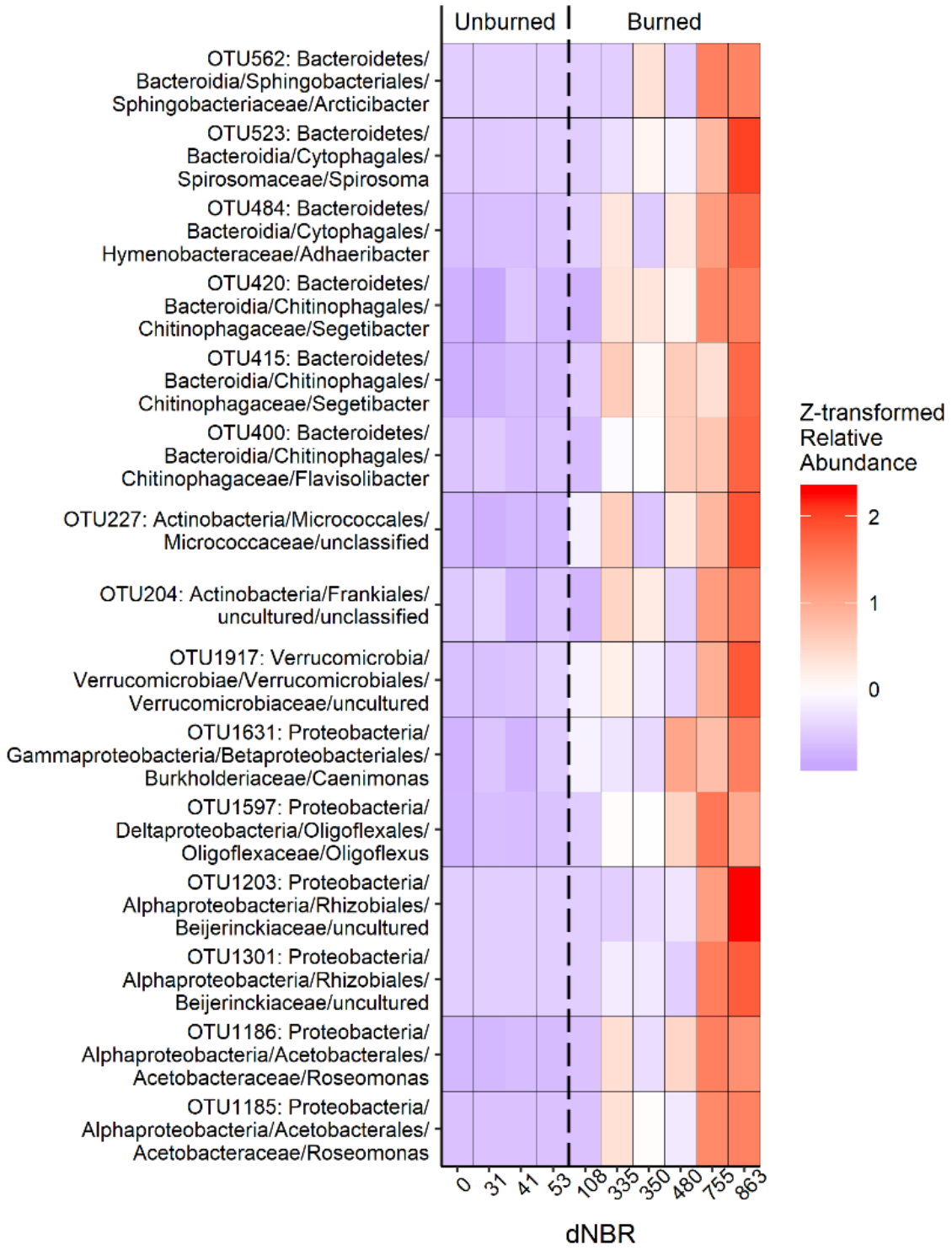

Figure 3.6 Heat map of showing z-transformed relative abundance of bacterial OTUs identified as severity responders. Severity responders were identified by performing indicator species analysis and linear mixed modelling. Abundances at each dNBR level are the means of four subplots.

Carbon degradation metabolic pathways

Using PICRUST2, I identified 135 MetaCyc metabolic pathways associated with C-degradation functions. PCoA on a Bray-Curtis matrix of the MetaCyc pathways grouped into common C-degradation functions indicated that the first axis explained 45.1% of variation and the second axis explained 22.1% (Fig. 3.7). Fire occurrence (r^2=0.16, p<0.001) and severity (r^2=0.41, p<0.001) were significantly correlated with the ordination. Additionally, several soil properties were significantly correlated with the ordination, including total C (p=0.009), C:N ratio (p=0.044), NH_4-N (p=0.008), TIN (p=0.047), extractable P (r^2=0.32, p=0.002), pH (p=0.010), and forest floor mass (p=0.007). Partial mantel tests between the distance matrix, a dNBR distance matrix, and a soil properties distance matrix indicated that, after accounting for soil properties, there was a significant correlation between severity and the metabolic pathways (Mantel statistic r=0.18, p=0.008).

AIC-based model comparisons for linear mixed models indicated that severity had more explanatory power for differences in carbohydrate degradation, alcohol degradation, amine and polyamine degradation, carboxylate degradation, and nucleotide and nucleoside degradation. Severity positively impacted the relative abundance of imputed pathways associated with carbohydrate degradation, alcohol degradation, amine and polyamine degradation, carboxylate degradation, and secondary metabolite degradation (Fig. 3.8). The relative abundance of amino acid degradation pathways was higher in burned areas than unburned areas (p=0.021). The relative abundances of aromatic compound degradation pathways and fatty acid and lipid degradation pathways were not related to fire occurrence or severity.

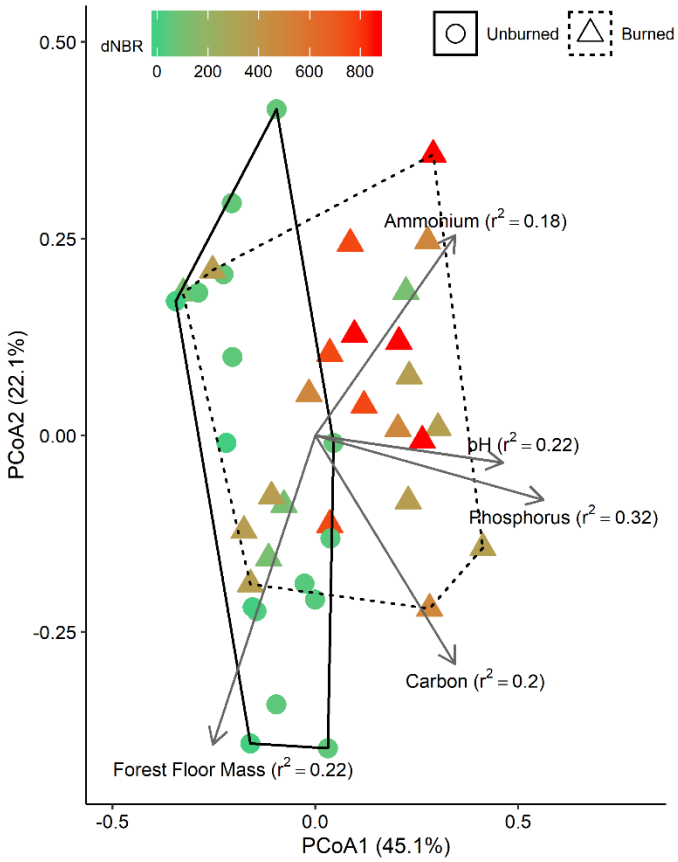

Figure 3.7 Principle coordinates analysis (PCoA) plots based on a Bray-Curtis distance matrix of imputed MetaCyc pathways grouped into common C-degradation functions. Vectors represent variables that are significantly correlated with one of the PCoA axes, and vector lengths are scaled based on r^2 values. Solid and dashed hulls depict the ordination space that encompasses all burned and unburned samples, respectively.

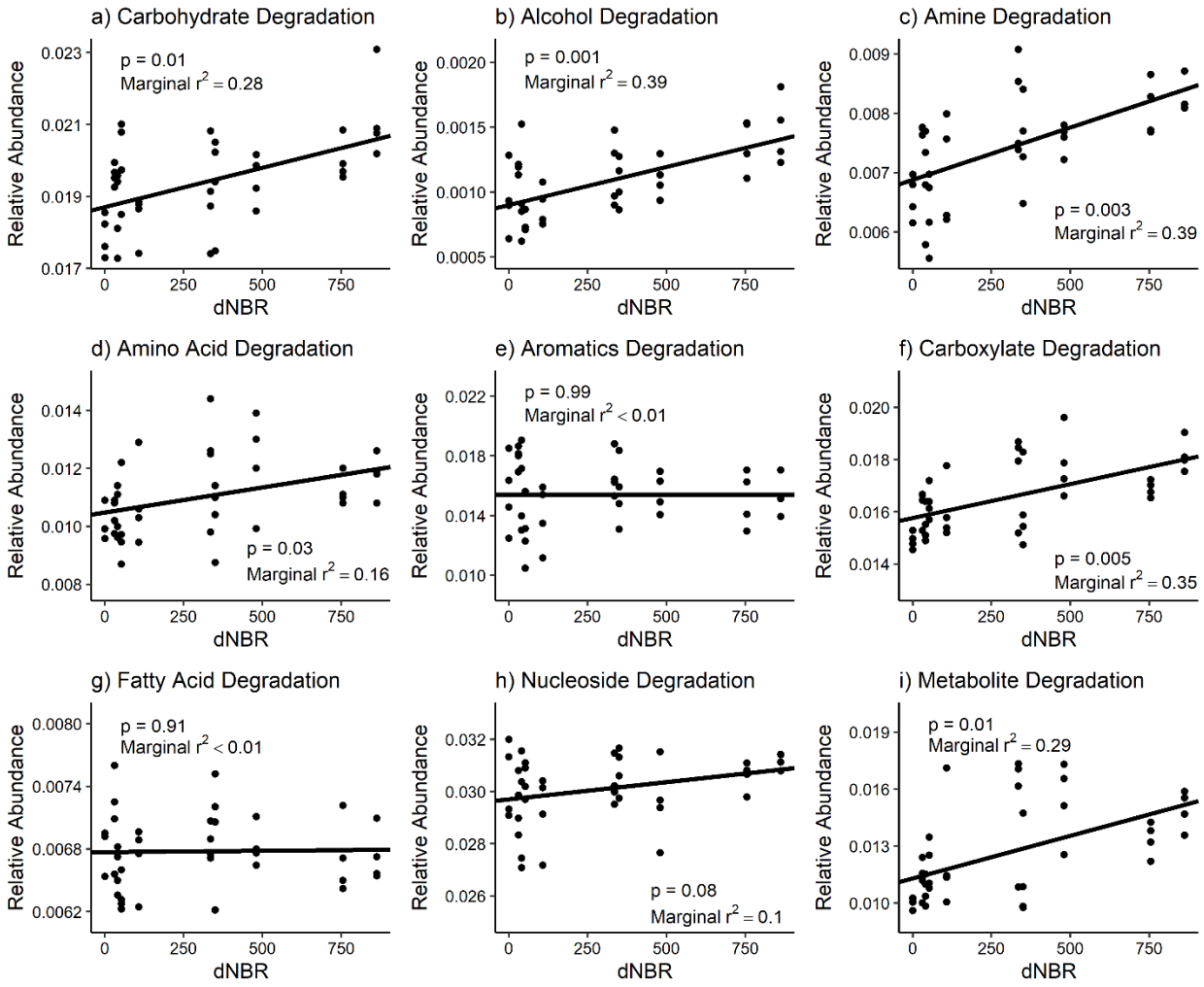

Figure 3.8 Relationships between burn severity and imputed C-degradation pathways estimated using PICRUST2.

3.4.4 Relationships between bacterial taxa, soil C pools, and soil nutrients

At the phyla level, *Proteobacteria*, *Latescibacteria*, and *Bacteroidetes* were positively correlated with C_a, whereas *Firmicutes* was negatively correlated with C_a (Fig 3.9). *Firmicutes* was also positively correlated with k_a, while several relatively rare bacterial phyla were negatively correlated with k_a. *Omnitrophicaeota* and *Elusimicrobia* were positively correlated with k_s, and no phyla were negatively correlated with k_s. *Firmicutes*, *FBP*, *Bacteroidetes* and *Actinobacteria* were the only phyla positively correlated with TIN or P. Several bacterial phyla were negatively correlated with these nutrients, including the relatively abundant *Verrucomicrobia*, *Planctomycetes*, and *Acidobacteria*. GLMs constructed using elastic net regularization selected seven bacterial phyla as associated with C_a, two phyla associated with k_a, and one phylum associated with k_s (Table S3.1).

Various relationships between bacteria, C pools, and nutrients emerged at the genera level (Table 3.3). *Proteobacteria*, *Bacteroidetes*, *Firmicutes*, and *Actinobacteria* are traditionally considered copiotrophic phyla. Within *Proteobacteria* and *Bacteroidetes*, more genera were positively correlated with C_a than were negatively correlated. More genera within these two phyla were positively correlated with TIN than were negatively correlated, but nearly 10% of genera within both phyla were negatively correlated with TIN. Within *Proteobacteria*, more genera were negatively correlated with P, and within *Bacteroidetes*, an equal proportion of genera were positively and negatively correlated with P. 46.8% of *Proteobacteria* genera and 45.8% of *Actinobacteria* genera were not significantly correlated within any of the considered variables.

Within *Firmicutes* and *Actinobacteria*, more genera were negatively correlated with C_a than were positively correlated, while more genera were positively correlated with TIN than

were negatively correlated. More *Firmicutes* genera were positively correlated P than were negatively correlated, whereas more *Actinobacteria* genera were negatively correlated with P than were positively correlated. For both phyla, more genera were positively correlated pH than were negatively correlated. 45.8% of *Firmicutes* genera and 42.7% of *Actinobacteria* genera were not significantly correlated with any of the considered variables.

Acidobacteria and *Verrucomicrobia* are typically considered oligotrophic phyla. Within both of these phyla, more genera were positively correlated with C_a than were negatively correlated. Additionally, more genera within both phyla were negatively correlated with TIN, P, and pH. 38.0% of *Acidobacteria* genera and 51.9% of *Verrucomicrobia* genera were not significantly correlated with any of the considered variables.

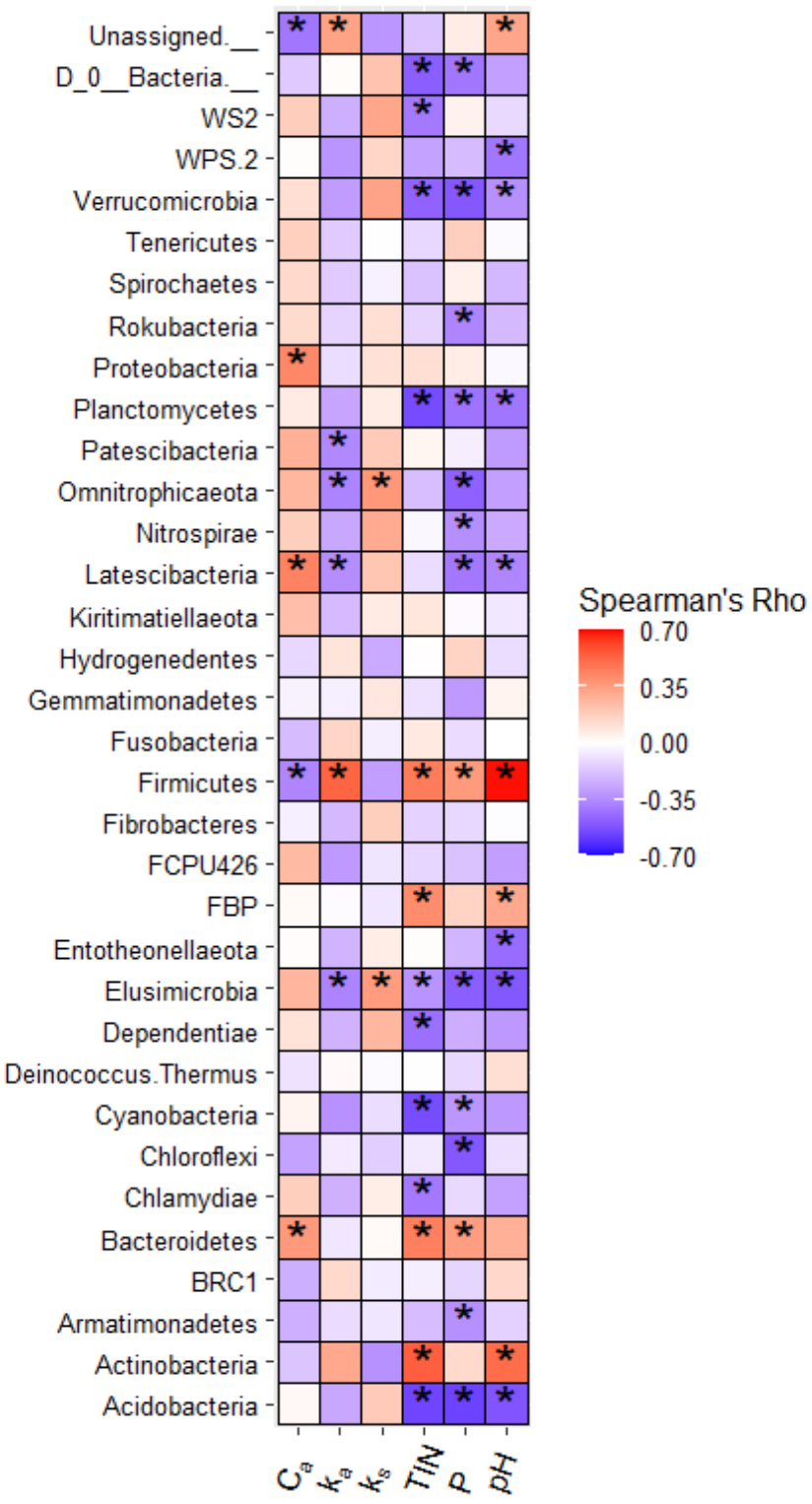

Figure 3.9 Correlations between bacterial phyla and active carbon pool size (C_a) and kinetic rate (k_a), non-active carbon pool kinetic rate (k_s), total inorganic nitrogen (TIN), phosphorus (P), and pH. Asterisks indicate correlations that were significant at α=0.05**.**

Table 3.3 Proportion of genera within selected phyla that are significantly correlated with soil carbon pools, total inorganic nitrogen (TIN), phosphorus (P), or pH**.** Correlations were performed using Spearman's rank correlation and were considered significant at α=0.05.

Phylum	Genera Count	C_a		k_a		k_s		TIN		P		pH	
		Pos. (%)	Neg. (%)	Pos. (%)	Neg. (%)	Pos. (%)	Neg. (%)	Pos. (%)	Neg. (%)	Pos. (%)	Neg. (%)	Pos. (%)	Neg. (%)
Proteobacteria	412	8.99	1.21	0.73	8.98	4.61	0.49	13.1	9.50	6.07	10.4	8.10	14.3
Bacteroidetes	131	7.63	1.53	0.00	13.0	9.16	2.29	16.0	9.92	6.87	6.87	13.0	12.2
Actinobacteria	157	3.18	4.46	3.18	6.37	1.91	3.18	12.7	8.28	3.18	15.9	16.6	8.92
Firmicutes	33	0.00	9.09	12.1	0.00	0.00	9.09	21.1	0.00	12.1	3.03	24.2	3.03
Verrucomicrobia	52	11.5	0.00	0.00	13.5	5.77	0.00	5.77	19.2	5.77	17.3	5.77	17.3
Acidobacteria	95	8.42	1.05	0.00	8.42	3.16	0.00	4.21	20.0	0.00	19.0	1.05	25.3

3.5 DISCUSSION

3.5.1 Hypothesis 1: Soil properties are related to differences in carbon pools across a burn severity gradient

Soil properties including forest floor mass, total N, and pH were related to C pools, but live and dead tree basal area also played an important role in explaining differences in C pools (Table 3.2). Dead tree basal area was related to several soil properties one-year post-fire, exhibiting direct links to total N and soil moisture and an indirect link to TIN (Fig. 3.1). I also observed a positive relationship between dead tree basal area and total N in a previous study (Adkins et al. 2020), an effect that could be caused by decomposition of dead tree roots leading to increased soil N inputs (Fahey et al. 1988). Root dynamics could also explain the direct negative link between dead tree basal area and C_a (Table 3.2), a relationship potentially resulting from decreased root exudation (Boddy et al. 2007; de Graaff et al. 2010). Along with forest floor mass and total N, dead tree basal area offset the direct positive link between severity and C_a, suggesting vegetation dynamics play an important role in mediating the response of soil C stability to fire. In my previous study performed three years post-fire, I found that forest floor mass was directly positively linked to live tree basal area (Adkins et al. 2020), whereas I found no such link here. This suggests that by one year post-fire, new litter inputs have not yet led to re-accumulation of forest floor, and litter deposition may not substantially increase forest floor mass until later in forest recovery.

The positive relationships of total N with C_a, and k_s are likely due to faster decomposition rates of high N (low C:N) soil organic matter (Aber and Melillo 1980; Melillo et al. 1982). Indeed, I found positive relationships between total N and C flux rate, and negative relationships between C:N and C flux rate during our soil incubation (data not shown). However,

total N did not vary with severity (Table 3.1), and thus does not account for k_s decreasing with severity. Similarly, although there was a tendency for C:N to increase with severity, this effect was not significant and therefore does not account for the decreased k_s. Interestingly, TIN was not related to C pool dynamics, despite indications that high TIN decreases organic matter decomposition rates in forests (Fog 1988; Janssens et al. 2010), and would therefore be expected to be negatively associated with k_a and/or k_s. There are several potential reasons why the impact of TIN on C cycling may be tempered in burned forests. First, TIN may primarily influence decomposition rates in organic surface horizons rather than in mineral soils (Janssens et al. 2010). This effect may therefore be minimal when fires lead to decreases in the forest floor layer, as I found here. Secondly, decreased decomposition in response to TIN may be partially attributable to acidifying effects of TIN on soil (Averill and Waring 2018). Increases in soil pH that typically occur following fires may therefore buffer against the acidifying effects of TIN and negate the potential impacts on decomposition. Finally, TIN may decrease decomposition by suppressing the abundance and activity of mycorrhizal (Phillips and Fahey 2007; Janssens et al. 2010) and lignolytic fungi (Fog 1988; DeForest et al. 2004; Entwistle et al. 2018). Mycorrhizal and saprotrophic fungal abundance is generally lower in burned versus unburned soils due to vegetation and litter loss, low tolerance for soil heating, and pH effects (Dooley and Treseder 2012; Pressler et al. 2018). Decomposition performed by these fungal groups is thus likely already lower in burned versus unburned areas, so higher TIN might not have any additional effects on their activities.

Although my SEMs displayed adequate goodness of fit statistics and identified several variables that were significantly related to C pool parameters, these SEMs do not appear to well explain the patterns of C pool kinetics across the severity gradient. For example, my non-linear

models indicated a strong negative effect of fire occurrence and burn severity on k_s, but the SEM indicated only a slightly negative effect. This suggests there are other unaccounted-for variables necessary for explaining relationships between fire and C pool kinetics. Despite the shortcomings of these SEMs, I present them here because they were still successful at identifying individual variables that are related to C pool sizes and kinetics, including ecosystem properties that are affected by fire and severity. For example, live and dead tree basal area, forest floor mass, pH, and pyrogenic C content are all properties that are associated with fire (Certini 2005; Hart et al. 2005; Miesel et al. 2018) and were directly linked to one or more C pool parameter in my SEMs.

Differences in soil organic matter composition across the severity gradient could account for the inability of the SEMs to represent the overall relationship between severity and C pool kinetics. For example, soil carbohydrate content decreased immediately following wildfires in *P. pinaster* forests of Spain (Martín et al. 2009), and lignin was found to be a more predominant component of soil organic matter in areas of high burn severity in coniferous and deciduous forests of northern Minnesota, USA (Miesel et al. 2015). The slower decomposition of lignin relative to carbohydrates could possibly account for the lower k_s in burned areas, especially if fire also decreases lignolytic fungal abundance. Accounting for soil organic matter composition could also capture the effects of colonization of burned areas by early successional herbs and shrubs during post-fire recovery (Hart et al. 2005; Collins and Roller 2013), which likely results in greater inputs of high N, low lignin deciduous litter over the short- to intermediate term (Hart et al. 2005). Differences in soil texture could also influence soil C pools in ways that were not accounted for in my SEMs. For example, fire can lead to altered soil textures by disrupting aggregates, degrading clay at high soil temperatures (>400 °C), and due to convective forces

generated by fire transporting fine soil particles (Certini 2005; Neary and DeBano 2005; Alcañiz et al. 2018). Soil C is stabilized via occlusion in aggregates and associations with clay (Jastrow et al. 2007), so changes to these soil physical properties could alter C pool structure and kinetics. In the field, soil microclimate differences between burned and unburned areas could also influence soil C pool kinetics in ways that are difficult to account for during lab-based soil incubations. For example, less canopy shading and decreased insulation from forest floor in high burn severity areas could result in higher temperatures and lower soil moisture in mineral soils (Hart et al. 2005; Kasischke and Johnstone 2005), thereby influencing microbial activity and C pool kinetics.

3.5.2 Hypothesis 2: Bacteria previously identified as fire responders are positively associated with burn severity

In support of my hypothesis, some of the genera harboring the severity-responsive OTUs (Fig. 3.6) have previously been identified as fire-responsive taxa (e.g. *Adhaeribacter*, *Roseomonas*, and *Flavisolibacter*) (Weber et al. 2014; Whitman et al. 2019). All of the genera harboring the severity-responsive OTUs were positively correlated with either TIN or P, suggesting copiotrophic life-strategies. To the best of my knowledge, other OTUs I identified as severity-responders have not previously been characterized as fire-responders. For example, *Segetibacter* accounted for two severity-responsive OTUs (and three positive fire-responsive OTUs) but has not been identified as fire-responsive in previous studies. However, *Segetibacter* was identified as responding positively to PyC additions in a lab incubation study, suggesting post-fire affinity (Woolet and Whitman 2020). I identified several genera as positive fire-responders (but not severity-responders) that other studies have also identified, including *Aeromicrobia*, *Blastococcus*, *Massilia*, *Phenylobacterium*, and *Devosia* (Weber et al. 2014;

Whitman et al. 2016; Huffman and Madritch 2018). Conversely, other studies have consistently identified *Arthrobacter* as a positive fire-responder (Weber et al. 2014; Huffman and Madritch 2018; Whitman et al. 2019), but I did not. My identification of unique severity responsive OTUs suggests that high burn severity may cause soil function to become dissimilar from pre-fire conditions. This is further evidenced by the positive associations of several imputed C-metabolism pathways with severity. The negative responses of bacterial phylogenetic diversity, OTU richness, and phyla-level oligotrophic-to-copiotrophic ratio to fire and burn severity agrees with my previous research where I found similar patterns three years post-fire in another mixed-conifer forest (Fig. 3.3; Adkins et al. 2020). This suggests that short- to intermediate-term decreases in bacterial diversity and oligotrophic-to-copiotrophic ratio are common responses to fire in mixed-conifer forests.

3.5.3 Hypothesis 3: Burned areas have a higher abundance of copiotrophic bacteria

The abundances of several dominant bacterial phyla were associated with fire, and in support of my hypothesis, phyla traditionally classified as copiotrophic tended to be more abundant and oligotrophic phyla less abundant in burned compared to unburned areas. The relative abundance of *Bacteroidetes* was higher and *Acidobacteria* was lower in burned areas compared to unburned areas, a dynamic that has often been observed following fires (Weber et al. 2014; Xiang et al. 2014b; Rodríguez et al. 2018; Pérez-Valera et al. 2019; Whitman et al. 2019). *Actinobacteria* and *Firmicutes* had higher relative abundance in burned areas one-year post-fire, which contrasts with my previous research where I found no differences in *Actinobacteria* and *Firmicutes* abundance three years after fire (Adkins et al. 2020). Other studies have found increased *Actinobacteria* and *Firmicutes* abundance in burned areas in several forest types (Ferrenberg et al. 2013; Weber et al. 2014; Fultz et al. 2016; Prendergast-Miller et al.

2017; Huffman and Madritch 2018; Pérez-Valera et al. 2019), and, like the present study, those studies all occurred within one year post-fire (range: one day to one year post-fire). The lack of studies encompassing longer timeframes makes it difficult to determine whether a parabolic-shaped response of *Actinobacteria* and *Firmicutes* abundance in mixed-conifer forests is typical, as suggested by this study and Adkins et al. (2020) together. The increased abundance of *Firmicutes* and *Actinobacteria* following fires is likely due to spore-forming ability (Prendergast-Miller et al. 2017), and thus the abundance of these phyla could decrease later in the post-fire recovery period as environmental characteristics become more important drivers of microbial communities (Ferrenberg et al. 2013; Whitman et al. 2019). The lower abundance of *Verrucomicrobia* and *Planctomycetes* in burned areas supports a previous study that identified a similar pattern in three months post-fire in ponderosa pine and mixed-conifer forest in New Mexico (Weber et al. 2014).

My hypothesis that greater copiotrophic bacterial abundance is related to post-fire increases in nutrient availability is supported by the positive relationships between TIN and *Bacteroidetes* and between P and *Firmicutes*. Support for my hypothesis that copiotrophic bacteria would be associated with higher C_a is mixed: *Bacteroidetes* and *Proteobacteria* abundance was positively associated with C_a while *Firmicutes* was negatively associated. The positive association of *Bacteroidetes* with C_a is particularly interesting because *Bacteroidetes* abundance increased with severity, but C_a was unchanged. This suggests that *Bacteroidetes* do not necessarily respond to labile C and nutrient availability simultaneously and that higher TIN concentrations maintain the greater *Bacteroidetes* populations in burned areas. Given that *Bacteroidetes* is the most abundant phylum in these soils, the response of *Bacteroidetes* to greater TIN could influence C cycling in ways that diverge with time post-fire. In the short term,

increased TIN could lead to more efficient C use by *Bacteroidetes* by allowing them to preferentially decompose labile C substrates that have high C:N ratios. However, if aboveground vegetation losses result in decreased labile C inputs in the long-term, *Bacteroidetes* may switch to recalcitrant C substrates, requiring greater investment in exoenzymes, and consequently, greater C mineralization (Malik et al. 2020).

Shifting abundances of C degradation pathways also supported the hypothesis that bacterial communities are more copiotrophic in burned areas. Higher ratios of genes associated with carbohydrate degradation versus aromatic compound degradation is a metagenomic indicator of community level copiotrophy (Hartman et al. 2017), and I found that carbohydrate degradation pathway abundance increased with severity while aromatic degradation pathway abundance was unchanged (Fig. 3.7). This approach can be extended to other compound types. Amino acids are labile C substrates, and amino acid degradation pathway abundance increased with severity. In contrast, fatty-acids and lipids are slow to decompose, and the abundance of pathways associated with their degradation was unrelated to severity, patterns that also suggest community-level copiotrophy increases with severity. Inputs of recalcitrant C compounds to soil may be high after fire due to the formation of pyrogenic organic matter and wood deposition resulting from tree mortality. If the input of this recalcitrant C is not accompanied by increases in the metabolic pathways associated with its degradation, recalcitrant C could accumulate in soil, leading to larger C_s $pool_s$ and soil C stocks over the long-term.

Validity of copiotroph-oligotroph classifications depends on bacterial taxonomic level

Although I found support for my hypothesis that phyla-level copiotroph versus oligotroph bacterial abundance differed between burned and unburned areas, I also found that these life-history classification depended on the resource (i.e. nutrients versus C) and taxonomic level

considered. Copiotrophic abundance is frequently associated both with labile C and nutrient availability, and, when considered at the phylum level, traditional ecological classifications appeared to agree with this framework. For example, in addition to *Proteobacteria* and *Bacteroidetes* increasing in abundance with C_a, the copiotrophic phyla *Actinobacteria* increased in abundance with TIN. Furthermore, the oligotrophic phyla *Acidobacteria* and *Verrucomicrobia* were negatively associated with nutrient concentrations, suggesting they are outcompeted by copiotrophs at high nutrient availability. A notable exception to the phyla-level oligotroph-copiotroph framework occurred for *Firmicutes*, which is typically classified as a copiotroph. *Firmicutes* increased in abundance with nutrient concentrations, suggesting copiotrophy, but was negatively correlated with C_a, suggesting oligotrophy. The oligotrophic traits of *Firmicutes* could be due to evolutionary tradeoffs related to endospore-forming ability (Malik et al. 2020). Maintaining sporulation ability is energetically costly, and, in environments that do not select for this trait, *Firmicutes* often lose the capacity for spore-formation and in turn achieve faster growth rates (Filippidou et al. 2016). Greater post-fire abundance of *Firmicutes* is likely due to the heat-tolerance of endospores (Ferrenberg et al. 2013; Prendergast-Miller et al. 2017), so post-fire soils may be dominated by slow-growing *Firmicutes* genera that are less able to rapidly respond to labile C availability. This indicates, that even at the phylum level, ecological classification of bacteria depends on specific environmental characteristics, as well as the resource or trait considered, and may oversimplify the metabolic diversity of bacteria within phyla (Hartmann et al. 2017; Ho et al. 2017).

The limitations of the oligotroph-copiotroph framework became even clearer when considered at the genus level. For example, despite their copiotrophic classification, a substantial proportion of *Proteobacteria* and *Bacteroidetes* genera were negatively related to TIN (Table

3.3). Furthermore, more than half of the genera harbored within *Proteobacteria* and *Bacteroidetes* were not significantly correlated with C_a or nutrient concentrations. This suggests that phyla-level ecological classification may be based on a minority of genera and fail to encompass taxa that are oligotrophic or neutral in their response to resources, especially if responses to C and nutrients are not considered in conjunction.

Similar divergence of ecological traits were apparent among genera harbored within the oligotrophically classified *Acidobacteria* and *Verrucomicrobia* phyla. Although a greater proportion of genera exhibited oliogotrophic tendencies in their relationships with nutrient availability, more genera were copiotrophic in their relationships with labile C availability. Only one of the nine *Acidobacteria* genera that was positively related to C_a was correlated with nutrient concentrations, and 50% of the *Verrucomicrobia* genera that were positively related to C_a were negatively correlated with nutrient concentrations. This suggests tradeoffs in traits related to C versus nutrient acquisition at the genus level (Malik et al. 2020), and that genera within the same phylum occupy different ecological niches. Niche differentiation among *Acidobacteria* taxa could explain the divergent response of subgroups within this phyla to fire (Weber et al. 2014; Adkins et al. 2020). The divergence of ecological strategies at the genera level contributes to a growing body of evidence suggesting that ecological classification of bacteria should occur at a finer taxonomic resolution than the phylum-scale (Hartmann et al. 2017; Ho et al. 2017; Sauvadet et al. 2019). Furthermore, my results show that the same taxon can exhibit both copiotrophic and oligotrophic traits depending on whether C or nutrients are the resources of interest. The oligotroph-copiotroph dichotomy may therefore fail to capture the metabolic breadth of bacteria, and a three-dimensional competitor-stress-ruderal framework (Ho et al. 2013; Malik et al. 2020) may be a more suitable alternative, especially in disturbed

ecosystems. Nevertheless, despite the apparent shortcoming of taxonomy-based life-history classifications, the fact that all of the OTUs that were positively associated with burn severity were also positively associated with nutrient concentrations supports the hypothesis that bacterial communities are more copiotrophic in burned areas than unburned areas.

3.5.4 Hypothesis 4: Bacterial taxa are associated with carbon pool kinetic rates

My hypothesis that k_a would be positively associated with copiotrophic bacterial taxa is not well supported. *Firmicutes* was the only phylum that was positively associated with k_a, and, although *Firmicutes* is often considered copiotrophic, I found that this phyla exhibited both copiotrophic and oligotrophic characteristics. In contrast, I found that k_s was positively associated with *Elusimicrobia* abundance. Although *Elusimicrobia* has not been classified as either copiotrophic or oligotrophic, my results and others suggest that *Elusimicrobia* is oligotrophic. *Elusimicrobia* is a recently defined bacterial phylum that appears to be metabolically diverse, with various lineages capable of N-fixation and nitrate reduction (Meheust et al. 2019). *Elusimicrobia* may preferentially utilize recalcitrant forms of C as substrate (Chávez-Romero et al. 2016), which may explain its association with k_s. In fact, *Elusimicrobia* have been identified as degraders of lignin (Wilhelm 2016), a plant compound that degrades slowly when other bioavailable C compounds are not available to provide energy for its decomposition (Klotzbücher et al. 2011). Considered with my observed negative relationship of *Elusimicrobia* with TIN and P, this suggests *Elusimicrobia* is an oligotrophic phylum. *Elusimicrobia* was a relatively rare phyla in my soils, exhibiting a relative abundance of only 0.21%, so likely is an indicator rather than a driver of higher k_s.

3.6 CONCLUSIONS

My results suggest that soil C is more persistent in burned than unburned areas one year after fire (as indicated by lower k_s), and that this effect is at least partially influenced by top-down controls exerted by vegetation on soil properties and bacterial communities. Dead tree basal area specifically was directly or indirectly linked to soil moisture, total N, and TIN, and, through these linkages, influenced soil bacterial communities. In concert with the positive association between live tree basal area and k_s, these results suggest that vegetation structure has a downstream effect on soil C persistence during post-fire recovery. The increase in C persistence may partially offset ecosystem C losses from biomass combustion while vegetation recovers, but it is possible that the positive relationship between fire and fast C-cycling copiotrophic bacterial taxa may negate some of these effects.

Differences in bacterial community structure between burned and unburned areas could be explained by the copiotroph-oligotroph life-history framework when considered at the phylum level but was less effective in explaining differences at the genus level. This suggests that coarse life-history classifications fail to capture the metabolic breadth of bacterial taxa and may therefore limit the ability to predict the influence of microbial communities on ecosystem function during post-fire recovery. Certain bacterial taxa were associated with C pool and kinetics. Although my study cannot disentangle correlation versus causation of bacterial communities on soil C pools, these results suggest that post-fire changes in microbial composition are linked to soil C cycling. Future research could incorporate isotopic tracing techniques to further elucidate which bacterial taxa drive differences in C cycling and whether life-history strategy explains these differences. Such information could be incorporated into

global ecosystem models to help anticipate the effects of fire regime change on the global C cycle.

APPENDIX

SUPPLEMENTAL FIGURES

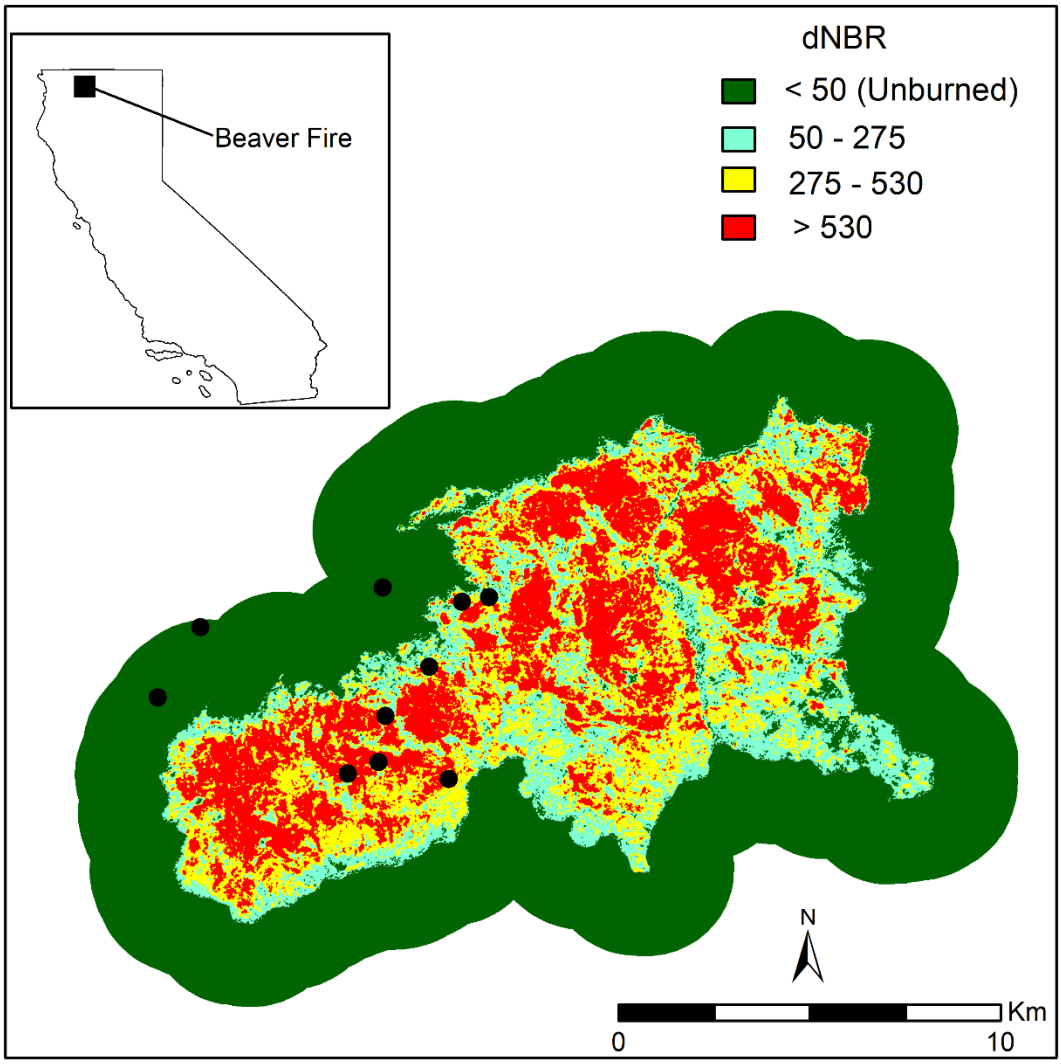

Figure S3.1. Locations of field plots within a burn severity matrix resulting from the Beaver Fire. dNBR values are grouped into unburned, low, moderate, and high severity thresholds identified by the Monitoring Trends in Burn Severity team.

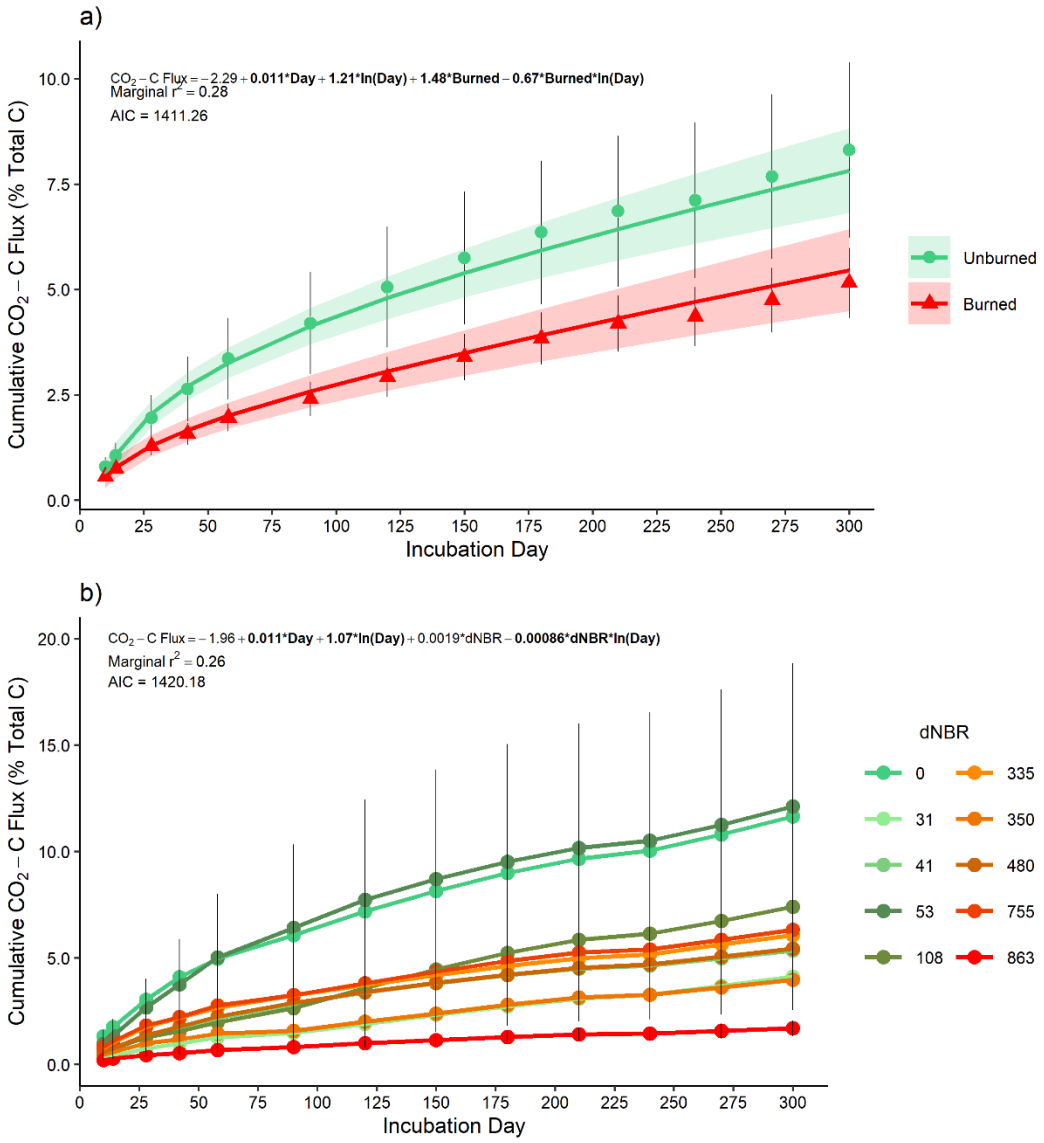

Figure S3.2 Mean (± SE) cumulative CO_2-C efflux (points) over a 300-day laboratory incubation of mineral soils (0-5 cm) grouped by fire-occurrence (a) and severity (b). In panel a, colored lines represent the fitted model, ribbons are the standard error of prediction, and vertical lines are standard errors of means (n=4 for unburned, n=6 for burned). In panel b, colored lines represent change in cumulative CO_2-C efflux between sampling days, and verticals bars are standard errors of means (n=3 or 4 per plot).

SUPPLEMENTAL TABLES

Table S3.1 Elastic-Net selected Generalized Linear Models explaining C-pool parameters based on bacterial phyla abundance.

Response Variable	Elastic-Net Selected Generalized Linear Model
C_a	$-888 - 10.6\text{Armatimonadetes} + 118.\text{Bacteroidetes} + 134\text{FCPU426} - 208\text{Firmicutes} + 209\text{Kiritimatiellaeota} + 203.\text{Proteobacteria} + 17.1\text{WS2} - 69.0\text{Unclassified}$
k_a	$0.020 + 0.0016\text{Firmicutes} - 0.00015\text{Omnitrophicaetoa}$
k_s	$0.00014 + 2.48\times10^{-6}\text{Elusimicrobia} - 3.00\times10^{-6}\text{Unclassified}$

REFERENCES

REFERENCES

Aber JD, Melillo JM (1980) Litter decomposition: measuring relative contributions of organic matter and nitrogen to forest soils. Can J Bot 58:416–421. doi: 10.1139/b80-046

Adkins J, Docherty KM, Gutknecht JLM, Miesel JR (2020) How do soil microbial communities respond to fire in the intermediate term? Investigating direct and indirect effects associated with fire occurrence and burn severity. Sci Total Environ 745:140957. doi: 10.1016/j.scitotenv.2020.140957

Adkins J, Sanderman J, Miesel J (2019) Soil carbon pools and fluxes vary across a burn severity gradient three years after wildfire in Sierra Nevada mixed-conifer forest. Geoderma 333:10–22. doi: 10.1016/j.geoderma.2018.07.009

Alcañiz M, Outeiro L, Francos M, Úbeda X (2018) Effects of prescribed fires on soil properties: A review. Sci Total Environ 613–614:944–957. doi: 10.1016/j.scitotenv.2017.09.144

Allison SD, Martiny JBH (2008) Colloquium paper: resistance, resilience, and redundancy in microbial communities. Proc Natl Acad Sci U S A 105 Suppl:11512–9. doi: 10.1073/pnas.0801925105

Averill C, Waring B (2018) Nitrogen limitation of decomposition and decay: How can it occur? Glob Chang Biol 24:1417–1427. doi: 10.1111/gcb.13980

Barbera P, Kozlov AM, Czech L, et al (2018) EPA-ng: Massively Parallel Evolutionary Placement of Genetic Sequences. Syst Biol 68:365–369. doi: 10.1093/sysbio/syy054

Boddy E, Hill PW, Farrar J, Jones DL (2007) Fast turnover of low molecular weight components of the dissolved organic carbon pool of temperate grassland field soils. Soil Biol Biochem 39:827–835. doi: 10.1016/j.soilbio.2006.09.030

Bokulich NA, Kaehler BD, Rideout JR, et al (2018) Optimizing taxonomic classification of marker-gene amplicon sequences with QIIME 2's q2-feature-classifier plugin. Microbiome 6:90. doi: 10.1186/s40168-018-0470-z

Bolyen E, Rideout JR, Dillon MR, et al (2019) Reproducible, interactive, scalable and extensible microbiome data science using QIIME 2. Nat Biotechnol 37:852–857. doi: 10.1038/s41587-019-0209-9

Box GEP, Cox DR (1964) An Analysis of Transformations. J R Stat Soc Ser B 26:211–243. doi: 10.1111/j.2517-6161.1964.tb00553.x

Callahan BJ, McMurdie PJ, Rosen MJ, et al (2016) DADA2: High-resolution sample inference from Illumina amplicon data. Nat Methods 13:581–583. doi: 10.1038/nmeth.3869

Caporaso JG, Kuczynski J, Stombaugh J, et al (2010) QIIME allows analysis of high- throughput community sequencing data Intensity normalization improves color calling in SOLiD sequencing. Nat Publ Gr 7:335–336. doi: 10.1038/nmeth0510-335

Caspi R, Billington R, Fulcher CA, et al (2018) The MetaCyc database of metabolic pathways and enzymes. Nucleic Acids Res 46:D633–D639. doi: 10.1093/nar/gkx935

Certini G (2005) Effects of fire on properties of forest soils: a review. Oecologia 143:1–10. doi: 10.1007/s00442-004-1788-8

Chávez-Romero Y, Navarro-Noya YE, Reynoso-Martínez SC, et al (2016) 16S metagenomics reveals changes in the soil bacterial community driven by soil organic C, N-fertilizer and tillage-crop residue management. Soil Tillage Res 159:1–8. doi: 10.1016/j.still.2016.01.007

Collins BM, Roller GB (2013) Early forest dynamics in stand-replacing fire patches in the northern Sierra Nevada, California, USA. Landsc Ecol 28:1801–1813. doi: 10.1007/s10980-013-9923-8

Collins HP, Elliott ET, Paustian K, et al (2000) Soil carbon pools and fluxes in long-term Corn Belt agroecosystems. Soil Biol Biochem 32:157–168. doi: 10.1016/S0038-0717(99)00136-4

Czech L, Barbera P, Stamatakis A (2020) Genesis and Gappa: processing, analyzing and visualizing phylogenetic (placement) data. Bioinformatics. doi: 10.1093/bioinformatics/btaa070

De Caceres M, Legendre P (2009) Associations between species and groups of sites: indices and statistical inference. Ecology

de Graaff M-A, Adkins J, Kardol P, Throop HL (2015) A meta-analysis of soil biodiversity impacts on the carbon cycle. Soil 1:257–271. doi: 10.5194/soil-1-257-2015

de Graaff M-A, Classen AT, Castro HF, Schadt CW (2010) Labile soil carbon inputs mediate the soil microbial community composition and plant residue decomposition rates. New Phytol 188:1055–1064. doi: 10.1111/j.1469-8137.2010.03427.x

DeForest JL, Zak DR, Pregitzer KS, Burton AJ (2004) Atmospheric nitrate deposition and the microbial degradation of cellobiose and vanillin in a northern hardwood forest. Soil Biol Biochem 36:965–971. doi: 10.1016/j.soilbio.2004.02.011

Dennison PE, Brewer SC, Arnold JD, Moritz MA (2014) Large wildfire trends in the western

United States, 1984-2011. Geophys Res Lett 41:2928–2933. doi: 10.1002/2014GL059576

Doane TA, Horwáth WR (2003) Spectrophotometric determination of nitrate with a single reagent. Anal Lett 36:2713–2722. doi: 10.1081/AL-120024647

Domeignoz-Horta LA, Pold G, Liu X-JA, et al (2020) Microbial diversity drives carbon use efficiency in a model soil. Nat Commun 11:3684. doi: 10.1038/s41467-020-17502-z

Dooley SR, Treseder KK (2012) The effect of fire on microbial biomass: A meta-analysis of field studies. Biogeochemistry 109:49–61. doi: 10.1007/s10533-011-9633-8

Douglas GM, Maffei VJ, Zaneveld J, et al (2019) PICRUSt2: An improved and extensible approach for metagenome inference. bioRxiv. doi: 10.1101/672295

Dove NC, Safford HD, Bohlman GN, et al (2020) High-severity wildfire leads to multi-decadal impacts on soil biogeochemistry in mixed-conifer forests. Ecol Appl 0:1–18. doi: 10.1002/eap.2072

Entwistle EM, Zak DR, Argiroff WA (2018) Anthropogenic N deposition increases soil C storage by reducing the relative abundance of lignolytic fungi. Ecol Monogr 88:225–244. doi: 10.1002/ecm.1288

Fahey TJ, Hughes JW, Pu M, Arthur MA (1988) Root decomposition and nutrient flux following whole-tree harvest of northern hardwood forest. For Sci 34:744–768. doi: 10.1093/forestscience/34.3.744

Faith DP (1992) Conservation evaluation and phylogentic diversity. Biol Conserv 61:1–10. doi: 10.1890/0012-9658(2006)87[1465:ATTFHF]2.0.CO;2

Fernández I, Cabaneiro A, Carballas T (1997) Organic matter changes immediately after a wildfire in an atlantic forest soil and comparison with laboratory soil heating. Soil Biol Biochem 29:1–11. doi: 10.1016/S0038-0717(96)00289-1

Ferrenberg S, O'neill SP, Knelman JE, et al (2013) Changes in assembly processes in soil bacterial communities following a wildfire disturbance. ISME J 7:1102–1111. doi: 10.1038/ismej.2013.11

Fierer N (2017) Embracing the unknown: Disentangling the complexities of the soil microbiome. Nat Rev Microbiol 15:579–590. doi: 10.1038/nrmicro.2017.87

Fierer N, Bradford MA, Jackson RB (2007) Toward an ecological classification of soil bacteria. Ecology 88:1354–1364. doi: 10.1890/05-1839

Fierer N, Lauber CL, Ramirez KS, et al (2012) Comparative metagenomic, phylogenetic and physiological analyses of soil microbial communities across nitrogen gradients. ISME J 6:1007–1017. doi: 10.1038/ismej.2011.159

Filippidou S, Wunderlin T, Junier T, et al (2016) A combination of extreme environmental conditions favor the prevalence of endospore-forming firmicutes. Front Microbiol 7:1–11. doi: 10.3389/fmicb.2016.01707

Flannigan MD, Krawchuk MA, de Groot WJ, et al (2009) Implications of changing climate for global wildland fire. Int J Wildl Fire 483–507. doi: 10.1071/WF08187

Fog K (1988) The effect of added nitrogen on the rate of decompositon of organic matter. Biol Rev 63:433–462. doi: 10.1111/j.1469-185X.1988.tb00725.x

Friedman J, Hastie T, Tibshirani R (2010) Regularizaton paths for generalized linear models via coordinate descent. J Stat Softw 33:1–22.

Fultz LM, Moore-kucera J, Davinic M, et al (2016) Forest wildfire and grassland prescribed fire effects on soil biogeochemical processes and microbial communities: Two case studies in the semi-arid Southwest. Appl Soil Ecol 99:118–128.

Grace JB, Scheiner SM, Schoolmaster DR (2015) Structural equation modeling: building and evaluating causal models. In: Fox GA, Negrete-Yankelevich S, Sosa VJ (eds) Ecological Statistics: Contemporary Theory and Application. Oxford University Press, pp 168–199

Graham EB, Knelman JE, Schindlbacher A, et al (2016) Microbes as engines of ecosystem function: When does community structure enhance predictions of ecosystem processes? Front Microbiol 7:1–10. doi: 10.3389/fmicb.2016.00214

Greenfield LG, Gregorich EG, van Kessel C, et al (2013) Acid hydrolysis to define a biologically-resistant pool is compromised by carbon loss and transformation. Soil Biol Biochem 64:122–126. doi: 10.1016/j.soilbio.2013.04.009

Hart SC, DeLuca TH, Newman GS, et al (2005) Post-fire vegetative dynamics as drivers of microbial community structure and function in forest soils. For Ecol Manage 220:166–184. doi: 10.1016/j.foreco.2005.08.012

Hartman WH, Ye R, Horwath WR, Tringe SG (2017) A genomic perspective on stoichiometric regulation of soil carbon cycling. ISME J 11:2652–2665. doi: 10.1038/ismej.2017.115

Hartmann M, Brunner I, Hagedorn F, et al (2017) A decade of irrigation transforms the soil microbiome of a semi-arid pine forest. Mol Ecol 26:1190–1206. doi: 10.1111/mec.13995

Ho A, Di Lonardo DP, Bodelier PLE (2017) Revisiting life strategy concepts in environmental microbial ecology. FEMS Microbiol Ecol 93:1–14. doi: 10.1093/femsec/fix006

Ho A, Kerckhof FM, Luke C, et al (2013) Conceptualizing functional traits and ecological characteristics of methane-oxidizing bacteria as life strategies. Environ Microbiol Rep 5:335–345. doi: 10.1111/j.1758-2229.2012.00370.x

Holden SR, Rogers BM, Treseder KK, Randerson JT (2016) Fire severity influences the response of soil microbes to a boreal forest fire. Environ Res Lett 11:035004. doi: 10.1088/1748-9326/11/3/035004

Huffman MS, Madritch MD (2018) Soil microbial response following wildfires in thermic oak-pine forests. Biol Fertil Soils 54:985–997. doi: 10.1007/s00374-018-1322-5

Janssens IA, Dieleman W, Luyssaert S, et al (2010) Reduction of forest soil respiration in response to nitrogen deposition. Nat Geosci 3:315–322. doi: 10.1038/ngeo844

Jastrow JD, Amonette JE, Bailey VL (2007) Mechanisms controlling soil carbon turnover and their potential application for enhancing carbon sequestration. Clim Change 80:5–23. doi: 10.1007/s10584-006-9178-3

Kashian DM, Romme WH, Tinker DB, et al (2006) Carbon storage on landscapes with stand-replacing fires. Bioscience 56:598–606. doi: 10.1641/0006-3568(2006)56[598:CSOLWS]2.0.CO;2

Kasischke ES, Johnstone JF (2005) Variation in postfire organic layer thickness in a black spruce forest complex in interior Alaska and its effects on soil temperature and moisture. Can J For Res 35:2164–2177. doi: 10.1139/x05-159

Katoh K, Standley DM (2013) MAFFT multiple sequence alignment software version 7: Improvements in performance and usability. Mol Biol Evol 30:772–780. doi: 10.1093/molbev/mst010

Klotzbücher T, Kaiser K, Guggenberger G, Kalbitz K (2011) A new model for the fate of lignin in decomposing. Ecology 95:1052–1062. doi: 10.2307/41151233

Kurth VJ, MacKenzie MD, DeLuca TH (2006) Estimating charcoal content in forest mineral soils. Geoderma 137:135–139. doi: 10.1016/j.geoderma.2006.08.003

Kuzyakov Y (2011) How to link soil C pools with CO2 fluxes? Biogeosciences 8:1523–1537. doi: 10.5194/bg-8-1523-2011

Lefcheck JS (2016) piecewiseSEM: Piecewise structural equation modelling in r for ecology,

evolution, and systematics. Methods Ecol Evol 7:573–579. doi: 10.1111/2041-210X.12512

Louca S, Doebeli M (2017) Efficient comparative phylogenetics on large trees. Bioinformatics 34:1053–1055. doi: 10.1093/bioinformatics/btx701

Lozupone C, Knight R (2005) UniFrac : a New Phylogenetic Method for Comparing Microbial Communities UniFrac : a New Phylogenetic Method for Comparing Microbial Communities. Appl Environ Microbiol 71:8228–8235. doi: 10.1128/AEM.71.12.8228

Malik AA, Martiny JBH, Brodie EL, et al (2020) Defining trait-based microbial strategies with consequences for soil carbon cycling under climate change. ISME J 14:1–9. doi: 10.1038/s41396-019-0510-0

Martín A, Díaz-Raviña M, Carballas T (2009) Evolution of composition and content of soil carbohydrates following forest wildfires. Biol Fertil Soils 45:511–520. doi: 10.1007/s00374-009-0363-1

Meheust R, Castelle CJ, Carnevali PBM, et al (2019) Aquatic Elusimicrobia are metabolically diverse compared to gut microbiome Elusimicrobia and some have novel nitrogenase-like gene clusters. bioRxiv. doi: 10.1101/765248

Melillo JM, Aber JD, Muratore JF (1982) Nitrogen and Lignin Control of Hardwood Leaf Litter Decomposition Dynamics. Ecology 63:621–626.

Miesel J, Reiner A, Ewell C, et al (2018) Quantifying Changes in Total and Pyrogenic Carbon Stocks Across Fire Severity Gradients Using Active Wildfire Incidents. Front Earth Sci 6:1–21. doi: 10.3389/feart.2018.00041

Miesel JR, Hockaday WC, Kolka RK, Townsend PA (2015) Soil organic matter composition and quality across fire severity gradients in coniferous and deciduous forests of the southern boreal region. J Geophys Res Biogeosciences 120:1124–1141. doi: 10.1002/2015JG002959

MTBS (2017) Monitoring trends in burn severity. https://www.mtbs.gov.

NCEI-NOAA (2017) National centers for environmental information. https://www.ncei.noaa.gov.

Neary D., DeBano L. (2005) Wildland fire in ecosystems effects of fire on soil and water.

Oksanen J, Blanchet FG, Friendly M, et al (2019) vegan: Community Ecology Package.

Olsen SR, Cole CV, Watanable FS, Dean LA (1954) Estimation of available phosphorus in soils by extraction with sodium bicarbonate.

Parsons A, Robichaud PR, Lewis S a, et al (2010) Field guide for mapping post-fire soil burn severity. Gen. Tech. Rep. RMRS-GTR-243

Paul EA, Morris SJ, Conant RT, Plante AF (2006) Does the acid hydrolysis-incubation method measure meaningful soil organic carbon pools? Soil Sci Soc Am J 70:1023–1035. doi: 10.2136/sssaj2005.0103

Pedregosa F, Varoquaux G, Gramfort A, et al (2011) Scikit-learn: Machine learning in Python. J Mach Learn Res 12:2825–2830.

Pérez-Valera E, Goberna M, Faust K, et al (2017) Fire modifies the phylogenetic structure of soil bacterial co-occurrence networks. Environ Microbiol 19:317–327. doi: 10.1111/1462-2920.13609

Pérez-Valera E, Goberna M, Verdú M (2019) Fire modulates ecosystem functioning through the phylogenetic structure of soil bacterial communities. Soil Biol Biochem 129:80–89. doi: 10.1016/j.soilbio.2018.11.007

Perry DA, Oren R, Hart SC (2008) Forest Ecosystems. Johns Hopkins University Press, Baltimore

Phillips RP, Fahey TJ (2007) Fertilization effects on fineroot biomass, rhizosphere microbes and respiratory fluxes in hardwood forest soils. New Phytol 176:655–664. doi: 10.1111/j.1469-8137.2007.02204.x

Pinheiro J, Bates D, Debroy S, Sarkar D (2019) nlme: Linear and nonlinear mixed effects models.

Pinheiro JC, Bates DM (2000) Mixed-effects models in S and S-Plus. Springer-Verlag, New York

Prendergast-Miller MT, de Menezes AB, Macdonald LM, et al (2017) Wildfire impact: Natural experiment reveals differential short-term changes in soil microbial communities. Soil Biol Biochem 109:1–13. doi: 10.1016/j.soilbio.2017.01.027

Pressler Y, Moore JC, Cotrufo MF (2018) Belowground community responses to fire: meta-analysis reveals contrasting responses of soil microorganisms and mesofauna. Oikos 1–19. doi: 10.1111/oik.05738

Price MN, Dehal PS, Arkin AP (2010) FastTree 2 - Approximately maximum-likelihood trees for large alignments. PLoS One. doi: 10.1371/journal.pone.0009490

Prosser JI, Martiny JBH (2020) Conceptual challenges in microbial community ecology. Philos

Trans R Soc B Biol Sci 375:2–4. doi: 10.1098/rstb.2019.0241

Quast C, Pruesse E, Yilmaz P, et al (2013) The SILVA ribosomal RNA gene database project: Improved data processing and web-based tools. Nucleic Acids Res 41:590–596. doi: 10.1093/nar/gks1219

R Core Team (2019) R: A language and environment for statistical computing.

Ramirez KS, Craine JM, Fierer N (2012) Consistent effects of nitrogen amendments on soil microbial communities and processes across biomes. Glob Chang Biol 18:1918–1927. doi: 10.1111/j.1365-2486.2012.02639.x

Rodríguez J, González-Pérez JA, Turmero A, et al (2018) Physico-chemical and microbial perturbations of Andalusian pine forest soils following a wildfire. Sci Total Environ 634:650–660. doi: 10.1016/j.scitotenv.2018.04.028

Rodríguez J, González-Pérez JA, Turmero A, et al (2017) Wildfire effects on the microbial activity and diversity in a Mediterranean forest soil. Catena 158:82–88. doi: 10.1016/j.catena.2017.06.018

Ruefenacht B, Finco MV, Nelson MD, et al (2008) Conterminous U.S. and Alaska Forest Type Mapping Using Forest Inventory and Analysis Data. Photogramm Eng Remote Sens 74:1379–1388. doi: 10.14358/PERS.74.11.1379

Sáenz de Miera LE, Pinto R, Gutierrez-Gonzalez JJ, et al (2020) Wildfire effects on diversity and composition in soil bacterial communities. Sci Total Environ. doi: 10.1016/j.scitotenv.2020.138636

Sauvadet M, Fanin N, Chauvat M, Bertrand I (2019) Can the comparison of above- and below-ground litter decomposition improve our understanding of bacterial and fungal successions? Soil Biol Biochem 132:24–27. doi: 10.1016/j.soilbio.2019.01.022

Schimel JP, Schaeffer SM (2012) Microbial control over carbon cycling in soil. Front Microbiol 3:1–11. doi: 10.3389/fmicb.2012.00348

Schmidt MWI, Torn MS, Abiven S, et al (2011) Persistence of soil organic matter as an ecosystem property. Nature 478:49–56. doi: 10.1038/nature10386

Sinsabaugh RL, Reynolds H, Long TM (2000) Rapid assay for amidohydrolase (urease) activity in environmental samples. Soil Biol Biochem 32:2095–2097. doi: 10.1016/S0038-0717(00)00102-4

Soil Survey Staff Official soil series descriptions. In: Nat. Resour. Conserv. Serv. United States

Dep. Agric. www.nrcs.usda.gov.

Soil Survey Staff Web Soil Survey. In: Nat. Resour. Conserv. Serv. United States Dep. Agric. http://websoilsurvey.sc.egov.usda.gov/.

Torn MS, Kleber M, Zavaleta ES, et al (2013) A dual isotope approach to isolate soil carbon pools of different turnover times. Biogeosciences 10:8067–8081. doi: 10.5194/bg-10-8067-2013

Treseder KK, Balser TC, Bradford MA, et al (2012) Integrating microbial ecology into ecosystem models: challenges and priorities. Biogeochemistry 109:7–18. doi: 10.1007/s10533-011-9636-5

Trumbore S (2000) Age of soil organic matter and soil respiration: radiocarbon constraints of belowground C dynamics. Ecol Appl 10:399–411.

Wagg C, Schlaeppi K, Banerjee S, et al (2019) Fungal-bacterial diversity and microbiome complexity predict ecosystem functioning. Nat Commun 10:1–10. doi: 10.1038/s41467-019-12798-y

Wan S, Hui D, Luo Y (2001) Fire effects on nitrogen pools and dynamics in terrestrial ecosystems: A meta-analysis. Ecol Appl 11:1349–1365.

Wang Q, Zhong M, Wang S (2012) A meta-analysis on the response of microbial biomass, dissolved organic matter, respiration, and N mineralization in mineral soil to fire in forest ecosystems. For Ecol Manage 271:91–97. doi: 10.1016/j.foreco.2012.02.006

Weber CF, Lockhart JS, Charaska E, et al (2014) Bacterial composition of soils in ponderosa pine and mixed conifer forests exposed to different wildfire burn severity. Soil Biol Biochem 69:242–250. doi: 10.1016/j.soilbio.2013.11.010

Westerling AL (2006) Warming and Earlier Spring Increase Western U.S. Forest Wildfire Activity. Science 313:940–943. doi: 10.1126/science.1128834

Whitman T, Pepe-Ranney C, Enders A, et al (2016) Dynamics of microbial community composition and soil organic carbon mineralization in soil following addition of pyrogenic and fresh organic matter. ISME J 10:2918–2930. doi: 10.1038/ismej.2016.68

Whitman T, Whitman E, Woolet J, et al (2019) Soil bacterial and fungal response to wildfires in the Canadian boreal forest across a burn severity gradient. Soil Biol Biochem 138:107571. doi: 10.1016/j.soilbio.2019.107571

Wilhelm RC (2016) Deciphering decomposition and the effects of disturbance in forest soil

microbial communities with metagenomics and stable isotope probing. University of British Columbia

Woolet J, Whitman T (2020) Pyrogenic organic matter effects on soil bacterial community composition. Soil Biol Biochem 141:107678. doi: 10.1016/j.soilbio.2019.107678

Xiang X, Shi Y, Yang J, et al (2014) Rapid recovery of soil bacterial communities after wildfire in a Chinese boreal forest. Sci Rep 4:1–8. doi: 10.1038/srep03829

Ye Y, Doak TG (2009) A Parsimony Approach to Biological Pathway Reconstruction/Inference for Genomes and Metagenomes. PLOS Comput Biol 5:e1000465.

CHAPTER 4:

POST-FIRE EFFECTS OF SOIL HEATING INTENSITY AND PYROGENIC ORGANIC MATTER ON MICROBIAL ANABOLISM: A LABORATORY-BASED APPROACH

4.1 ABSTRACT

Wildfires result in direct and indirect CO_2 emissions due to combustion and post-fire decomposition. Approximately half of temperate forest ecosystem carbon (C) is stored in soil, so post-fire soil C cycling likely impacts the strength of forest C sinks. Soil C sink strength is in part determined by soil microbial anabolism versus catabolism, which dictates the amount of C stored in microbial biomass versus respired as CO_2. Fires affect soil C availability and composition, changes that could alter carbon use efficiency (CUE) and microbial biomass production, and thus potentially influence recovery of the forest C sink. Wildfire intensity is forecast to increase in forests of the western United States and understanding the impacts of fire intensity on the amount of C retained in soil versus respired to the atmosphere is necessary for predicting fire-climate feedbacks. My objective was to determine the influence of soil heating intensity and pyrogenic organic matter (PyOM) on microbial anabolism. I determined the short-term impacts of these factors on microbial anabolism by measuring the accumulation of microbial biomass carbon (MBC), C mineralization, and a proxy for CUE. I simulated the effects of fire intensity by heating soils to 100 or 200 °C for 30 minutes in a muffle furnace, and I amended the soils with charred or uncharred organic matter. Higher intensity soil heating (200 °C) consistently led to lower MBC accumulation, greater metabolic C respiration, and lower CUE proxies compared to unheated soils. In contrast, lower intensity soil heating (100 °C) resulted in MBC accumulation and estimated CUE that was similar to unheated soils. Soils amended with PyOM exhibited similar MBC accumulation compared to the uncharred organic matter, but CO_2 emissions were lower in soils amended with PyOM. These results indicate that

high intensity soil heating decreases soil C-sink strength over the short-term by decreasing the amount of microbial anabolism relative to catabolism. These findings suggest that increased wildfire intensity will have detrimental impacts of on soil C storage over the short-term.

4.2 INTRODUCTION

Wildfire disturbances are common in mixed-conifer forests of the western United States, resulting in direct CO_2 emissions during biomass combustion (Flannigan et al. 2009; Chen et al. 2017). Over the long-term, these emissions have a neutral impact on atmospheric carbon (C) concentrations as CO_2-C is assimilated by plant regrowth during forest recovery, but, over the short-term, represent a decrease in the size of forest C sink (Bowman et al. 2009; Loehman et al. 2014). Temperate forests store ~50% of ecosystem C in soils (Pan et al. 2011), so losses to soil C due to combustion (Campbell et al. 2007), and post-fire necromass decomposition could make substantial contributions to fire-induced C emissions (Meigs et al. 2009; Zhao et al. 2012; Campbell et al. 2016). Understanding the amount of soil C retained versus respired in the aftermath of fire is thus necessary for accurate representation of the influence of fire on the strength of the forest C sink.

The relative amount of microbial anabolism (biomass production) versus catabolism (C mineralization) determines the fate of soil C over both short and long timescales (Schimel and Schaeffer 2012; Liang et al. 2017a). Microbial carbon use efficiency (CUE) represents the balance between anabolic and catabolic processes over short timeframes (Manzoni et al. 2012; Sinsabaugh et al. 2013; Spohn et al. 2016a). An index of the amount of total C uptake that is assimilated into microbial biomass during decomposition (Geyer et al. 2016), CUE is the proximal driver determining whether C is lost to atmosphere versus retained in soil (Cotrufo et al. 2013). High CUE indicates more C accumulated in microbial biomass, whereas low CUE

indicates more C respired to the atmosphere. Microbial anabolism also influence C storage over longer time scales because microbial necromass is more efficiently stabilized in soils compared to other types of organic matter and may account for >50% of total soil C (Liang et al. 2019; Ni et al. 2020). The physiological responses of soil microbes to fire may therefore dictate the magnitude of post-fire soil emissions in the short term, and affect the size of soil C stocks and soil-climate feedbacks over the long-term (Allison et al. 2010; Frey et al. 2013; Wieder et al. 2013; Liang et al. 2019). Identifying the mechanistic processes that impact C sequestration following disturbance has been identified as a key component of managing forests for C storage in the future (Birdsey et al. 2006). Determining post-fire patterns in microbial anabolism and catabolism will thus contribute to understanding of C source/sink strength of burned ecosystems.

CUE and microbial biomass production are influenced by substrate quality and complexity, microbial community structure, nutrient availability, and environmental factors such as soil temperature and moisture (Frey et al. 2013; Geyer et al. 2016; Spohn et al. 2016b; Liang et al. 2019; Domeignoz-Horta et al. 2020). For example, CUE is lower for structurally complex/stable molecules (e.g. lignin, aromatic molecules) that require a larger enzyme investment compared to simpler, labile molecules (e.g. sugars) (Manzoni et al. 2012; Frey et al. 2013; Sinsabaugh et al. 2013). Relatedly, CUE decreases when nutrient availability is low due to microbial direction of metabolism toward catabolic processes that support nutrient acquisition, for example mining of nutrients from complex organic molecules (Geyer et al. 2016; Spohn et al. 2016b; Chen et al. 2020; Soong et al. 2020). In some cases, CUE increases with microbial diversity (Domeignoz-Horta et al. 2020), and may differ for fungi versus bacteria as consequence of differences in microbial biomass stoichiometry (Six et al. 2006; Keiblinger et al. 2010; Manzoni et al. 2012; Sinsabaugh et al. 2013).

Fire alters soil C chemistry, nutrient availability, and microbial community structure, with potentially contrasting impacts on microbial biomass production. Fire induces temporary pulses in soil dissolved organic carbon (Wang et al. 2012) and inorganic nitrogen (N) (Wan et al. 2001), potentially increasing microbial biomass production and CUE via positive effects on labile C and N availability. However, fire also generates pyrogenic organic matter (PyOM), which is more chemically stable and aromatic than its precursor material (Preston and Schmidt 2006; Bird et al. 2015), and thus may be used less efficiently. The conversion of organic matter to PyOM may therefore lead to less bioavailable C and lower microbial biomass production. There is a dearth of information on the influence of PyOM on microbial anabolism in burned systems, but biochar amendment studies can provide some insight. Biochar is a form of PyOM produced under controlled pyrolysis conditions and applied as a soil amendment in agricultural systems. Biochar additions to soil have frequently been found to increase microbial biomass, potentially via beneficial effects on soil nutrient retention, pH, soil moisture, and by providing microhabitat (Lehmann et al. 2011). A study in temperate pastures found that biochar-CUE was lower than values typically reported for non-biochar feedstock (Fang et al. 2018), but other studies have found that biochar increases overall CUE via beneficial effects on soil bio-physiochemical properties (Jiang et al. 2016; Guo et al. 2020). In addition to influencing C and N chemistry, fire increases the predominance of bacteria relative to fungi (Dooley and Treseder 2012; Pressler et al. 2018), in part due lower sensitivity of bacteria to soil heating (Neary and DeBano 2005). Bacteria may use simple C substrates more efficiently than fungi when N is abundant, exhibit rapid growth rates, and act as the primary decomposers of the labile fraction of PyOM; in contrast, fungi may more efficiently decompose the recalcitrant fraction of PyOM and

PyOM derived from wood (Steinbeiss et al. 2009; Lehmann et al. 2011; Yu et al. 2018; Pérez-Guzmán et al. 2020).

Fire intensity is predicted to increase in ecosystems across the globe (Flannigan et al. 2009), and there are reasons to suspect that effects of fire on microbial anabolic and catabolic processes vary with fire intensity and/or severity. For example, the amount of PyOM generated has been shown to increase with fire intensity (Czimczik et al. 2003; Sawyer et al. 2018) and severity (Miesel et al. 2015), which could have negative impacts on microbial anabolism by decreasing C bio-availability, or positive impacts via beneficial effects on soil properties. Changes to labile C and nutrient availability could also influence microbial anabolism, but there is a dearth of information regarding the immediate impacts of fire intensity on salt-water extractable organic carbon (EOC) and inorganic-N pools. Used as an alternative to field-based research, lab-based soil heating studies have indicated that EOC increases with soil heating temperature up to at least ~300 °C (Bárcenas-Moreno and Bååth 2009). Various experiments have found that inorganic-N concentrations exhibit no changes to moderate increases in soils heated from 150-210 °C (Serrasolsas and Khanna 1995; Choromanska and DeLuca 2002; Prieto-Fernández et al. 2004; Guerrero et al. 2005), with larger increases beginning to occur at ~400 °C (Raison 1979; Choromanska and DeLuca 2002). Laboratory-based heating studies have also assessed the effects of heating intensity on microbial biomass carbon (MBC), and microbial community structure (Serrasolsas and Khanna 1995; Díaz-Raviña et al. 1996; Fernández et al. 1997; Prieto-Fernández et al. 1998; Guerrero et al. 2005; Bárcenas-Moreno and Bååth 2009), but whether these characteristics lead to post-heating changes in the balance between microbial anabolism and catabolism is not well studied.

Small changes in the balance between microbial anabolism and catabolism can have substantial impacts on soil C emissions and stocks (Allison et al. 2010; Schimel and Schaeffer 2012; Wieder et al. 2013; Liang et al. 2017a), potentially exacerbating or modulating the effects of fire intensity on ecosystem C loss. Here, my objectives are to determine 1) how a proxy for CUE and the balance of MBC accumulation versus C mineralization vary with soil heating intensity and 2) whether PyOM influences these processes differently in soil subjected to contrasting soil heating intensities. I hypothesized that 1) estimated CUE and MBC accumulation will increase with soil heating intensity due to greater EOC availability, and 2) estimated CUE and MBC accumulation will be higher in soils amended with uncharred organic matter compared to charred organic matter regardless of soil heating intensity. I used factorial incubation experiments in which I subjected a forest soil to two levels of heating intensity and applied two C substrates in charred and uncharred form and multiple types of charred and uncharred plant litter to determine a proxy for CUE and the level of MBC accumulation versus C mineralization.

4.3 MATERIALS AND METHODS

4.3.1 Site description and sample collection

I collected soil and litter samples from the Plumas National Forest in the Sierra Nevada Mountain Range, California, USA. The ecosystem is a dry mixed-conifer forest dominated by *Pinus ponderosa, P. lambertiana, P. jeffreyi, Abies concolor, Pseudotsuga menziesii,* and *Calocedrus decurrens,* with lesser cover by *Quercus kelloggii*. Dry mixed-conifer forests of the region are fire-adapted, having exhibited a mean fire rotation of 23 years prior to Euro-American settlement (1500-1850 C.E.) (Mallek et al. 2013). Soils in my plots are from the Skalan series, a loamy-skeletal, isotic, mesic Vitrandic Haploxerlaf (Soil Survey Staff 2018). The 30 year mean annual precipitation is 1080 mm and mean annual temperature is 10.6 ºC.

From four sites within the forest that did not exhibit evidence of recent fire activity (i.e. no charred biomass), I collected mineral soil at two sampling points located 40 m apart. At each sampling location, I removed the litter (Oi) and duff (Oe + Oa) layers overlying the mineral soil, and then collected mineral soil to 10 cm depth using a 10 cm diameter soil auger. I then collected three types of litter from the forest, including *Q. kelloggii* (black oak), *P. ponderosa* (ponderosa pine), and mixed litter. I collected black oak and ponderosa pine litter samples from the litter surface directly under a tree of each species, and I collected only leaf material that was recognizable as belonging to the target tree species. The mixed litter sample included litter recognizable as deriving from *P. ponderosa* and litter that was derived from either *A. concolor*, *P. menziesii* or both. Mineral soils and litter samples were stored on ice until being transported to the lab, after which mineral soils were stored at -20 °C, and litter samples were air-dried and stored at ambient temperature until the commencement of the lab experiments.

4.3.2 Generation of pyrogenic organic matter

I generated PyOM from two simple C substrates (glucose, ascorbic acid) and from the three litter types collected in the field. Glucose is commonly used in CUE and substrate induced respiration experiments, and ascorbic acid has been demonstrated to effectively induce differential respiration responses among soil types (Degens and Harris 1997). I charred glucose (210 °C) and ascorbic acid (200 °C) at temperatures at the lower end of their thermal degradation ranges (Örsi 1973; Jingyan et al. 2013). I weighed ~5 g of each substrate into a small aluminum dish, covered the dish with aluminum foil, and heated in a muffle furnace by ramping to the target temperature over 30 minutes and then holding at temperature for another 30 minutes.

I sterilized the litter via autoclave (121 °C) for 30 minutes and then oven-dried overnight at 65 °C. I charred the litter by placing aluminum-foil wrapped sterile litter in a muffle furnace

that had been pre-heated to 200 °C and held at temperature for one hour. I then ramped the temperature to 300 °C and held at temperature for another hour. The litter was then homogenized using a mortar and pestle to pass a 500-micron sieve. I measured charred substrate and litter C and N concentrations of single replicates using a dry-combustion elemental analyzer (Costech Analytical Technologies Inc., Valencia, CA, USA), with acetanilide as the quantification standard.

4.3.3 Experimental design

I conducted two experiments to assess the amount microbial anabolism versus catabolism after a soil heating disturbance. In one experiment, I measured a proxy for community-scale CUE which quantifies gross production efficiency of the microbial community over short timescales (up to 48 hours) before biomass turnover occurs (Geyer et al. 2016). In the second experiment, I measured net MBC accumulation and net C mineralization over 14 days. To account for potential heterogeneity of soil across my sampling sites, I composited equal masses of sieved (2 mm) mineral soil from the plots before evaluating the short-term impacts of soil heating and PyOM on CUE and MBC accumulation.

Carbon use efficiency experiment

I determined impacts of soil heating and substrate pyrolysis on a CUE proxy using a fully-factorial experiment in which I applied two levels of soil heating (plus unheated controls) and two labile substrate types (glucose, ascorbic acid) in charred and uncharred form. Each treatment was replicated 18 times, equally divided between two incubation blocks that were performed consecutively. For each incubation block, I pre-incubated nine soil replicates for seven days. For each replicate, I weighed 130 g (dry mass equivalent (DME)) of soil into 0.473 L

mason jars, added water to bring soil moisture to 40% water-holding capacity (WHC), and incubated in the dark at ambient temperature (~23 °C).

After pre-incubation, I applied heat treatments of 100 °C or 200 °C by covering the mason jars with aluminum foil and heating the jars in a muffle furnace for 45 minutes. Following heating, I weighed 5 g (DME) subsamples into 50 mL centrifuge tubes, adjusted soil moisture to 50% WHC, capped the tubes with septa-fitted lids, and incubated in the dark at ambient temperature. Before adding substrates, I measured CO_2-C respiration daily until respiration rates differed by <10% among soil heating treatments, which occurred after five days. I waited until respiration rates were similar so that CUE estimates would not be influenced by differences in basal respiration. I measured soil respiration rates by flushing the incubation tubes with ambient air, tightly capping, and measuring CO_2-C concentrations of 1 mL gas aliquots after ~30 minutes and again after ~6 hours using an infrared gas analyzer (LI-COR Inc., Lincoln, NE, USA).

On the sixth day after heating, I added charred and uncharred substrates to the incubation tubes at 1 mg substrate-C g^{-1} soil in 0.5 mL DI water. I monitored respiration rates over 24 hours by measuring CO_2-C concentrations after ~1.5, 4, 8, 12, and 24 hours. I extracted three replicates per treatment in each block for determination of EOC immediately after substrate addition, and I extracted the remaining six replicates after 24 hours. I performed EOC extractions by adding 25 mL K_2SO_4 directly to the incubation tubes, agitating on a reciprocating shaker for 1 hour, and filtering through 11 µm pore-size filters (Whatman Grade 1). I determined EOC concentrations in the extracts spectrophotometrically after potassium-dichromate oxidation (Cai et al. 2011). I calculated CUE over the 24 hours after substrate addition as:

$$CUE = \frac{(\Delta EOC - \Sigma CO_2\ C)}{\Delta EOC} \quad (1)$$

where ΔEOC is the change in EOC over the 24 hours after substrate addition and is assumed to represent total microbial C uptake; ΣCO_2-C is cumulative C respired over the 24 hours (Tiemann and Billings 2011; Geyer et al. 2016). This calculation is a proxy for CUE because I did not apply isotopically labeled substrates and so cannot directly quantify the amount of substrate-C uptake and respiration.

Microbial biomass carbon accumulation experiment

I determined impacts of soil heating and substrate pyrolysis on MBC accumulation and cumulative C mineralization using a fully-factorial experiment in which I applied two levels of soil heating (plus unheated controls) and three litter types (ponderosa pine, black oak, and mixed litter) in charred and uncharred form. Each treatment was replicated 18 times, equally divided between two incubation blocks that were performed consecutively, except for mixed litter treatments which were replicated nine times and incubated in a single block.

Soil pre-incubation was performed as described above, except that replicates were 150 g (DME) and pre-incubated for ten days. After pre-incubation, I applied heat treatments of 100 °C or 200 °C as described above. I then weighed 10 g (DME) subsamples into 50 mL centrifuge tubes, added 80 ± 5 mg charred or uncharred litter to each tube, mixed by vortexing for 30 seconds, and added water to bring soil moisture to 50% WHC. I incubated the soils for 14 days, measuring respiration on days 1, 2, 3, 4, 5, 7, 9, and 13.

Twenty-four hours after heat treatments, I extracted a subset of unamended samples (n=6 per heat treatment) for EOC and microbial biomass C (MBC) using direct chloroform fumigation (Witt et al. 2000). 14 days after applying treatments, I extracted the remaining soils (n=12 per treatment combination). I measured MBC as the difference in EOC between fumigated and

unfumigated samples, divided by a correction factor of 0.33 (Cai et al. 2011). I calculated net accumulation of MBC as the difference in MBC between days 1 and 14 of the incubation.

For one incubation block, I determined fungal and bacterial activity in a subset of soils < 24 hours after heating (n=6 per heat treatment) using selective respiratory inhibition (Anderson and Domsch 1973). Additionally, I incubated an extra set of heated and unheated soils amended with uncharred or charred pine material (n=6) to determine post-incubation differences in fungal and bacterial activity. For selective respiratory inhibition, I weighed four equal soil masses (2.5 g DME) from each incubation tube into septa-capped 20 mL scintillation vials, applied glucose at 8 mg g^{-1} in 0.2 mL DI water, and agitated on a reciprocating shaker for 1 hour. I then applied one of four biocide treatments to each of the vials: no biocide addition, the bactericide bronopol at 100 µg g^{-1}, the fungicide cycloheximide at 8 mg g^{-1}, or the addition of both biocides at these concentrations. Vials were capped and placed on a reciprocating shaker for 6 hours, after which accumulated CO_2-C was measured with an infrared gas analyzer. Fungal and bacterial activity was determined as:

$$Fungal\ (or\ Bacterial)\ Activity = \frac{A-B(or\ C)}{A-D} \quad (3)$$

Where A is respiration in the absence of inhibitors, B is respiration in the presence of the fungicide, C is respiration in the presence of bactericide, and D is respiration in the presence of both biocides. The inhibitor additivity ratio (IAR), a measure of non-target or antagonistic effects of the antibiotics was determined as:

$$IAR = \frac{(A-B)+(A-C)}{A-D} \quad (4)$$

The concentrations of glucose and antibiotics for determination of bacterial and fungal activity were selected based on the optimization procedures described by Bailey et al. (2003) using the

same soil as was used for the CUE experiments. These preliminary procedures yielded an IAR of 1.01 ± 0.07 (SD). An IAR of 1.0 indicates no non-target or antagonistic effects.

4.3.4 Statistical analysis

I performed all statistical analysis in the R statistical computing environment (v 3.6.1) (R Core Team 2019). I applied linear mixed-models using the nlme package (v 3.1.140) (Pinheiro et al. 2019) to assess the response of C respiration, EOC, MBC, and CUE to my experimental treatments. All models initially included soil heating level, litter or substrate type, and char status as main effects, all possible two- and three-way interaction effects, and incubation block as a random effect. Interaction effects that exhibited p-values ≥ 0.15 were sequentially removed from the models. For main effects that were significant at $\alpha=0.05$, I compared marginal means using Tukey-adjusted p-values using the emmeans package (v.1.4.4) (Lenth 2020). For the MBC accumulation experiment, I also applied general linear models to determine impact of soil heating and uncharred and charred pine litter on fungal and bacterial activity.

4.4 RESULTS

4.4.1 Carbon use efficiency experiment

Soil heating caused an immediate increase in soil respiration rate that was positively associated with heating intensity ($p<0.001$; Table 4.1). Compared to unheated soils, heating soils to 100 °C caused a pulse in respiration that lasted two days, and heating soils to 200 °C caused a pulse that lasted four days. By five days after heating, the heated soils did not differ in respiration rates compared to unheated soils. Over five days post-heating, soils heated to 100 °C respired 8.6% more CO_2-C, and soils heated to 200 °C respired 58.9% more CO_2-C compared to unheated soils.

Table 4.1 Respiration rate by day and cumulative CO_2-C respired over five days after soil heating and prior to adding substrates for the carbon use efficiency experiment (mean ± SE). Lower-case letters indicate Tukey-adjusted significant differences in respiration among soil heating treatments (α=0.05).

Respiration Rate (mg CO_2-C kg^{-1} d^{-1})	Unheated (n=84)	100 °C (n=84)	200 °C (n=84)
Day 1	22.7 ± 0.4 a	31.4 ± 0.5 b	43.7 ± 3.1 c
Day 2	25.5 ± 0.5 a	30.2 ± 1.2 b	56.4 ± 1.2 c
Day 3	22.5 ± 0.4 a	23.5 ± 0.6 a	40.4 ± 0.4 b
Day 4	27.3 ± 0.6 a	27.7 ± 0.6 a	36.6 ± 0.6 b
Day 5	31.6 ± 1.9 a	28.2 ± 1.9 a	28.7 ± 1.8 a
Cumulative Respired (mg CO_2-C kg^{-1})	130 ± 2.6 a	141 ± 2.7 b	206 ± 3.4 c

Table 4.2 Carbon and nitrogen concentrations for uncharred and charred carbon substrates and litters used in the carbon use efficiency and microbial biomass carbon accumulation experiment.

	C (%)		N (%)	
	Uncharred	Charred	Uncharred	Charred
Glucose	40.0	42.6	–	–
Ascorbic Acid	40.9	41.1	–	–
P. Ponderosa Litter	50.6	63.6	0.25	0.43
Q. Kellogii Litter	47.2	65.8	2.54	3.31
Mixed Litter	35.0	52.9	0.59	0.75

Charring of glucose and ascorbic acid resulted in visual changes in appearance (Fig. S4.1) and slight increases in C concentration (Table 4.2). There were significant effects of soil heating ($p<0.001$) and a heating × substrate identity interaction ($p<0.001$) on the CUE proxy, but no main effects of substrate identity or charring on the estimate (Fig. 4.1). Soils heated to 200 °C exhibited ~68% lower estimated CUE in response to ascorbic acid application than the other soil heating treatments. The CUE proxy is driven by the level of EOC uptake and CO_2-C respired, so I separately assessed the response of these metabolic functions to the treatments. There were significant effects of soil heating ($p<0.001$) and a charring × substrate interaction ($p<0.001$) on EOC uptake. Additionally, there were marginally significant differences of substrate identity ($p=0.070$) and a heating × substrate interaction ($p=0.067$). For soils receiving ascorbic acid, differences in EOC uptake were driven by heating effects: soils heated to 200 °C exhibited ~42% less EOC uptake than unheated soils (Fig. 4.2). In contrast, EOC uptake in soils that received glucose was driven by both charring and soil heating: within heating treatments, EOC uptake was ~32-56% lower for charred glucose than uncharred glucose. Within charring treatments, EOC uptake was ~27-30% lower for soils heated to 100 °C compared to unheated soils. For CO_2-C respired, there were significant effects of soil heating ($p<0.001$) and a charring × substrate interaction ($p<0.001$). Similar to EOC uptake, drivers of differences in CO_2-C respiration varied among substrate type. For soils receiving ascorbic acid, differences in respiration were driven by heating, with soils heated to 100 °C respiring ~28% less CO_2-C than the other treatments. Soils that received glucose exhibited differences in respiration due to both substrate charring and soil heating. Within heating treatments, soils respired ~28-60% less CO_2-C in response to charred glucose application, and, within charring treatments, soils heated to 100 °C respired ~6-40% less CO_2-C.

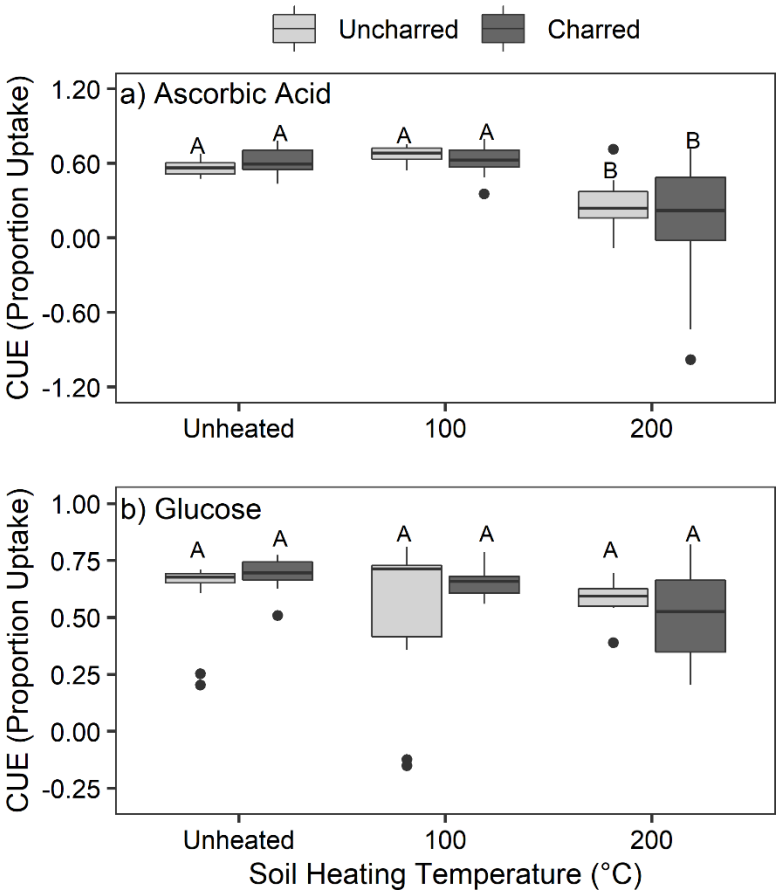

Figure 4.1 A proxy for carbon use efficiency (CUE) for unheated soils and soils heated to 100 °C and 200 °C that received ascorbic acid (a) or glucose (b) in uncharred or charred form. Shading of boxplots indicates whether soils received uncharred or charred substrates. Each boxplot represents the distribution of 12 replicates. Upper-case letters indicate Tukey-adjusted significant differences among the heating × charring treatment combinations within substrate types (α=0.05).

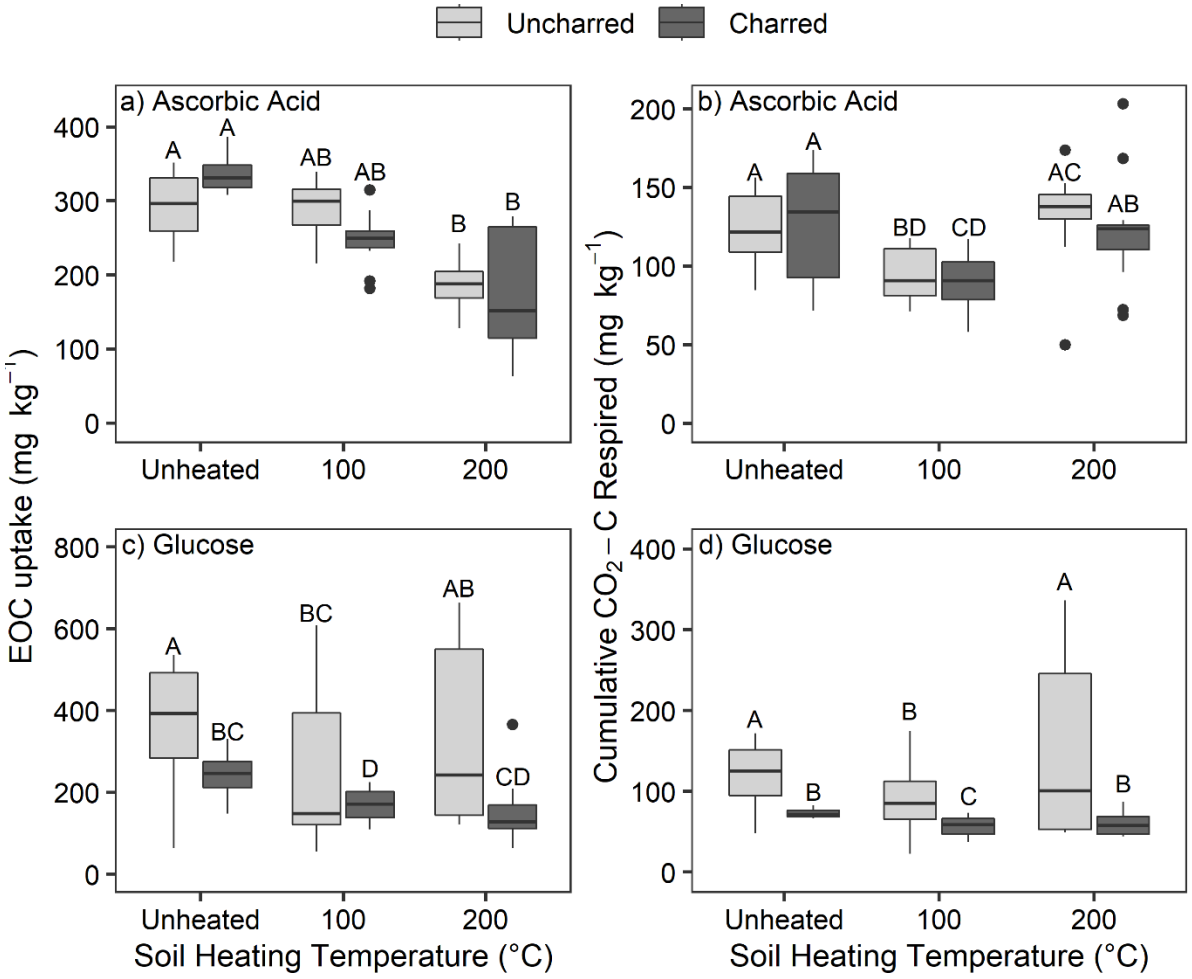

Figure 4.2 Uptake of extractable organic carbon (a and c) and 24-hour cumulative respired CO_2-C (b and d) for unheated soils and soils heated to 100 °C and 200 °C that received ascorbic acid or glucose in uncharred or charred form. Shading of boxplots indicates whether soils received uncharred or charred substrates. Each boxplot represents the distribution of 12 replicates. Upper-case letters indicate Tukey-adjusted significant differences among the heating × charring treatment combinations within substrate types (α=0.05).

4.4.2 Microbial biomass accumulation experiment

Soil heating led to increases in EOC in soils extracted 24 hours after heating: unheated soils contained 40.4 ± 3.1 mg kg^{-1} EOC compared to 60.6 ± 2.2 and 121 ± 2.0 mg kg^{-1} for soils heated to 100 °C and 200 °C, respectively. Microbial biomass was decreased only in soils heated to 100 °C, where MBC was 85.1 ± 12.2 mg kg^{-1} compared to 138 ± 13.5 and 134 ± 8.0 mg kg^{-1}

for unheated soils and soils heated to 200 °C, respectively. Litter charring led to increases in C and N concentrations compared to uncharred litter (Table 4.2).

MBC decreased over the incubation period in soils heated to 200 °C for all litter types (Fig. 4.3), while CO_2-C respiration was elevated by ~6-105% compared to unheated soils ($p=0.001$). CO_2-C respiration was also elevated in soils heated to 100 °C for soils that received no litter, uncharred oak, and uncharred pine by ~32-59%, but these soils also accumulated 28-390% more MBC over the incubation. Within soils that received oak or pine litter, the charred version induced 33-61% less CO_2-C respiration compared to the uncharred counterpart and exhibited similar MBC accumulation. Within soils that received mixed litter, CO_2-C respiration and MBC accumulation were similar between charred and uncharred forms. After the 14-day incubation, soils heated to 200 °C had 28-76% less MBC than unheated soils, and soils heated to 100 °C had similar MBC to unheated soils. MBC was similar between charred and uncharred litter among all soil heat treatments.

EOC uptake over the 14-day incubation increased with soil heating intensity for soils that did not receive litter inputs ($p<0.001$). EOC uptake was 3.9 ± 1.2 mg kg^{-1} for unheated soils, 21.4 ± 1.5 mg kg^{-1} for soils heated to 100 °C, and 40.5 ± 1.3 mg kg^{-1} for soils heated to 200 °C. When considered on a relative basis, EOC uptake was similar for soils heated to 100 °C (34.7 ± 2.4% of initial EOC) and 200 °C (33.5 ± 1.0%), both of which exhibited greater EOC uptake than unheated soils (9.7 ± 2.9%). Cumulative 14-day respiration was positively correlated with EOC uptake only for soils heated to 100 °C ($r=0.61$, $p=0.037$), and MBC accumulation was positively correlated with EOC uptake only for soils heated to 200 °C ($r=0.71$, $p=0.014$).

Despite my IAR values being very near the target value of 1.0 during preliminary optimization procedures (see methods), the IAR values I observed during the CUE_E experiment

were substantially higher. Immediately post heating, IAR was 1.42 ± 0.03, and after the 14-day incubation IAR was 1.27 ± 0.04. These values indicate non-target effects of one of the antibiotics (Bailey et al. 2003; Rousk et al. 2009). The bactericide was very likely responsible for the non-target effects because the inhibition resulting from bactericide application alone was similar to the inhibition that resulted from application of both biocides in conjunction. Thus, I limit the dissemination of my results to the impacts of treatments on fungal activity only. Immediately after heating, fungal activity did not differ among the soil heating treatments. After the 14-day incubation, there were significant main effects of soil heating ($p=0.017$) and litter charring ($p=0.047$) on fungal activity, but no interaction effects ($p=0.12$). Fungi contributed to 31.4 ± 3.5% of respiration in soils heated to 200 °C, which was significantly less than 47.7 ± 5.5% in unheated soils. At 40.4 ± 5.2%, fungal respiration in soils heated to 100 °C did not differ from the other treatments. Although the results of my general linear model indicated that soils amended with charred versus uncharred pine litter exhibited higher fungal activity, pairwise means comparisons did not uncover differences in fungal activity between these treatments. Fungal activity did not significantly affect cumulative C respired or change in MBC.

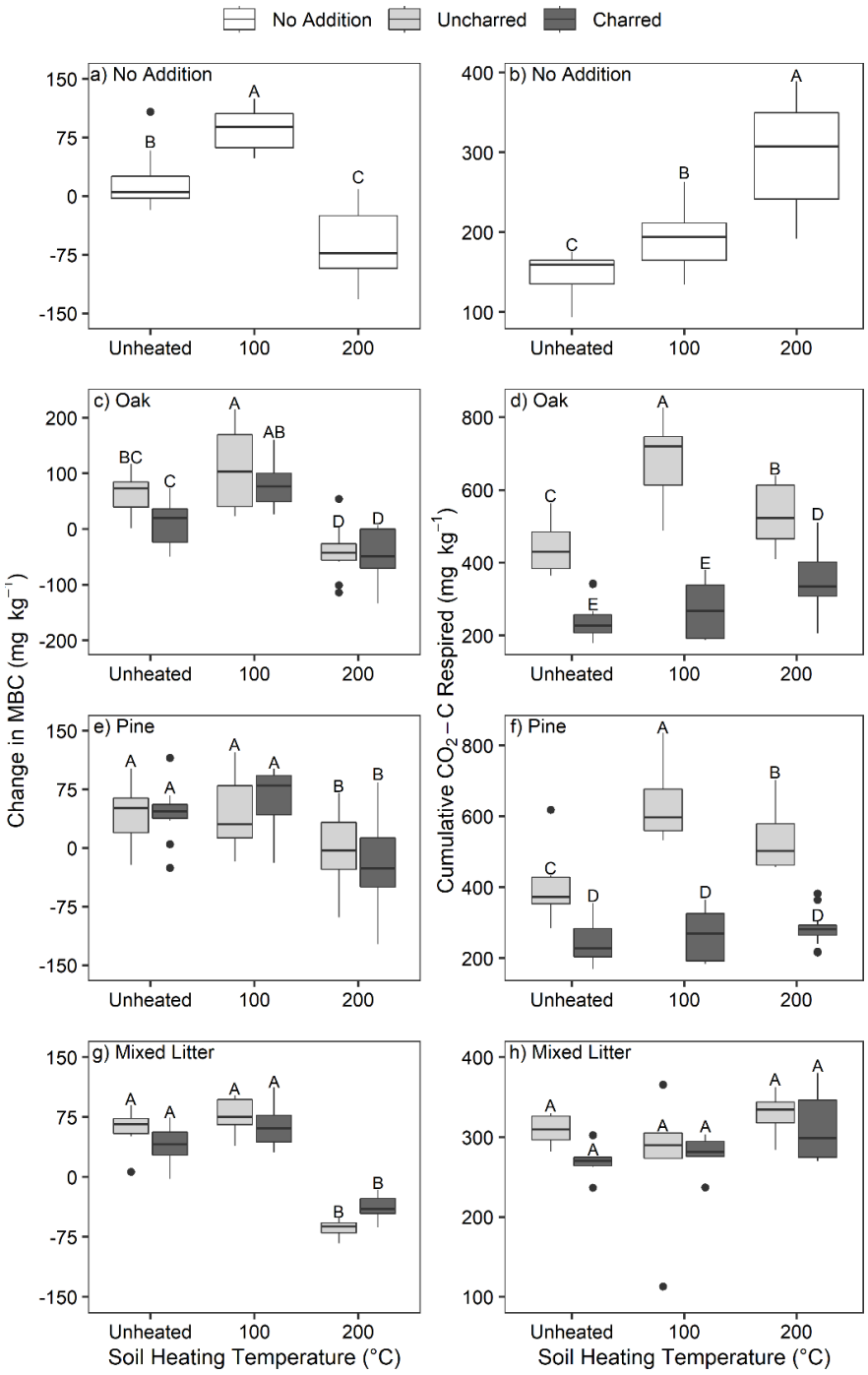

Figure 4.3 Change in microbial biomass carbon (a, c, e, g) and 14-day cumulative respired CO_2-C (b, d, f, h) for unheated soils and soils heated to 100 °C and 200 °C that no litter, *Q. kelloggii* (Oak), *P. ponderosa* (Pine), or mixed leaf litter in uncharred or charred form. Shading of boxplots indicates whether soils received uncharred or charred litter. Each boxplot represents the distribution of 12 replicates, except for mixed litter treatments which had 6 replicates. Upper-case letters indicate Tukey-adjusted significant differences among the heating × charring treatment combinations within litter treatments (α=0.05).

4.5 DISCUSSION

4.5.1 Soil heating intensity underlies estimated carbon use efficiency and microbial biomass accumulation

I did not find support for my hypothesis that the CUE proxy and MBC accumulation would be positively correlated with soil heating intensity. Rather, heating soils to 200 °C decreased the CUE proxy and led to net negative MBC accumulation. Interestingly, in the MBC accumulation experiment, MBC content measured 24 hours after heating was lower in soils heated to 100 °C than those heated to 200 °C. This suggests rapid microbial growth in the 24 hours after heating in soils heated to 200 °C. EOC content increased with heating intensity, and the assimilation of this flushed EOC by the surviving microbial community could have fueled the rapid growth in the soils heated to 200 °C. Indeed, a laboratory heating study performed on soils collected from *Pinus halepensis* forest in Spain found that bacterial growth was several times higher in soils heated between 80 and 400 °C than unheated controls within 2-4 days of soil heating (Bárcenas-Moreno and Bååth 2009). Furthermore, Bárcenas-Moreno and Bååth (2009) found that peak growth rate was greater and occurred earlier in soils heated to higher temperatures, an effect that correlated with greater initial increases in EOC.

Differences in the balance between anabolism versus catabolism in heated soils are likely due to the combined effects of heating on labile C availability, nutrient availability, and microbial biomass stoichiometry. For example, the greater MBC accumulation in soils heated to 100 °C versus 200 °C could be related to the combined effects of microbial cell lysis and threshold effects of heating on organic molecules impacting the quality of available C. Microbial lysis during heating results in the release of labile organic molecules, for example carbohydrates, proteins, and amino acids (González-Pérez et al. 2004). Such molecules are likely to be

efficiently utilized by the surviving microbial populations in the absence of nutrient limitation (Cotrufo et al. 2013), potentially explaining why MBC accumulation sometimes increased in soils heated to 100 °C compared to unheated soils. Additionally, protein and amino acids represent labile forms of organic N (Jones et al. 2004; Schimel and Bennett 2004; Kielland et al. 2007), and 100 °C is below the threshold of N volatilization (Bodí et al. 2014). Thus, low intensity soil heating could potentially increase labile organic N availability and allow fast-growing microorganisms with high nutrient demands to rapidly increase in biomass. Concurrently, increased N availability could suppress less efficient decomposition of complex and recalcitrant organic matter (Janssens et al. 2010) and decrease the need for N-mining (Moorhead and Sinsabaugh 2006; Craine et al. 2007).

In contrast, heating soils to 200 °C likely caused greater mortality to the microbial community (Pingree and Kobziar 2019) and thus greater input of organic molecules, but 200 °C is above or near the threshold at which these labile organic molecules are destructively distilled, volatized, or pyrolyzed (González-Pérez et al. 2004; Massman et al. 2010). Thus, although there was an overall increase in EOC after 200 °C heating, this C may be in a less bioavailable form. Studies assessing chemical changes of plant biomass during pyrolysis indicate that loss of thermally labile compounds and aromatization reactions occur at 200 °C (Hatton et al. 2016), and carbohydrate loss and transformation is one of the first processes to occur (Chatterjee et al. 2012). Moreover, soil carbohydrate content derived from both plants and microbes has been found to decrease immediately following wildfire, and remain depressed for at least 15 months (Martín et al. 2009). Greater carbohydrate loss and increased dominance of lignin and pyrogenic compounds appears to occur at higher fire severity (Miesel et al. 2015), and water-extractable organic matter is more aromatic after both prescribed fires and wildfires (Vergnoux et al. 2011;

Hobley et al. 2019). Thus, at higher soil heating intensity, the low MBC accumulation could be due to low availability of labile C that can be efficiently transformed into MBC.

In addition to the potential effects on C quality, 200 °C represents the lower threshold for N-volatilization and loss of soil proteins (Russell et al. 1974; Bodí et al. 2014; Lozano et al. 2016), potentially leading to decreased N availability and increasing the need for N-mining and investment in extracellular enzymes. For example, Prieto-Fernández et al. (2004) found that chemically labile (acid hydrolysable) organic N was not impacted when soils were heated to 150 °C, but decreased by >50% when heated to 210 °C and by a similar amount in soils collected immediately after a wildfire. Some of this organic N will be converted to inorganic N and retained in soil as available N, but substantial increases in inorganic N might not occur until soil is heated at much higher temperatures (~400 °C) than I employed (Raison 1979; Choromanska and DeLuca 2002; Guerrero et al. 2005). Even if N availability increased slightly in soils heated to 200 °C, changes in microbial community composition in response to soil heating could affect CUE and MBC accumulation by leading to a disconnect between microbial biomass stoichiometry and nutrient availability. If soil heating induces a shift in the microbial community from fungi and oligotrophic bacteria with high C:N biomass ratios—and thus lower nutrient requirements—towards copiotrophic bacteria with lower C:N ratios and higher nutrient requirements (Fierer et al. 2007; Sinsabaugh et al. 2013), decomposition of labile C could be coupled to *ex vivo* catabolic processes in order to obtain limiting nutrients from complex organic matter (Moorhead and Sinsabaugh 2006; Craine et al. 2007; Manzoni et al. 2017). Microbial communities that have lower fungal-to-bacterial ratios and/or a greater abundance of copiotrophic bacteria are less efficient at scavenging for limiting nutrients from complex organic matter, leading to greater C mineralization per unit biomass and therefore lower CUE and MBC

accumulation. In fact, I found that fungal activity was significantly decreased in soils heated to 200 °C, and research has shown that the relative abundance of bacterial phyla typically classified as copiotrophic increase within one day to one week post-fire (Pérez-Valera et al. 2017; Prendergast-Miller et al. 2017), suggesting shifts to microbial communities with higher nutrient requirements. Indeed, the high respiration rates and lack of associated MBC accumulation (Fig. 4.3) supports the explanation that catabolic, rather than anabolic, processes are dominant in soils heated to 200 °C. Similarly, the lower CUE proxy in 200 °C soils that received ascorbic acid could be due to the decomposition of this labile C substrate being coupled to nutrient acquisition.

Importantly, higher MBC accumulation in soils heated to 100 °C does not necessarily reflect increased C sequestration compared to unheated soils. In fact, greater C respiration in the absence of new C inputs reflects a net loss of C, regardless of an associated accumulation of MBC. Thus, the increased C respiration in soils heated to 100 °C compared to unheated soils indicates a net loss of soil C during the immediate post-heating period (Table 4.1 and Fig. 4.3). However, the high MBC accumulation does represent efficient C recycling, limiting the contribution of microbial mortality to post-fire emissions and suggests microbial anabolism is high following low-intensity soil heating. In contrast, soils heated to 200 °C exhibited high post-heating respiration rates, continuing decreases in microbial biomass, and lower estimated CUE even in soils amended with a relatively labile C source (Figs. 4.1 and 4.3). This suggests that the effects of high-intensity soil heating results in high microbial catabolism which exacerbates C emissions after heating, at least in the short term.

4.5.2 Pyrogenic organic matter decreases soil respiration

I did not find support for my hypothesis that estimated CUE and MBC accumulation would be higher in soils amended with uncharred organic matter compared to charred organic

matter. In most cases, regardless of soil heating intensity, application of PyOM led to decreases in C respiration without negatively affecting EOC uptake or MBC accumulation compared to the uncharred counterpart (Figs 4.2 and 4.3). These findings indicate that PyOM addition decreases microbial catabolism in soils without negatively impacting anabolism. The decrease in catabolism was likely not due to pyrolysis releasing labile C that could be used more efficiently, because EOC extractions of charred and uncharred litter indicated that there was ~90% less extractable C in charred litter. One possible explanation for these patterns is that PyOM additions positively affected soil properties in ways that increased the efficiency of decomposition. For example, PyOM has been shown to increase CUE and microbial abundance by increasing nutrient availability, soil oxygen concentrations, pH, and by providing sorption sites for bacteria (Lehmann et al. 2011; Jiang et al. 2016; Fang et al. 2018). Alternatively, low-intensity soil heating could select for microbial groups that are adapted to efficient use of PyOM (Whitman et al. 2019). The lower amounts of catabolism in response to PyOM addition could also be due to low bio-availability of the charred biomass. However, low microbial use of PyOM may depend on the availability of an alternative labile C pool, and EOC can remain depressed for decades following wildfire (Prieto-Fernández et al. 1998). In the case of high intensity fires, aboveground plant mortality and biomass combustion may be high, removing a source of future labile soil C inputs from litter deposition and root inputs (González-Pérez et al. 2004; Grady and Hart 2006; Kavanagh et al. 2010). In these cases, the microbial community may switch to use of PyOM after the residual labile C pool is depleted, leading to less efficient C use over the intermediate or long term. An analogous substrate-limitation mechanism has been found to explain lignin degradation when soil carbohydrate pools becomes depleted (Hall et al. 2020).

There was a clear negative impact of soil heating on fungal activity, supporting other research finding that fungal biomass is more negatively affected by fire than bacterial biomass (Dooley and Treseder 2012). Although I did not observe a relationship between fungal respiration and MBC accumulation, decreased fungal biomass could negatively impact MBC accumulation in soils with high PyOM concentrations because fungi may be better able to utilize organic matter characterized by high aromaticity and C:N (Jastrow et al. 2007; Keiblinger et al. 2010; Dungait et al. 2012).

4.6 CONCLUSIONS

High intensity soil heating decreases the strength of soil C sink over the short term by decreasing the microbial anabolism and increasing catabolism. Higher soil heating intensity likely increases the amount of C lost to combustion during fire events. My results suggest that this effect may be exacerbated by low CUE, low accumulation of MBC, and high soil respiration rates over the short-term in soils that experience high heating intensity. In addition to exacerbating short-term C losses, the decreased anabolism could lead to long-term reductions in soil C storage via less microbial necromass, which is a persistent stock of C. Fire intensity is predicted to increase in many fire-prone ecosystems, and a negative relationship between intensity and microbial anabolism could lead to positive fire-climate feedbacks. Disrupted fire regimes are already being observed in temperate coniferous forests of the western United States, and if these altered fire regimes lead to lower anabolism and decreased CUE, the C sequestration ability of these forests could be permanently reduced. I found some beneficial impacts of PyOM in ameliorating C losses via decreased respiration, but over longer timeframes, PyOM could either negatively influence CUE due to its chemical recalcitrance, or positively influence CUE via beneficial effects on soil physicochemical properties. My study used lab-based soil heating to

estimate direct effects of fire on a CUE proxy and MBC accumulation, but field-based research is needed to determine whether the influences of soil heating and PyOM on CUE and MBC accumulation persist over the long-term.

APPENDIX

SUPPLEMENTAL FIGURES

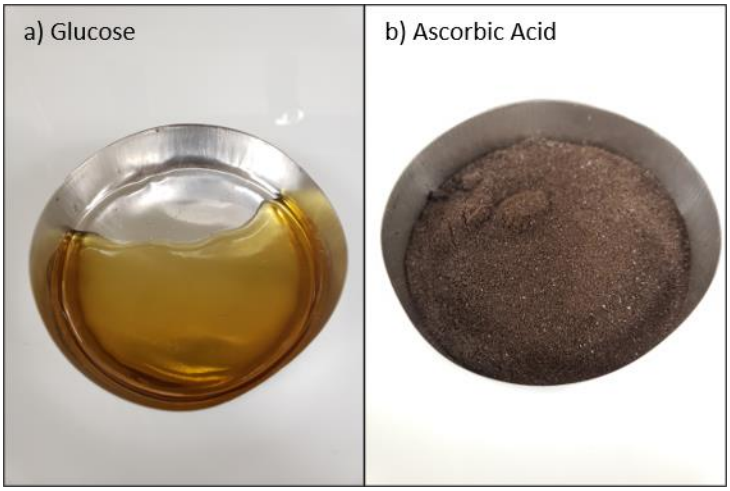

Figure S4.1 Glucose (a) and ascorbic acid (b) after charring in a muffle furnace at 210 °C and 200 °C, respectively.

REFERENCES

REFERENCES

Anderson JPE, Domsch KH (1973) Quantification of bacterial and fungal contributions to soil respiration. Arch Mikrobiol 93:113–127. doi: 10.1007/BF00424942

Bailey VL, Smith JL, Bolton H (2003) Novel antibiotics as inhibitors for the selective respiratory inhibition method of measuring fungal:bacterial ratios in soil. Biol Fertil Soils 38:154–160. doi: 10.1007/s00374-003-0620-7

Bárcenas-Moreno G, Bååth E (2009) Bacterial and fungal growth in soil heated at different temperatures to simulate a range of fire intensities. Soil Biol Biochem 41:2517–2526. doi: 10.1016/j.soilbio.2009.09.010

Bird MI, Wynn JG, Saiz G, et al (2015) The pyrogenic carbon cycle. Annu Rev Earth Planet Sci 43:273–298. doi: 10.1146/annurev-earth-060614-105038

Birdsey R, Pregitzer K, Lucier A (2006) Forest carbon management in the United States. J Environ Qual 35:1461. doi: 10.2134/jeq2005.0162

Bodí MB, Martin D a., Balfour VN, et al (2014) Wildland fire ash: Production, composition and eco-hydro-geomorphic effects. Earth-Science Rev 130:103–127. doi: 10.1016/j.earscirev.2013.12.007

Bowman DMJS, Balch JK, Artaxo P, et al (2009) Fire in the earth system. Science 324:481–484. doi: 10.1126/science.1163886

Cai Y, Peng C, Qiu S, et al (2011) Dichromate digestion-spectrophotometric procedure for determination of soil microbial biomass carbon in association with fumigation-extraction. Commun Soil Sci Plant Anal 42:2824–2834. doi: 10.1080/00103624.2011.623027

Campbell J, Donato D, Azuma D, Law B (2007) Pyrogenic carbon emission from a large wildfire in Oregon, United States. J Geophys Res Biogeosciences. doi: 10.1029/2007JG000451

Campbell JL, Fontaine JB, Donato DC (2016) Carbon emissions from decomposition of fire-killed trees following a large wildfire in Oregon, United States. J Geophys Res Biogeosciences 121:718–730. doi: 10.1002/2015JG003165

Chatterjee S, Santos F, Abiven S, et al (2012) Elucidating the chemical structure of pyrogenic organic matter by combining magnetic resonance, mid-infrared spectroscopy and mass spectrometry. Org Geochem 51:35–44. doi: 10.1016/j.orggeochem.2012.07.006

Chen G, Hayes DJ, David McGuire A (2017) Contributions of wildland fire to terrestrial ecosystem carbon dynamics in North America from 1990 to 2012. Global Biogeochem Cycles 31:878–900. doi: 10.1002/2016GB005548

Chen X, Xia Y, Rui Y, et al (2020) Microbial carbon use efficiency, biomass turnover, and necromass accumulation in paddy soil depending on fertilization. Agric Ecosyst Environ 292:106816. doi: 10.1016/j.agee.2020.106816

Choromanska U, DeLuca TH (2002) Microbial activity and nitrogen mineralization in forest mineral soils following heating: Evaluation of post-fire effects. Soil Biol Biochem 34:263–271. doi: 10.1016/S0038-0717(01)00180-8

Cotrufo MF, Wallenstein MD, Boot CM, et al (2013) The Microbial Efficiency-Matrix Stabilization (MEMS) framework integrates plant litter decomposition with soil organic matter stabilization: do labile plant inputs form stable soil organic matter? Glob Chang Biol 19:988–995. doi: 10.1111/gcb.12113

Craine JM, Morrow C, Fierer N (2007) Microbial nitrogen limitation increases decomposition. Ecology 88:2105–2113. doi: 10.1890/06-1847.1

Czimczik CI, Preston CM, Schmidt MWI, Schulze E-D (2003) How surface fire in Siberian scots pine forests affects soil organic carbon in the forest floor: Stocks, molecular structure, and conversion to black carbon (charcoal). Global Biogeochem Cycles. doi: 10.1029/2002GB001956

Degens BP, Harris J a. (1997) Development of a physiological approach to measuring the catabolic diversity of soil microbial communities. Soil Biol Biochem 29:1309–1320. doi: 10.1016/S0038-0717(97)00076-X

Díaz-Raviña M, Prieto A, Bååth E (1996) Bacterial activity in a forest soil after soil heating and organic amendments measured by the thymidine and leucine incorporation techniques. Soil Biol Biochem 28:419–426. doi: 10.1016/0038-0717(95)00156-5

Domeignoz-Horta LA, Pold G, Liu X-JA, et al (2020) Microbial diversity drives carbon use efficiency in a model soil. Nat Commun 11:3684. doi: 10.1038/s41467-020-17502-z

Dooley SR, Treseder KK (2012) The effect of fire on microbial biomass: A meta-analysis of field studies. Biogeochemistry 109:49–61. doi: 10.1007/s10533-011-9633-8

Dungait J a J, Hopkins DW, Gregory AS, Whitmore AP (2012) Soil organic matter turnover is governed by accessibility not recalcitrance. Glob Chang Biol 18:1781–1796. doi: 10.1111/j.1365-2486.2012.02665.x

Fang Y, Singh BP, Luo Y, et al (2018) Biochar carbon dynamics in physically separated fractions and microbial use efficiency in contrasting soils under temperate pastures. Soil Biol Biochem 116:399–409. doi: 10.1016/j.soilbio.2017.10.042

Fernández I, Cabaneiro A, Carballas T (1997) Organic matter changes immediately after a wildfire in an atlantic forest soil and comparison with laboratory soil heating. Soil Biol Biochem 29:1–11. doi: 10.1016/S0038-0717(96)00289-1

Fierer N, Bradford MA, Jackson RB (2007) Toward an ecological classification of soil bacteria. Ecology 88:1354–1364. doi: 10.1890/05-1839

Flannigan MD, Krawchuk MA, de Groot WJ, et al (2009) Implications of changing climate for global wildland fire. Int J Wildl Fire 483–507. doi: 10.1071/WF08187

Frey SD, Lee J, Melillo JM, Six J (2013) The temperature response of soil microbial efficiency and its feedback to climate. Nat Clim Chang 3:395–398. doi: 10.1038/nclimate1796

Geyer KM, Kyker-Snowman E, Grandy AS, Frey SD (2016) Microbial carbon use efficiency: accounting for population, community, and ecosystem-scale controls over the fate of metabolized organic matter. Biogeochemistry 127:173–188. doi: 10.1007/s10533-016-0191-y

González-Pérez JA, González-Vila FJ, Almendros G, Knicker H (2004) The effect of fire on soil organic matter--a review. Environ Int 30:855–870. doi: 10.1016/j.envint.2004.02.003

Grady KC, Hart SC (2006) Influences of thinning, prescribed burning, and wildfire on soil processes and properties in southwestern ponderosa pine forests: A retrospective study. For Ecol Manage 234:123–135. doi: 10.1016/j.foreco.2006.06.031

Guerrero C, Mataix-Solera J, Gómez I, et al (2005) Microbial recolonization and chemical changes in a soil heated at different temperatures. Int J Wildl Fire 14:385–400. doi: 10.1071/WF05039

Guo K, Zhao Y, Liu Y, et al (2020) Pyrolysis temperature of biochar affects ecoenzymatic stoichiometry and microbial nutrient-use efficiency in a bamboo forest soil. Geoderma 363:114162. doi: 10.1016/j.geoderma.2019.114162

Hall SJ, Huang W, Timokhin VI, Hammel, KE (2020) Lignin lags, leads, or limits the decomposition of litter and soil organic carbon. Ecology 101:1–7. doi: 10.1002/ecy.3113

Hatton PJ, Chatterjee S, Filley TR, et al (2016) Tree taxa and pyrolysis temperature interact to control the efficacy of pyrogenic organic matter formation. Biogeochemistry 130:103–116. doi: 10.1007/s10533-016-0245-1

Hobley EU, Zoor LC, Shrestha HR, et al (2019) Prescribed fire affects the concentration and aromaticity of soluble soil organic matter in forest soils. Geoderma 341:138–147. doi: 10.1016/j.geoderma.2019.01.035

Janssens IA, Dieleman W, Luyssaert S, et al (2010) Reduction of forest soil respiration in response to nitrogen deposition. Nat Geosci 3:315–322. doi: 10.1038/ngeo844

Jastrow JD, Amonette JE, Bailey VL (2007) Mechanisms controlling soil carbon turnover and their potential application for enhancing carbon sequestration. Clim Change 80:5–23. doi: 10.1007/s10584-006-9178-3

Jiang X, Denef K, Stewart CE, Cotrufo MF (2016) Controls and dynamics of biochar decomposition and soil microbial abundance, composition, and carbon use efficiency during long-term biochar-amended soil incubations. Biol Fertil Soils 52:1–14. doi: 10.1007/s00374-015-1047-7

Jingyan S, Yuwen L, Zhiyong W, Cunxin W (2013) Investigation of thermal decomposition of ascorbic acid by TG-FTIR and thermal kinetics analysis. J Pharm Biomed Anal 77:116–119. doi: 10.1016/j.jpba.2013.01.018

Jones DL, Shannon D, Murphy D V., Farrar J (2004) Role of dissolved organic nitrogen (DON) in soil N cycling in grassland soils. Soil Biol Biochem 36:749–756. doi: 10.1016/j.soilbio.2004.01.003

Kavanagh KL, Dickinson MB, Bova AS (2010) A way forward for fire-caused tree mortality prediction: Modeling a physiological consequence of fire. Fire Ecol 6:80–94. doi: 10.4996/fireecology.0601080

Keiblinger KM, Hall EK, Wanek W, et al (2010) The effect of resource quantity and resource stoichiometry on microbial carbon-use-efficiency. FEMS Microbiol Ecol 73:no-no. doi: 10.1111/j.1574-6941.2010.00912.x

Kielland K, McFarland JW, Ruess RW, Olson K (2007) Rapid cycling of organic nitrogen in taiga forest ecosystems. Ecosystems 10:360–368. doi: 10.1007/s10021-007-9037-8

Lehmann J, Rillig MC, Thies J, et al (2011) Biochar effects on soil biota – A review. Soil Biol Biochem 43:1812–1836. doi: 10.1016/j.soilbio.2011.04.022

Lenth R (2020) emmeans: Estimated Marginal Means, aka Least-Squares Means. R package version 1.4.4.

Liang C, Amelung W, Lehmann J, Kästner M (2019) Quantitative assessment of microbial necromass contribution to soil organic matter. Glob Chang Biol 25:3578–3590. doi:

10.1111/gcb.14781

Liang C, Schimel JP, Jastrow JD (2017) The importance of anabolism in microbial control over soil carbon storage. Nat Microbiol. doi: 10.1038/nmicrobiol.2017.105

Loehman RA, Reinhardt E, Riley KL (2014) Wildland fire emissions, carbon, and climate: Seeing the forest and the trees – A cross-scale assessment of wildfire and carbon dynamics in fire-prone, forested ecosystems. For Ecol Manage 317:9–19. doi: 10.1016/j.foreco.2013.04.014

Lozano E, Chrenková K, Arcenegui V, et al (2016) Glomalin-related Soil Protein Response to Heating Temperature: A Laboratory Approach. L Degrad Dev 27:1432–1439. doi: 10.1002/ldr.2415

Mallek CM, Safford H, Viers J, Miller JD (2013) Modern departures in fire severity and area vary by forest type, Sierra Nevada and southern Cascades, California, USA. Ecosphere 4:1–28. doi: 10.1890/ES13-00217

Manzoni S, Čapek P, Mooshammer M, et al (2017) Optimal metabolic regulation along resource stoichiometry gradients. Ecol Lett 20:1182–1191. doi: 10.1111/ele.12815

Manzoni S, Taylor P, Richter A, et al (2012) Environmental and stoichiometric controls on microbial carbon-use efficiency in soils. New Phytol 196:79–91. doi: 10.1111/j.1469-8137.2012.04225.x

Martín A, Díaz-Raviña M, Carballas T (2009) Evolution of composition and content of soil carbohydrates following forest wildfires. Biol Fertil Soils 45:511–520. doi: 10.1007/s00374-009-0363-1

Massman WJ, Frank JM, Mooney SJ (2010) Advancing investigation and physical modeling of first-order fire effects on soils. Fire Ecol 6:36–54. doi: 10.4996/fireecology.0601036

Meigs GW, Donato DC, Campbell JL, et al (2009) Forest fire impacts on carbon uptake, storage, and emission: The role of burn severity in the eastern Cascades, Oregon. Ecosystems 12:1246–1267. doi: 10.1007/s10021-009-9285-x

Miesel JR, Hockaday WC, Kolka RK, Townsend PA (2015) Soil organic matter composition and quality across fire severity gradients in coniferous and deciduous forests of the southern boreal region. J Geophys Res Biogeosciences 120:1124–1141. doi: 10.1002/2015JG002959

Moorhead DL, Sinsabaugh RL (2006) A theoretical model of litter decay and microbial interaction. Ecol Monogr 76:151–174.

Neary D., DeBano L. (2005) Wildland fire in ecosystems effects of fire on soil and water.

Ni X, Liao S, Tan S, et al (2020) The vertical distribution and control of microbial necromass carbon in forest soils. Glob Ecol Biogeogr 29:1829–1839. doi: 10.1111/geb.13159

Örsi F (1973) Kinetic studies on the thermal decomposition of glucose and fructose. J Therm Anal 5:329–335. doi: 10.1007/BF01950381

Pan Y, Birdsey RA, Fang J, et al (2011) A large and persistent carbon sink in the world's forests. Science 333:988–993. doi: 10.1126/science.1201609

Pérez-Valera E, Goberna M, Faust K, et al (2017) Fire modifies the phylogenetic structure of soil bacterial co-occurrence networks. Environ Microbiol 19:317–327. doi: 10.1111/1462-2920.13609

Pérez-Guzmán L, Lower BH, Dick RP (2020) Corn and hardwood biochars affected soil microbial community and enzyme activities. Agrosystems, Geosci Environ 3:1–12. doi: 10.1002/agg2.20082

Pingree MRA, Kobziar LN (2019) The myth of the biological threshold: A review of biological responses to soil heating associated with wildland fire. For Ecol Manage 432:1022–1029. doi: 10.1016/j.foreco.2018.10.032

Pinheiro J, Bates D, Debroy S, Sarkar D (2019) nlme: Linear and nonlinear mixed effects models.

Prendergast-Miller MT, de Menezes AB, Macdonald LM, et al (2017) Wildfire impact: Natural experiment reveals differential short-term changes in soil microbial communities. Soil Biol Biochem 109:1–13. doi: 10.1016/j.soilbio.2017.01.027

Pressler Y, Moore JC, Cotrufo MF (2018) Belowground community responses to fire: meta-analysis reveals contrasting responses of soil microorganisms and mesofauna. Oikos 1–19. doi: 10.1111/oik.05738

Preston CM, Schmidt MWI (2006) Black (pyrogenic) carbon: a synthesis of current knowledge and uncertainties with special consideration of boreal regions. Biogeosciences 3:397–420. doi: 10.5194/bg-3-397-2006

Prieto-Fernández A, Acea MJ, Carballas T (1998) Soil microbial and extractable C and N after wildfire. Biol Fertil Soils 27:132–142. doi: 10.1007/s003740050411

Prieto-Fernández Á, Carballas M, Carballas T (2004) Inorganic and organic N pools in soils burned or heated: Immediate alterations and evolution after forest wildfires. Geoderma

121:291–306. doi: 10.1016/j.geoderma.2003.11.016

R Core Team (2019) R: A language and environment for statistical computing.

Raison RJ (1979) Modification of the soil environment by vegetation fires, with particular reference to nitrogen transformations: A review. Plant Soil 51:73–108. doi: 10.1007/BF02205929

Rousk J, Demoling LA, Bååth E (2009) Contrasting short-Term antibiotic effects on respiration and bacterial growth compromises the validity of the selective respiratory inhibition technique to distinguish fungi and bacteria. Microb Ecol 58:75–85. doi: 10.1007/s00248-008-9444-1

Russell JD, Fraser AR, Watson JR, Parsons JW (1974) Thermal decomposition of protein in soil organic matter. Geoderma 11:63–66. doi: 10.1016/0016-7061(74)90007-X

Sawyer R, Bradstock R, Bedward M, Morrison RJ (2018) Fire intensity drives post-fire temporal pattern of soil carbon accumulation in Australian fire-prone forests. Sci Total Environ 610–611:1113–1124. doi: 10.1016/j.scitotenv.2017.08.165

Schimel JP, Bennett J (2004) Nitrogen mineralization: challenges of a changing paradigm. Ecology 85:591–602.

Schimel JP, Schaeffer SM (2012) Microbial control over carbon cycling in soil. Front Microbiol 3:1–11. doi: 10.3389/fmicb.2012.00348

Serrasolsas I, Khanna PK (1995) Changes in heated and autoclaved forest soils of S.E. Australia. I. Carbon and nitrogen. Biogeochemistry 29:3–24. doi: 10.1007/BF00002591

Sinsabaugh RL, Manzoni S, Moorhead DL, Richter A (2013) Carbon use efficiency of microbial communities: Stoichiometry, methodology and modelling. Ecol Lett 16:930–939. doi: 10.1111/ele.12113

Six J, Frey SD, Thiet RK, Batten KM (2006) Bacterial and Fungal Contributions to Carbon Sequestration in Agroecosystems. Soil Sci Soc Am J 70:555. doi: 10.2136/sssaj2004.0347

Soil Survey Staff Official soil series descriptions. In: Nat. Resour. Conserv. Serv. United States Dep. Agric. www.nrcs.usda.gov.

Soong JL, Fuchslueger L, Marañon-Jimenez S, et al (2020) Microbial carbon limitation: The need for integrating microorganisms into our understanding of ecosystem carbon cycling. Glob Chang Biol 26:1953–1961. doi: 10.1111/gcb.14962

Spohn M, Klaus K, Wanek W, Richter A (2016a) Microbial carbon use efficiency and biomass turnover times depending on soil depth - Implications for carbon cycling. Soil Biol Biochem 96:74–81. doi: 10.1016/j.soilbio.2016.01.016

Spohn M, Pötsch EM, Eichorst SA, et al (2016b) Soil microbial carbon use efficiency and biomass turnover in a long-term fertilization experiment in a temperate grassland. Soil Biol Biochem 97:168–175. doi: 10.1016/j.soilbio.2016.03.008

Steinbeiss S, Gleixner G, Antonietti M (2009) Effect of biochar amendment on soil carbon balance and soil microbial activity. Soil Biol Biochem 41:1301–1310. doi: 10.1016/j.soilbio.2009.03.016

Tiemann LK, Billings SA (2011) Changes in variability of soil moisture alter microbial community C and N resource use. Soil Biol Biochem 43:1837–1847. doi: 10.1016/j.soilbio.2011.04.020

Vergnoux A, Di Rocco R, Domeizel M, et al (2011) Effects of forest fires on water extractable organic matter and humic substances from Mediterranean soils: UV-vis and fluorescence spectroscopy approaches. Geoderma 160:434–443. doi: 10.1016/j.geoderma.2010.10.014

Wan S, Hui D, Luo Y (2001) Fire effects on nitrogen pools and dynamics in terrestrial ecosystems: A meta-analysis. Ecol Appl 11:1349–1365.

Wang Q, Zhong M, Wang S (2012) A meta-analysis on the response of microbial biomass, dissolved organic matter, respiration, and N mineralization in mineral soil to fire in forest ecosystems. For Ecol Manage 271:91–97. doi: 10.1016/j.foreco.2012.02.006

Whitman T, Whitman E, Woolet J, et al (2019) Soil bacterial and fungal response to wildfires in the Canadian boreal forest across a burn severity gradient. Soil Biol Biochem 138:107571. doi: 10.1016/j.soilbio.2019.107571

Wieder WR, Bonan GB, Allison SD (2013) Global soil carbon projections are improved by modelling microbial processes. Nat Clim Chang 3:909–912. doi: 10.1038/nclimate1951

Witt C, Gaunt JL, Galicia CC, et al (2000) A rapid chloroform-fumigation extraction method for measuring soil microbial biomass carbon and nitrogen in flooded rice soils. Biol Fertil Soils 30:510–519. doi: 10.1007/s003740050030

Yu Z, Chen L, Pan S, et al (2018) Feedstock determines biochar-induced soil priming effects by stimulating the activity of specific microorganisms. Eur J Soil Sci 69:521–534. doi: 10.1111/ejss.12542

Zhao H, Tong DQ, Lin Q, et al (2012) Effect of fires on soil organic carbon pool and

mineralization in a Northeastern China wetland. Geoderma 189–190:532–539. doi: 10.1016/j.geoderma.2012.05.013

CHAPTER 5:

SOIL HEATING INTENSITY AND PYROGENIC ORGANIC MATTER HAVE IMMEDIATE IMPACTS ON THE STRUCTURE AND KINETICS OF SOIL CARBON POOLS

5.1 ABSTRACT

Increases in tree density and fuel loads in the mixed-conifer forests of California (USA) have led to increases in wildfire intensity, potentially leading to positive feedbacks between carbon (C) emissions and climate. In addition to emissions resulting from combustion, high intensity fires could alter soil C mineralization rates immediately post-fire due to direct impacts of soil heating on soil properties; however, high intensity fires could also produce more pyrogenic organic matter (PyOM), a source of persistent C. The influence of soil heating and PyOM on the relative sizes and stability of the active and slow cycling soil C pools could have long-lasting effects on forest C storage and determine the strength of fire-climate feedbacks. Here, I disentangle the impacts of soil heating intensity and PyOM on the size and kinetic rates of the active (C_a) and non-active (C_s) C pools in forest soils. I hypothesized that C_a size and mineralization rate will increase with soil heating intensity, C_s size will increase with PyOM additions, and that C_s mineralization rates will be inversely related to temperature of PyOM formation. I conducted a laboratory experiment in which I manipulated soil heating temperature (unheated, 200 °C, 300 °C, 400 °C) and char formation temperature (uncharred, 300 °C, 550 °C), and incubated soils for 390 days to determine the sizes and kinetic rates of the C_a and C_s pools. The C_a pool size and mineralization rate increased at the two highest soil heating intensities, and char additions increased C_s pool size. Char formation temperature did not influence the size or mineralization rates of either the C_a or C_s pools. My results suggest that soil C pools are resistant to low intensity soil heating, whereas high intensity soil heating leads to immediate decreases in

soil C persistence. Over the long term, the impacts of high intensity soil heating could be offset by the persistence of PyOM. This research advances understanding of C persistence in fire-prone forests, and suggests that forest C accounting should consider the impacts of fire intensity on soil C.

5.2 INTRODUCTION

Carbon (C) stored in temperate forest soils accounts for ~50% of the ecosystem C stock (Pan et al. 2011), so disturbance-induced changes to the persistence of soil C could have substantial impacts on the global C balance (Luo and Weng 2011). In California's mixed-conifer forests, selective logging and fire suppression have resulted in forests that are more densely populated with small, fire-sensitive trees and have higher surface fuel loads compared to historical reference conditions (Skinner and Taylor 2006; Earles et al. 2014; Taylor et al. 2014). These structural changes have led to increased wildfire intensity (Taylor et al. 2014), which, coupled with greater surface fuel loads, can result in greater heat flux to soil during wildfires (Neary and DeBano 2005; Massman et al. 2010; Busse et al. 2013). Soil heating can directly impact the amount and composition of soil organic matter (González-Pérez et al. 2004; Knicker 2007), potentially influencing both the size and persistence of the soil C sink. Understanding the effects of soil heating intensity on soil C dynamics is important for predicting the feedbacks between fire and climate under disrupted fire regimes, as well as for determining whether fuel removal treatments designed to decrease fire severity and intensity are also effective at promoting resilience of soil functions.

The magnitude, depth, and duration of soil heating during a fire can vary substantially, largely depending on pre-fire fuel load and moisture content. Temperatures of 100-300 °C are typical at the soil surface, but instantaneous temperatures can exceed 700-1000 °C under heavy

fuel loads (Certini 2005; Neary and DeBano 2005). Mineral soil is a poor heat conductor, so temperatures at 5 cm below the mineral soil surface are generally less than 150 °C (Certini 2005), but can exceed temperatures of 200 °C for several hours under wood piles or smoldering duff (Neary and DeBano 2005; Busse et al. 2013). Soil heating intensity likely influences soil C cycling due to progressive changes in soil chemistry and biology with temperature (González-Pérez et al. 2004). For example, soluble organic C content has been shown to increase with soil heating temperature up to ~300 °C, and then exhibit rapid declines (Bárcenas-Moreno and Bååth 2009). Protein denaturation begins at temperatures <100 °C (Knicker 2007), cellulose and hemicellulose are lost or transformed at temperatures ~200 °C, and lignin appears to be lost at temperatures >300 °C (Fernández et al. 1997; González-Pérez et al. 2004). From a biological standpoint, microbial biomass losses increase with soil heating temperature (Choromanska and DeLuca 2002; Bárcenas-Moreno and Bååth 2009), and soil heating leads to lower fungal-to-bacterial ratios due to greater heat-sensitivity of fungi (Dunn et al. 1985; Guerrero et al. 2005).

Soil C can be conceptually modeled as discrete pools that vary in persistence: an active C pool (C_a) with a mean residence time (MRT) of days to months, and a non-active C pool (C_s) with an MRT of years to decades. The C_s pool can be an order of magnitude larger than the C_a pool, so fire-induced changes to its size or persistence may be especially important for determining the strength of the soil C sink. Some C pool models include a third "passive" or "resistant" C pool, but research indicates that methods for isolating such a pool result in inaccurate estimates (Greenfield et al. 2013). Pyrogenic organic matter (PyOM) encompasses a range of fire-affected organic matter, from slightly charred biomass to highly condensed aromatic compounds (Masiello 2004; Bird et al. 2015), and tends to exhibit longer MRT in soils compared to uncharred biomass (Kuzyakov et al. 2009; Santos et al. 2012; Kuzyakov et al.

2014). PyOM may therefore primarily contribute to the C_s pool, representing a persistent C sink that offsets C losses resulting from biomass combustion (Jones et al. 2019). However, a portion of PyOM decomposes relatively quickly in soil, and the size of this fast-cycling PyOM pool is inversely related to pyrolysis temperature (Nguyen et al. 2010; Bird et al. 2015), indicating that fire intensity may influence the persistence of PyOM. Furthermore, PyOM decomposition can be primed by labile C (Kuzyakov et al. 2009), and fungi may decompose PyOM more efficiently than bacteria (Zimmermann et al. 2012), suggesting that the impacts of heating intensity on soil chemical and biological properties can indirectly influence PyOM decomposition dynamics.

Previous research has indicated that wildfire can lead to immediate increases in the size of the C_a pool and the kinetic rates of both the C_a and C_s pools (Fernández et al. 1997; Fernández et al. 1999). However, by months to years post-fire in *Pinus sylvestris* (Fernández et al. 1997; Fernández et al. 1999) and Sierra-Nevada mixed-conifer forests (Adkins et al. 2019b), the opposite trend is apparent: C_a pool size and mineralization rates of the C_a and C_s pools are lower in burned areas versus unburned areas. This suggests that fire has immediate and distinct impacts on soil C pool dynamics that are not captured by assessments later during ecosystem recovery. The immediate impacts of fire intensity on soil C pool dynamics has not been investigated, nor has it been determined whether changes are related to soil chemical or biological properties. A better understanding of the immediate impacts of fire on soil C persistence could improve forest C accounting and inform the management of fire-prone forests for C storage under novel fire regimes. Here, I performed a laboratory study to disentangle the direct and indirect impacts of fire on the structure and persistence of C_a and C_s pools by manipulating soil heating intensity, PyOM additions, and microbial communities independently of one another. I hypothesized that 1) C_a pool size and kinetic rates would progressively increase with soil heating intensity due to

increases in extractable C; 2) C_s size would increase with PyOM additions; and 3) C_s kinetic rates would be inversely related to the temperature of PyOM formation.

5.3 MATERIALS AND METHODS

5.3.1 Site description and sample collection

I collected soil samples from the Lassen National Forest in the Sierra Nevada Mountain Range, California, USA. The forest is a dry mixed-conifer forest dominated by *Pinus ponderosa*, *P. lambertiana, P. jeffreyi, Abies concolor, Pseudotsuga menziesii, Calocedrus decurrens*, and *Quercus kelloggii*. Soils at my sites are from the Skalan soils series, a loamy-skeletal, isotic, mesic Vitrandic Haploxerlaf (Soil Survey Staff). From five sites within the forest, I collected soil along a transect with sampling locations spaced ~15 cm apart until I collected ~10 L of mineral soil. At each sampling location, I removed the organic horizon, inserted a 15.7 cm diameter cylinder to 5 cm, and collected mineral soil using a stainless-steel scoop. I sieved (4 mm) and air dried the soil at time of sampling. After transport to the lab, I composited equal masses of soils from each of the five sampling sites and sieved to 2 mm.

I collected *P. taeda* (loblolly pine) wood samples from the Duke Forest in Durham, North Carolina, USA. The forest is dominated by *P. taeda*, with an understory of *Liquidambar styracifua*, *Acer rubrum*, *Cercis canadensis*, and *Cornus florida* (Hobbie et al. 2014). Within each plot, I collected five pieces of wood (2.54-7.62 cm diameter) from the surface of the forest floor. Duke Forest is a former Free Air Carbon Enrichment (FACE) site, and wood produced under CO_2 fumigation is depleted in ^{13}C compared to wood produced under CO_2 natural abundance. I collected wood samples from Duke Forest instead of Lassen National Forest to trace accumulation of C from wood and char into microbial biomass, but I do not report those results here.

5.3.2 Experimental design

I performed a full-factorial experiment in which I manipulated soil heating intensity (unheated soil, and soil heated to 200 °C, 300 °C, or 400 °C), wood/char additions (no addition, uncharred wood addition, and addition of char generated at 300 °C or 550 °C), and soil inoculum type to manipulate microbial communities (250-2000 µm soil fraction and a ≤250 µm soil fraction). Each treatment combination was replicated 18 times (N=576), and replicates were divided between four incubation blocks that were destructively sampled after incubating for 30, 100, 200, and 390 days.

Treatment applications and soil incubation

I created char by individually wrapping ~15 cm lengths of loblolly pine wood in aluminum foil and heating in a muffle furnace for four hours at the target temperature. I then pulverized charred and uncharred wood to pass a 250 µm sieve. For soil heating treatments, I weighed ~1600 g of soil into an aluminum baking dish, added DI water to bring soils to 25% water-filled pore-space (WFPS), and mixed the soil to achieve even moisture throughout. I then covered the dish with aluminum foil and heated in a muffle furnace for 90 minutes at the target temperature. I measured C and N concentrations of soil, wood, and char using a dry-combustion elemental analyzer (Costech Analytical Technologies Inc., Valencia, CA, USA), using acetanilide as the quantification standard.

I weighed 31.0 ± 1.0 g replicates of the post-heated soils into 90 mL specimen cups. For microcosms receiving wood or char additions, I added 0.310 ± 0.010 g of material to the soils and stirred to mix. I readjusted the soils to 25% WFPS, capped the specimen cups, and sterilized the samples by autoclaving at 121 °C for 30 minutes. Following sterilization, I sought to manipulate the soil microbial community by reinoculating the sterilized soils with either 0.75 ±

0.10 g of unsterilized soil that had passed a 250 µm sieve, or 1.50 ± 0.10 g of soil that did not pass the sieve (i.e. 250-2000 µm fraction). The different masses of the two inoculum types were selected to apply approximately equal microbial biomass, determined via substrate-induced respiration in preliminary experiments. Previous research indicates that soil fractions differ in microbial community composition (Wagg et al. 2014; Wagg et al. 2019), and preliminary experiments based on selectively-inhibited substrate-induced respiration suggested that the 0-250 µm fraction had a higher fungal-to-bacterial ratio than the 250-2000 µm fraction (1.45 ± 0.34 vs 0.68 ± 0.06; p=0.024; Fig. S5.1). After soil inoculation, I adjusted soil moisture of each microcosm to 50% WFPS, placed each specimen cup in a loosely capped 0.473 L glass jar, and incubated in the dark at ambient temperature (23 °C).

Determination of extractable organic carbon and microbial biomass carbon

I destructively sampled incubation blocks at 30, 100, 200, and 390 days for determination of extractable organic carbon (EOC) and microbial biomass carbon (MBC). From each microcosm, I weighed four ~5 g subsamples into 50 mL centrifuge tubes. Two subsamples were immediately extracted for EOC, and the other two were directly exposed to chloroform for 24 hours to lyse microbial cells prior to extraction (Witt et al. 2000). I also determined EOC from each soil heating treatment at day 0 by extracting three autoclaved and unamended soil replicates. I extracted EOC by adding 25 mL of 0.5 M K_2SO_4 to the centrifuge tubes, agitating on a reciprocating shaker for 1 hour, and filtering through 11 µm pore-size filters (Whatman Grade 1). I determined EOC concentrations spectrophotometrically after potassium-dichromate oxidation (Cai et al. 2011). Wet-oxidation methods have been shown to underestimate EOC concentrations compared to combustion methods (Bolan et al. 1996), but conversion factors between methods are not available in the published literature. MBC was determined as the

difference in EOC between fumigated and unfumigated subsamples, divided by a correction factor of 0.33 (Cai et al. 2011).

My original intent was to measure fungal-to-bacterial ratios using selectively-inhibited substrate-induced respiration on each sampling date to determine whether the two soil inoculum treatments affected microbial community structure (Anderson and Domsch 1973; Bailey et al. 2003). Prior to initiating the experiment, I optimized the selective-inhibition procedure on unheated and unsterilized soils collected from the same site and achieved acceptable results. However, when I applied the procedure on day 30, the inhibition additivity ratio was too high (>1.3) to accept the results. Thus, I did not continue using this technique on the remaining sampling dates. Selectively-inhibited substrate-induced respiration requires extensive optimization, and different soils require different inhibitor types and concentrations to produce acceptable results (Bailey et al. 2003; Rousk et al. 2009). This suggests that differences in soil biological characteristics affect the performance of this procedure, and I suspect that changes in the soil biological community over the course of the incubation impacted its efficacy.

Determination of carbon mineralization rates

For one incubation block, I measured C mineralization rates on incubation days 9, 11, 21, 31, 40, 50, 60, 74, 90, 102, 119, 143, 180, 221, 265, 305, 347, and 389. On measurement days 9 and 11, I determined CO_2-C production by tightly capping each jar with a septum-fitted lid and measuring the CO_2 concentrations of 13 mL gas aliquots using a gas chromatograph (Thermo Fisher Scientific Inc., Waltham, MA, USA). Measurements were taken ~30 minutes and 6 hours after capping. Due to equipment malfunction, not all replicates were measured on day 21, so this data were not analyzed. For the remaining sampling days, I measured CO_2 concentrations of 1 mL gas aliquots using an infrared gas analyzer (LI-COR Inc., Lincoln, NE, USA). For these

sampling days, CO_2 was allowed to accumulate in the capped jars for 24-96 hours prior to measurement, with the longer accumulation times occurring later in the incubation when C mineralization rates were low.

Carbon Pool Models

I applied single- and double-pool decay models to my C mineralization data to determine the size and rate constants of soil C pools (Kuzyakov 2011). The single-pool model was fit as:

$$C_t = C_m(1 - e^{-k_m * t}) \quad (1)$$

where C_t is cumulative CO_2-C respired at day t, C_m is the initial size of the carbon pool available for mineralization, and k_m is its kinetic rate constant. The double-pool model was fit as:

$$C_t = C_a(1 - e^{-k_a * t}) + C_s(1 - e^{-k_s * t}) \quad (2)$$

where C_a is the size of the active (or fast cycling) pool, C_s is the size of the non-active pool, and k_a and k_s are the respective kinetic rate constants. In this model, C_s is constrained to be the difference between total C in the microcosms (soil C + char C) and C_a. The soil and char C values used for this constraint were treatment means. I used both single- and double-pool decay models because visual inspection of cumulative C mineralization curves suggested that two treatment combinations (unheated soil + uncharred wood, 200 °C soil + uncharred wood) would be better estimated by single-pool models. I did not include a passive C pool in my models, because methods for isolating such a pool do not provide biologically meaningful estimates (Greenfield et al. 2013).

5.3.3 Statistical Analysis

I performed all analyses in the R statistical computing environments (v 3.6.1) (R Core Team 2019) using the nlme package (v 3.1.140) (Pinheiro et al. 2019). I used general linear models to assess the responses of EOC and MBC and linear mixed models to assess the

responses of C mineralization rate and cumulative C mineralization. Models initially included main effects of time, soil heating, char type, and inoculum type, and all possible two- and three-way interactions. The mixed models also included a microcosm identifier as a random effect. Non-significant three-way interactions were removed from the models. Additionally, inoculum treatment main and interactive effects were never significant and were removed from all models, but all other effects were retained. Model residuals for the two C mineralization models were not normally distributed. For the C mineralization rate model, this was rectified by specifying time as a continuous covariate and adding a *log*(time) term. For the cumulative C mineralization model, residual non-normality was rectified by specifying time as a factor and an autoregressive correlation structure to account for non-independence of within-group (microcosm) observations (Pinheiro and Bates 2000).

I fit the single- and double-pool decay models by first performing separate non-linear regressions for each incubation replicate, with cumulative C mineralization in units of mg kg^{-1} soil. To fit a single model encompassing all replicates, I then used data visualization approaches as described by Pinheiro and Bates (2000) to determine which parameters were associated with random and interactive effects. These procedures resulted in models that included random intercepts and two-way interactions associated with C_a and k_s, whereas k_a was associated only with main effects. I then fit additional models with cumulative C mineralization in units of percent total microcosm C to obtain estimates of pool sizes on both a soil mass fraction basis and relative to total C. Because C_s is constrained in the double-pool models, it is not estimated independently of C_a. I therefore calculated 95% confidence intervals for C_s by subtracting the confidence limits of C_a from total microcosm C, and I considered differences in C_s to be significant if the confidence intervals did not overlap. For all other parameters, if main effects

were significant at $\alpha \leq 0.05$, I performed pairwise comparisons of marginal means using Tukey's adjustment in the emmeans package (v 1.4.4) (Lenth 2020).

5.4 RESULTS

5.4.1 Soil and char carbon concentrations

There were no statistically significant effects of soil heating on C concentrations ($p=0.79$; $n=3$), although soils heated to 400 °C had slightly lower C concentrations than the pooled average (3.7 ± 0.4% and 3.9 ± 0.2%, respectively). C concentrations were 48.7% for uncharred wood, 66.1% for 300 °C char, and 71.7% for 550 °C char.

5.4.2 Extractable organic carbon and microbial biomass carbon

Soil heating had immediate impacts on EOC concentrations ($p<0.001$; Fig. 5.1). EOC increased with heating temperature up to 300 °C, then decreased in soils heated to 400 °C. Compared to unheated soils, EOC concentrations were 45.0% higher in soils heated to 300 °C and 12.5% lower in soils heated to 400 °C. There were significant main and interactive effects on both EOC and MBC measured over the incubation (Table 5.1). EOC was lowest in soils heated to 400 °C on all four sampling dates regardless of char treatment (Fig. 5.2). Averaged across all char × time combinations, soils heated to 400 °C exhibited 50.2%-55.0% less EOC than the other soil heating treatments. On day 30, unheated soils generally exhibited higher EOC than soils heated to 400 °C, and soils heated to 200 °C and 300 °C exhibited intermediate values. On day 100, soils heated to 200 °C exhibited the greatest EOC for soils that with uncharred wood or no addition, while unheated soils exhibited greatest EOC for soils with 550 °C char. Although there were temperature-based differences in EOC on days 200 and 390, these differences did not exhibit a clear pattern.

Soils with uncharred wood tended to have greater EOC than the soils with char or no addition throughout the incubation. Averaged across all soil heating × time combinations, soil that received uncharred wood exhibited 8.6%-18.2% more EOC than the other addition treatments. In soils that were heated to 200 °C, EOC was lowest in soils that received 550 °C char at all sampling dates, averaging 23.9%-31.3% less EOC than the other char treatments.

On day 30, unheated soil generally exhibited lower MBC than heated soils (Fig. 5.3). Averaged across all char treatments, MBC was 39.1%-67.6% lower in unheated soils at this time point compared to the other soil heat treatments. Soils heated to 300 °C and 400 °C exhibited MBC that was higher than the other heat treatments by 1.7-2.1 fold on day 30. Soil heating impacted patterns in MBC over time. MBC decreased by 55.4% between days 30 and 390 in soils heated to 300 °C and by 74.9% in soils heated to 400 °C. In contrast, MBC in soils heated to 200 °C only decreased by 16.9% and increased by 48.4% in unheated soils. The impacts of charcoal on MBC did not exhibit a clear pattern.

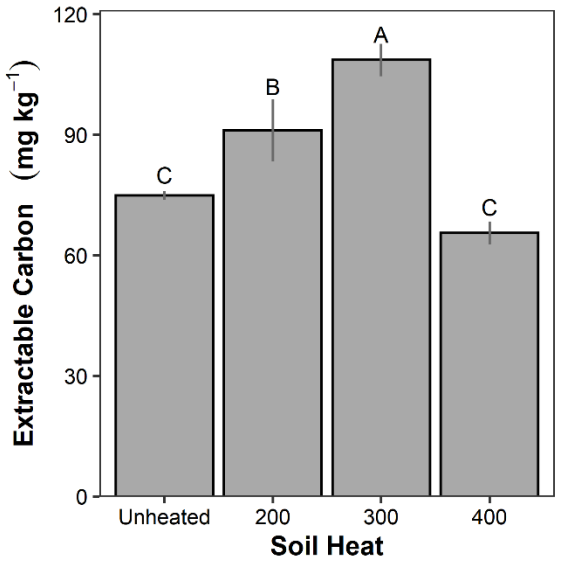

Figure 5.1 Extractable organic carbon of pre-incubated soils exposed to four different heating intensities and then autoclaved. The heights of the bars are treatment means (n=3) and error bars are 95% confidence intervals. Letters above bars represent pairwise significant differences among treatments.

Table 5.1 ANOVA tables for extractable organic carbon (EOC) and microbial biomass carbon (MBC) for soils destructively sampled four times over the 390 day incubation.

	Explanatory Variable	F-value	P-value
EOC	Intercept	527.45	<0.001
	Time	0.16	0.686
	Soil Heat Treatment	52.03	<0.001
	Char Treatment	5.16	0.002
	Time × Soil Heat	1.81	0.144
	Time × Char	6.37	<0.001
	Soil Heat × Char	4.08	<0.001
	Time × Soil Heat × Char	4.59	<0.001
MBC	Intercept	33.01	<0.001
	Time	2.83	0.038
	Soil Heat Treatment	30.02	<0.001
	Char Treatment	0.07	0.978
	Time × Soil Heat	7.72	<0.001
	Time × Char	2.24	0.019
	Soil Heat × Char	23.48	<0.001
	Time × Soil Heat × Char	6.51	<0.001

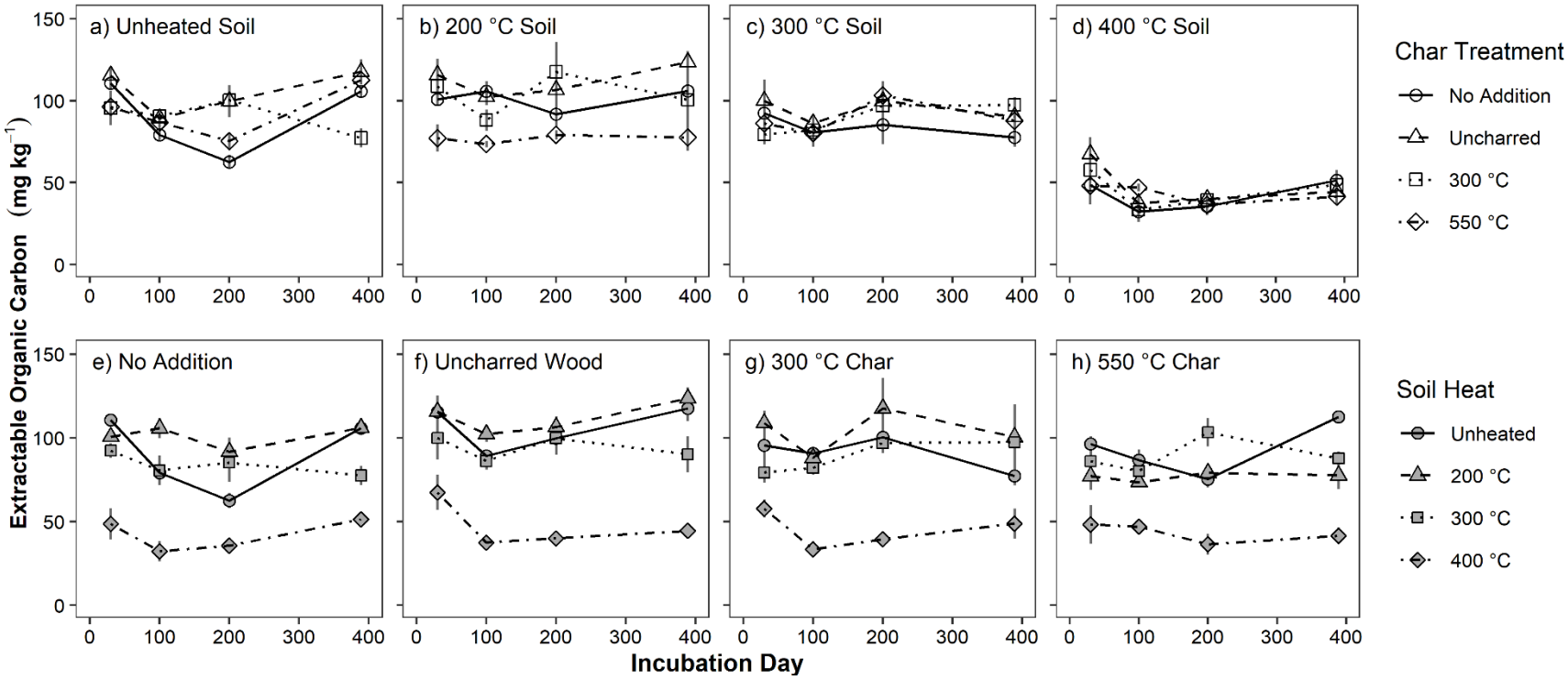

Figure 5.2 Extractable organic carbon on four destructive sampling days of soils exposed to different heating intensities and receiving different char additions. The top row of figures (a-d) displays char treatments grouped into levels of soil heating, and the bottom row of figures (e-h) displays soil heating treatments grouped into levels of char treatments. Points are treatment means (n=9) and error bars are 95% confidence intervals.

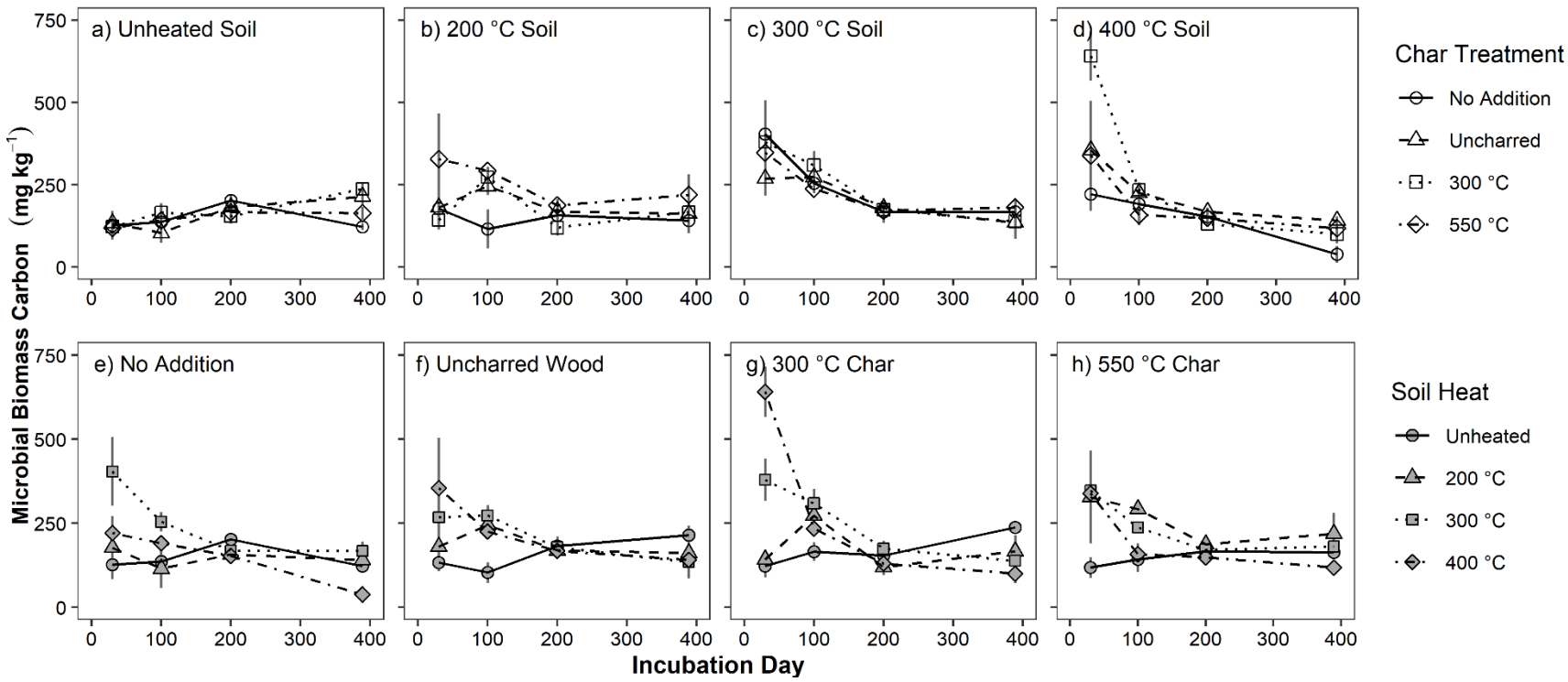

Figure 5.3 Microbial biomass carbon on four destructive sampling days of soils exposed to different heating intensities and receiving different char additions. The top row of figures (a-d) displays char treatments grouped into levels of soil heating, and the bottom row of figures (e-h) displays soil heating treatments grouped into levels of char treatments. Points are treatment means (n=9) and error bars are 95% confidence intervals.

5.4.3 Carbon mineralization

Cumulative C mineralization (mg CO_2-C kg^{-1} soil C) was not influenced by main effects of soil heating or char treatments, but all interactions involving time were significant (Table 5.2). By the end of the incubation, soil heating impacted cumulative C mineralized only for the uncharred wood or 300 °C char treatments (Fig. 5.4). For soils with uncharred wood, the unheated and 200 °C treatments resulted in 34.8%-44.6% more C mineralized than the other soil heating treatments. For soils with 300 °C char, the 400 °C treatment led to 27.6% more C mineralized than the unheated treatments. Char treatments impacted cumulative C mineralization at all soil heating intensities. In unheated and soils heated to 200 °C, soils with uncharred wood mineralized 1.5-2.1 times more C than the other char treatments. In soils heated to 300 °C, uncharred wood resulted in ~ 33% more total C mineralization than either char type; and in soils heated to 400 °C, uncharred wood led to 25.8% more C mineralization than 550 °C char. For all soil heating temperatures, soils with char exhibited total C mineralization that was less than or equal to soils that received no addition.

All main and interactive effects impacted C mineralization rate (mg CO_2-C kg^{-1} soil C d^{-1}) (Table 5.2). The effect of soil heating on C mineralization changed over time. Early in the incubation, mineralization rate was positively associated with soil heating intensity, with the 300 °C and 400 °C treatments consistently exhibiting the highest mineralization rates, regardless of char treatment. The opposite pattern was present late in the incubation, with the 300 °C and 400 °C heating treatments typically exhibiting lower mineralization rates compared to the unheated and 200 °C treatments. The effect of char treatments on mineralization rates depended on levels of soil heating and varied with time. Early in the incubation, soils with no additions exhibited the highest mineralization rates for unheated and 200 °C treatments. Within the 400 °C heat

treatment, soils with no additions or uncharred wood exhibited higher mineralization rates than soils with char. Late in the incubation, uncharred wood treatments exhibited the highest mineralization rates in soils that were unheated or heated to 200 °C or 300 °C. Soils that received char did not differ in mineralization rates from those that received no additions.

Table 5.2 ANOVA tables for carbon mineralization rate and cumulative carbon mineralization over the 390 day incubation.

	Explanatory Variable	F-value	P-value
C Mineralization Rate ($mg\ CO_2\text{-}C\ kg^{-1}\ soil\ C\ d^{-1}$)	Intercept	2307.01	<0.001
	Time	63.55	<0.001
	log(Time)	1774.87	<0.001
	Soil Heat Treatment	8.99	<0.001
	Char Treatment	12.61	<0.001
	Time × Soil Heat	11.80	<0.001
	Time × Char	17.33	<0.001
	Soil Heat × Char	6.66	<0.001
	Time × Soil Heat × Char	20.43	<0.001
Cumulative C Mineralization ($mg\ CO_2\text{-}C\ kg^{-1}\ soil\ C$)	Intercept	20.04	<0.001
	Time	69.66	<0.001
	Soil Heat Treatment	0.36	0.78
	Char Treatment	0.73	0.54
	Time × Soil Heat	11.70	<0.001
	Time × Char	10.32	<0.001
	Soil Heat × Char	0.36	0.95
	Time × Soil Heat × Char	5.96	<0.001

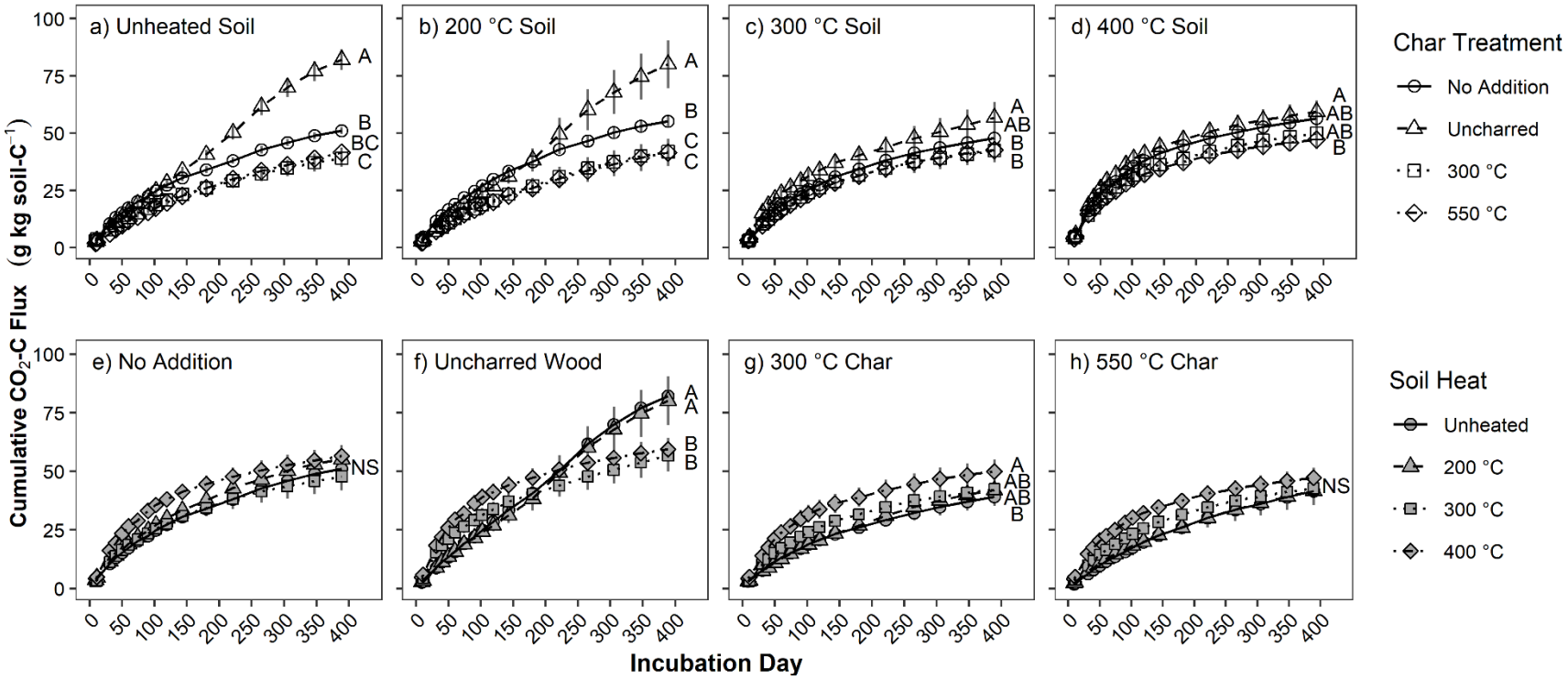

Figure 5.4 Carbon mineralization over 390 days of soils exposed to different heating intensities and receiving different char additions. The top row of figures (a-d) displays char treatments grouped into levels of soil heating, and the bottom row of figures (e-h) displays soil heating treatments grouped into levels of char treatments. Points are treatment means of cumulative C mineralization (n=9) and error bars are 95% confidence intervals. The slope of the lines between points represent mineralization rates. Letters represent pairwise significant differences in cumulative carbon mineralization at the end of the incubation.

5.4.4 Carbon pools: single pool model

C_m was impacted by char treatments and by a soil heat × char interaction, and k_m was impacted by all main and interactive effects (Table 5.3). Uncharred wood increased C_m by ~4.5-5.5 times in unheated soils and by ~4.1-4.3 times in soils heated to 200 °C (Fig. 5.5; Table S5.1). This pattern was consistent whether C_m pool size was considered on a soil mass fraction basis or relative to total C. C_m was otherwise unaffected by soil heat and char treatments. Similarly, k_m decreased in response to uncharred wood additions in unheated soils and soils heated to 200 °C but was otherwise unchanged.

Table 5.3 ANOVA tables for single and double carbon pool models. Values are from models fit to cumulative respiration per g soil data. ANOVAs for models fits to cumulative respiration per g soil C are not presented but are similar to the results provided here.

	Explanatory Variable	F-value	P-value
Single Pool Model			
C_m	Intercept	59.40	<0.001
	Soil Heat Treatment	0.25	0.859
	Char Treatment	66.69	<0.001
	Soil Heat × Char	30.60	<0.001
k_m	Intercept	85.02	<0.001
	Soil Heat Treatment	10.17	<0.001
	Char Treatment	12.93	<0.001
	Soil Heat × Char	5.51	<0.001
Double Pool Model			
C_a	Intercept	146.01	<0.001
	Soil Heat Treatment	6.85	<0.001
	Char Treatment	23.26	<0.001
	Soil Heat × Char	13.03	<0.001
k_a	Intercept	456.37	<0.001
	Soil Heat Treatment	19.78	<0.001
	Char Treatment	32.78	<0.001
k_s	Intercept	74.38	<0.001
	Soil Heat Treatment	2.72	0.043
	Char Treatment	90.73	<0.001
	Soil Heat × Char	21.18	<0.001

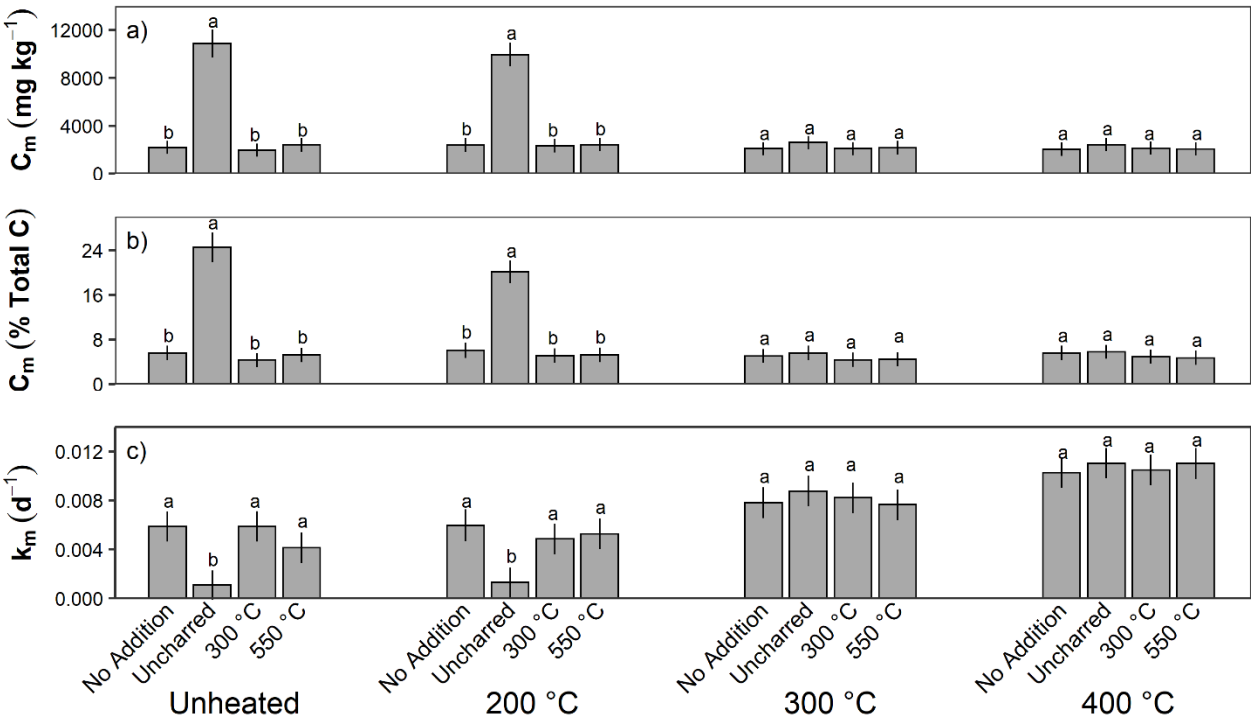

Figure 5.5 Bar charts illustrating the parameters of the single carbon pool model. The size of the potential mineralizable C pool (C_m) is presented in both absolute size (a) and relative to total soil C (b). The kinetic rate constant (k_m) is presented as d^{-1} (c). The heights of the bars represent the marginal means of the parameter estimates, and the error bars represent the 95% confidence intervals of the estimates. Letters above bars indicate pairwise significant differences between char treatments within soil heating levels. Pairwise comparisons for soil heating levels within char treatments are provided in table S1.

5.4.5 Carbon pools: double pool model

Pool sizes on soil mass fraction basis

C_a was affected by both soil heating and char treatments (Table 5.3). Within soils that received no additions, C_a was 22.6%-38.9% larger in soils heated to 400 °C than the other heat treatments (Fig. 5.6; Table S5.2). For soils with uncharred wood, C_a was 8.9-13.1 times larger in the 300 °C and 400 °C treatments than the other heating treatments. For char soils with char, C_a was 1.5-2.1 times larger in the 300 °C and 400 °C treatments than the other heating treatments. C_a generally did not differ between soils that received char additions from those that received no

additions. An exception occurred in soils heated to 200 °C, where C_a was 29.2% smaller for the 300 °C char treatment compared to the no addition treatment. Among all char treatments, C_s was smallest in soils heated to 400 °C and largest for soils heated to 300 °C. C_s showed a consistent pattern of increasing with char treatments as follows: no addition < uncharred < 300 °C < 550 °C.

Pool sizes relative to total carbon

Soils heated to 400 °C had C_a pools that were 1.5-6.2 times larger than the other heat treatments (Fig. 5.6; Table S5.2). For soils with wood or char additions, soils heated to 300 °C had 1.5-4.9 fold larger C_a pools than the unheated and 200 °C treatments. For soils with uncharred wood, unheated soils and soils heated to 200 °C had the largest C_s pools. For soils that received char, the 400 °C heat treatment resulted in the smallest C_s pools, and the 300 °C treatment had smaller C_s pools than the unheated and 200 °C treatments. Within unheated and 200 °C heated soils, uncharred wood led to the largest C_s pools. Char additions increased C_s pool size compared to no additions in soils heated to 200 °C.

Kinetic rate constants

Soils heated to 400 °C exhibited larger k_a values than the other soil heating treatments. Compared to unheated soils, the larger k_a values in these soils represent a decrease in C_a mean residence time (MRT) of 9.8-18.6 days. Soils with uncharred wood exhibited the largest k_a values at all soil heating treatments, representing a decrease of 16.0-24.9 days in C_a MRT. In addition to significant main effects, k_s was affected by a soil heat × char interaction. For soils with uncharred wood, k_s was largest in the unheated soils and 200 °C treatments, representing a decrease of 25.8-34.2 years in C_s MRT. For soils with 300 °C char, k_s was higher in soils heated to 200 °C than in soils heated to 400 °C, representing a 27.1 year difference in MRT. Within

soils that received 550 °C char, k_s was higher for the unheated treatments than for the 200 °C and 400 °C treatments, representing a difference in C_s MRT of 17.9-36.6 years. Soils with uncharred wood had the largest k_s values in soils that were unheated or heated to 200 °C, representing a 22.9-37.7 year decrease in C_s MRT compared to the two higher soil heating treatments.

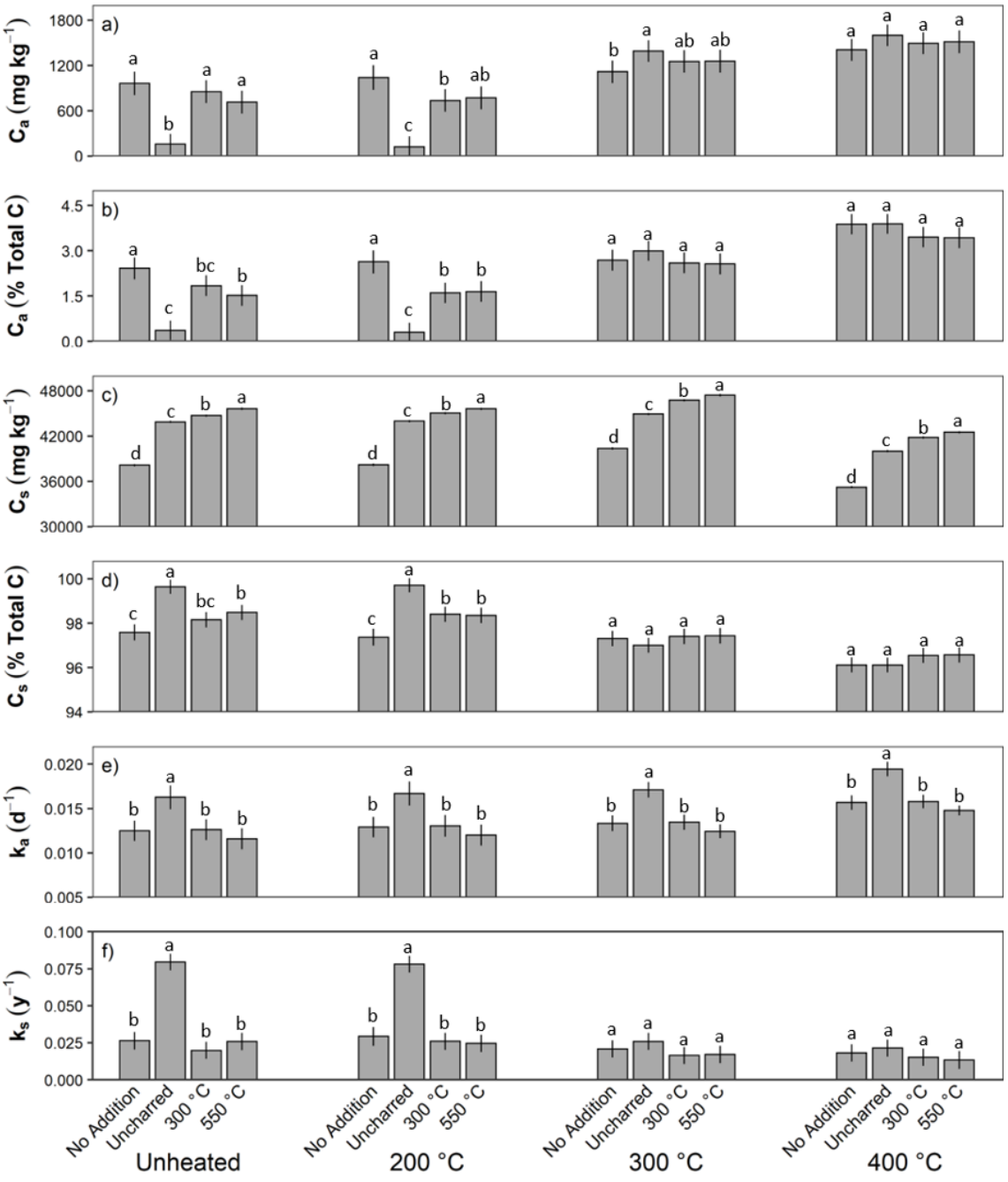

Figure 5.6 Bar charts illustrating the parameters of the double carbon pool model. The sizes of the active (C_a) and non-active (C_s) pools are presented in both absolute size (a and c) and relative to total soil C (b and d). The active C pool kinetic rate constant (k_a) is presented as d^{-1} (e), and slow C pool kinetic rate constant (k_s) is presented as y^{-1} (f). The heights of the bars represent the marginal means of the parameter estimates, and the error bars represent the 95% confidence intervals of the estimates. Letters above bars indicate pairwise significant differences between char treatments within soil heating levels. Pairwise comparisons for soil heating levels within char treatments are provided in table S2.

5.5 DISCUSSION

5.5.1 High intensity soil heating decreases soil carbon persistence over the short term

I found support for my hypothesis that C_a pool size and kinetic rates would increase with soil heating intensity. The two highest intensity soil heating treatments increased k_m, k_a and C_a pool size, and the highest intensity decreased C_s pool size, all of which indicate lower soil C persistence over the short term. Thus, in addition to causing greater C emissions during the combustion event itself, high intensity fires could increase soil C emissions via impacts on the structure and stability of soil C pools. My results support previous, field-based research that found increased C_a pools and k_a values in burned vs unburned mineral soils collected immediately (1 day) after wildfires in *P. sylvestris* dominated forests in northwestern Spain (Fernández et al. 1997; Fernández et al. 1999). My previous research found that C_a size is lower in burned areas than unburned areas three years post-fire (Adkins et al. 2019), suggesting the direct effects of soil heating on C_a are transient. My experiment suggests that the immediate changes to C_a size and persistence are likely due to the direct effects of heat flux on soil characteristics. For example, soil heating can directly affect soluble C content (Certini 2005; Knicker 2007), which could in turn influence C_a pool size and kinetics, because soluble C is a fast-cycling C source that is often positively correlated with soil respiration rates (Neff and Asner 2001; Wang et al. 2003). However, contrary to my hypothesis, increases in C_a and k_a in heated soils do not appear to be related to EOC: soils heated to 400 °C had the largest C_a and k_a values, but the lowest EOC. This suggests that nutrient availability may be a stronger driver of active C cycling in heated soils. For example, N volatilization increases with temperature from 200 to 500 °C, at which point >50% of N is lost (Knicker 2007; Bodí et al. 2014). Lower N availability could increase the need for N-mining from organic matter (Moorhead and

Sinsabaugh 2006), a C inefficient process that could lead to higher C mineralization rates. In addition to changes to C and nutrient availability, soil heating could influence C pools by destabilizing soil aggregates and degrading clay (Certini 2005; Mataix-Solera et al. 2011). Soil aggregation and clay associations are important mechanisms of C stabilization (Jastrow et al. 2007), so disruption of these mechanisms could explain the higher C_a and k_a.

Additionally, the higher mineralization rates and k_a values in soils heated to 300 °C and 400 °C could be due to indirect effects of soil heating on MBC via changes to soil abiotic properties. Microbes drive heterotrophic respiration and MBC may account for a portion of C_a (Wang et al. 2003; Lawrence et al. 2009), and, early in the incubation, MBC was greatest in soils subjected to high heating intensity. Soil heating can directly impact MBC by inducing microbial mortality (Choromanska and DeLuca 2002; Certini 2005; Bárcenas-Moreno and Bååth 2009); however, I sterilized and reinoculated the microcosms to ensure similar initial microbial biomass among soil heating treatments. Thus, differences in MBC were likely indirectly affected by soil heating. Furthermore, although soil heating can directly impact microbial community structure via differential survival of fungi vs bacteria and by selecting for heat-resistant bacterial taxa (Dooley and Treseder 2012; Prendergast-Miller et al. 2017), the lack of difference in C pool structure or kinetics between my two inoculation treatments indicates that initial differences in microbial community structure did not drive C cycling. These results further support the interpretation that top-down impacts of heating on soil abiotic characteristics determine C pool structure and kinetics.

5.5.2 Char increases the size and persistence of the non-active carbon pool

I found support for my hypothesis that C_s would increase with PyOM additions, but not for my hypothesis that k_s would be inversely related to the temperature of PyOM formation. My

findings that char increased the size of the C_s pool on a soil mass fraction basis suggest that char generated during fires can ameliorate the negative influence of soil heating on C persistence. This is further supported by my finding that high intensity soil heating decreased k_s only in soils with charred or uncharred wood. Previous research has shown that a high intensity wildfire had minimal immediate impacts on k_s (Fernández et al. 1997). However, research performed months to years following wildfires in mixed-conifer (Adkins et al. 2019b) and *P. sylvestris* forests (Fernández et al. 1999) indicate that the absolute size of C_s was higher and k_s lower at these intermediate time points in post-fire recovery in burned vs unburned areas. Considered with my present results, this suggests that increased C_s size and persistence is an indirect effect of fire that may emerge later during ecosystem recovery as char formed from aboveground biomass becomes incorporated into soil (Abney et al. 2017). Charcoal production increases with fire intensity and severity (Czimczik et al. 2003; Miesel et al. 2015; Sawyer et al. 2018), and I found that C_s size increased with charring temperature. Therefore, high intensity fire could result in a large and persistent C pool that offsets the negative direct effects of high intensity soil heating on C persistence.

Previous research has shown that char can contribute to the C_a pool (Abney et al. 2019), because a portion of char-associated C is easily decomposed (Kuzyakov et al. 2014; Bird et al. 2015), and char can induce positive priming of native soil C (Maestrini et al. 2015). However, I observed no statistically significant effects of char on C_a or k_a, again suggesting that char primarily led to higher soil C persistence. This effect may be partially attributable to the relatively high charring temperatures I employed, as previous research has indicated that forest soils amended with char generated at 200 °C exhibited larger C_a pools than soils amended with higher temperature chars (Abney et al. 2019). Additionally, the chemical properties of char, and

the influence of char on soil respiration varies with source material (Michelotti and Miesel 2015; Hatton et al. 2016). In contrast, adding uncharred wood often increased both k_a and k_s, indicating less persistent C_a and C_s pools. Although wildfires cause immediate declines in woody debris at the soil surface (Miesel et al. 2018), uncharred wood could reaccumulate over time via fallen branches and stems of fire-killed trees. For example, by 4-5 years after a wildfire in *P. ponderosa* dominated forest in Oregon, USA, woody debris accounted for a larger proportion of aboveground C stocks in burned areas compared to unburned areas (Meigs et al. 2009).

5.6 CONCLUSIONS

High intensity fires likely result in greater ecosystem C losses due to combustion. My results suggest that this effect may be exacerbated over the short term by increases in the size and kinetic rate of the active C pool. However, over the long term, these losses could be offset by char incorporation into soil, which increases the size of the non-active C pool. The non-active C pool is an order of magnitude larger than the active C pool and exhibits MRT of decades, so char incorporation could substantially increase the strength of the soil C sink during forest recovery. These results suggest that accurate estimates of the impacts of disrupted fire regimes on forest C stocks and persistence should account for the influence of fire intensity on the soil C cycle. Low intensity soil heating had minimal impacts on soil C pools and MBC, suggesting that soils are resistant and/or resilient to low intensity fires. Therefore, fuel reduction treatments that decrease soil heating intensity could effectively promote resilience of soil functions. Additionally, low intensity prescribed fires could be an effective management tool for reducing forest fuel loads and restoring forest structure without adversely affecting soil C storage. Previous research has shown that the reductions in fire severity resulting from fuel removal treatments enhance permanence of aboveground forest C stocks (North and Hurteau 2011); my results suggest that

fuel removal that decreases soil heating intensity could also contribute to maintaining the persistence of soil C.

APPENDIX

SUPPLEMENTAL FIGURES

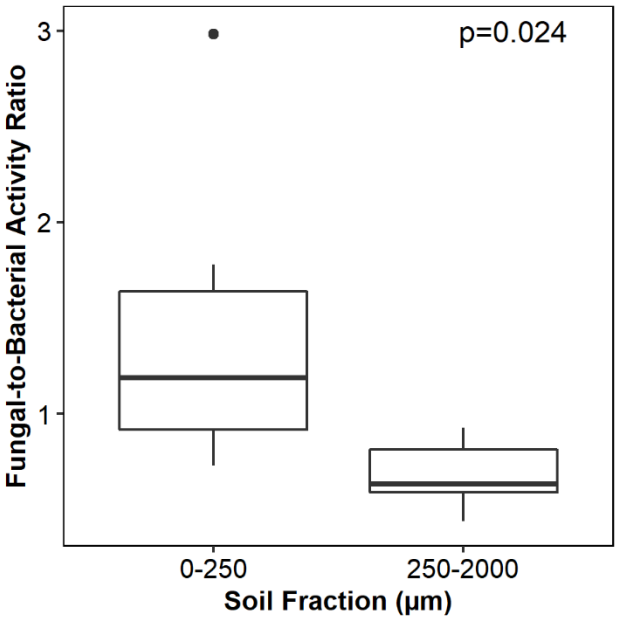

Figure S5.1 Fungal-to-bacterial activity ratio for the two soil fractions used to reinoculate sterilized soil microcosms. Fungal-to-bacterial activity ratio was determined using selectively inhibited substrate-induced respiration.

SUPPLEMENTAL TABLES

Table S5.1 Parameters estimated from single pool carbon models. Pool size parameters expressed in mg kg^{-1} are derived from models fit to cumulative respiration per g soil, and pool size parameters expressed in percent total C are from models fit to respiration per g soil C. Ranges are 95% confidence intervals. Lower-case letters indicate significant differences between soil heating treatments within levels of char treatments. Data is the tabular form of the data shown in figure 5.5.

Single Pool Models			
	C_m (mg kg^{-1})	C_m (%)	k_m (d^{-1})
No Addition			
Unheated Soil	1630.37-2733.38 a	4.31-6.85 a	0.0046-0.0071 b
200 °C Soil	1782.96-2952.22 a	4.69-7.38 a	0.0046-0.0073 b
300 °C Soil	1525.99-2626.69 a	3.74-6.28 a	0.0065-0.0091 b
400 °C Soil	1488.64-2587.81 a	4.30-6.83 a	0.0090-0.0115 a
Uncharred Wood			
Unheated Soil	9727.08-12046.08 a	21.82-27.17 a	-0.0001-0.0023 b
200 °C Soil	8966.37-10928.08 a	18.07-22.15 a	0.0001-0.0025 b
300 °C Soil	2036.83-3136.63 b	4.32-6.86 b	0.0075-0.0100 a
400 °C Soil	1848.34-2947.23 b	4.49-7.03 b	0.0098-0.0123 a
300 °C Char			
Unheated Soil	1408.86-2513.14 a	3.03-5.58 a	0.0046-0.0071 b
200 °C Soil	1768.12-2878.11 a	3.79-6.35 a	0.0036-0.0061 b
300 °C Soil	1524.94-2624.76 a	3.05-5.59 a	0.0070-0.0095 a
400 °C Soil	1563.46-2662.53 a	3.61-6.15 a	0.0092-0.0117 a
550 °C Char			
Unheated Soil	1843.00-2955.72 a	3.89-6.46 a	0.0029-0.0053 c
200 °C Soil	1867.29-2983.54 a	3.92-6.50 a	0.0040-0.0065 c
300 °C Soil	1617.30-2717.82 a	3.18-5.72 a	0.0064-0.0089 b
400 °C Soil	1506.79-2605.96 a	3.40-5.94 a	0.0098-0.0123 a

Table S5.2 Parameters estimated from double pool carbon models. Pool size parameters expressed in mg kg^{-1} are derived from models fit to cumulative respiration per g soil, and pool size parameters expressed in percent total C are from models fit to respiration per g soil C. Ranges are 95% confidence intervals. Lower-case letters indicate significant differences between soil heating treatments within levels of char treatments. Data is the tabular form of the data shown in figure 5.6.

Double Pool Models	C_a (mg kg^{-1})	C_a (% Total C)	C_s (mg kg^{-1})	C_s (% Total C)	k_a (d^{-1})	k_s (y^{-1})
No Addition						
Unheated Soil	807.19-1116.94 b	2.06-2.78 b	37983.06-38292.81 b	97.22-97.94 a	0.011-0.014 b	0.020-0.032 a
200 °C Soil	875.44-1201.66 b	2.25-3.02 b	38028.34-38354.56 b	96.98-97.75 a	0.012-0.014 b	0.023-0.036 a
300 °C Soil	968.37-1266.18 b	2.34-3.04 b	40203.82-40501.63 a	96.96-97.75 a	0.012-0.014 b	0.015-0.027 a
400 °C Soil	1261.72-1552.01 a	3.54-4.22 a	35077.99-35368.28 c	95.78-98.46 a	0.015-0.016 a	0.012-0.024 a
Uncharred Wood						
Unheated Soil	19.20-293.05 b	0.05-0.68 c	43740.95-44014.80 b	99.32-99.95 a	0.015-0.018 b	0.074-0.085 a
200 °C Soil	-14.72-258.74 b	-0.02-0.61 c	43845.23-44118.69 b	99.39-100.02 a	0.015-0.018 b	0.072-0.084 a
300 °C Soil	1246.56-1533.40 a	2.67-3.33 b	44767.48-45054.32 a	96.67-97.33 b	0.016-0.018 b	0.020-0.032 b
400 °C Soil	1458.23-1741.11 a	3.56-4.22 a	39865.78-40148.66 c	95.78-96.44 c	0.019-0.020 a	0.016-0.027 b
300 °C Char						
Unheated Soil	700.43-1003.07 b	1.50-2.19 c	44561.97-44864.61 c	97.81-98.50 a	0.011-0.014 b	0.014-0.026 ab
200 °C Soil	588.18-883.22 b	1.26-1.94 c	44893.58-45188.62 b	98.06-98.74 a	0.012-0.014 b	0.020-0.032 a
300 °C Soil	1103.95-1404.03 a	2.26-2.94 b	46610.47-46910.55 a	97.06-97.74 b	0.013-0.014 b	0.011-0.023 ab
400 °C Soil	1349.35-1639.80 a	3.11-3.79 a	41677.56-41968.01 d	96.21-96.89 c	0.015-0.017 a	0.010-0.021 b
550 °C Char						
Unheated Soil	563.34-865.99 b	1.18-1.86 c	45476.68-45779.33 b	98.14-98.82 a	0.010-0.013 b	0.020-0.032 a
200 °C Soil	617.36-920.20 b	1.30-1.99 c	45459.69-45762.53 b	98.01-98.70 a	0.011-0.013 b	0.019-0.030 a
300 °C Soil	1103.51-1408.03 a	2.22-2.92 b	47268.30-47572.82 a	97.08-97.78 b	0.012-0.013 b	0.011-0.023 ab
400 °C Soil	1364.11-1665.19 a	3.08-3.78 a	42351.51-42652.59 c	96.22-96.91 c	0.014-0.015 a	0.007-0.019 b

REFERENCES

REFERENCES

Abney RB, Jin L, Berhe AA (2019) Soil properties and combustion temperature: Controls on the decomposition rate of pyrogenic organic matter. CATENA 182:104127. doi: 10.1016/j.catena.2019.104127

Abney RB, Sanderman J, Johnson D, et al (2017) Post-wildfire erosion in mountainous terrain leads to rapid and major redistribution of soil organic carbon. Front Earth Sci 5:1–16. doi: 10.3389/feart.2017.00099

Adkins J, Sanderman J, Miesel J (2019a) Soil carbon pools and fluxes vary across a burn severity gradient three years after wildfire in Sierra Nevada mixed-conifer forest. Geoderma. doi: 10.1016/j.geoderma.2018.07.009

Adkins J, Sanderman J, Miesel J (2019b) Soil carbon pools and fluxes vary across a burn severity gradient three years after wildfire in Sierra Nevada mixed-conifer forest. Geoderma 333:10–22. doi: 10.1016/j.geoderma.2018.07.009

Anderson JPE, Domsch KH (1973) Quantification of bacterial and fungal contributions to soil respiration. Arch Mikrobiol 93:113–127. doi: 10.1007/BF00424942

Bailey VL, Smith JL, Bolton H (2003) Novel antibiotics as inhibitors for the selective respiratory inhibition method of measuring fungal:bacterial ratios in soil. Biol Fertil Soils 38:154–160. doi: 10.1007/s00374-003-0620-7

Bárcenas-Moreno G, Bååth E (2009) Bacterial and fungal growth in soil heated at different temperatures to simulate a range of fire intensities. Soil Biol Biochem 41:2517–2526. doi: 10.1016/j.soilbio.2009.09.010

Bird MI, Wynn JG, Saiz G, et al (2015) The pyrogenic carbon cycle. Annu Rev Earth Planet Sci 43:273–298. doi: 10.1146/annurev-earth-060614-105038

Bodí MB, Martin D a., Balfour VN, et al (2014) Wildland fire ash: Production, composition and eco-hydro-geomorphic effects. Earth-Science Rev 130:103–127. doi: 10.1016/j.earscirev.2013.12.007

Bolan NS, Baskaran S, Thiagarajan S (1996) An evaluation of the methods of measurement of dissolved organic carbon in soils, manures, sludges, and stream water. Commun Soil Sci Plant Anal 27:2723–2737. doi: 10.1080/00103629609369735

Busse MD, Shestak CJ, Hubbert KR (2013) Soil heating during burning of forest slash piles and

wood piles. Int J Wildl Fire 22:786–796. doi: 10.1071/WF12179

Cai Y, Peng C, Qiu S, et al (2011) Dichromate digestion-spectrophotometric procedure for determination of soil microbial biomass carbon in association with fumigation-extraction. Commun Soil Sci Plant Anal 42:2824–2834. doi: 10.1080/00103624.2011.623027

Certini G (2005) Effects of fire on properties of forest soils: a review. Oecologia 143:1–10. doi: 10.1007/s00442-004-1788-8

Choromanska U, DeLuca TH (2002) Microbial activity and nitrogen mineralization in forest mineral soils following heating: Evaluation of post-fire effects. Soil Biol Biochem 34:263–271. doi: 10.1016/S0038-0717(01)00180-8

Czimczik CI, Preston CM, Schmidt MWI, Schulze E-D (2003) How surface fire in Siberian scots pine forests affects soil organic carbon in the forest floor: Stocks, molecular structure, and conversion to black carbon (charcoal). Global Biogeochem Cycles. doi: 10.1029/2002GB001956

Dooley SR, Treseder KK (2012) The effect of fire on microbial biomass: A meta-analysis of field studies. Biogeochemistry 109:49–61. doi: 10.1007/s10533-011-9633-8

Dunn PH, Barro SC, Poth M (1985) Soil moisture affects survival of microorganisms in heated chaparral soil. Soil Biol Biochem 17:143–148.

Earles JM, North MP, Hurteau MD (2014) Wildfire and drought dynamics destabilize carbon stores of fire-suppressed forests. Ecol Appl 24:732–740. doi: 10.1890/13-1860.1

Fernández I, Cabaneiro A, Carballas T (1997) Organic matter changes immediately after a wildfire in an atlantic forest soil and comparison with laboratory soil heating. Soil Biol Biochem 29:1–11. doi: 10.1016/S0038-0717(96)00289-1

Fernández I, Cabaneiro A, Carballas T (1999) Carbon mineralization dynamics in soils after wildfires in two Galician forests. Soil Biol Biochem 31:1853–1865. doi: 10.1016/S0038-0717(99)00116-9

González-Pérez JA, González-Vila FJ, Almendros G, Knicker H (2004) The effect of fire on soil organic matter--a review. Environ Int 30:855–870. doi: 10.1016/j.envint.2004.02.003

Greenfield LG, Gregorich EG, van Kessel C, et al (2013) Acid hydrolysis to define a biologically-resistant pool is compromised by carbon loss and transformation. Soil Biol Biochem 64:122–126. doi: 10.1016/j.soilbio.2013.04.009

Guerrero C, Mataix-Solera J, Gómez I, et al (2005) Microbial recolonization and chemical

changes in a soil heated at different temperatures. Int J Wildl Fire 14:385–400. doi: 10.1071/WF05039

Hatton PJ, Chatterjee S, Filley TR, et al (2016) Tree taxa and pyrolysis temperature interact to control the efficacy of pyrogenic organic matter formation. Biogeochemistry 130:103–116. doi: 10.1007/s10533-016-0245-1

Hobbie EA, Hofmockel KS, van Diepen LTA, et al (2014) Fungal carbon sources in a pine forest: evidence from a 13C-labeled global change experiment. Fungal Ecol 10:91–100. doi: 10.1016/j.funeco.2013.11.001

Jastrow JD, Amonette JE, Bailey VL (2007) Mechanisms controlling soil carbon turnover and their potential application for enhancing carbon sequestration. Clim Change 80:5–23. doi: 10.1007/s10584-006-9178-3

Jones MW, Santín C, van der Werf GR, Doerr SH (2019) Global fire emissions buffered by the production of pyrogenic carbon. Nat Geosci 12:742–747. doi: 10.1038/s41561-019-0403-x

Knicker H (2007) How does fire affect the nature and stability of soil organic nitrogen and carbon? A review. Biogeochemistry 85:91–118. doi: 10.1007/s10533-007-9104-4

Kuzyakov Y (2011) How to link soil C pools with CO2 fluxes? Biogeosciences 8:1523–1537. doi: 10.5194/bg-8-1523-2011

Kuzyakov Y, Bogomolova I, Glaser B (2014) Biochar stability in soil: Decomposition during eight years and transformation as assessed by compound-specific ^{14}C analysis. Soil Biol Biochem 70:229–236. doi: 10.1016/j.soilbio.2013.12.021

Kuzyakov Y, Subbotina I, Chen H, et al (2009) Black carbon decomposition and incorporation into soil microbial biomass estimated by 14C labeling. Soil Biol Biochem 41:210–219. doi: 10.1016/j.soilbio.2008.10.016

Lawrence CR, Neff JC, Schimel JP (2009) Does adding microbial mechanisms of decomposition improve soil organic matter models? A comparison of four models using data from a pulsed rewetting experiment. Soil Biol Biochem 41:1923–1934. doi: 10.1016/j.soilbio.2009.06.016

Lenth R (2020) emmeans: Estimated Marginal Means, aka Least-Squares Means. R package version 1.4.4.

Luo Y, Weng E (2011) Dynamic disequilibrium of the terrestrial carbon cycle under global change. Trends Ecol Evol 26:96–104. doi: 10.1016/j.tree.2010.11.003

Maestrini B, Nannipieri P, Abiven S (2015) A meta-analysis on pyrogenic organic matter

induced priming effect. GCB Bioenergy 7:577–590. doi: 10.1111/gcbb.12194

Masiello CA (2004) New directions in black carbon organic geochemistry. Mar Chem 92:201–213. doi: 10.1016/j.marchem.2004.06.043

Massman WJ, Frank JM, Mooney SJ (2010) Advancing investigation and physical modeling of first-order fire effects on soils. Fire Ecol 6:36–54. doi: 10.4996/fireecology.0601036

Mataix-Solera J, Cerdà A, Arcenegui V, et al (2011) Fire effects on soil aggregation: A review. Earth-Science Rev 109:44–60. doi: 10.1016/j.earscirev.2011.08.002

Meigs GW, Donato DC, Campbell JL, et al (2009) Forest fire impacts on carbon uptake, storage, and emission: The role of burn severity in the eastern Cascades, Oregon. Ecosystems 12:1246–1267. doi: 10.1007/s10021-009-9285-x

Michelotti L, Miesel J (2015) Source Material and Concentration of Wildfire-Produced Pyrogenic Carbon Influence Post-Fire Soil Nutrient Dynamics. Forests 6:1325–1342. doi: 10.3390/f6041325

Miesel J, Reiner A, Ewell C, et al (2018) Quantifying Changes in Total and Pyrogenic Carbon Stocks Across Fire Severity Gradients Using Active Wildfire Incidents. Front Earth Sci 6:1–21. doi: 10.3389/feart.2018.00041

Miesel JR, Hockaday WC, Kolka RK, Townsend PA (2015) Soil organic matter composition and quality across fire severity gradients in coniferous and deciduous forests of the southern boreal region. J Geophys Res Biogeosciences 120:1124–1141. doi: 10.1002/2015JG002959

Moorhead DL, Sinsabaugh RL (2006) A theoretical model of litter decay and microbial interaction. Ecol Monogr 76:151–174.

Neary D., DeBano L. (2005) Wildland fire in ecosystems effects of fire on soil and water.

Neff JC, Asner GP (2001) Dissolved organic carbon in terrestrial ecosystems: Synthesis and a model. Ecosystems 4:29–48. doi: 10.1007/s100210000058

Nguyen BT, Lehmann J, Hockaday WC, et al (2010) Temperature sensitivity of black carbon decomposition and oxidation. Environ Sci Technol 44:3324–3331. doi: 10.1021/es903016y

North MP, Hurteau MD (2011) High-severity wildfire effects on carbon stocks and emissions in fuels treated and untreated forest. For Ecol Manage 261:1115–1120. doi: 10.1016/j.foreco.2010.12.039

Pan Y, Birdsey RA, Fang J, et al (2011) A large and persistent carbon sink in the world's forests.

Science 333:988–993. doi: 10.1126/science.1201609

Pinheiro J, Bates D, Debroy S, Sarkar D (2019) nlme: Linear and nonlinear mixed effects models.

Pinheiro JC, Bates DM (2000) Mixed-effects models in S and S-Plus. Springer-Verlag, New York

Prendergast-Miller MT, de Menezes AB, Macdonald LM, et al (2017) Wildfire impact: Natural experiment reveals differential short-term changes in soil microbial communities. Soil Biol Biochem 109:1–13. doi: 10.1016/j.soilbio.2017.01.027

R Core Team (2019) R: A language and environment for statistical computing.

Rousk J, Demoling LA, Bååth E (2009) Contrasting short-Term antibiotic effects on respiration and bacterial growth compromises the validity of the selective respiratory inhibition technique to distinguish fungi and bacteria. Microb Ecol 58:75–85. doi: 10.1007/s00248-008-9444-1

Santos F, Torn MS, Bird JA (2012) Biological degradation of pyrogenic organic matter in temperate forest soils. Soil Biol Biochem 51:115–124. doi: 10.1016/j.soilbio.2012.04.005

Sawyer R, Bradstock R, Bedward M, Morrison RJ (2018) Fire intensity drives post-fire temporal pattern of soil carbon accumulation in Australian fire-prone forests. Sci Total Environ 610–611:1113–1124. doi: 10.1016/j.scitotenv.2017.08.165

Skinner CN, Taylor AH (2006) Southern Cascades Bioregion. 195–224.

Soil Survey Staff Official soil series descriptions. In: Nat. Resour. Conserv. Serv. United States Dep. Agric. www.nrcs.usda.gov.

Taylor AH, Vandervlugt AM, Maxwell RS, et al (2014) Changes in forest structure, fuels and potential fire behaviour since 1873 in the Lake Tahoe Basin, USA. Appl Veg Sci 17:17–31. doi: 10.1111/avsc.12049

Wagg C, Bender SF, Widmer F, van der Heijden MGA (2014) Soil biodiversity and soil community composition determine ecosystem multifunctionality. Proc Natl Acad Sci 111:5266–5270. doi: 10.1073/pnas.1320054111

Wagg C, Schlaeppi K, Banerjee S, et al (2019) Fungal-bacterial diversity and microbiome complexity predict ecosystem functioning. Nat Commun 10:1–10. doi: 10.1038/s41467-019-12798-y

Wang WJ, Dalal RC, Moody PW, Smith CJ (2003) Relationships of soil respiration to microbial biomass, substrate availability and clay content. Soil Biol Biochem 35:273–284. doi: 10.1016/S0038-0717(02)00274-2

Witt C, Gaunt JL, Galicia CC, et al (2000) A rapid chloroform-fumigation extraction method for measuring soil microbial biomass carbon and nitrogen in flooded rice soils. Biol Fertil Soils 30:510–519. doi: 10.1007/s003740050030

Zimmermann M, Bird MI, Wurster C, et al (2012) Rapid degradation of pyrogenic carbon. Glob Chang Biol 18:3306–3316. doi: 10.1111/j.1365-2486.2012.02796.x

CHAPTER 6:

MANAGEMENT IMPLICATIONS: POST-FIRE FOREST MANAGEMENT MAY IMPROVE RECOVERY OF SOIL CARBON STORAGE

Altered forest structure in forests of the western United States has led to increased forest ecosystem carbon (C) stocks due to greater tree density and dead fuel accumulation (North et al. 2009; Earles et al. 2014; Hurteau et al. 2014). Forest densification has allowed these forests to act as strong C sinks and offset a substantial portion CO_2-C emissions (Goodale et al. 2002; Pan et al. 2011). However, compared to forests that are structurally similar to historical (i.e. pre fire-suppression) forests, these C stocks are inherently less stable because dense forests are more susceptible to C losses due to drought and insect-based disturbances (Earles et al. 2014; Hurteau et al. 2014; Stephens et al. 2020) and could transition to C sources under future climate scenarios (Loudermilk et al. 2013; Liang et al. 2017c). Furthermore, these dense forests are more susceptible to stand-replacing fires that lead to immediate losses of forest C stocks and are slow to recover the lost stocks due to low post-fire net ecosystem productivity (Kashian et al. 2006; Meigs et al. 2009). High-severity fires can therefore act as "tipping-point" disturbances in which centuries of accumulated C are rapidly lost, and the large magnitude of change to the ecosystem prevents the forest from fully recovering the lost C stocks (Adams 2013). Approximately half of ecosystem C in temperate forests is stored in soils (Pan et al. 2011), so understanding the impacts of fire and fire-management on soil C storage is important for managing forests for C sequestration and climate change mitigation (Birdsey et al. 2006). Here, I discuss the implications of my research on fire's impacts on soil C storage and soil microbial communities for forest and fire management.

My research shows soil C storage is lower in burned compared to unburned forest stands, likely due to forest floor mass loss, and this effect increases in magnitude with burn severity

(Fig. 1.3). High intensity soil heating also induces short-term increases in soil C mineralization and decreases C stored in microbial biomass (Table 4.1 and Fig. 4.3). Together, these results indicate that increased burn severity has negative impacts on soil C storage. However, despite the short-term effects of soil heating on mineral soil C, total mineral soil C storage does not vary among severity levels by three years post-fire (Fig 1.3), and, in fact, may be more stable (Table 1.4). This indicates that recovery of forest soil C storage is primarily dependent on re-accumulation of forest floor.

The importance of forest floor for dictating post-fire soil C storage suggests that managing forests for vegetation recovery will have associated benefits on soil. I found that live tree coverage is substantially lower in high severity areas (Fig. 2.1d), and previous research has indicated that a negative relationship between severity and tree coverage is common in California mixed-conifer forests (Miller et al. 2016). Considered with my finding that forest floor mass is positively associated with live tree basal area (Fig. 2.4), this further supports the idea that vegetation management is necessary for achieving recovery of soil C storage in high burn severity areas. This has implications for both pre- and post-fire forest management. From a pre-fire perspective, it suggests forest management practices designed to limit the incidence of high-severity fires will have a positive impact on soil C storage. Severity-reduction treatments (e.g. prescribed fire, stand thinning, fuel removal) have been shown to have numerous positive outcomes, including promoting biodiversity, increasing water availability, and stabilizing aboveground C stocks (Stephens et al. 2020). Severity-reduction treatments stabilize aboveground C stocks by limiting tree mortality when wildfires burn treated areas, decreasing combustion emissions and allowing for post-fire photosynthetic C gains (Liang et al. 2018). My research suggests that the stabilizing effects of severity-reduction treatments may also apply to

soil C: lower fire severity leads to more C retained in forest floor and faster re-accumulation due to greater tree survival. Additionally, treatments that decrease soil heating (e.g. coarse woody debris removal) could have marginal benefits on soil C storage by limiting losses to soil C via microbial biomass loss and post-fire increases in C mineralization. Fire exclusion has led to forest floor accumulation in some forest stands, and prescribed fires in these areas could result in high intensity soil heating due to forest floor combustion. In these cases, prescribed fires may have a temporary negative impact on soil C storage, but, over the long term, could have a positive impact if prescribed fires lead to lower wildfire severity.

From a post-fire perspective, my results suggest that management decisions designed to increase tree regeneration in areas of high burn severity could increase the rate of soil C recovery. Management strategies that promote C storage and are compatible with other goals such as forest restoration or timber production have been identified as integral for forest C management in the 21st century (Birdsey et al. 2006). Post-fire seedling planting may represent a management application with multi-faceted benefits by improving forest regeneration following wildfires (Ouzts et al. 2015), with corollary benefits on the recovery of soil C storage. Post-fire tree planting is controversial because successful establishment from these practices can be low, and dense plantations can promote high severity fires (Thompson et al. 2007; Ouzts et al. 2015). However, natural tree regeneration can be low or absent in areas of high burn severity due to poor site conditions and greater distance to seed sources (Crotteau et al. 2013; Feddema et al. 2013; Lopez Ortiz et al. 2019), potentially precipitating a "state-change" shift to a different vegetation type (Barton 2002; Savage and Mast 2005; Roccaforte et al. 2012; Tepley et al. 2017). Due to negative impacts of high severity fire on natural forest recovery, the need for post-fire restoration is becoming increasingly recognized, especially during a critical 3-5 year post-fire

window when regeneration is most likely to be successful (Tepley et al. 2017; Stewart et al. 2020). My research indicates that certain site conditions in areas of high burn severity may have a positive influence on artificial regeneration efforts. Shrub coverage was positively correlated with severity three years post-fire (Fig. 2.1f), and inorganic nitrogen concentrations were greater in areas of high burn severity at 1-3 years post fire (Fig. 1.5 and Table 3.1) Shrubs can positively influence regeneration by acting as "nurse objects" that improve soil microclimate conditions (Keyes et al. 2009), and greater nitrogen availability ameliorates nutrient limitation (Taboada et al. 2017). However, previous research has shown that elevated inorganic nitrogen in burned stands generally does not persist longer than approximately five years post-fire (Wan et al. 2001). This suggests that artificial regeneration efforts are more likely to be successful in this timeframe, supporting arguments that the 3-5 year post-fire window is key for successful regeneration (Tepley et al. 2017; Stewart et al. 2020). By focusing restoration efforts in high severity areas with elevated nutrient concentrations and shrub coverage, forest managers could maximize the success of artificial regeneration efforts and increase the rate of soil C recovery.

Changes to soil microbial communities could have consequences for post-fire forest management. Using phospholipid fatty acid (PLFA) analysis, I found that fungal biomass was negatively related to severity three years post-fire (Fig. 2.5a). The change in fungal biomass could reflect losses to ectomycorrhizal fungi, which are known to be sensitive to fire (Dahlberg et al. 2001; Holden et al. 2013). Loss of ectomycorrhizal fungi could negatively impact both natural regeneration and artificial restoration efforts because these fungi form symbiotic associations with conifer roots, improving nitrogen and phosphorus acquisition in exchange for carbohydrates (Heijden et al. 2015). This suggests that artificial regeneration efforts that use seedling transplants, which already have developed mycorrhizal networks, may be more

effective than direct seeding, which depend on an existing soil bank of ectomycorrhizal spores. Indeed, *in situ* mycorrhizal colonization decreases following fires (Dove and Hart 2017). Moreover, transplant of seedlings that have been inoculated with ectomycorrhiza has been shown to improve seedling performance during reforestation following a variety of disturbance types, including for post-fire restoration in *Pinus pinaster* stands (Policelli et al. 2020).

Differences in soil bacterial communities in areas of high burn severity also highlight the importance of actively managing areas of high burn severity for forest regeneration and C recovery. The abundance of copiotrophic bacteria, which have higher nutrient requirements than oligotrophic bacteria (Fierer et al. 2007; Ho et al. 2017), was positively correlated with severity 1-3 years post-fire (Figs. 2.6f and 3.3f). Plants and microbes compete for nutrients (Kaye and Hart 1997; Kuzyakov and Xu 2013), and the higher nutrient requirements of copiotrophic bacteria could result in increased competition between plants and microbes. Increased competition could decrease plant performance following fire, hindering natural forest regeneration and the recovery of both aboveground and soil C stocks. Additionally, copiotrophs exhibit faster decomposition rates than oligotrophs (Orwin et al. 2018), potentially leading to continued soil C losses in the years post-fire. This further highlights the importance of inoculating seedling transplants with ectomycorrhizal fungi, which improve the competitive ability of plants for nutrients.

Overall, my results indicate that high burn severity has detrimental impacts on soil C storage and that microbial communities are altered in ways that could hinder natural forest recovery. Fortunately, these negative effects can be overcome by vegetation management practices that are already common in forest ecosystems, and the development of new soil-specific management tools does not appear necessary. However, achieving recovery of soil C

storage in areas of high burn severity likely requires active forest management rather than relying on natural regeneration.

REFERENCES

REFERENCES

Adams M (2013) Mega-fires, tipping points and ecosystem services: Managing forests and woodlands in an uncertain future. For Ecol Manage 294:250-261. doi: 10.1016/j.foreco.2012.11.039

Barton AM (2002) Intense wildfire in southeastern Arizona: Transformation of a Madrean oak-pine forest to oak woodland. For Ecol Manage 165:205–212. doi: 10.1016/S0378-1127(01)00618-1

Birdsey R, Pregitzer K, Lucier A (2006) Forest carbon management in the United States. J Environ Qual 35:1461. doi: 10.2134/jeq2005.0162

Crotteau JS, Morgan Varner J, Ritchie MW (2013) Post-fire regeneration across a fire severity gradient in the southern Cascades. For Ecol Manage 287:103–112. doi: 10.1016/j.foreco.2012.09.022

Dahlberg A, Schimmel J, Taylor AFS, Johannesson H (2001) Post-fire legacy of ectomycorrhizal fungal communities in the Swedish boreal forest in relation to fire severity and logging intensity. Biol Conserv 100:151–161. doi: 10.1016/S0006-3207(00)00230-5

Dove NC, Hart SC (2017) Fire reduces fungal species richness and in situ mycorrhizal colonization: A meta-analysis. Fire Ecol 13:37–65. doi: 10.4996/fireecology.130237746

Earles JM, North MP, Hurteau MD (2014) Wildfire and drought dynamics destabilize carbon stores of fire-suppressed forests. Ecol Appl 24:732–740. doi: 10.1890/13-1860.1

Feddema JJ, Mast JN, Savage M (2013) Modeling high-severity fire, drought and climate change impacts on ponderosa pine regeneration. Ecol Modell 253:56–69. doi: 10.1016/j.ecolmodel.2012.12.029

Fierer N, Bradford MA, Jackson RB (2007) Toward an ecological classification of soil bacteria. Ecology 88:1354–1364. doi: 10.1890/05-1839

Goodale CL, Apps MJ, Birdsey R a, et al (2002) Forest carbon sinks in the Northern Hemisphere. Ecol Appl 12:891–899. doi: Doi 10.2307/3060997

Heijden MG a Van Der, Martin FM, Selosse M-AA, et al (2015) Mycorrhizal ecology and evolution: the past, the present, and the future. New Phytol 205:1406–1423. doi: 10.1111/nph.13288

Ho A, Di Lonardo DP, Bodelier PLE (2017) Revisiting life strategy concepts in environmental microbial ecology. FEMS Microbiol Ecol 93:1–14. doi: 10.1093/femsec/fix006

Holden SR, Gutierrez A, Treseder KK (2013) Changes in Soil Fungal Communities, Extracellular Enzyme Activities, and Litter Decomposition Across a Fire Chronosequence in Alaskan Boreal Forests. Ecosystems 16:34–46. doi: 10.1007/s10021-012-9594-3

Hurteau MD, Bradford JB, Fulé PZ, et al (2014) Climate change, fire management, and ecological services in the southwestern US. For Ecol Manage 327:280–289. doi: 10.1016/j.foreco.2013.08.007

Kashian DM, Romme WH, Tinker DB, et al (2006) Carbon storage on landscapes with stand-replacing fires. Bioscience 56:598–606. doi: 10.1641/0006-3568(2006)56[598:CSOLWS]2.0.CO;2

Kaye JP, Hart SC (1997) Competition for nitrogen between plants and soil microorganisms. Trends Ecol Evol 12:139–142.

Keyes CR, Maguire DA, Tappeiner JC (2009) Recruitment of ponderosa pine seedlings in the Cascade Range. For Ecol Manage 257:495–501. doi: 10.1016/j.foreco.2008.09.024

Kuzyakov Y, Xu X (2013) Competition between roots and microorganisms for nitrogen: Mechanisms and ecological relevance. New Phytol 198:656–669. doi: 10.1111/nph.12235

Liang S, Hurteau MD, Westerling AL (2017) Potential decline in carbon carrying capacity under projected climate-wildfire interactions in the Sierra Nevada. Sci Rep 7:1–7. doi: 10.1038/s41598-017-02686-0

Liang S, Hurteau MD, Westerling AL (2018) Large-scale restoration increases carbon stability under projected climate and wildfire regimes. Front Ecol Environ. doi: 10.1002/fee.1791

Lopez Ortiz MJ, Marcey T, Lucash MS, et al (2019) Post-fire management affects species composition but not Douglas-fir regeneration in the Klamath Mountains. For Ecol Manage 432:1030–1040. doi: 10.1016/j.foreco.2018.10.030

Loudermilk EL, Scheller RM, Weisberg PJ, et al (2013) Carbon dynamics in the future forest: The importance of long-term successional legacy and climate-fire interactions. Glob Chang Biol 19:3502–3515. doi: 10.1111/gcb.12310

Meigs GW, Donato DC, Campbell JL, et al (2009) Forest fire impacts on carbon uptake, storage, and emission: The role of burn severity in the eastern Cascades, Oregon. Ecosystems 12:1246–1267. doi: 10.1007/s10021-009-9285-x

Miller JD, Safford HD, Welch KR (2016) Using one year post-fire fire severity assessments to estimate longer-term effects of fire in conifer forests of northern and eastern California, USA. For Ecol Manage 382:168–183. doi: 10.1016/j.foreco.2016.10.017

North M, Hurteau M, Innes J (2009) Fire supression and fuels treatment effects on mixed-conifer carbon stocks and emissions. Ecol Appl 19:1385–1396. doi: 10.1890/08-1173.1

Orwin KH, Dickie IA, Holdaway R, Wood JR (2018) A comparison of the ability of PLFA and 16S rRNA gene metabarcoding to resolve soil community change and predict ecosystem functions. Soil Biol Biochem 117:27–35. doi: 10.1016/j.soilbio.2017.10.036

Ouzts J, Kolb T, Huffman D, Sánchez Meador A (2015) Post-fire ponderosa pine regeneration with and without planting in Arizona and New Mexico. For Ecol Manage 354:281–290. doi: 10.1016/j.foreco.2015.06.001

Pan Y, Birdsey RA, Fang J, et al (2011) A large and persistent carbon sink in the world's forests. Science 333:988–993. doi: 10.1126/science.1201609

Policelli N, Horton TR, Hudon AT, et al (2020) Back to Roots: The Role of Ectomycorrhizal Fungi in Boreal and Temperate Forest Restoration. Front For Glob Chang. doi: 10.3389/ffgc.2020.00097

Roccaforte JP, Fulé PZ, Chancellor WW, Laughlin DC (2012) Woody debris and tree regeneration dynamics following severe wildfires in Arizona ponderosa pine forests. Can J For Res 42:593–604. doi: 10.1139/x2012-010

Savage M, Mast JN (2005) How resilient are southwestern ponderosa pine forests after crown fires? Can J For Res 35:967–977. doi: 10.1139/x05-028

Stephens SL, Westerling ALR, Hurteau MD, et al (2020) Fire and climate change: conserving seasonally dry forests is still possible. Front Ecol Environ 18:354–360. doi: 10.1002/fee.2218

Stewart JAE, van Mantgem PJ, Young DJN, et al (2020) Effects of postfire climate and seed availability on postfire conifer regeneration. Ecol Appl. doi: 10.1002/eap.2280

Taboada A, Tárrega R, Marcos E, et al (2017) Fire recurrence and emergency post-fire management influence seedling recruitment and growth by altering plant interactions in fire-prone ecosystems. For Ecol Manage 402:63–75. doi: 10.1016/j.foreco.2017.07.029

Tepley AJ, Thompson JR, Epstein HE, Anderson-Teixeira KJ (2017) Vulnerability to forest loss through altered postfire recovery dynamics in a warming climate in the Klamath Mountains. Glob Chang Biol 23:4117–4132. doi: 10.1111/gcb.13704

Thompson JR, Spies TA, Ganio LM (2007) Reburn severity in managed and unmanaged vegetation in a large wildfire. Proc Natl Acad Sci U S A 104:10743–10748. doi: 10.1073/pnas.0700229104

Wan S, Hui D, Luo Y (2001) Fire effects on nitrogen pools and dynamics in terrestrial ecosystems: A meta-analysis. Ecol Appl 11:1349–1365.